



HAL
open science

Fabrication et caractérisation d'un pansement électrofilée bicouche moderne pour les applications biomédicales

Tabinda Riaz

► **To cite this version:**

Tabinda Riaz. Fabrication et caractérisation d'un pansement électrofilée bicouche moderne pour les applications biomédicales. Autre. Université de Haute Alsace - Mulhouse, 2020. Français. NNT : 2020MULH4004 . tel-03435013

HAL Id: tel-03435013

<https://theses.hal.science/tel-03435013v1>

Submitted on 18 Nov 2021

HAL is a multi-disciplinary open access archive for the deposit and dissemination of scientific research documents, whether they are published or not. The documents may come from teaching and research institutions in France or abroad, or from public or private research centers.

L'archive ouverte pluridisciplinaire **HAL**, est destinée au dépôt et à la diffusion de documents scientifiques de niveau recherche, publiés ou non, émanant des établissements d'enseignement et de recherche français ou étrangers, des laboratoires publics ou privés.

Année 2020

N° d'ordre: -----

UNIVERSITÉ DE HAUTE-ALSACE
UNIVERSITE DE STRASBOURG

THÈSE

Pour l'obtention du grade de
DOCTEUR DE L'UNIVERSITÉ DE HAUTE-ALSACE
ECOLE DOCTORALE : Sciences Chimiques (ED 222)
Discipline : Chimie des Matériaux

Présentée et soutenue publiquement
par

Tabinda RIAZ

Le 10 novembre 2020

Fabrication & Characterization of A Modern Bilayer Electrospun Wound Dressing for Biomedical Applications

Sous la direction des Pr. Christelle DELAITE et Dominique C. ADOLPHE

Jury :

Pr. Leonard ATANASE	University "Apollonia" Iasi-Romania Faculty of Dental Medicine	Président
Dr. Ahsan NAZIR	National Textile University, Faisalabad-Pakistan	Rapporteur
Pr. Fabien SALAUN	ENSAIT, GEMTEX, Roubaix-France	Rapporteur
Dr. Nabyl KHENOUSI	KAS Consulting, Mulhouse-France	Examineur
Pr. Christelle DELAITE	Université de Haute-Alsace	Directrice
Pr. Dominique ADOLPHE	Université de Haute-Alsace	Co-Directeur

Dedication

«-----»

I dedicate this honor to my three pillars of strength in life, without whom this wouldn't have been possible. To my dearest mother, my beloved husband Atif and my beautiful children Haram and Haroon.

«-----»

Acknowledgement

First and foremost, I am grateful to God for blessing me with His eternal grace, mercy and provision during what ended up being the most challenging yet beautiful years of my life.

Next, I would like to express my sincere gratitude to the driving force of this thesis, my supervisor Pr. Christelle DELAITE for her unwavering support, encouragement and facilitation. I am indebted to her moral and scientific assistance. Napoleon Hill once said: *"It is literally true that you can succeed best and quickest by helping others to succeed"* and I found Christelle as a living example of this quote. I am also obliged to my co-supervisor Pr. Dominique ADOLPHE for being so kind, generous and helpful throughout these years. It was his invaluable feedback and guidance that enlightened my way.

I gratefully acknowledge the intellectual contribution of Dr. Nabyl KHENOUSSI who introduced me to this progressive topic and paved my beginnings with his technical advice. I would like to extend my heartfelt appreciations to Pr. Leonard ATANASE for his unconditional support and inspiration. A huge thanks to his research team as well for assisting me in my research.

Last but not the least, I am truly thankful to all my colleagues from LPIM and LPMT specially, Mr. Gaetan GARREFFA and Ms. Floriane LECLINCHE for their kindness and cooperation.

Abbreviations

Materials

AgNPs : Silver nanoparticles

CS : Chitosan

Chl : Chloramphenicol

Cur : Curcumin

DMF : Dimethylformamide

DOX : Doxorubicin hydrochloride

E. coli. : Escherichia coli (gram-negative bacteria)

EUG : Eugenol oil

GE : Gelatin

GAG : Glycosaminoglycan

HA : Sodium Hyaluronate

IBU : Ibuprofen

MSNs : Mesoporous silica nanoparticles **THF** : Tetrahydrofuran

Na-IBU : Sodium salt of Ibuprofen

NCs : Nanocapsules of chitosan

NCs.Na-IBU : Nanocapsules of chitosan loaded with sodium salt of Ibuprofen

NSAIDs : Non-steroidal anti-inflammatory drugs

PCL : Poly(ϵ -caprolactone)

PEG : Polyethylene glycol

PEO : Polyethylene oxide

PLLA : Poly(l-lactic acid)

PLGA : Poly(lactic-co-glycolic acid)

PVA : Polyvinyl alcohol

S. epidermidis. : Staphylococcus epidermidis (gram-positive bacteria)

SiO₂ : Silicone dioxide/silica

Terms and Equipment

CV% : Coefficient of variation

D : Needle-collector distance

DOE : Design of experiment

DSC : Differential Scanning Calorimetry

ECM: Extracellular matrix

F.R : Feed rate

ΔH_m : Melting enthalpy

kV : Kilo volts

MPa : Mega Pascal

MD : Mean diameter

N : Newton

N₂ : Nitrogen gas

NHDF : Normal human dermal fibroblast

nm : Nanometers

PCA : Principal Component Analysis

%RE : Percentage release efficiency

rpm : Rotation per min

SEM: Scanning Electron Microscopy

SD : Standard deviation

TGA : Thermogravimetric Analysis

T_g: Glass transition temperature

T_m : Melting temperature

UV : Ultra violet

μm : Micrometers

X_c % : Percentage crystallinity ratio of nanofibers

Table of Contents

GENERAL INTRODUCTION.....	16
INTRODUCTION:	18
GENERAL INTRODUCTION	20
CHAPTER 1: LITERATURE REVIEW	23
CHAPITRE 1: BIBLIOGRAPHIE	25
1. ELECTROSPINNING HISTORY AND ITS BASIC PRINCIPLES.....	27
2. TYPES OF ELECTROSPINNING AND THEIR SCOPE.....	30
2.1 <i>Single-needle electrospinning</i>	31
2.2 <i>Needleless electrospinning</i>	32
3. ELECTROSPINNING PARAMETERS AND THEIR IMPACT ON NANOFIBERS PROPERTIES.....	34
3.1 <i>Polymer concentration and viscosity</i>	35
3.2 <i>Feed rate</i>	35
3.3 <i>Needle to collector distance</i>	36
3.4 <i>Applied voltage</i>	36
3.5 <i>Ambient environment</i>	37
4. BIOMATERIALS FOR WOUND DRESSINGS	37
4.1 <i>Natural polymers</i>	38
4.2 <i>Synthetic polymers and their blending</i>	39
5. PCL ELECTROSPINNING.....	41
6. PCL/PEG BLEND ELECTROSPINNING.....	44
7. INCORPORATION OF DRUGS AND NANOPARTICLES INTO PCL NANOFIBERS	46
7.1 <i>Incorporation of drugs</i>	46
7.2 <i>Incorporation of nanoparticles</i>	48
8. NANOFIBERS AS DRUG DELIVERY SYSTEMS IN WOUND DRESSINGS.....	49
9. CONCLUSION	53
REFERENCES	55
CHAPTER 2: MATERIALS & METHODS.....	66
CHAPITRE 2: MATÉRIEL ET MÉTHODES.....	68

1. MATERIALS	70
1.1 Poly(ϵ-caprolactone) (PCL)	70
1.2 Polyethylene glycol (PEG)	70
1.3 Ibuprofen (IBU)	70
1.4 Dispersing agents	71
1.5 Gelatin and Hyaluronan	71
1.6 Solvents	72
2. METHODS	72
2.1 Electrospinning solution preparation	72
2.2 Elaboration of Na-IBU loaded nanocapsules of chitosan	73
2.3 Single-needle electrospinning set-up	74
2.4 Needleless electrospinning equipment	81
2.5 GE/HA film preparation	83
2.6 Fabrication of bilayer structure	84
3. CHARACTERIZATION	84
3.1 Viscosity analysis of PCL solution	84
3.2 Scanning Electron Microscopy (SEM) of nanofibers	84
3.3 Contact angle measurements	86
3.4 Differential Scanning Calorimetry (DSC) analysis of nanofibers	87
3.5 Thermogravimetric analysis (TGA) of nanofibers	87
3.6 Particle size distribution measured by light scattering	88
3.7 Optical Microscopy	88
3.8 Tensile strength testing of nanofibers	88
4. BIOLOGICAL TESTING	90
4.1 Drug release kinetics	90
4.2 In-vitro antimicrobial assay	91
5. CONCLUSION	93
REFERENCES	94
CHAPTER 3: SINGLE-NEEDLE ELECTROSPINNING & CHARACTERIZATION OF PCL NANOFIBERS	95

CHAPITRE 3: ELECTROFILAGE À UNE AIGUILLE ET CARACTÉRISATION DES NANOFIBRES PCL ET PCL/PEG	97
1. INTRODUCTION	99
2. VISCOSITY OF PCL IN DIFFERENT SOLVENTS	100
3. MORPHOLOGY OF NANOFIBERS	102
3.1 Pure PCL nanofibers	102
3.2 PCL/PEG-10% nanofibers	105
3.3 PCL/PEG-20% nanofibers	108
4. STATISTICAL OPTIMIZATION OF ELECTROSPINNING PARAMETERS FOR PCL AND PCL/PEG NANOFIBERS	111
4.1 Observations of PCA for 10wt% PCL nanofibers	111
4.2 Observations of PCA for PCL/PEG-10%	113
4.3 Observations of PCA for PCL/PEG-20%	116
4.4 Comparison between electrospinning parameters of PCL and PCL/PEG-10%, PCL/PEG-10% and PCL/PEG-20%	118
5. CRYSTALLINITY OF PCL AND PCL/PEG NANOFIBERS	120
Impact of PEG-400 on the crystallinity of PCL nanofibers	122
6. TAILORING THE WETTABILITY OF PCL NANOFIBERS WITH PEG-400	123
7. THERMAL ANALYSIS OF PCL AND PCL/PEG NANOFIBERS	124
8. INCORPORATION OF NANOCAPSULES OF CHITOSAN	126
8.1 Morphology of 1%NCs+PCL nanofibers	127
8.2 Morphology of 1%NCs+PCL/PEG-10% nanofibers	129
8.3 Incorporation of drug encapsulated nanocapsules of chitosan	131
8.4 Agglomerations of NCs.Na-IBU into PCL solution	131
8.5 Size distribution analysis of NCs.Na-IBU with dispersing agents	132
8.6 Incorporation of NCs.Na-IBU into PCL/PEG-10% nanofibers	134
9. INCORPORATION OF PURE IBU INTO PCL AND PCL/PEG NANOFIBERS	138
9.1 Morphology of 5%IBU+PCL nanofibers	138
9.2 Morphology of 7%IBU+PCL/PEG-10% nanofibers	140
9.3 Crystallinity of IBU loaded nanofibers	143
9.4 Presence of IBU in nanofibers determined by thermal analysis	144
10. MECHANICAL PROPERTIES OF NANOFIBERS	147

10.1	<i>Influence of PEG-400 concentration</i>	148
10.2	<i>Impact of IBU on mechanical properties of nanofibers</i>	149
11.	IBU RELEASE KINETICS OF NANOFIBERS	150
12.	CONCLUSION	152
	REFERENCES	154
CHAPTER 4: NEEDLELESS ELECTROSPINNING AND CHARACTERIZATION OF PCL AND PCL/PEG NANOFIBERS		159

CHAPITRE 4: ELECTROSPINNING SANS AIGUILLE ET CARACTÉRISATION DES NANOFIBRES PCL ET PCL/PEG		
		161
1.	INTRODUCTION	163
2.	NEEDLELESS ELECTROSPINNING OF PURE PCL, PCL/PEG AND IBU LOADED NANOFIBERS	164
	<i>Morphology of nanofibers</i>	164
3.	NEEDLELESS ELECTROSPINNING OF PCL NANOFIBERS WITH NA-IBU	167
	<i>Morphology of Na-IBU loaded PCL nanofibers</i>	168
4.	CRYSTALLINITY OF PCL AND PCL/PEG NANOFIBERS ELECTROSPUN BY NEEDLELESS ELECTROSPINNING	171
	<i>Impact of PEG-400 and IBU on the crystallinity ratios of PCL nanofibers</i>	175
5.	THERMAL ANALYSIS OF NANOFIBERS ELECTROSPUN BY NEEDLELESS ELECTROSPINNING	176
	<i>Presence of IBU in nanofibers determined by thermal analysis</i>	177
6.	IBU RELEASE KINETICS	180
7.	COMPARISON BETWEEN TWO ELECTROSPINNING TECHNIQUES	183
8.	CONCLUSION	185
	REFERENCES	186

CHAPTER 5: FABRICATION & CHARACTERIZATION OF BILAYER ELECTROSPUN WOUND DRESSING		188
--------------------------------------------------------------------------------------------------	--	------------

CHAPITRE 5: FABRICATION ET CARACTÉRISATION DU PANSEMENT BICOUCHE ÉLECTROFILÉ		
		190
1.	INTRODUCTION	192
2.	PREPARING THE FIRST LAYER WITH GE/HA HYDROGEL	194

3. INCORPORATION OF SODIUM HYALURONATE (HA) INTO PCL NANOFIBERS	194
4. FABRICATION OF BILAYER WOUND DRESSING	196
5. CHARACTERIZATION OF NANOFIBERS AND BILAYER WOUND DRESSING	198
5.1 Morphology of PCL, PCL/PEG nanofibers with HA and IBU	198
5.2 Crystallinity of PCL nanofibers with HA, PEG-400 and IBU.....	204
5.3 Thermal stability of GE/HA film and PCL nanofibers with HA and IBU.....	207
a) Degradation of GE/HA film.....	207
b) Degradation of PCL nanofibers with HA and IBU	208
5.4 Wettability of GE/HA film and nanofibers of bilayer wound dressing	211
5.5 Mechanical strength of GE/HA film.....	212
6. IBU RELEASE KINETICS OF HA/IBU LOADED NANOFIBERS AND BILAYER STRUCTURE	214
7. ANTIBACTERIAL ANALYSIS OF BILAYER WOUND DRESSING.....	216
8. CONCLUSION	219
REFERENCES.....	220
GENERAL CONCLUSION & FUTURE PROSPECTS	224
CONCLUSION ET PERSPECTIVES	226
GENERAL CONCLUSION AND FUTURE PROSPECTS.....	229

General Introduction

Introduction:

Les plaies formées sur la peau humaine sont induits par un traumatisme impliquant une multitude d'événements biochimiques endogènes et de réactions cellulaires du système immunitaire. Par conséquent, la cicatrisation des plaies est un processus complexe de régénération tissulaire que le corps humain subit pour anticiper la zone touchée avec des tissus cellulaires rompus. L'inflammation des plaies est un autre problème qui pourrait transformer une simple blessure en une plaie critique. Il existe une variété de traitements sur le marché permettant la gestion des plaies, tels que des films et des pansements en mousse contenant des agents biologiques pour faciliter la cicatrisation. Cependant, la question se pose de savoir comment faciliter et accélérer le processus de guérison? Les pansements conventionnels servent à protéger la plaie de l'environnement externe pour empêcher l'infection tout en maintenant un environnement humide pour favoriser une récupération rapide. Ces dernières années, d'importants progrès de recherche ont été documentés pour le développement de pansements multifonctionnels efficaces composés de différentes couches ayant des fonctionnalités différentes. Ils sont fabriqués à partir de divers matériaux naturels et synthétiques dans divers formats tels que des non tissés nanofibreux électrofilés, des hydrogels ou une combinaison des deux. Ces pansements sont équipés d'un système d'administration de médicament avec libération prolongée du médicament afin de guérir la douleur et l'inflammation. Les pansements non tissés électrofilés offrent non seulement une bonne couverture, mais sont également perméables à l'air et à l'humidité. Ces nanofibres peuvent être fabriquées en utilisant plusieurs techniques de traitement, telles que la lyophilisation d'une émulsion, l'électropulvérisation et la séparation de phase. Mais la technique d'électrofilage est recommandée pour la fabrication de pansements pour plaies car les nanofibres électrofilées obtenues présentent de grands rapports surface / volume et ont des diamètres allant du nanomètres

à quelques micromètres. De plus, l'électrofilage est une approche facile, rentable et polyvalente pour produire des nanofibres à partir de solutions polymères naturelles et synthétiques.

L'objectif principal de cette recherche était de fabriquer un pansement bicouche polyvalent ayant deux couches distinctes de caractéristiques diverses qui auront des rôles ciblés. La poly (ϵ -caprolactone) (PCL), un polymère synthétique biodégradable et biocompatible a été utilisée pour produire une couche nanofibreuse non tissée par électrofilage. La seconde partie est constituée d'une couche d'hydrogel composée de gélatine (GE) et de hyaluronate de sodium (HA), polymères naturels bien connus pour leurs propriétés de régénération cutanée et de réparation tissulaire. Cette couche d'hydrogel absorbera l'exsudat de la plaie tout en créant une atmosphère hydratée pour faciliter le processus de guérison. Les nanofibres PCL imiteront la matrice extracellulaire (ECM) de la peau, mais elles manquent d'hydrophilie pour la croissance cellulaire. Afin de contrer cette limitation, un biopolymère hydrophile, le polyéthylène glycol (PEG) de masse molaire M_n -400 g / mol a été ajouté aux nanofibres PCL. La solution de PCL a été préparée en utilisant un mélange de chloroforme: éthanol dans un rapport massique de 88:12. La nouveauté de cette recherche a été le choix d'une masse molaire aussi faible de PEG pour le mélange PCL, aucune publication n'ayant à ce jour été rapportée utilisant cette masse molaire de PEG. Ces nanofibres PCL / PEG ont ensuite été chargées avec deux concentrations différentes d'un médicament modèle, l'ibuprofène (IBU) pour développer un système contrôlé d'administration de médicaments. L'IBU est un médicament anti-inflammatoire non stéroïdien largement utilisé pour soigner la douleur et l'inflammation. Cette thèse présente les matières premières, les techniques d'électrofilage, les paramètres de traitement et les techniques de caractérisation qui ont été utilisés pour la fabrication et l'investigation de ce pansement bicouche.

General Introduction

Wounds are trauma induced defects of the human skin involving a multitude of endogenous biochemical events and cellular reactions of the immune system. Hence, wound healing is a complex tissue regeneration process that human body undergoes to anticipate the affected area with ruptured cellular tissues. Inflammation in wounds is another problem that could turn a simple injury into a critical wound. There is a variety of treatments offered in market for wound management such as films and foams dressings containing biological agents to aid healing. However, question arise as how to facilitate and expedite the healing process? Conventional dressings serve to protect the wound from external environment to prevent infection while maintaining a moist environment to promote rapid recovery. In recent years, extensive research progresses were documented for the development of efficient multifunctional wound dressings consisting of different layers with discrete functionalities. They are fabricated out of various natural and synthetic materials in diverse formats such as electrospun nanofibrous mats, hydrogels or combination of both. These wound dressings are equipped with drug delivery system with prolonged release of drug in order to cure pain and inflammation. Electrospun nonwoven wound dressings not only offer good coverage but are also permeable to air and moisture. These nanofibers can be fabricated using several processing techniques, such as emulsion freeze drying, electrospraying and phase separation. But, the electrospinning technique is recommended for the fabrication of wound dressings because the obtained electrospun nanofibers show large surface area to volume ratios and have diameters ranging from nanometers to few micrometers. Additionally, electrospinning is a facile, cost-effective and versatile approach to produce nanofibers from natural and synthetic polymer solutions.

The main objective of this research was, to fabricate a versatile bilayer wound dressing having two distinct composite layers of diverse features that will serve targeted roles. Poly(ϵ -caprolactone) (PCL), a biodegradable and biocompatible synthetic polymer was used to produce a nonwoven nanofibrous layer via electrospinning. The other part consists of a hydrogel layer composed of gelatin (GE) and sodium hyaluronate (HA), natural polymers well-known for their skin regeneration and tissue repair properties. This hydrogel layer will absorb wound exudate while creating a hydrated atmosphere to aid healing process. PCL nanofibers will mimic the extracellular matrix (ECM) of skin but they lack hydrophilicity for cells growth. To encounter this limitation, a hydrophilic biopolymer polyethylene glycol (PEG) of molar mass M_n -400 g/mol was added to PCL nanofibers. PCL solution was prepared by using a solvent mixture of chloroform: ethanol in 88:12 wt/wt ratio. The novelty of this research was the choice of such a low molar mass of PEG for PCL blending for the very first time as no publication has been reported yet using this molar mass of PEG. These PCL/PEG nanofibers were then loaded with two different concentrations of a model drug Ibuprofen (IBU) to develop a self-monitoring drug delivery system. IBU is a non-steroidal anti-inflammatory medicine that is widely used to heal pain and inflammation. This thesis narrates the raw materials, electrospinning techniques, processing parameters and characterization techniques that were employed for the fabrication and investigation of this bilayer wound dressing.

First chapter recounted the history of electrospinning and its basic principle, types of electrospinning and their scope, influence of applied parameters and concept of blend electrospinning. It further reviewed the role of nanofibers in biomedical applications specially as drug delivery systems in wound dressings and cited numerous studies related to this from last one decade. Second chapter described the materials and methods used in this study and provided the specifications and supplier information of all chemicals and equipment. All methods and techniques along with their applied conditions were documented in this section. Third chapter of

single-needle electrospinning reported the preliminary studies regarding the electrospinning of PCL, PCL/PEG and their IBU loaded nanofibers and optimization of electrospinning parameters. The physico-chemical properties of PCL nanofibers such as; morphology, crystallinity, thermal stability, wettability and tensile strength were comprehensively analyzed and described. The drug release kinetics of IBU loaded nanofibers were also studied. Further experiments were carried on by employing a semi-industrial needleless electrospinning technique that used NanoSpider equipment by [®]Elmarco company. Fourth chapter reported the production of PCL and PCL/PEG nanofibers alone and with IBU from this needleless technology and characterization of these nanofibers including their drug release analysis. A comparison between these two electrospinning techniques with respect to their nanofibers production process and nanofibers characteristics was presented at the end. Last chapter of this thesis documented the fabrication of a bilayer wound dressing step by step. It emphasized on the importance of use of gelatin (GE) and sodium salt of hyaluronic acid (HA) as hydrogel by providing references from literature. Results obtained from characterization of IBU/HA loaded PCL and PCL/PEG nanofibers and of bilayer scaffold were explained in this section. Biological aspects of this bilayer wound dressing were analyzed such as, drug release kinetics and antibacterial assay and their findings were stated in this last segment.

Chapter 1: Literature Review

Chapitre 1: Bibliographie

Ce chapitre présente l'histoire du processus d'électrofilage, son principe de base, les différents types d'électrofilage existants et leur portée, l'influence des paramètres appliqués et le concept d'électrofilage par mélange. Deux techniques majeures sont décrites: l'électrofilage à une seule aiguille et l'électrofilage sans aiguille. L'influence des paramètres appliqués sur les caractéristiques des nanofibres sont présentés. Le principe de base de l'électrofilage d'une solution de polymère est sa capacité à transporter une charge électrique. La viscosité de la solution doit également être suffisante pour permettre au polymère d'être étiré sans former de gouttelettes. Un appareil d'électrofilage à une aiguille se compose d'une seringue remplie de solution polymère connectée à une aiguille en acier inoxydable et comporte un tube capillaire, une alimentation haute tension pour maintenir le potentiel électrique requis pour étirer le jet de solution et une plaque collectrice mise à la terre sur laquelle les nanofibres sont déposées. Les nanofibres sont produites lorsque les gouttelettes de solution de polymère sont étirées sous l'influence de fortes forces électriques et sont entraînées vers le collecteur mis à la terre où elles sont finalement déposées. L'approche sans aiguille utilise quant à elle des électrodes en fil métallique à la place d'une aiguille. Ce chapitre explique le principe de fonctionnement de cette technologie sans aiguille ainsi que ses avantages. L'impact de divers paramètres du processus (tension appliquée, distance aiguille-collecteur et vitesse d'alimentation) sur la morphologie des nanofibres est également discuté. Une revue de la littérature concernant l'utilisation de polymères naturels et synthétiques pour la production de nanofibres est présentée. Dans le cadre de la thèse, la poly (ϵ -caprolactone) (PCL) a été sélectionnée comme polymère principal mélangé avec du poly (éthylène glycol) (PEG) tandis que l'ibuprofène (IBU) a été sélectionné comme médicament modèle. Un bref historique rapportant l'utilisation de PCL et de PEG pour la production de nanofibres vient donc conclure cette partie bibliographique. De nombreuses publications faisant référence à l'incorporation de divers

médicaments dans des nanofibres sont également citées, y compris celles faisant référence à l'utilisation d'IBU dans des nanofibres PCL. Les applications biomédicales des nanofibres sont dans un dernier temps décrites, en particulier les systèmes d'administration de médicaments dans les pansements pour plaies. Le processus de cicatrisation des plaies et ses défis sont ainsi abordés et les caractéristiques de base d'un pansement idéal ont été expliquées. Ce chapitre a non seulement présenté une vue historique des pansements électrofilés, mais a également lié ce contexte aux principaux objectifs de ce travail de recherche. En bref, cette section est une projection bibliographique de ce sujet de recherche particulier et aussi une brève introduction de ses objectifs.

CHAPTER 1

LITERATURE REVIEW

1. Electrospinning history and its basic principles

The technique to produce synthetic fibers with the aid of electrostatic forces was utilized a hundred years ago. This process is named as “electrospinning” that was first derived from term “electrostatic spinning” that too evolved from the electrospraying method. The first attempt was made by Rayleigh [1] in 1897, which was followed by Morton [2] and Cooley [3], who patented the method to disperse fluids using electrostatic forces. Later on, in 1914, Zeleny [4] reported the behavior of conductive fluid droplets at the end of metallic tubes in the presence of electrical field. Subsequently, efforts were made by Formhals [5], for the development of textile yarns and explained in a series of patents from 1934 to 1944. After this study, the focus shifted to explore the electrospinning process in its length and breadth.

In 1969, Taylor [6] elaborated the electrospinning by means of mathematical modeling of the conical shape formed by the fluid droplets at the tip of the needle under the influence of electric field. This cone has since been known as the “Taylor cone”, schematic diagram of which is shown in Figure 1.1. Several years later, the first research of electrospinning of melt polymers was carried out by Larrondo and Manley [7]. The method was not well established until early 1990’s when researchers started to acknowledge the vast potential of this technique for nanofibers production [8].

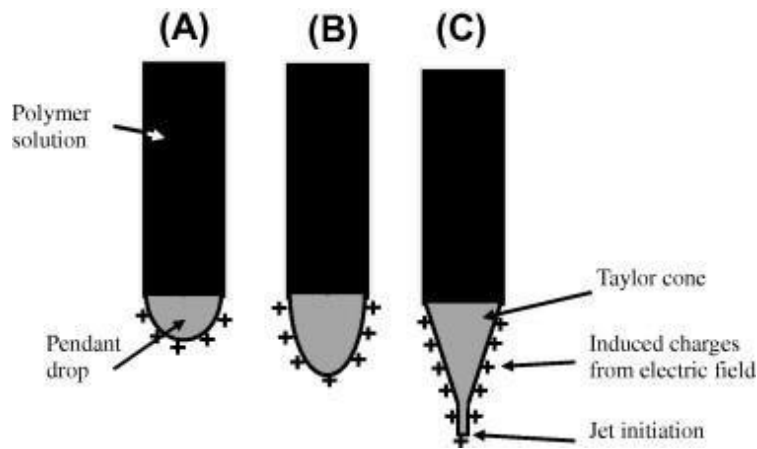


Figure 1.1. Schematic illustration of “Taylor Cone” initiation under increasing voltage from A to C

The basic principle of electrospinning of a polymer solution is its ability to carry an electric charge and have sufficient viscosity to be stretched without breaking up into droplets. A typical framework of electrospinning is illustrated in Figure 1.2. There are three main components that are predominantly utilized in this process. A syringe filled with polymer solution connected to a stainless steel needle with a capillary tube, a high voltage power supply to maintain a required electric potential for stretching the solution jet and a grounded collector plate on which the nanofibers are deposited. Initially, polymer solution is introduced into a capillary tube with a needle attached to its end. Then, a high voltage (between 10 to 30kV) is applied between droplets of polymer solution at the needle tip and a grounded collector. As the electric potential increases, the pendant droplet of polymer solution becomes highly electrified, thus inducing electric charge on the solution surface. This results in the stretching of polymer solution droplet into a conical shape, known as Taylor cone. When this electric potential reaches a critical value, the electrostatic repulsive forces overcome the surface tension of solution, hence a charged jet of polymer solution is ejected. This polymer jet ejected from the Taylor cone travels towards the grounded collector plate. On the way to the collector plate, this jet is stretched under electric field which results in

realignment of polymer chains and production of micro and nanofibers and solvent evaporation [1, 9].

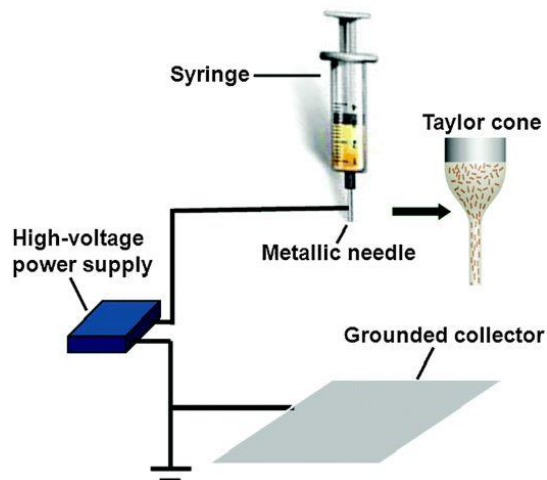


Figure 1.2. Typical needle electrospinning set-up

A typical electrospinning process yields long continuous fibers that can vary in diameters along their lengths and generally exhibit a solid interior with smooth surface. However, recent developments show that different nanofibers with specific shapes and structures like core/shell, porous, hollow, necklace-like, flat ribbon and multichannel tubular surfaces can also be prepared [10-15] as shown below in Figure 1.3. The morphology of the nanofibers can be different depending upon the type of polymer used, solvents and electrospinning conditions [1, 16, 17].

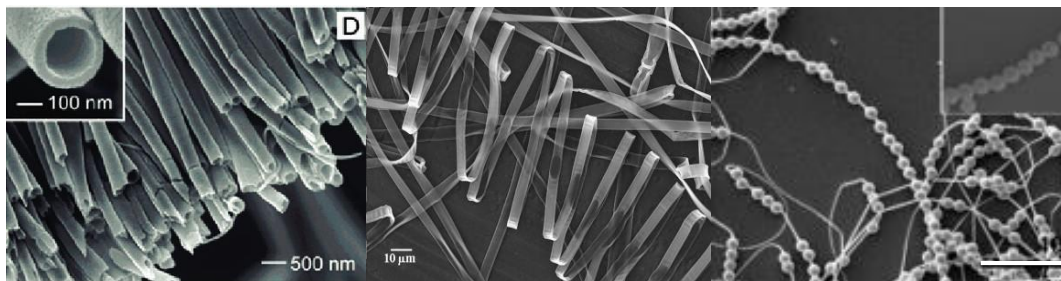


Figure 1.3. Core shell, flat/ribbon like and necklace shape nanofibers

2. Types of electrospinning and their scope

Hundreds of publications on electrospinning have paved the path for ever growing advancements in this technique. Various new dimensions are introduced such as, bioengineering, environmental protection, bio-sensors and smart electronics [18] [19] [20]. The ease of producing nanostructures from different kinds of raw materials, from natural to synthetic polymers to high tech composites consisting of organic and inorganic particles has attracted scientists around the globe. The research, in nanofibrous materials as biomedical composites and scaffolds, has seen humongous growth and expanded in last two decades. The scale of research interest in this field can be estimated by reviewing the number of published articles over a certain period of time as shown in Figure 1.4 [21].

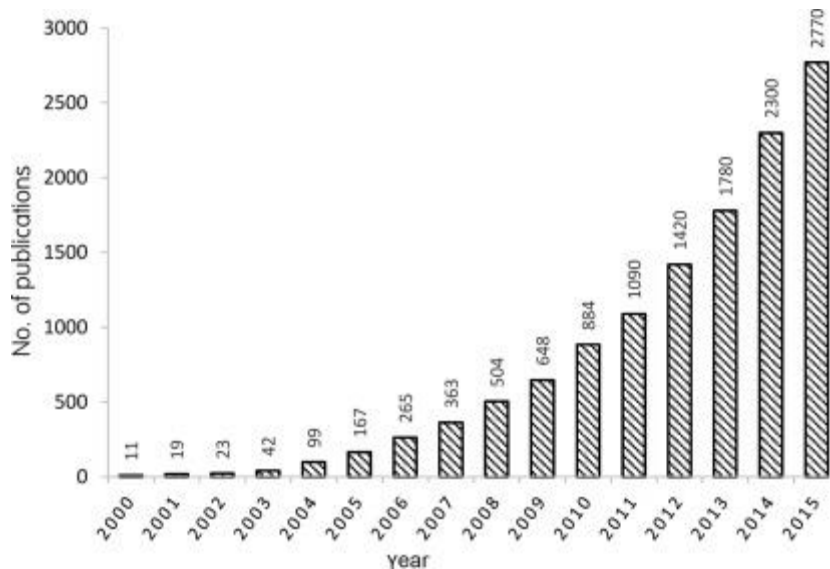


Figure 1.4. A bar chart elaborating the number of publications about electrospun nanofibrous scaffolds and nanocomposites for biomedical applications [21].

Electrospun scaffolds can be tailored according to their end applications. These hybrid nanofibers scaffolds facilitate environment for cell growth, adhesion and proliferation [22]. Besides, biomedical application, electrospun nanofibers have found their significant use for environment

protection as benign affinity membranes, both for air and water filtration purposes [23]. Also, these fine nanofibers can also be utilized to manufacture ultra-sensitive high-surface-area, chemical and biological nanosensors with enhanced sensibility for various hazardous substances like; nitro compounds, mercury, ferric ions and chromium ions in comparison to conventional dense membranes [24]. In addition to these chemical and biological sensors, polymeric optical sensors with high sensibility have been developed using electrospun nanofibers produced from fluorescent polymers [25].

Lately, electrospinning is garnering growing attention in the scientific community, as well as in industry due to its broad range of applications. So, advancements have been made to improve the production rate of nanofibers. For instance, after single-needle electrospinning, a modern and more efficient technique, needleless electrospinning was also introduced few years back. Needleless electrospinning was developed for higher productivity by producing hundreds of nanofibers simultaneously from a polymer solution carried by suitable support, i.e. metallic wire or a rotating drum. This technique is considered very encouraging for bulk production of nanofibers [26-28].

2.1 Single-needle electrospinning

This type of electrospinning has two standard setups, vertical and horizontal. Either setup consists of typically three main components: a syringe (with polymer solution attached to a needle at the end) with a feeding pump, a grounded collector plate and a high voltage power source. Polymer solution is pumped through the syringe at a constant feed rate forming a droplet at the tip of the needle. A high voltage source (between 10 to 30kV) maintains a potential difference between the polymer solution and the collector surface. the induced electric field overcomes the surface tension of the droplet and elongates to form a Taylor cone. Once the electric field reaches the critical value, a charged jet of polymer solution starts ejecting from the tip of the cone. This jet is accelerated

towards the collector plate while stretching the polymer chains on its way. Finally, it gets deposited in the form of nanofibers on the collector surface and this phenomenon continues. Solvent evaporation occurs during this stretching and whipping process of polymer solution jet caused by electrostatic repulsions. Different types of collectors, stationary or rotating, with varying shapes may be used to produce various kinds of nanofibers' structures as shown in the Figure 1.5 [29, 30].

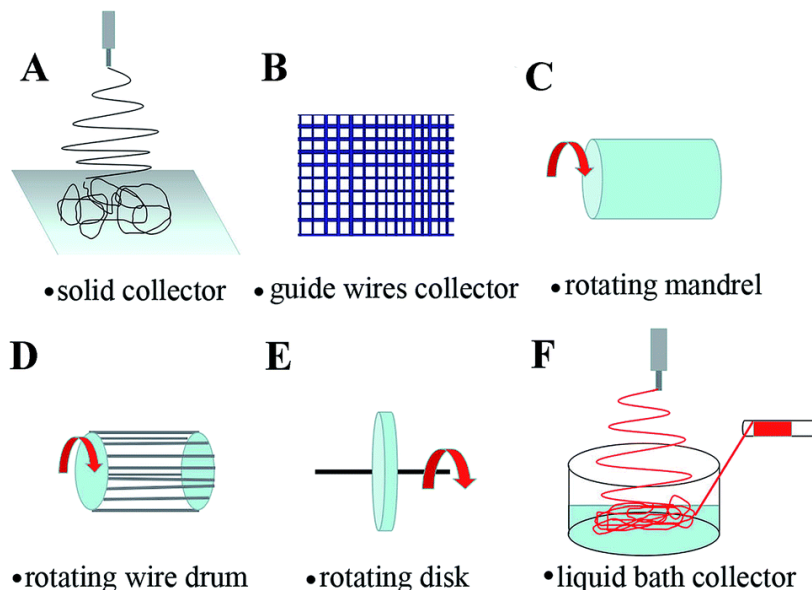


Figure 1.5. Different types of collectors for nanofibers

2.2 Needleless electrospinning

In recent years, needleless electrospinning emerged as an alternative electrospinning technology with the purpose of producing nanofibers on a large scale from a compact space. Needleless electrospinning is featured as electrospinning of nanofibers directly from an electrode dipped in open polymer solution. Numerous jets are formed simultaneously from the needleless electrode without the influence of capillary effect that is normally associated with needle technique. Since the jet initiation in needleless electrospinning is a self-organized process which happens on a free liquid surface, the spinning process is hard to control [27]. This method introduces the formation

of numerous polymer jets along the length of electrode from a free liquid surface. This novel technique was patented by Jirsak *et al.*, [31]. The needleless equipment, called NanoSpider was later developed by the [®]Elmarco company (Liberec, Czech Republic) as shown in Figure 1.6. This NanoSpider equipment has a production rate of ~100 g/h per meter [28]. The main advantage of this technology is that the jets are initiated naturally in the optimal positions.

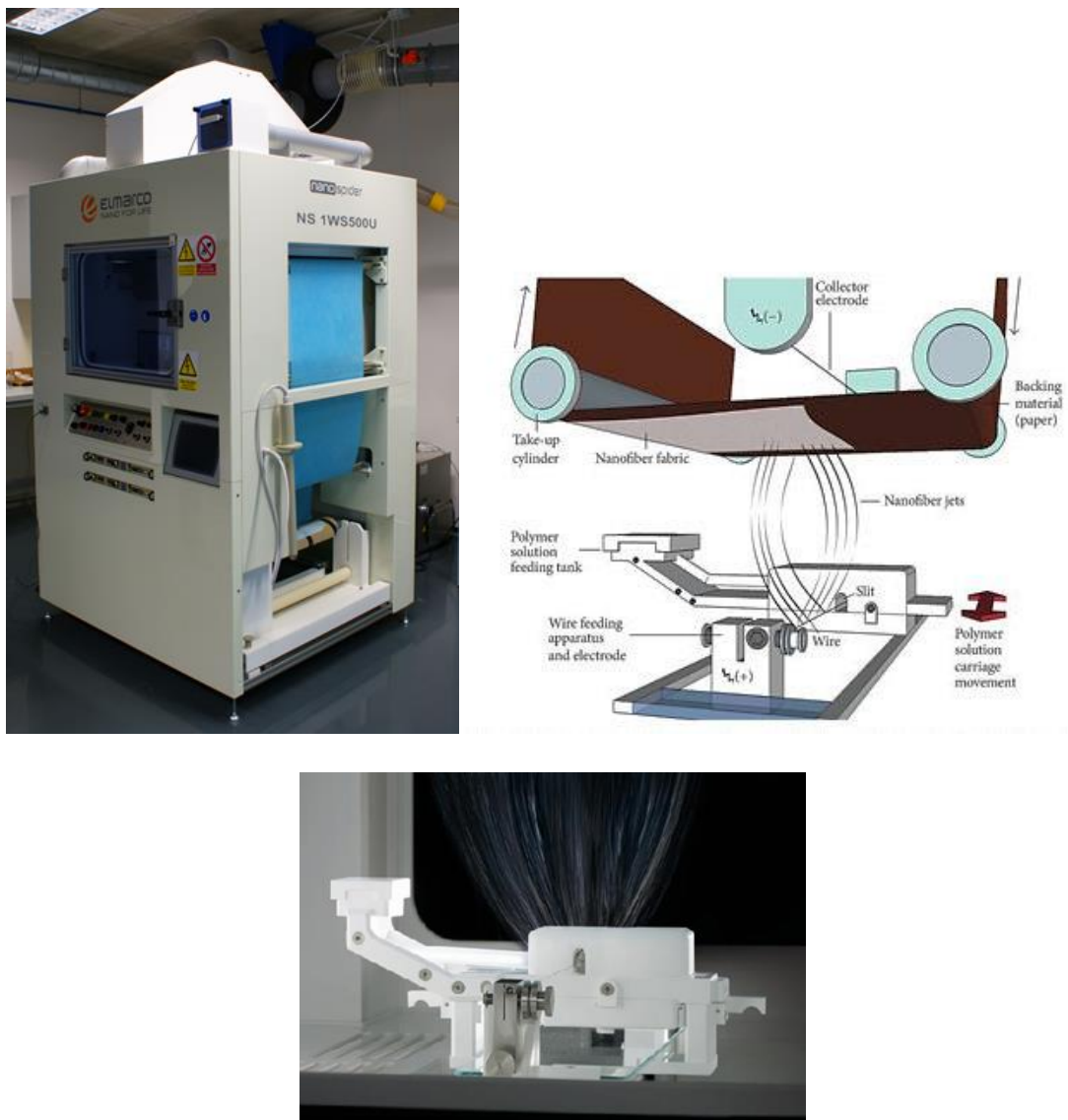


Figure 1.6. NanoSpider by ElMarco company (model 1WS500U) lab scale unit, schematic diagram of needleless electrospinning with wire electrode and image of multi-fiber jet initiating from that wire electrode.

The jet formation in needleless electrospinning has been proposed to follow four steps: (1) a thin layer of polymer solution is formed on the spinneret surface as a result of its partial immersion in the solution and rotation; (2) the rotation also causes perturbations on the solution layer thus inducing the formation of conical spikes on the solution surface; (3) when a high voltage is applied, the spikes concentrate electric forces thus intensifying the perturbations to form several initiating points; (4) polymer jets are stretched out from these initiating points and finally result in nanofibers with diameters in a range of 50-900nm [27]. These jets are distributed over the electrode surface with certain periodicity. This is one of the main advantages of needleless electrospinning, the number and location of jets is set up naturally in their optimal positions. In the case of multi-needle spinning heads, the jet distribution is made artificially. The mismatch between the 'natural' jet distribution and the real mechanical structure leads to instabilities in the process, and to the production of nanofiber layers which are not homogenous [28]. NanoSpider has shown the capability of producing nanofibers from both polymer solutions and polymer melts. Several types of rotating and stationary electrodes for free liquid surface electrospinning have been developed.

3. Electrospinning parameters and their impact on nanofiber properties

The characteristics of electrospun nanofibers depend on a number of parameters. These parameters are commonly divided into three categories: solution parameters (such as solution concentration and/or viscosity, solution surface tension, and solution conductivity), process parameters (such as feed rate, applied voltage, and tip to collector distance), and ambient conditions (like ambient temperature and humidity) [32, 33]. The following will discuss the influential parameters on morphology and diameter of fibers in the process of electrospinning.

3.1 Polymer concentration and viscosity

Solution concentration is one of those key parameters that determine the diameter of nanofibers. Fiber diameter is directly dependent on the solution concentration, if one increases the other too and vice versa. It has been found out that the polymer concentration affects the formation of beads. Fong *et al* [34] have reported that a higher polymer concentration resulted in fewer beads. However, if the concentration is increased to a greater extent, then beads or entanglements are the outcome of the electrospinning instead of continuous fibers. On the other hand, if concentration is less than a critical value, no fiber formation occurs and only droplets of polymer solution will be seen. So, it is very important to select the right concentration in order to produce homogeneous nanofibers with a definite morphology and diameter.

The solution viscosity has been strongly related to the concentration of the solution. An increase in solution viscosity or concentration gives rise to a large and more uniform nanofibers diameter. In electrospinning, the viscosity of a solution plays an important role in determining the range of concentrations from which continuous nanofibers can be obtained. For the solution of low viscosities, surface tension is the dominant factor and just beads or beaded nanofibers are formed while above critical concentration, a continuous nanofibers structure is obtained and its morphology is affected by the concentration of the solution [1, 35, 36].

3.2 Feed rate

Solution feed rate is another crucial factor that controls the diameter and morphology of nanofibers during electrospinning process. As the feed rate of polymer solution increase, the charge density will decrease. A high charge density may lead to the electrospinning jet undergoing secondary bending instabilities, which contributes to the formation of fibers having small diameters. So, with an increase in feed rate, there is a corresponding increase in diameter of the nanofibers. It is worth

noting that nanofibers with beads are formed when the feed rate of solution is too high due to not providing enough time for solvent evaporation [37-39].

3.3 Needle to collector distance

Both the diameters and the morphology of the nanofibers can be controlled by the distance between the tip and the collector, although the effect is not as notable as the other previously mentioned parameters [40]. A minimum distance that enables enough time for solvent evaporation before the fibers reach the collector is required in the process of electrospinning. Longer distance has yielded thinner fibers [41], and beads were observed when the needle to collector distance was either too far or too close [1].

3.4 Applied voltage

Deitzel *et al* [17] studied the impact of applied voltage on the morphology of PEO nanofibers and found that as the voltage increased, the resulting nanofibers with rough morphology are obtained. The applied voltage to the polymer solution is the most important parameter. This is because fiber formation only occurs when the applied voltage surpasses the threshold voltage (about $\sim 1\text{KV/cm}$, dependent on the solution). In most cases, applied voltage affects fiber diameter, but the level of significance varies with other parameters such as the polymer solution concentration and the distance between the tip and the collector [42].

As previously discussed, an increase in the applied voltage increases the electrostatic forces on the solution, which favors the stretching of the jet, ultimately leading to reduction in the fiber diameter. It has been found that changing the applied voltage will change the shape of the initial drop thereby bringing a change in the structure and morphology of the nanofibers [43].

3.5 Ambient environment

Apart from the solution and processing parameters, there are also ambient parameters that include humidity, temperature etc. Studies have been conducted to examine the effects of ambient parameters (i.e. temperature and humidity) on the electrospinning process [32, 33]. Both factors are related to the physical and chemical properties of employed polymer and solvent for electrospinning. For instance, hydrophilic or hydrophobic polymers would have different ambient humidity and temperature values for electrospinning. Similarly, some polymers are temperature sensitive, so their ability to form nanofibers will directly depend upon these two factors. For instance, the effect of temperature, on polyamide-6 nanofibers has been investigated from 25°C to 60°C and it has been established that with an increase in temperature, there is a yield of nanofibers with decreased diameters, and they attributed this decline in diameter to the decrease in the viscosity of the polymer solution at increased temperature [44].

Also, the effect of humidity on the formation of polystyrene nanofibers has been studied by Casper *et al* [45]. They established that the variation in humidity while spinning polystyrene solutions has shown that, by increasing humidity there is an appearance of small circular pores on the surface of nanofibers; a further increase in humidity leads to the pore coalescence. At very low humidity, volatile solvent dries rapidly since the evaporation of the solvent is faster.

4. Biomaterials for wound dressings

Fibers derived from electrospinning have gained popularity in the field of drug delivery and because of the flexibility of the method, it is considered as an ideal dressing material for wounds that can deliver various biological agents to local tissues at the wound site [46-48]. Not only they physically protect the wound, but also have the ability to carry large amount of drugs (up to 40% loading) and their release efficiency can be controlled by the type and composition of fibrous

material [49]. Various materials are available for the production of electrospun fibers to be used as medical fabrics for wound dressing [46], and these materials can be divided into natural and synthetic polymers [47, 50]. Hydrophilic polymers are also suitable for containing small molecules, proteins, peptides and gene carriers. The fast release rate of the hydrophilic system limits its long-term functionality. Whereas, the use of hydrophobic polymers is ideal for controlled release. However, this method requires the use of harmful organic solvents, which can affect the stability of the biological agent and reduce its pharmacological efficacy. This section summarizes, the polymers most commonly used in the electrospinning process of wound dressings.

4.1 Natural polymers

Natural polymers have many advantages, including considerable abundance and ease of use, and in most cases are biocompatible, biodegradable and non-toxic [51]. In addition, their structural resemblance to human skin's extracellular matrix (ECM) can promote and stimulate the wound healing process. Others have demonstrated the benefits of using natural polymers to repair damaged tissue and thus promote skin regeneration [52]. However, due to the molecular structure of natural polymers, their ability to be electrospun alone is compromised. This problem can be solved by introducing a synthetic polymer as a support coupled with a natural polymer. For example, chitosan is a naturally occurring polysaccharide that is popular as a wound dressing material since it is hemostatic, antibacterial, non-toxic/biocompatible and biodegradable and can retain drug delivery to promote wound healing [53, 54]. Chitosan is insoluble in water, so organic solvents are used for its electrospinning. In addition, when dissolved in organic solvents, it shows a high viscosity at low concentrations, which makes electrospinning very difficult. Pakravan *et al.* demonstrated how to solve this problem by blending chitosan and polyethylene oxide (PEO) to prepare solutions with different ratios [55]. Pairing of these two polymers improved

electrospinnability due to strong hydrogen bonds between chitosan and PEO chains. Other popular natural polymers commonly used for blend electrospinning for wound healing applications are alginate [56], gelatin [57, 58], cellulose [59], collagen [60, 61], hyaluronic acid [62-64], Keratin [65], silk fibroin [66] and zein [67].

4.2 Synthetic polymers and their blending

Biodegradable and biocompatible synthetic polymers are widely used for electrospinning for wound healing applications. They can be mixed with other synthetic or natural polymers to provide a sustained release of the drug [68, 69]. These polymers can be separated into water-soluble and insoluble polymers. This property has a major influence on the ability of the polymer to degrade over time, thereby determining the drug delivery mechanism.

Poly(ϵ -caprolactone) (PCL) is an aliphatic polyester that is very popular in the field of biomedical research due to its easy processing. The basic chemical structure of PCL is shown in Figure 1.7. In addition, it is non-toxic, biodegradable, biocompatible, compatible with many drugs and is easily available, these attributes make it an excellent candidate for long-term drug delivery carrier [70]. PCL is very hydrophobic and degrades over several months, so its life can be prolonged by mixing with hydrophilic polymers.

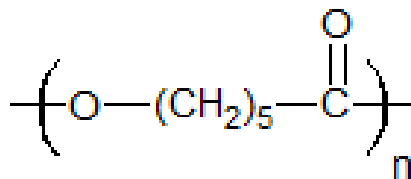


Figure 1.7. Chemical structure of Poly(ϵ -caprolactone)

Ponjavic *et al.* demonstrated the mixing of water-soluble PEG with PCL and showed that the surface properties have been greatly improved due to the hydrophilic nature of PEG [71]. Studies have also been performed to determine the effect of hydrophilic drugs on nanofibers formation and PCL fibers release profiles. Luong-Van *et al.*[72], in their results showed that increasing the amount of hydrophilic heparin leads to a reduction in nanofibers diameter and sustained release behavior for up to 14 days. Like PCL, PLGA is another biodegradable and biocompatible synthetic polyester. Its strong mechanical properties make it an ideal choice for drug delivery. PLGA and PCL show prolonged degradation time with $t_{1/2}$ of PLGA = 30 days and $t_{1/2}$ of PCL > 18 months [73-75]. Ranjbar-Mohammadi *et al.*, studied the potential of tailoring the hydrophilic tetracycline hydrochloride from blend and core-shell fibers using PLGA and xanthan gum [76]. The results showed that the blended fibers had higher cumulative release and initial burst of tetracycline hydrochloride than pure PLGA fibers within 75 days, while the core-shell structure showed a medium cumulative release curve between the blended fibers and the pure PLGA fibers.

Unlike water-insoluble polymers, the hydrophilic PEG ensures a faster degradation than hydrophobic polymers. Kim *et al.* explained the ability to modulate the release phenomenon of protein lysozyme by blending hydrophobic polymers (PCL, PLLA and PLGA) with hydrophilic PEG [77]. In vitro drug release elaborated that the PCL/PEG mixture received the smallest burst and the prolonged release profile. Polyethylene glycol (PEG) is a hydrophilic polymer investigated for drug delivery using blends with hydrophobic counterparts. Research suggests that PEG can help with the healing process of wounds. Bui *et al.* investigated the effect of curcumin-loaded PCL/PEG nanofibers on the rate of wound closure in rats. They found that the curcumin loaded blended fibers achieved a 99% wound closure as compared to 90% with just curcumin loaded PCL fibers in 10 days [78]. By controlling the hydrophobicity of these synthetic polymers, blends of polymer fibers are ideal for controlled drug delivery in wound healing applications [78-81].

5. PCL electrospinning

In past two decades, PCL and other biocompatible polymers have been studied extensively for their use in biomedical applications such as controlled drug delivery systems in wound dressings and tissue engineering scaffolds [82-84]. PCL is an aliphatic linear polyester with a glass transition temperature of -62°C and melting point around 60°C depending on the degree of crystallinity, which in turn is dictated by the molar mass of PCL and also by the electrospinning process of nanofibers [85-87]. Main advantages of using PCL are; it is a biocompatible, biodegradable and cost efficient synthetic polymer [88]. Its hydrophobic semi-crystalline nature is the reason behind its slow degradation rate which normally ranges from 2-4 years depending upon its molar mass and it also exhibits good mechanical properties [87]. Furthermore, it is an FDA (Food and Drug Administration) approved material [86], to be used clinically for the controlled drug release and as a suture material since 1980 (i.e. [®]Capronor, [®]SynBiosys, [®]Monocryl suture).

In comparison to other linear aliphatic polyesters like polyglycolic acid (PGA), polylactic acid (PLA) and their other copolymers, PCL has few unique attributes regarding its physical properties that hold the interest of researchers. Firstly, PCL monomers are arranged in a different manner than that of PLA which has three different forms: PDLA, PLLA and combinations to form PDLLA. So, their biological degradation and melting temperatures are distinct correspondingly. Whereas, the melting point of PCL is considerably lower than PLA, PGA and all of their variant combinations. This could be due to the greater polarity and tendency of hydrogen bonding of PGA and PLA compared to PCL. Secondly, PCL has some rheological and viscoelastic properties which allow its fabrication into various kinds of structures such as nanofibers mats, scaffolds and nanocomposites. This ease of fabricating a polymer into different end products using various techniques, is an extraordinary aspect that should not be undermined. PCL and its derivatives have

demonstrated this utility by being successfully processed by electrospinning [80], gravity spinning [89], phase separation, solid freeform fabrication [90, 91] and microparticles [92, 93] due to its low melting temperature and eminent blending compatibility.

PCL nanofibers were produced by many scientists for various applications in recent years, a summary of which will be described in this section. Electrospinning parameters and their effect on the nanofibers properties have been widely studied over the time. Beachley *et al.* [16] studied the effect of various electrospinning parameters on the length and diameter of PCL nanofibers. It was found that PCL concentration, applied voltage and collector plate size greatly affected the nanofibers morphology and collected the nanofibers with average diameters ranging from 350 nm to 1 μ m. Similarly, nanofibrous composites of PCL and nanohydroxyapatite (nHA) were prepared by Doustangi [94] and effect of electrospinning parameters on mean fiber diameter was investigated. Mean fiber diameter was in range of 300-650nm, which increased by decreasing needle to collector distance and feed rate of polymer solution. Applied voltage and polymer concentration were found directly proportional to the mean fiber diameter. Konstantinos *et al.* [95] reported the electrospinning of PCL nanofibers by using a binary solvent system 90% v/v chloroform/dimethyl sulfoxide. They analyzed the impact of process parameters on the fibers morphology and porosity. Average fibers diameter obtained was in range of 1.6-3.3 μ m and it was proven that applied voltage was the key parameter which impact the fibers diameter and surface morphology.

Solvent selection is one of the key factors which governs the electrospinnability and morphological attributes of nanofibers. In this regard, a study was performed by Qin *et al.* [96] about the effect of different solvents of PCL on the properties of nanofibers such as mean diameter, solution viscosity and shearing strength. Thermal properties of PCL nanofibers, the glass transition and melting temperature were compared depending upon the solvent used. Another research by

Bosworth *et al.* [97] documented the use of less toxic solvent, acetone as an alternative to hazardous solvents for PCL. It was also concluded that nanofibers with beads were yielded with lower polymer concentration. Whereas, the higher polymer concentrations produced bead-free nanofibers but with larger diameters. Recently, Zhang *et al.* [98] published an effort towards the use of benign solvents for PCL electrospinning and studied a combination of glacial acetic acid and water. Using PCL concentrations from 17wt% to 20wt%, ultrafine nanofibers with diameters ranging from 180-200nm were obtained.

Among all other properties of electrospun nanofibers, crystallinity ratio stands out as the crucial element when it comes to describe their degradation rate, wettability and mechanical resilience. In recent times, various scholars invested their efforts to determine the crystallinity ratio of PCL nanofibers and several other characteristics that are directly or indirectly linked to it. For instance, Wang *et al.* [99] studied the crystalline morphology of PCL nanofibers which showed a diameter range of 300-500nm. They reported that the crystallinity of aligned nanofibers was higher than their randomly aligned counterparts. Also, the crystallites were in nanofibers were highly arranged along their axis, likewise their molecular chains. Average size of a crystallite suggested that each nanofiber was comprised of dozens of nanofibrils and these nanofibrils were further composed of crystallites along the axis of nanofibers with amorphous regions of extended PCL molecular chains between the neighboring crystallites. Kostakova *et al.* [100] also performed a study about the crystallinity of electrospun and centrifugal spun nanofibrous materials. They documented the fact that crystallinity of PCL greatly affects the rate of degradation that is an important feature for biodegradable materials to be used in medical applications. Results of DSC analysis showed that there was no significant difference in crystallinity ratio of nanofibers produced by electrospinning or centrifugally spun nanofibers. However, molar mass of PCL showed great influence on

crystallinity, also mean diameter of nanofibers had no connection to the degree of crystallinity in nanofibers.

Another attempt of electrospinning PCL was made by Ferreira *et al.* [101] to produce nonwoven fibers mats by using glacial acetic acid as solvent. Various concentrations of PCL were tried and it was observed that only 20wt% and 23wt% of PCL concentrations produced high quality nanofibers, rest yielded beaded, irregular and fused fibers. These nonwoven mats were highly porous, showed good mechanical properties and nanofibers were semi-crystalline in nature. Cell proliferation assay proved that these mats could be used as scaffolds for tissue engineering applications. Sultana *et al.* [70] presented a research which narrates the synthesis of two distinct nanofiber mats: poly(ϵ -caprolactone)-poly(ethylene glycol methyl ether) and other with poly(ϵ -caprolactone)-chitosan. These mats were characterized for their nanofiber diameters, porosity, wettability and mechanical strength. *In vivo* cell viability and metabolic activity assay proved that these nanofibrous mats could serve as a potential vascular tissue-engineering material.

6. PCL/PEG blend electrospinning

PCL has many advantages such as prolonged degradation, good mechanical strength, low cost and ease of availability. However, the hydrophobicity and stiffness of PCL may limit its biomedical applications such as in wound dressings, where hydrophilicity is needed to absorb wound exudate and flexibility is required to be compatible with the skin [102, 103]. Whereas, polyethylene glycol (PEG) is a water soluble polyether available in wide range of molar masses and is biocompatible and bioresorbable. PEG is used in hydrogels and also for surface modification of other polymers to obtain co-polymers, with enhanced wettability and flexibility and it also supports cell growth and attachment. Therefore, a blend of PCL and PEG could lead to product with improved features, suitable to be used in drug delivery and wound healing applications [104, 105]. In literature,

blending of PEG with PCL has been reported to achieve diverse objectives. Repanas *et al.* [79] blended PCL with PEG (Mn 3500-4500 g/mol) to electrospin nanofibers scaffolds to test their suitability for the drug delivery system. Dipyridamole (DPA), which is an anti-thrombotic and anti-proliferative pharmaceutical agent was employed as a model drug. Two different chain lengths of PEG were used to investigate the morphological, mechanical and physiochemical properties of obtained nanofibers with and without DPA, and release kinetics of DPA were also studied. Bui *et al.* [78] explained the development of PCL/PEG nanofibers mats loaded with Curcumin (Cur), for prevention of infections and wound healing purpose. Biological testing of prepared mats was done such as: cell viability, cell attachment, anti-inflammatory, anti-bacterial activity and *in vivo* wound healing capability was examined. The surface morphology of PCL nanofibers was changed after blending with PEG as numerous pores were observed on the surface of nanofibers. SEM images showed cell growth and proliferation due to the presence of PEG. It was proved that PEG and Cur facilitated the rapid wound healing and cell growth in the PCL nanofibers matrix. Chen *et al.* [81] prepared PCL-PEG nanofibrous membranes to prevent peritendinous adhesion. Three PEG percentages were blended with PCL and were characterized for their mechanical and physiochemical behavior. *In vitro* cell adhesion and migration study with fibroblasts were showed that all membranes prevented cell penetration. Tiwari *et al.* [106] demonstrated how it is possible to tailor the properties of PCL electrospun nanofibers by introducing PEG. Heterogeneous PCL/PEG nanofibers were achieved as backbone of the structure along with ultrathin nano-nets interlacing the thicker fibers. SEM studies showed a bimodal structure of nanofibers with mean diameters ranging from 300-600nm, whereas pure PCL nanofibers were in a range of 600-800nm. A clear decrease in mean diameter was noticed in the presence of PEG. Moreover, results showed that PCL/PEG blended scaffolds displayed enhanced wettability, biocompatibility, mechanical stability and mineralization characteristics as compared to the pure PCL nanofibers.

7. Incorporation of drugs and nanoparticles into PCL nanofibers

7.1 Incorporation of drugs

The first study of using electrospun nanofibers as a drug delivery medium was reported back in 2002 by Kenawy [107]. Since then, numerous studies have been dedicated to document the use of electrospun nanofibers in drug delivery systems and wound healing procedures [108]. Due to their unique features like ease of drug loading during electrospinning, fine diameters but large surface area, highly interlinked structure and capability of surface modification, electrospun nanofibers had been the center of interest in biomedical research.

In modern pharmaceutical approaches, hydrophobic drugs present a common limitation of poor water-solubility and lack of targeted delivery to the affected site. Their dosage and application must be monitored to specific populations, especially in children and elder patients. Along with poor solubility, several technological issues are also associated like selection of right dosage and delivery method. In past year, nanofibers evolved as a rising and promising materials for targeted delivery of both hydrophobic and hydrophilic drugs in a number of biomedical applications. Controlled or burst release of a certain drug could also be achieved, by the right choice of electrospinning polymer and mode of drug loading. A model drug could either be loaded directly into the polymer solution that will eventually become the part of polymer matrix in nanofibers or, could be deposited on the surface of nanofibers.

Any type of polymer; synthetic, natural, biodegradable or non-biodegradable can be employed to tailor the drug release rate via diffusion or by combining diffusion and fiber degradation. Good selection of polymer will ensure the best recipe of mechanical and physiochemical attributes of resulting nanofibers [109]. In addition to the salient features of nanofibers like; very fine diameters,

high surface-to-volume ratio, porosity and diversity in surface morphology, the drug delivery rate could be tuned according to a special situation and application by altering the fiber composition, processing parameters and production technology [110]. Several researchers have studied all these factors in detail over the period of time in recent decades, a relevant summary of which is discussed in this section.

Low dissolution rate and poor solubility of IBU in water, limits its delivery to certain organs and its bioavailability. Masoumi *et al.* [111] attempted to improve the aqueous dissolution of IBU by preparing supramolecular nanocontainers of IBU/cyclodextrin via inclusion complex. The encapsulation of IBU in cyclodextrin cavity enhanced its solubility, *in vitro* dissolution rate and controlled the IBU release for long-term delivery. Likewise, Kocbeck *et al.* [112] published a study of PCL electrospinning loaded with two different model drugs, IBU and carvedilol and also PCL films with these two drugs were casted for comparison. It was noticed that addition of these drugs reduced the crystallinity of nanofibers, whereas, an increase in diameters was observed. The incorporation of the drugs in electrospun nanofibers visibly improved their dissolution rate. IBU showed a burst release and all the amount of incorporated drug was released during first 4h of analysis but carvedilol rather showed a controlled release during the same period of time. Hang Liu *et al.* [113] electrospun the PCL nanofibers containing ampicillin sodium salt and twisted them into yarns for their potential use as surgical sutures. These nanofibrous yarns, loaded with drug, were investigated for their diameters, crystallinity, *in vitro* drug release and *in vitro* antimicrobial properties. An initial burst release of ampicillin in first hour followed by a complete cycle in 96 hours was analyzed. Tran *et al.* [114] demonstrated the controllable and switchable release of Ibuprofen from PCL nanofibers with average diameter from 500nm to 3 μ m. Chen *et al.* [115] prepared composite nanofibers of PCL and nanohydroxyapatite for osteogenic differentiation of mesenchymal stem cells with diameters 340 \pm 30nm. Karuppuswamy and Reddy [116] fabricated

PCL nanofibers with different concentrations of the antibiotic drug (tetracycline hydrochloride 2%, 3%, 4% and 5%) for the controlled drug delivery. The nanofibers obtained were smaller in diameters measuring 419 nm without drug and 643 nm with 2wt% of tetracycline hydrochloride. Madhaiyan *et al.* [117] produced PCL nanofibers mediated sustained release of the hydrophilic drug (Vitamin B12) and studied its applicability as the transdermal delivery system. The fiber diameter was within the range from 700nm to 2.5 μ m.

7.2 Incorporation of nanoparticles

The burst release of drugs is an undesirable phenomenon which occurs most of the times when they are incorporated into nanofibers. In order to control the drug release and turn it into a slow sustainable release, many scientists have used different kinds of inorganic nanoparticles along with these drugs to counter their problem. For instance, silica particles are chosen as drug carriers because of their high surface area and porous interior which can be utilized as a drug loading site both for hydrophobic and hydrophilic drugs. Gohary *et al.* [118] reported about loading anti-cancer drug, doxorubicin hydrochloride (DOX) into electrospun PCL nanofibers via silica nanoparticles. DOX was added to silica nanoparticles (SiO₂) via sol-gel method and DOX@SiO₂ was obtained that was subsequently incorporated to PCL/PEO blend solution for electrospinning. DOX in its free state and as DOX@SiO₂ were investigated for their impact on nanofibers diameter, morphology and drug release rate. A continued release of DOX for several days was realized from PCL/PEO nanofibers. Another attempt was made by Lopez *et al.* [119], they produced PCL nanofibers with silver nanoparticles and investigated their antimicrobial activity against gram-positive and gram-negative bacteria. The minimum diameter of the nanofibers obtained was 160nm with 1-10mM of silver nanoparticles. Silver nanoparticles (AgNPs) have gained attention in recent times because of their anti-bacterial and disinfectant properties. Al-Omair [120]

demonstrated the use of these AgNPs with electrospun PCL/MMA (polymethacrylic acid) graft copolymer nanofibers. Nanofibers morphology, AgNPs content, water up take of nanofibers and anti-microbial efficacy were analyzed. AgNPs showed good dispersion in PCL/MMA and nanofibers with average diameter range of 200-570nm was achieved. Diameter and nanofibers uniformity was unaffected by these AgNPs. Resulting nanofibers with silver nanoparticles showed appreciable hydrophilic and excellent anti-bacterial properties against Gram-negative bacteria *E.coli* and *P. aeruginosa* and Gram-positive bacteria *Bacillus thuringiensis* and *Staphylococcus aureus* with clear inhibition zones of about 22mm and 53mm. Chen *et al.* [121] achieved a sustained antibiotic (gentamicin) release by electrospinning PCL nanofibers comprising entrapped mesoporous silica nanoparticles (MSNs-PCL). Gentamicin loaded PCL nanofibers showed great resilience against *E coli.* and retained bioactivity.

8. Nanofibers as drug delivery systems in wound dressings

When human skin suffers any kind of injury, it under goes a complex process of tissue revival that anticipates the affected area, this phenomenon is called “wound healing”. There are so many challenges during this wound healing process that human skin has to face and counteract. Most common is the inflammation in the injured area that can turn a simple wound to a critical one majorly in case of diabetic patients or people with weak immunity system. Usually there are three basic issues to be addressed; wound secrets exudate that should be absorbed, wound dressing should be equipped to cure the pain and should protect the wounded skin from microorganisms which can cause serious infections [122]. In clinical practice, wounds are first cleaned with antiseptic solutions followed by the application of antiseptic gel or ointment which is then covered by a sterile dressing material, usually a muslin. These antiseptic ointments are typically loaded with 5wt% of drug at maximum and dressing material is required to be changed at regular time

intervals, which in itself is a painful, labor intensive practice [123]. Hence, this gave birth to the idea of advanced wound dressings, with incorporated drugs and healing agents which must be capable of preventing infections, healing pain and expedite tissue regeneration process. These multifunctional wound dressings were envisioned to be sustainable, biodegradable, embrace good mechanical stability and be equipped with controllable drug delivery system [124]. Following this direction, great deal of research was conducted around the globe which is discussed in this section as a nut-shell review.

Wound dressings have been fabricated out of different types of materials and various formats, for example; nanofiber mats and hydrogels, and may contain additives like anti-bacterial nanoparticles or pharmaceutical drugs. Recent progresses in the development of advanced wound dressings has focused on the application of electrospun nanofibers for drug delivery to affected area of skin. Nanofibers help to encapsulate the therapeutic agents in their structure and on their surface to form a drug delivery system. In addition, electrospun fibers maintain the integrity and bioactivity of the drug molecules due to the mild processing parameters. Localized inoculation of medicines in wound treatment using electrospun fibers as delivery vehicles can significantly reduce the systemic absorption of the drug and prevent/reduce any side effects from the drugs. In addition, the efficacy of the drug would also improve due to localization of the treatment. The release of the drug is then dependent on the degradation of the polymer fibers and thus can be properly controlled [125].

Lei *et al.* [126] explained the fabrication of an elastomeric, photoluminescent and antibacterial wound dressing, consisted of hybrid polypeptide-based nanofibers. This specialized wound dressing was prepared to resist against multi-drug resistant (MDR) bacteria and to accelerate wound healing. The hybrid nanofibrous matrix was composed of poly(citrate)- ϵ -poly-lysine (PCE) and poly(ϵ -caprolactone) (PCL). This wound dressing not only efficiently prevented the MDR and

infections related to it, but also killed the bacteria capacity, showed elastomeric behavior and supported skin regeneration. Kwon *et al.* [127] designed a blended scaffold of synthetic and natural polymeric nanofibers using polyurethane (PU) and gelatin. An antibiotic, silver-sulfadiazine (SSD) was also incorporated into the blended solution for electrospinning of nanofibers which were capable to cure burn-wounds. SSD release was capable to prevent the growth of many bacteria as well as augmented the wound healing process by preventing infection.

Natural materials such as gelatin and chitosan had remained the preferred choice in order to develop burn wound dressing materials by electrospinning technique. Such an example is the work done by Kossovich *et al.* [128] which narrates the production of chitosan nanofibrous mats, as a dressing material for IIIa and IIIb degree burn wounds. These chitosan nanofibrous mats effectively absorbed the wound exudate, showed air permeability, protected the wound from external threats and speeded the skin revival. Effect of material thickness on the regeneration and degradation was studied and mechanical properties were also analyzed. Chen *et al.* [129] also used chitosan (CS) with poly(ϵ -caprolactone) (PCL) to create a cationic chitosan graft copolymer (CS-PCL). A hybrid scaffold was prepared by CS-PCL/PCL nanofibers by electrospinning for damaged retinal tissue repair. Characterization of nanofibrous scaffolds was done to measure the fiber diameter and content of amino groups on their surface. It was found that CS-PCL/PCL (20/80) wt/wt scaffolds showed better mice cell proliferation and growth and favored the retinal tissue repair as compared to other prepared ratios.

A novel bilayer wound dressing was manufactured by Corriea *et al.* [130] with a top dense layer of PCL nanofibers, designed to provide mechanical support and a bottom porous layer composed of chitosan and Aloe Vera, aimed to act as bacterial barrier and aids healing process. Fibroblast cells were able to adhere, spread and proliferate on the membrane surface and these asymmetric membranes also showed good antimicrobial properties. Gouveia *et al.* [131] published their study

about novel electrospun, Poly(ϵ -caprolactone) (PCL)/Polyvinyl Alcohol (PVA)/Chitosan (CS) nanofibers mats loaded with Eugenol (EUG), an essential oil, known for its therapeutic properties. Prepared fiber mats were characterized by FTIR, SEM, total porosity measurements and water contact angle analysis. *In vitro* EUG release profile and antibacterial efficacy against *Staphylococcus aureus* and *Pseudomonas aeruginosa* were investigated. PCL/PVA/CS nanofibers mats showed a burst release of EUG in first 8h of analysis with a complete release till 120h. It also presented an efficient antibacterial ability with 90% inhibition ratios and *in vitro* cytotoxicity assay showed that the normal human dermal fibroblast (NHDF) remained sustainable for at least 7 days, while in contact with electrospun nanofibers mats. These findings justified the use of these EUG loaded, electrospun PCL/PVA/CS nanofiber mats as potential wound dressing material for rapid wound healing by preventing bacterial wound infections.

9. Conclusion

This chapter is a review about electrospinning history, its operating principles and parameters, types of electrospinning techniques and their scope, biomedical applications of electrospun nanofibers, electrospinning of natural and synthetic polymers and their blending, incorporation of drugs and nanoparticles in nanofibers and their use as drug delivery systems in various kinds of wound dressings. Electrospinning technique is versatile, robust and economical approach for the production of very fine polymeric fibers to be used in several industries. It is a very simple yet resourceful process which gives the liberty of tailoring the characteristics of electrospun nanofibers significantly, by merely altering the operating parameters such as voltage, needle to collector distance, feed rate, viscosity and concentration. Among these key variables, temperature and relative humidity also contributes in shaping the morphology and physiochemical properties of nanofibers. Due to the hydrophobic or hydrophilic nature of polymers, these two factors predominantly impact the nanofibers production and their end results. Viscosity, selection of solvent and concentration are also very important to be analyzed as they greatly affect the success or failure of electrospinning phenomenon. Moreover, it was proven from the literature that blending PCL with different polymers having different characteristics is a progressive and fruitful method. Because of this blending, one can achieve desirable set of properties in one product according to its potential end use. An overview of PCL electrospinning and its blending is also narrated in this section. The subsequent use of PCL based nanofibrous materials for drug deliver and tissue engineering is also discussed.

From previously reported research, it was emphasized that single needle electrospinning is an adaptable method of electrospinning to produce small lab scale samples to perform preliminary studies about the characteristics of selected polymer, solvent selection, finalizing the concentration

and gauging its ability to be electrospun. Whereas, the needleless Nanospider technique is rather large scale production of nanofibers and it offers a higher range of applied voltage and shapes of electrodes such as metallic wire or rotating drums with varying diameters.

A lot of research has already been published about the biomedical applications of nanofibers and specially for wound dressing materials. A number of polymer blends and drugs were tested to produce nanofibers and were investigated for their biocompatibility, antimicrobial behavior, cytotoxicity, drug release efficiency in a certain time frame, cell adhesion and proliferation etc. But, there is still enough room for new blends of PCL and its fabrication methods, to be tested and verified as viable product to be used as a topical wound dressing. PCL blends with PEG have already been studied by many scholars, but most of these publications reported the use of high molar masses of PEG (which are mentioned in above section).

In this study, for the first time a low molar mass of PEG (M_n -400 Da) is blended with PCL (M_n -80,000 Da) to study its impact on the electrospinning process and properties of PCL nanofibers. In addition to this new approach, a bilayer wound dressing is the target of this research by utilizing a biopolymer, gelatin (GE) and hyaluronic acid (HA) as a base for IBU and HA loaded electrospun PCL nanofibers. This bilayer membrane equipped with drug delivery system is investigated for its potential use as a topical wound dressing which cures the pain, prevents inflammation and accelerates the wound healing process.

References

1. Bhardwaj, N. and S.C. Kundu, *Electrospinning: a fascinating fiber fabrication technique*. Biotechnol Adv, 2010. **28**(3): p. 325-47.
2. Morton, W.J., *Method of dispersing fluids.*, U.S.P. Office., Editor 1902: United States. p. 4.
3. Cooley, J.F., *Apparatus for ellectrically dispersing fluids.*, U.S.P. Office., Editor 1902. p. 7.
4. Zeleny, J., *Instability of Electrified Liquid Surfaces*. Physical Review, 1917. **10**(1): p. 1-6.
5. Formhals, A., *Process and apparatus for preparing artificial threads*, U.S.P. Office., Editor 1934: United States. p. 7.
6. Sir Taylor G., *Electrically driven jets*. Proc. Roy. Soc. Lond. A, 1969. **313**: p. 453-475.
7. Larrondo L., M.J.R.S., *Electrostatic Fiber Spinning from Polymer Melts. I. Experimental Observations on Fiber Formation and Properties*. Journal of Polymer Science: Polymer Physics Edition, 1981. **19**: p. 909-920.
8. Li D and Xia Y., *Electrospinning of Nanofibers: Reinventing the Wheel?* Advanced Materials, 2004. **16**(14): p. 1151-1170.
9. Hu X, L.S., Zhou G, Huang Y, Xie Z, Jing X, *Electrospinning of polymeric nanofibers for drug delivery applications*. J Control Release, 2014. **185**: p. 12-21.
10. Alves da Silva ML, M.A., Costa-Pinto AR, Costa P, Faria S, Gomes M, Reis RL, Neves NM, *Cartilage tissue engineering using electrospun PCL nanofiber meshes and MSCs*. Biomacromolecules, 2010. **11**: p. 3228-3236.
11. Jin Y, Y.D., Kang D, Jiang X, *Fabrication of necklace-like structures via electrospinning*. Langmuir, 2009. **26**(2): p. 1186-1190.
12. Koombhongse S, L.W., Reneker DH, *Flat polymer ribbons and other shapes by electrospinning*. J. Polym. Sci. Part B: Polym. Phys., 2001. **39**: p. 2598-2606.
13. Nguyen TT, G.C., Hwang SG, Chanunpanich N, Park JS, *Porous core/sheath composite nanofibers fabricated by coaxial electrospinning as a potential mat for drug release system*. . Int. J. Pharm., 2012. **439**: p. 296-306.
14. Dror Y, S.W., Avrahami R, Zussman E, Yarin A, Dersch R, Greiner A, Wendorff J, *One-step production of polymeric microtubes by co-electrospinning*. Small, 2007. **3**(6): p. 1064-1073.

15. Zhao Y, C.X., Jiang L, *Bio-mimic multichannel microtubes by a facile method*. J. Am. Chem. Soc., 2007. **129**(4): p. 764-765.
16. Beachley, V. and X. Wen, *Effect of electrospinning parameters on the nanofiber diameter and length*. Mater Sci Eng C Mater Biol Appl, 2009. **29**(3): p. 663-668.
17. Deitzel, J.M.K., J.; Harris, D. & Beck Tan, N.C., *The effect of processing variables on the morphology of electrospun nanofibers and textiles*. Polymer, 2001. **42**(1): p. 261-272.
18. Lee, H.J., et al., *Biomedical Applications of Magnetically Functionalized Organic/Inorganic Hybrid Nanofibers*. Int J Mol Sci, 2015. **16**(6): p. 13661-77.
19. Sridhar, R., et al., *Electrospun inorganic and polymer composite nanofibers for biomedical applications*. J Biomater Sci Polym Ed, 2013. **24**(4): p. 365-85.
20. Sapountzi, E., et al., *Recent Advances in Electrospun Nanofiber Interfaces for Biosensing Devices*. Sensors (Basel), 2017. **17**(8).
21. Liverani L., R.J.A., Boccaccini A. R., *Nanofiber composites in bone tissue engineering*. Nanofiber Composites for Biomedical Applications. , 2017: p. 301-323.
22. Haider A., K.S., Huh M. -W., Kang I. -K., , *Hybrid nanofiber scaffold stimulates osteoblastic cells growth*. . BioMed. Res. Int., 2015. **2015**.
23. Subramanian S., S.R., *New directions in nanofiltration applications—are nanofibers the right materials as membranes in desalination?* . Desalination, 2013. **308**: p. 198-208.
24. Schulte J., *Nanotechnology: Global Strategies, Industry Trends and Applications*. , 2005, John Wiley & Sons Ltd, : Southern Gate, Chichester, West Sussex, PO19 8SQ, England. p. 1450.
25. Lee S.H., K.B.C., Wang X., Samuelson L.A., Kumar J.,. *Design, synthesis and electrospinning of a novel fluorescent polymer for optical sensor applications*. in *Mater. Res. Soc. Symp. Proc.* . 2002.
26. Teo W.E, I.R., Ramakrishna S.,, *Technological advances in electrospinning of nanofibers*. . Science and Technology of Advanced Materials, 2011. **12**(1).
27. Haitao N., T.L., *Fiber Generators in Needleless Electrospinning*. Journal of Nanomaterials., 2012.
28. Petrik S., M.M. *Production Nozzle-Less Electrospinning Nanofiber Technology*. in *Symposium WW – Polymer Nanofibers – Fundamental Studies and Emerging Applications*. 2009. Cambridge University Press.

29. Huang Z.M., Z.Y.Z., Kotaki M. & Ramakrishna S., *A review on polymer nanofibers by electrospinning and their applications in nanocomposites*. Composites Science and Technology of Advanced Materials, 2003. **63**: p. 2223-2253.
30. Doshi J. & Reneker D. H., *Electrospinning process and applications of electrospun fibers*. Journal of Electrostatics, 1995. **35**: p. 151-160.
31. Jirsak O., S.F., Lukas D., Kotek V., Martinova L. and Chaloupek J., *A method of nanofibres production from a polymer solution using electrostatic spinning and a device for carrying out the method.*, in *World Intellectual Property Organization*, C.P. Application, Editor 2005, Technicka Univerzita v Liberci: Canada.
32. Yao S, W.X., Liu X, Wang R, Deng C and Cui F., *Effects of ambient relative humidity and solvent properties on the electrospinning of pure hyaluronic acid nanofibers*. Journal of Nanoscience and Nanotechnology, 2013. **13**(7): p. 4752-4758.
33. Vrieze S.D, C.T.V., Nelvig A, Hagstrom B, Westbroek P and Clerck K. De., *The effect of temperature and humidity on electrospinning*. Journal of Materials Science, 2009. **44**(5): p. 1357-1362.
34. Fong H, C.I.a.R.D.H., *Beaded nanofibers formed during electrospinning*. Polymer, 1999. **40**: p. 4585–4592.
35. Khan W.S, A.R., Ceylan M and Jabbarnia A., *Recent progress on conventional and non-conventional electrospinning processes*. Fiber Polym., 2013. **14**: p. 1235-1247.
36. Huang L, N.K., Apkarian R.P and Chaikof E.L., *Engineered collagen-PEO nanofibers and fabrics*. J. Biomater. Sci. Polym., 2001. **12**: p. 979-999.
37. Andradý A.L, *Factors affecting nanofiber quality*. Science and technology of polymer nanofibers.2008. 81-110.
38. Okutan N, T.P.a.A.F., *Affecting parameters on electrospinning process and characterization of electrospun gelatin nanofibers*. Food Hydrocolloids, 2014. **39**: p. 19-26.
39. Pham Q.P, S.U.a.M.A.G., *Electrospinning of polymeric nanofibers for tissue engineering applications: a review*. . Tissue. Eng., 2006. **12**(5): p. 1197-1211.
40. Doshi J and Reneker D.H. *Electrospinning process and applications of electrospun fibers*. in *Proceedings of the Conference Record of the IEEE*. 1993. Toronto, Canada.
41. Hu A and Apblett A, *Nanotechnology for Water Treatment and Purification*. Vol. 22. 2014, Berlin, Germany: Springer.

42. Yordem O. S, P.M.a.M.Y.Z., *Effects of electrospinning parameters on polyacrylonitrile nanofiber diameter: an investigation by response surface methodology*. Materials & Design., 2008. **29**(1): p. 34-44.
43. Baumgarten P. K, *Electrostatic spinning of acrylic microfibers*. Journal of Colloid and Interface Science, 1971. **36**(1): p. 71-79.
44. Mit-uppatham C, N.M.a.S.P., *Ultrafine electrospun polyamide-6 fibers: effect of solution conditions on morphology and average fiber diameter*. Macromolecular Chemistry Physics., 2004. **25**: p. 1883-1890.
45. Casper C.L, S.J.S., Tassi N.G, Chase D.B and Rabolt J.F., *Controlling Surface Morphology of Electrospun Polystyrene Fibers: Effect of Humidity and Molecular Weight in the Electrospinning Process*. Macromolecules, 2004. **37**(2): p. 573-578.
46. Liu M, D.X.P., Li Y.M, Yang D.P and Long Y.Z., *Electrospun nanofibers for wound healing*. Mater. Sci. Eng. C, 2017. **76**: p. 1413-1423.
47. M, W.J.a.W., *Functional electrospun fibers for the treatment of human skin wounds*. Eur. J. Pharm. Biopharm., 2017. **119**: p. 283-299.
48. Ahmadi M.S, R.K.M., Moshtaghian S.J, Talebi A and Khezri M., *Application of Chitosan/PVA Nano fiber as a potential wound dressing for streptozotocin-induced diabetic rats*. Int. J. Biol. Macromol. , 2016. **92**: p. 1162-1168.
49. Chou S.F and Woodrow K.A, *Relationships between mechanical properties and drug release from electrospun fibers of PCL and PLGA blends*. J. Mech. Behav. Biomed. Mater. , 2017. **65**: p. 724-733.
50. Chen S, B.S.K., Batra S.K, Li X and Xie J., *Emerging roles of electrospun nanofibers in cancer research*. Adv. Healthc. Mater., 2018. **7**.
51. Mogosanu G.D and Grumezescu A.M, *Natural and synthetic polymers for wounds and burns dressing*. Int. J. Pharm., 2014. **463**: p. 127-136.
52. Huang S and Fu X, *Naturally derived materials-based cell and drug delivery systems in skin regeneration*. J. Control. Release, 2010. **142**(2): p. 149-159.
53. Dai T, T.M., Huang Y.Y and Hamblin M.R., *Chitosan preparations for wounds and burns: Antimicrobial and wound-healing effects*. Expert Rev. Anti-Infect. Ther., 2011. **9**(7): p. 857-879.
54. Bano I, A.M., Yasin T, Ghauri M.A and Younus M., *Chitosan: A potential biopolymer for wound management*. Int. J. Biol. Macromol., 2017. **102**: p. 380-383.

55. Pakravan M, H.M.C.a.A.A., *A fundamental study of chitosan/PEO electrospinning*. . Polymer, 2011. **52**(21): p. 4813-4824.
56. Lu, J.-W.Z., Y.-L.; Guo, Z.-X.; Hu, P.; Yu, J. , *Electrospinning of sodium alginate with poly(ethylene oxide)*. Polymer, 2006. **47**(23): p. 8026-8031.
57. Topuz F and Uyar T, *Electrospinning of gelatin with tunable fiber morphology from round to flat/ribbon*. Mater. Sci. Eng. C, 2017. **80**: p. 371-378.
58. Butchera A.L, K.C.T.a.O.M.L., *Systematic mechanical evaluation of electrospun gelatin meshes*. Journal of the Mechanical Behavior of Biomedical Materials, 2017. **69**: p. 412-419.
59. Zhang K, L.Z., Kang W, Deng N, Yan J, Ju J, Liu Y and Cheng B., *Preparation and characterization of tree-like cellulose nanofiber membranes via the electrospinning method*. Carbohydr. Polym., 2018. **183**: p. 62-69.
60. Bak S.Y, Y.G.J., Lee S.W and Kim H.W, , *Effect of humidity and benign solvent composition on electrospinning of collagen nanofibrous sheets*. Materials Letters, 2016. **181**: p. 136-139.
61. Sadeghi-Avalshahr A, N.S., Molavi A.M, Khorsand-Ghayeni M and Mahdavi-Shahri M., *Synthesis and characterization of collagen/PLGA biodegradable skin scaffold fibers*. Regenerative Biomaterials 2017. **4**(5): p. 309-314.
62. Kutlusoy T, O.B., Apohan N.K, Süleymanoglu M and Kuruca S.E., *Chitosan-co-Hyaluronic acid porous cryogels and their application in tissue engineering*. Int. J. Biol. Macromol., 2017. **103**: p. 366-378.
63. Liu Y, M.G., Fang D, Xu J, Zhang H and Nie J., *Effects of solution properties and electric field on the electrospinning of hyaluronic acid*. . J. Carbohydr. Polym., 2011. **83**(2): p. 1011-1015.
64. Brenner E.K, S.J.D., Thompson E.A, Toth L.J and Schauer C.L., *Electrospinning of hyaluronic acid nanofibers from aqueous ammonium solutions*. Carbohydr. Polym., 2012. **87**(1): p. 926-929.
65. Esparza Y, U.A., Boluk Y and Wu J, , *Preparation and characterization of thermally crosslinked poly(vinyl alcohol)/feather keratin nanofiber scaffolds*. Mater. Des., 2017. **133**: p. 1-9.
66. Yukseloglu S.M, S.N.a.C.S., *Biomaterial applications of silk fibroin electrospun nanofibres*. Microelectron. Eng., 2015. **146**: p. 43-47.

67. Dias Antunes M, d.S.D.G., Fiorentini Â.M, Pinto V.Z, Lim L.T, da Rosa Zavareze E and Dias A.R.G., *Antimicrobial electrospun ultrafine fibers from zein containing eucalyptus essential oil/cyclodextrin inclusion complex*. Int. J. Biol. Macromol. Part A, 2017. **104**: p. 874-882.
68. Chou S.F., C.D., Woodrow K.A., *Current strategies for sustaining drug release from electrospun nanofibers*. J. Control. Release, 2015(220): p. 584-591.
69. Chou S.-F., G.S., Kiellani M.H.H., Thottempudi V.V.K., Neuenschwander P., Nie H., *A review of injectable and implantable biomaterials for treatment and repair of soft tissues in wound healing*. J. Nanotechnol., 2017. **2017**: p. 1-15.
70. Sultana, T., et al., *Preparation and characterization of polycaprolactone-polyethylene glycol methyl ether and polycaprolactone-chitosan electrospun mats potential for vascular tissue engineering*. J Biomater Appl, 2017. **32**(5): p. 648-662.
71. Ponjavic M. Nikolic M.S., N.-R.J., Jeremic S., Stevanovic S. and Djonlagic J., *Degradation behaviour of PCL/PEO/PCL and PCL/PEO block copolymers under controlled hydrolytic, enzymatic and composting conditions*. Polym. Test., 2017. **57**: p. 67-77.
72. Luong-Van E., G.L., Chua K.N., Leong K.W., Nurcombe V. and Cool S.M., *Controlled release of heparin from poly(ϵ -caprolactone) electrospun fibers*. Biomaterials, 2006. **27**(9): p. 2042-2052.
73. Lu L., G.C.A.a.M.A.G., *In vitro degradation of thin poly(DL-lactic-co-glycolic acid) films*. J. Biomed. Mater. Res., 1999. **46**: p. 236-244.
74. Park T.G., *Degradation of poly(lactic-co-glycolic acid) microspheres: Effect of copolymer composition*. Biomaterials, 1995. **16**(15): p. 1123-1130.
75. Peña J., C.T., Izquierdo-Barba I., Doadrio A.L. and Vallet-Regí M., *Long term degradation of poly(ϵ -caprolactone) films in biologically related fluids*. . Polym. Degrad. Stab., 2006. **91**(7): p. 1424-1432.
76. Ranjbar-Mohammadi M., Z.M., Prabhakaran M.P., Bahrami S.H. and Ramakrishna S., *Electrospinning of PLGA/gum tragacanth nanofibers containing tetracycline hydrochloride for periodontal regeneration*. Mater. Sci. Eng. C, 2016. **58**: p. 521-531.
77. Kim T.G., L.D.S.a.P.T.G., *Controlled protein release from electrospun biodegradable fiber mesh composed of poly(ϵ -caprolactone) and poly(ethylene oxide)*. Int. J. Pharm., 2007. **338**(1-2): p. 276-283.

78. Bui H. T., C.O.H., Cruz J. D. and Park J. S., *Fabrication and characterization of electrospun curcumin-loaded polycaprolactone-polyethylene glycol nanofibers for enhanced wound healing*. *Macromolecular Research*, 2014. **22**(12): p. 1288-1296.
79. Repanas A, W.W.F., Grykshov O, Müller M. and Glasmacher B., *PCL/PEG electrospun fibers as drug carriers for the controlled delivery of dipyridamole*. *Journal of In Silico & In Vitro Pharmacology*, 2015. **1**(1:2): p. 1-10.
80. Detta, N., et al., *Melt electrospinning of polycaprolactone and its blends with poly(ethylene glycol)*. *Polymer International*, 2010. **59**(11): p. 1558-1562.
81. Chen, C.H., Chen, S. H., Shalumon, K. T. and Chen, J. P., *Prevention of peritendinous adhesions with electrospun polyethylene glycol/polycaprolactone nanofibrous membranes*. *Colloids. Surf. B: Biointerfaces*, 2015. **133**: p. 221-30.
82. Dash T. K. and Konkimalla V. B., *Poly-ε-caprolactone based formulations for drug delivery and tissue engineering: A review*. *J. Control. Release.*, 2012. **158**(1): p. 15-33.
83. McEachin Z. and Lozano K., *Effects of expandable graphite and modified ammonium polyphosphate on the flame-retardant and mechanical properties of wood flour-polypropylene composites*. *Polym. Polym. Compos.*, 2013. **21**(7): p. 449-456.
84. Aditya N. , R.P.R., Avula U. S., and Vats R., *Poly (ε-caprolactone) nanocapsules for oral delivery of raloxifene: process optimization by hybrid design approach, in vitro and in vivo evaluation*. *J. Microencapsul.*, 2014. **31**(5): p. 508-518.
85. Nair L. S. and Laurencin C. T., *Biodegradable polymers as biomaterials*. *Prog. Polym. Sci.*, 2007. **32**: p. 762-798.
86. Middleton J. C. and Tipton A. J., *Synthetic biodegradable polymers as orthopedic devices*. *Biomaterials.*, 2000. **21**(23): p. 2335-2346.
87. Engelberg I. and Kohn J., *Physico-mechanical properties of degradable polymers used in medical applications: a comparative study*. *Biomaterials.*, 1991. **12**: p. 292-304.
88. Woodruff M. and Hutmacher D., *The return of a forgotten polymer—polycaprolactone in the 21st century*. *Prog. Polym. Sci.*, 2010. **35**(10): p. 1217-1256.
89. Williamson M. R. and Coombes A. G. A., *Gravity spinning of polycaprolactone fibers for applications in tissue engineering*. *Biomaterials.*, 2004. **25**(3): p. 459-465.
90. Hutmacher D. W. and Cool S., *Concepts of scaffold-based tissue engineering—the rationale to use solid free-form fabrication techniques*. *J. Cell. Mol. Med.*, 2007. **11**(4): p. 654-669.

91. Hutmacher D. W., S.M.a.R.M.V., *Scaffold-based tissue engineering: rationale for computer-aided design and solid free-form fabrication systems*. Trends Biotechnol., 2004. **22**(7): p. 354-362.
92. Coccoli V., L.A., Orsi S., Guarino V., Causa F. and Netti P. A., *Engineering of poly(ϵ -caprolactone) microcarriers to modulate protein encapsulation capability and release kinetic*. Mater. Sci.: Mater. Med., 2008. **19**(4): p. 1703-1711.
93. Luciani A., C.V., Orsi S., Ambrosio L. and Netti P. A., *PCL microspheres based functional scaffolds by bottom-up approach with predefined microstructural properties and release profiles*. Biomaterials., 2008. **29**(36): p. 4800-4807.
94. Doustgani, A., *Effect of electrospinning process parameters of polycaprolactone and nanohydroxyapatite nanocomposite nanofibers*. Textile Research Journal, 2015. **85**(14): p. 1445-1454.
95. Georgiadou, K.A.G.K.G.T.V.S., *Porous electrospun polycaprolactone fibres: Effect of process parameters*. Journal of Polymer Science Part B: Polymer Physics, 2016. **54**: p. 1878-1888.
96. Qin, X. and D. Wu, *Effect of different solvents on poly(caprolactone) (PCL) electrospun nonwoven membranes*. Journal of Thermal Analysis and Calorimetry, 2011. **107**(3): p. 1007-1013.
97. Bosworth, L.A. and S. Downes, *Acetone, a Sustainable Solvent for Electrospinning Poly(ϵ -Caprolactone) Fibres: Effect of Varying Parameters and Solution Concentrations on Fibre Diameter*. Journal of Polymers and the Environment, 2012. **20**(3): p. 879-886.
98. Li W., S.L., Zhang X., Liu K., Ismat Ullah and Cheng P., *Electrospinning of polycaprolactone nanofibers using H₂O as benign additive in polycaprolactone/glacial acetic acid solution*. Journal of Applied Polymer Science, 2018. **135**.
99. Wang, X., et al., *Crystalline Morphology of Electrospun Poly(ϵ -caprolactone) (PCL) Nanofibers*. Industrial & Engineering Chemistry Research, 2013. **52**(13): p. 4939-4949.
100. Kostakova E. K., M.L., Maskova G., Blazkova L., Turcsan T. and Lukas D., *Crystallinity of Electrospun and Centrifugal Spun Polycaprolactone Fibers: A Comparative Study*. Journal of Nanomaterials, 2017. **2017**: p. 1-9.
101. Ferreira J. L., G.S., Henriques C., Borges J. P. and Silva J. C., *Electrospinning Polycaprolactone Dissolved in Glacial Acetic Acid*. Journal of Applied Polymer Science, 2014. **131**.

102. Bolgen N., V.I., Korkusuz P., Menciloglu Y.Z. and Piskin E., *In vivo performance of antibiotic embedded electrospun PCL membranes for prevention of abdominal adhesions*. J. Biomed. Mater. Res. B: Appl. Biomater., 2007. **81**(2): p. 530-543.
103. Mir M., A.M.N., Barakullah A., Gulzar A., Arshad M., Fatima S. and Asad M., *Synthetic polymeric biomaterials for wound healing: a review*. Progress in Biomaterials, 2018. **7**: p. 1-21.
104. Jiang W., L.L., Zhang D., Huang S., Jing Z., Wu Y., Zhao Z., Zhao L. and Zhou S., *Incorporation of aligned PCL-PEG nanofibers into porous chitosan scaffolds improved the orientation of collagen fibers in regenerated periodontium*. Acta Biomater., 2015. **25**: p. 240-252.
105. Han N., J.J.K., Bradley P.A., Parikh K.S., Lannutti J.J. and Winter J.O., *Cell attachment to hydrogel-Electrospun fiber mat composite materials*. J. Funct. Biomater., 2012. **3**: p. 497-513.
106. Tiwari A. P., J.M.K., Lee J., Bikendra M., Ko S. W., Park C. H. and Kim C. S., *Heterogeneous electrospun polycaprolactone/polyethylene glycol membranes with improved wettability, biocompatibility, and mineralization*. Colloids and Surfaces A: Physicochemical and Engineering Aspects., 2017. **520**: p. 105-113.
107. Kenawy E. -R., B.G.L., Mansfield K., Layman J., Simpson D. G., Sanders E. H., Wnek G. E., *Release of Tetracycline Hydrochloride from Electrospun Poly(Ethylene-Co-Vinylacetate), Poly(Lactic Acid), and a Blend*. J. Controlled Release., 2002. **81**(1-2): p. 57-64.
108. Gizaw, M., et al., *Electrospun Fibers as a Dressing Material for Drug and Biological Agent Delivery in Wound Healing Applications*. Bioengineering (Basel), 2018. **5**(1).
109. Meinel, A.J., Germershaus, O., Luhmann, T., Merkle, H.P., Meinel, L., *Electrospun matrices for localized drug delivery: current technologies and selected biomedical applications*. Eur. J. Pharm. Biopharm., 2012(81): p. 1-13.
110. Sill, T.J., von Recum, H. A., *Electrospinning: applications in drug delivery and tissue engineering*. Biomaterials, 2008. **29**: p. 1989-2006.
111. Masoumi, S., S. Amiri, and S.H. Bahrami, *PCL-based nanofibers containing ibuprofen/cyclodextrins nanocontainers: A potential candidate for drug delivery application*. Journal of Industrial Textiles, 2018. **48**(9): p. 1420-1438.

112. Potrc, T., et al., *Electrospun polycaprolactone nanofibers as a potential oromucosal delivery system for poorly water-soluble drugs*. Eur J Pharm Sci, 2015. **75**: p. 101-13.
113. Liu H., L.K.K.a.Z.Y., *Antimicrobial Properties and Release Profile of Ampicillin from Electrospun Poly(ϵ -caprolactone) Nanofiber Yarns*. Journal of Engineered Fibers and Fabrics, 2010. **5**(4): p. 1024-1031.
114. Tran T., H.M., Patel D., Burns E., Peterman V. and Wu J., *Controllable and switchable drug delivery of ibuprofen from temperature responsive composite nanofibers*. Nano Convergence., 2015. **2**(15).
115. Chen J. P., L.G.C., and Chang Y. S., *Preparation of composite electrospun nanofibers of polycaprolactone and nanohydroxyapatite for osteogenic differentiation of stem cells.*, in *3rd Int. Nanoelectron. Conf. (INEC)*, 2010: Hong Kong, China. p. 1395-1396.
116. Karuppuswamy P. and Reddy J., *Polycaprolactone nano fibers for the controlled release of tetracycline hydrochloride*. Mater. Lett., 2015. **141**: p. 180-186.
117. Madhaiyan K., S.R., Sundarrajan S., Venugopal J. R. and Ramakrishna S., *Vitamin B12 loaded polycaprolactone nanofibers: A novel transdermal route for the water soluble energy supplement delivery.*, Int. J. Pharm., 2013. **444**(1-2): p. 70-76.
118. Gohary, M.I.E., et al., *Electrospinning of doxorubicin loaded silica/poly(ϵ -caprolactone) hybrid fiber mats for sustained drug release*. Advances in Natural Sciences: Nanoscience and Nanotechnology, 2018. **9**(2): p. 025002.
119. Efrén Amador Hinojos-Márquez, J.L.-E., León Francisco Espinosa- and A.D.-C. Cristóbal, and Simón Yobanny Reyes-López, *Antimicrobial activity of silver nanoparticles in polycaprolactone nanofibers against Gram-positive and negative bacteria*. Industrial and Engineering Chemistry Research, 2016. **55**(49): p. 12532-12538.
120. Al-Omair, M., *Synthesis of Antibacterial Silver–Poly(ϵ -caprolactone)-Methacrylic Acid Graft Copolymer Nanofibers and Their Evaluation as Potential Wound Dressing*. Polymers (Basel), 2015. **7**(8): p. 1464-1475.
121. Chen, X., C. Xu, and H. He, *Electrospinning of silica nanoparticles-entrapped nanofibers for sustained gentamicin release*. Biochem Biophys Res Commun, 2019. **516**(4): p. 1085-1089.
122. Strodbeck, F., *Physiology of wound healing*. . Newborn and Infant Nursing Reviews., 2001. **1**(1): p. 43-52.

123. Sidgwick, G.P., McGeorge, D., Bayat, A., *A comprehensive evidence-based review on the role of topicals and dressings in the management of skin scarring.* Arch. Dermatol. Res., 2015. **307**: p. 461-477.
124. Chou, S.-F., Carson, D., Woodrow, K. A., *Current strategies for sustaining drug release from electrospun nanofibers.* J. Control. Release., 2015. **220**: p. 584-591.
125. Farrugia B.L., M.Y., Kim H.N., Whitelock J.M., Baker S.M., Wiesmann W.P., Li Z., Maitz P. and Lord M.S., *Chitosan-based heparan sulfate mimetics promote epidermal formation in a human organotypic skin model.* Adv. Funct. Mater., 2018. **28**(36): p. 1802818.
126. Xi, Y., et al., *Biomimetic Elastomeric Polypeptide-Based Nanofibrous Matrix for Overcoming Multidrug-Resistant Bacteria and Enhancing Full-Thickness Wound Healing/Skin Regeneration.* ACS Nano, 2018. **12**(11): p. 10772-10784.
127. Heo, D.N., et al., *Burn-wound healing effect of gelatin/polyurethane nanofiber scaffold containing silver-sulfadiazine.* J Biomed Nanotechnol, 2013. **9**(3): p. 511-5.
128. L.Y. Kossovich, Y.S., I.V. Kirillova. *Electrospun Chitosan Nanofiber Materialas burn dressing.* 2010.
129. Chen, H., et al., *Electrospun chitosan-graft-poly (varepsilon-caprolactone)/poly (varepsilon-caprolactone) nanofibrous scaffolds for retinal tissue engineering.* Int J Nanomedicine, 2011. **6**: p. 453-61.
130. Miguel S. P., R.M.P., Coutinho P., Correia I. J., *Electrospun Polycaprolactone/Aloe Vera_Chitosan Nanofibrous Asymmetric Membranes Aimed for Wound Healing Applications.* Polymers., 2017. **9**(183).
131. Mouro C., S.M., Gouveia I. C., *Emulsion Electrospun Fiber Mats of PCL/PVA/Chitosan and Eugenol for Wound Dressing Applications.* Advances in Polymer Technology., 2019. **2019**.

Chapter 2: Materials & Methods

Chapitre 2: Matériel et Méthodes

Le deuxième chapitre comprend les spécifications et les informations sur les fournisseurs de l'ensemble des produits chimiques qui ont été utilisés, ainsi que les méthodes de filage et de caractérisation appliquées pour atteindre les objectifs visés. Les étapes de préparation de la solution d'électrofilage ont été expliquées et l'élaboration de nanocapsules de chitosane a également été mentionnée. La solution de polymère a été électrofilée dans un premier temps en utilisant un équipement vertical conventionnel à une seule aiguille puis en utilisant un équipement semi-industriel sans aiguille appelé «NanoSpider». Les deux configurations d'électrofilage ont été expliquées et leurs composants de base ont été présentés. Différents ensembles de plans d'expériences (DOE) ont été établis afin de déterminer l'impact de différents paramètres d'électrofilage sur la morphologie des nanofibres. Les résultats obtenus de ces DOE ont été analysés à l'aide d'un outil d'analyse statistique appelé «Analyse des Composantes Principales». L'approche analytique de cet outil statistique a été décrite en détail. De plus, les étapes de fabrication du pansement bicouche ont été décrites, notamment la préparation du film gélatine/acide hyaluronique (GE/HA).

La caractérisation physico-chimique des nanofibres PCL a été réalisée en utilisant diverses techniques. La viscosité de la solution de PCL dans divers solvants a été mesurée en utilisant un rhéomètre plan-plan, à température ambiante. La morphologie des nanofibres produites a été étudiée par microscopie électronique à balayage (SEM). Avant l'analyse SEM, tous les échantillons ont été métallisés par pulvérisation à l'or à l'aide d'un métalliseur afin de les rendre conducteurs. Les diamètres moyens des nanofibres ont été mesurés à l'aide du logiciel ImageJ en prenant 50 mesures par échantillon. Pour déterminer la mouillabilité des nanofibres PCL et PCL / PEG, leurs angles de contact avec l'eau ont été mesurés. Une analyse par calorimétrie différentielle à balayage (DSC) des nanofibres PCL a été effectuée afin de déterminer leurs taux de cristallinité.

La tenue thermique des nanofibres a été étudiée par analyse thermo-gravimétrique (TGA). La résistance mécanique des nanofibres et des films GE/HA a été déterminée grâce à une machine d'essai de traction MTS et leurs courbes contrainte-déformation ont été enregistrées.

La caractérisation biologique des nanofibres PCL chargées d'IBU et de la structure bicouche comprenait la cinétique de libération de médicament in vitro qui a été étudiée par spectroscopie UV-vis et l'analyse antibactérienne du matériau bicouche. Cette section a également expliqué la préparation des cultures bactériennes et présente les étapes de l'analyse antibactérienne.

CHAPTER 2

MATERIALS AND METHODS

The selection of materials and methods was done carefully in order to achieve the goal of this research that is a bilayer wound dressing. Preparation of electrospinning solution to electrospinning of nanofibers by using two different techniques, incorporation of PEG and IBU to the PCL nanofibers, optimization of electrospinning parameters and characterization of electrospun PCL nanofibers, preparing the first GE/HA layer to fabricate a bilayer structure, all these steps are explained in this chapter.

1. Materials

1.1 Poly(ϵ -caprolactone) (PCL)

In this study, PCL with a molar mass of M_w - 80,000 g/mol was used as core component to produce electrospun nanofibers. The physical form of PCL was white round pellets and was purchased from Sigma-ALDRICH. It was used as received without further processing.

1.2 Polyethylene glycol (PEG)

To blend PCL with a hydrophilic polymer, a low molar mass of PEG was selected. PEG with molar mass M_n -400 g/mol was sourced from Sigma-ALDRICH and was used as received.

1.3 Ibuprofen (IBU)

IBU in pure form >98% (M_w = 206.28 g/mol) was purchased from Sigma-ALDRICH and was used as received.

1.4 Dispersing agents

Three different dispersing agents i.e., W966 supplied by BYK, G079 and G127 supplied by Mader company were used to disperse the nanocapsules of chitosan.

1.5 Gelatin and Hyaluronan

Gelatin (GE) type A, from porcine skin was supplied by Sigma-Aldrich. Hyaluronan (sodium hyaluronate) (HA) of cosmetic grade was purchased from Aroma-zone. Both products were used as received. The specifications and supplier information of above mentioned materials are given in Table 2.1.

Table 2.1. Specifications of all the materials with their supplier information

Product	Molar Mass (g/mol)/Type	Form	Supplier
PCL	Mn-80,000	Pellets (~3mm)	Sigma-ALDRICH
PEG	Mn-400	Liquid	Sigma-ALDRICH
IBU	Mw-206.28	Powder	Sigma-ALDRICH
GE	Type A from porcine skin	Powder	Sigma-ALDRICH
HA	Cosmetic grade	Powder	Aroma-Zone
W966	---	Wax	BYK
G079	---	Wax	Mader
G127	---	Wax	Mader

1.6 Solvents

Different solvents were selected to measure the viscosity of 10wt% PCL solution for electrospinning. For this purpose, chloroform, chloroform: ethanol (88:12 wt/wt ratio), acetone, tetrahydrofuran (THF) and o-xylene were used. The technical data of these solvents is listed in the Table 2.2.

Table 2.2. Description of solvents.

Solvents	Supplier	Purity
Chloroform	Carlo Erba, France	>99.0%
THF	Carlo Erba, France	>99.0%.
Acetone	Honeywell, France	>99.5%
Ethanol	Honeywell, France	>99.5%
o-xylene	Sigma-ALDRICH, France	98.0%

2. Methods

2.1 Electrospinning solution preparation

A homogeneous solution of 10wt% PCL was prepared in a solvent mixture of chloroform: ethanol (88:12 wt/wt) ratio. To obtain a clear solution of PCL, the solution was magnetically stirred overnight at room temperature [1, 2]. After 12h, PEG was added to this clear PCL solution and was stirred for 15min with magnetic stirrer. Both concentrations of PEG 10wt% and 20wt% were calculated with respect to the weight of PCL. Similarly, 5wt% and 7wt% IBU calculated with respect to the weight of PCL were added directly to the clear PCL and PCL/PEG solutions respectively with a subsequent magnetic stirring for 10min each solution. Finally, all the solutions

were left in ultrasonic bath for 5-7min to remove air bubbles. The weight in grams of all the chemicals used is enlisted in Table 2.3.

Table 2.3. Weight in grams of all chemicals used in various concentrations

Materials	10%PCL	PCL/PEG-10%	PCL/PEG-20%	PCL+IBU 5wt%	PCL/PEG-10%+5%IBU	PCL+7%IBU	PCL/PEG-10%+7%IBU
PCL	4.5 g	4.5 g	4.5 g	4.5 g	4.5 g	4.5 g	4.5 g
Solvents	40.7 g	40.7 g	40.7 g	40.7 g	40.7 g	40.7 g	40.7 g
PEG	×	0.45 g	0.9 g	×	0.45 g	×	0.45 g
IBU	×	×	×	0.22 g	0.22 g	0.31 g	0.31

2.2 Elaboration of Na-IBU loaded nanocapsules of chitosan

The first attempt of electrospinning the drug loaded nanofibers was done by incorporating nanocapsules of chitosan loaded with sodium salt of Ibuprofen (Na-IBU) into PCL and PCL/PEG nanofibers. These nanocapsules of chitosan were synthesized and loaded with drug by Pr. Leonard-Ionut Atanase at Faculty of Dental Medicine, University “Apollonia”, Iasi-Romania.

The synthesis of nanocapsules of chitosan was documented by Rata *et al.* [3]. For encapsulation, 100mg nanocapsules of chitosan were dispersed in 4 ml of solution containing 80mg/ml Na-IBU and was maintained for 24h under stirring at 120rpm. The nanocapsules were separated by ultracentrifugation at 7,000rpm at room temperature for 10min and using a Laborzentrifugen equipment type SIGMA 3–30K ultracentrifuge. The amount of Na-IBU loaded into nanocapsules was calculated by the difference between the initial amount of Na-IBU and the amount of Na-IBU from supernatant using a UV Spectrometer (Nanodrop ONE) at 254nm. The efficiency of Na-IBU encapsulation (Eef %) into nanocapsules was calculated as follows:

$$\text{Eef\%} = \frac{mi - ms}{mi} \times 100$$

$$ml = mi - ms$$

Where, *ml* is the amount of loaded Na-IBU (mg), *mi* is the initial amount of Na-IBU (mg) and *ms* is the amount of Na-IBU found in supernatant (mg). The encapsulation efficiency of Na-IBU into nanocapsules and amount of loaded drug (Na-IBU/g nanocapsules) are presented in Table 2.4.

Table 2.4. Loading efficiency and amount of Na-IBU encapsulated into 1g of chitosan nanocapsules.

Sample code	Mean loading efficiency (%)	Mean loaded Na-IBU (g)/g nanocapsules
CN-1	88	2.8/1

2.3 Single-needle electrospinning set-up

In 2006, the Laboratoire de Physique et Mecanique Textiles (LPMT) devised a homemade set-up of vertical single-needle electrospinning as shown in Figure 2.1. The preliminary studies of PCL electrospinning, optimization of electrospinning parameters, PCL blending with PEG and incorporation of IBU were performed on this equipment.

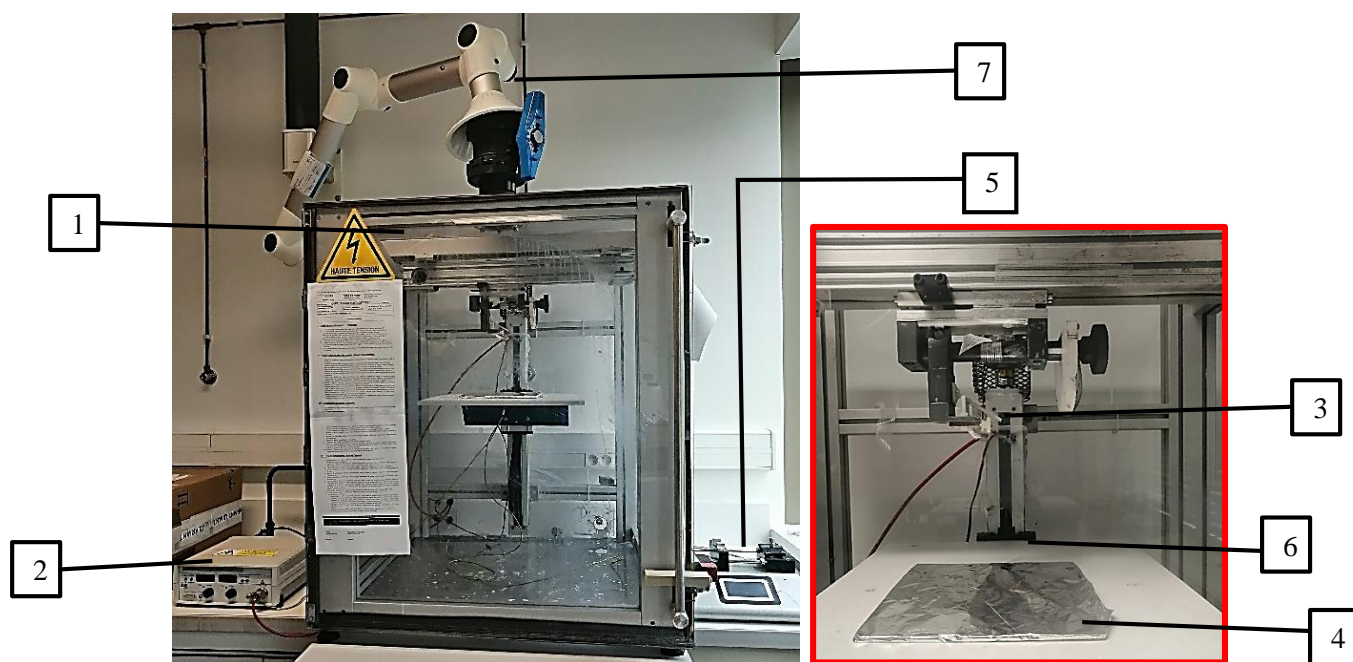


Figure 2.1. A homemade set-up of vertical single-needle electrospinning.

The main components of this single-needle electrospinning machine are shown and labeled in Figure 2.1. It consists of (1) an enclosed poly(methyl methacrylate) chamber, (2) connected to a high voltage (DC) source (10-30 kV) to create a potential difference between (3) the needle with a metallic tip to eject the polymer solution and (4) a grounded collector plate covered with aluminum foil, (5) an automated feeding pump is used to push the polymer solution contained in a plastic syringe through a tube towards the needle at a constant flow rate. The height of collector plate is adjustable by means of a mechanical adjustment tool attached to it (6). This enclosed chamber is connected to a vacuum ventilation hub (7) for removing evaporated solvents in order to avoid any health hazards. A security system is also installed in this equipment in the form of an electronic circuit that prevents the user from any risk of high voltage or electrical discharge. For all experiments the humidity and temperature were kept at $35 \pm 4\%$ and $25 \pm 2^\circ\text{C}$ respectively. All specifications and manufacturer details of the above mentioned parts are given in the Table 2.5.

Table 2.5. Specifications of different components of single-needle electrospinning equipment.

Components	Specifications/Model	Manufacturer
Automatic Feeding Pump	KD Scientific Legato 200 syringe pump	Delta Labo, France
High Voltage Source	LNC 30 kV-DC source	Heinzinger, Germany
Solution Syringe	20 mL, 2 cm inner diameter	BD Plastipak, USA
Collector	Aluminum foil of 0.016 mm thickness/ Teflon® plate 20×20 cm	Carl Roth, France
Needle	0.4 mm inner diameter	Terumo, Belgium

a) Design of experiment

For the production of nanofibers, a defined set of experiments called DOE (design of experiments) was outlined by keeping one electrospinning parameter constant while varying the others. This DOE was followed to investigate the effect of different electrospinning parameters on the electrospinnability of PCL solutions and optimization of these parameters in order to select the best of them which produce bead free nanofibers. Five different DOEs were followed to carry out several electrospinning experiments in order to investigate the effect of electrospinning parameters as shown in Tables 2.6, 2.7, 2.8, 2.9 and 2.10.

Table 2.6. DOE for 10wt% PCL by varying applied voltage (V)

Exp.#	Materials	PCL (wt%)	FR (mL/h)	V (kV)	D (cm)
1	PCL	10	0.5	15	25
2				18	
3				20	
4				23	
5				25	
6				28	
7				30	

Table 2.7. DOE for 10wt% PCL by varying needle to collector distance (D)

Exp.#	Materials	PCL (wt%)	FR (mL/h)	V (kV)	D (cm)
1	PCL	10	0.5	25	15
2					17
3					19
4					21
5					23
6					25
7					27
8					29
9					31
10					33

Table 2.8. DOE for PCL/PEG-10% by varying applied voltage (kV) and needle to collector distance (D) with feed rate (FR) 0.5 mL/h

Exp.#	Materials	PCL (wt%)	FR (mL/h)	V (kV)	D (cm)
1	PCL/PEG-10%	10	0.5	18	25
2				19	
3				20	
4	PCL/PEG-10%	10	0.5	18	20
5				19	
6				20	
7				21	
8	PCL/PEG-10%	10	0.5	18	15
9				19	
10				20	
11				21	

Table 2.9. DOE for PCL/PEG-10% by varying applied voltage (kV) and needle to collector distance (D) with feed rate (FR) 0.1 mL/h

Exp.#	Materials	PCL (wt%)	FR (mL/h)	V (kV)	D (cm)
1	PCL/PEG-10%	10	0.1	18	25
2				19	
3				20	
4	PCL/PEG-10%	10	0.1	18	20
5				19	
6				20	
7	PCL/PEG-10%	10	0.1	18	15
8				19	
9				20	

Table 2.10. DOE for PCL/PEG-10% by varying applied voltage (kV) and needle to collector distance (D) with feed rate (FR) 0.5 mL/h

Exp.#	Materials	PCL (wt%)	FR (mL/h)	V (kV)	D (cm)
1	PCL/PEG-20%	10	0.5	16	25
2				17	
3				18	
4				19	
5	PCL/PEG-20%	10	0.5	17	20
6				18	
7				19	
8				20	

By following these DOEs, a series of experiments was conducted to study the impact of each electrospinning parameter (applied voltage, needle to collector distance and feed rate) on the homogeneity of nanofibers and their morphology.

b) Statistical analysis to optimize ES parameters

In order to deduce a relationship between the homogeneity of nanofibers and applied electrospinning parameters, a statistical tool called Principal Component Analysis (PCA) was used to present all the results in a coordinate system to highlight their impact.

Principal Component Analysis (PCA) is a multidimensional descriptive statistical tool that extracts useful information when there is a lot of quantitative data to interpret. In addition, a graphic representation of the variables is possible in order to visualize their existing correlations. It highlights the similarities between individuals and the links between variables while minimizing the loss of information. The use of PCA therefore makes it possible to reduce the space of study of the variables and to clarify the inter-variable, inter-individual and variable-individual correlations. Moreover, the analysis can be carried out on reduced centered data, the so-called standardized PCA. The principle of this method is based on a linear transformation of the initial variables in a small dimensional space. The original variables are thus replaced by the new non-correlated maximum variance variables. These new variables are called principal components and define factorial plans allowing the graphic representation of the initial variables. The cumulative percentage of variance makes it possible to select the adequate number of principal components. Generally speaking, percentages of the order of 70 to 90 are recommended.

In standardized PCA, the variables are projected onto the factorial plane defined inside a circle of unit radius. In general, the more a variable will be projected towards the edge of the circle, the better the variable will be represented and therefore the more significant it will be. The cosine square (\cos^2) value of the angle between the vector of the variable and the main component of the projection makes it possible to objectively assess the quality representation of the variable on the circle. If two correctly represented variables are close to each other, then they will be positively

correlated. Conversely, if they are on opposite side of the circle, then they will be negatively correlated. Note that an orthogonality between the two variables will translate an absence of linear correlation. An example of a graphical representation of the results of a PCA is presented in Figure

2.2. Following facts are elaborated in it:

- The variables of the set being close to the center of the unit circle are not considered significant (group E).
- Each group of variables represents a set of positively correlated variables, as is the case of groups A and B.
- An opposition of groups of variables with respect to an axis (group A and B or C and D) reflects a negative correlation between them.
- When the groups are opposed along the two axes, for example groups B and F, the choice of axis depends on the closest groups. So, in case of groups B and F, we will therefore choose the horizontal axis.

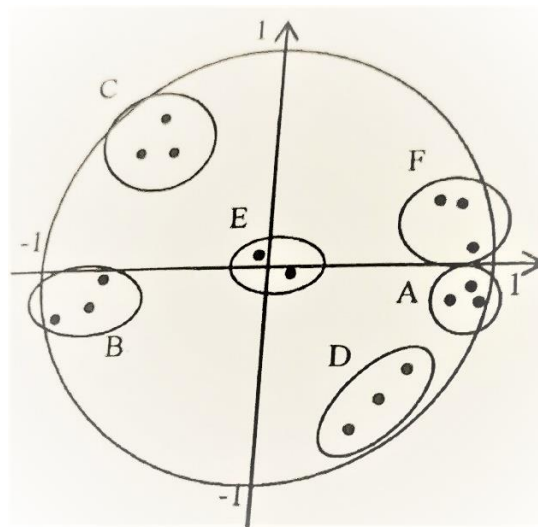


Figure 2.2. An example of graphical representation of PCA variables.

2.4 Needleless electrospinning equipment

Another electrospinning technique used to produce nanofibers was needleless electrospinning. All the samples of PCL, PCL/PEG and IBU loaded nanofibers were prepared using this technique. The electrospinning equipment used for this study was [®]Elmarco's needleless machine known as "NanoSpider" (Model NS 1WS500U, Czech Republic) is shown in Figure 2.3. This was an automated industrial electrospinning machine with a capacity of producing a continuous sample of nanofibers with a production rate of ~100g/h per meter. Two voltages (positive and negative) were applied ranging from 10-50kV and ΔV could reach 100kV. This technology does not use any needles instead; a wire electrode was installed at the base which acted as a fiber generator when a solution carrier moved across and coated it with the polymer solution. Description of all components of this machine are indicated in Figure 2.3 along with their respective numbers. This wire electrode (1) was 0.2mm in thickness and was positively charged. The wire passed through an orifice (2) (0.5 mm gauge was used for this study) fixed into the solution carrier (3) and it deposited an even layer of polymer solution on the wire as carrier moved back and forth. Another negatively charged wire electrode was situated above it (4) and a substrate passed under this wire at a predefined traverse rate (5). Under the influence of strong electric field, thousands of polymer jets were initiated as the solution carrier moved across the wire. These polymers jets moved towards the upper wire and on their way they encountered the substrate and were deposited in the form of nanofibers. In this phenomenon, nanofibers are produced by following the "free surface technology" principle. The humidity level inside the electrospinning chamber was controlled by the help of an in-built air flow regulator system. For all experiments the humidity and temperature were kept at $35 \pm 4\%$ and $25 \pm 2^\circ\text{C}$ respectively.

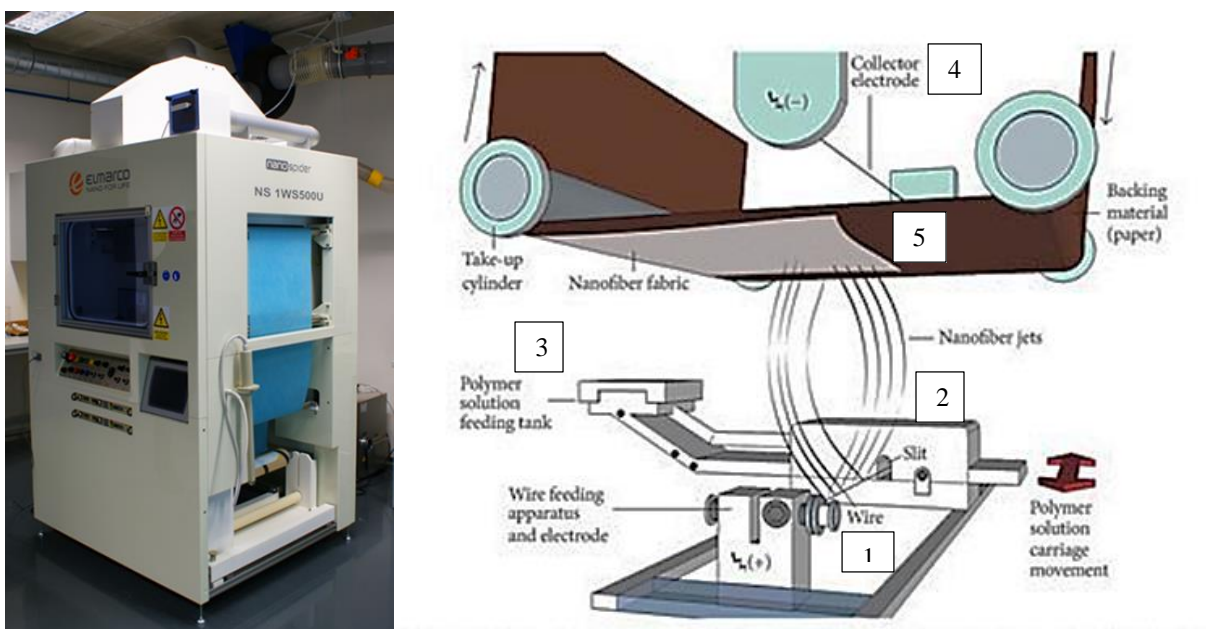


Figure 2.3. [®]Elmarco's lab unit of NanoSpider (Model-1WS500U) and schematic diagram of needleless electrospinning with wire electrodes

Design of experiment

Electrospinning of nanofibers was carried out by following the previous formulations and concentrations of PCL, PEG and IBU. All the nanofibers produced by needleless electrospinning and their electrospinning parameters are shown in the Table 2.11. Several preliminary experiments were done to finalize the optimum conditions of electrospinning for each sample.

Table 2.11. Nanofibers electrospun by NanoSpider and their applied electrospinning conditions

Exp.#	Materials	V (kV)	D (mm)	Nozzle Size (mm)
1	10wt% PCL	45	220	0.5
2	PCL/PEG-10%	40		
3	PCL/PEG-20%	43		
4	5%IBU+PCL	45		
5	5%IBU+PCL/PEG-10%	50		
6	5%IBU+PCL/PEG-20%	45		
7	7%IBU+PCL	45		
8	7%IBU+PCL/PEG-10%	50		
9	7%IBU+PCL/PEG-20%	50		

*Note: V is applied voltage and D is the distance between wire electrode and substrate.

2.5 GE/HA film preparation

In order to prepare the GE/HA film, 10% GE solution was prepared. To do so, 2g of GE was dissolved in 18g of distilled water to make a 10% GE solution. This solution was in gel form at room temperature so, it was heated to 40°C in a water bath with continuous stirring to get a liquid solution. In a separate container, 2.5% HA solution was prepared in distilled water (0.5 g of HA was added to 19.5g of distilled water). 2.5% HA gel was added to 10% GE solution in a quantity of 8.5g to have a GE/HA solution. This GE/HA solution was finally put in an ultrasonic bath for 5min to remove air bubbles. This GE/HA solution in liquid state was poured on a Teflon sheet and a smooth film was casted with the help of manual bar coater of 100µm thickness.

2.6 Fabrication of bilayer structure

To fabricate a bilayer nanofibrous structure, the electrospinning of IBU loaded PCL and PCL/PEG nanofibers was performed on the GE/HA film. The GE/HA coated Teflon sheet was immediately mounted in the NanoSpider machine and afterwards, the nanofibers of PCL and PCL/PEG with IBU were deposited on the wet GE/HA film via electrospinning at the optimum conditions. The coated Teflon sheet acted as nanofibers substrate and nanofibers adhered to the wet GE/HA film. The relative humidity RH% was $35 \pm 4\%$ and the temperature was kept at $25 \pm 2^\circ\text{C}$.

3. Characterization

To investigate the morphology, thermal and mechanical properties of nanofibers, various characterization techniques were utilized. The detail of all these instruments and procedures followed for the characterization of nanofibers are discussed in this section.

3.1 Viscosity analysis of PCL solution

To measure the viscosity of 10wt%PCL solutions in all the solvents, Anton Par MCR-302 plate-plate Rheometer was employed. All measurements were taken at room temperature (25°C) with a shear rate of 100s^{-1} . For each sample, 20 measuring points were taken and for each point time setting was 12s. All solutions were clear and homogeneous and viscosity was measured as a function of time.

3.2 Scanning Electron Microscopy (SEM) of nanofibers

Electrospun nanofibers were observed under Scanning Electron Microscope in order to determine their morphology, homogeneity and nanofibers diameters. For this purpose, JEOL's JSM-IT100 series SEM equipment and S-2360N Hitachi/Japan model were employed. Prior SEM analysis, all

samples were sputter coated with gold using a metallizer (POLARON E5100-France) to make them conductive as shown in Figure 2.4. After gold coating, samples were analyzed at a scale of 10 μ m-50 μ m. To assure accuracy, three images of each sample were taken from different points.

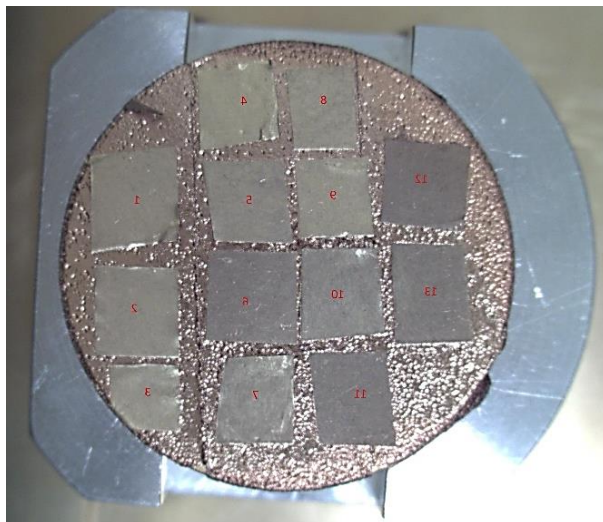


Figure 2.4. Gold coated SEM sample stub

a) Sample preparation

For SEM analysis, all samples of nanofibers were cut with great care in order to avoid any deformation during their handling process. A sharp cutter was used to cut nanowebs into $\sim 5\text{mm} \times 5\text{mm}$ square samples and were lifted with the help of forceps to avoid any distortions. These specimens were pasted on the SEM sample stub by using double sided conductive carbon tape. After preparation, these specimens were transported in a closed glass container to avoid contaminations.

b) Diameter measurements by ImageJ software

Diameters of nanofibers were measured by using ImageJ software by taking bar measurements of nanofibers depicted in SEM micrographs. Fifty random measurements were made per sample to ensure accuracy and to cover maximum area of sample. Mean diameters and standard deviation (SD) of nanofibers were calculated by the ImageJ software. The coefficient of variation (CV%) was calculated to conclude the overall morphology and homogeneity of nanofiber by following the Equation 1:

$$\text{CV\%} = \text{SD} / \text{Mean} \times 100 \quad (1)$$

3.3 Contact angle measurements

Water contact angle measurements were carried out by Drop Shape Analyzer (DSA 100 KRUSS GmbH, Germany) apparatus by Sessile drop method. A water droplet of 2 μl was dispensed from the needle and was dropped on the samples placed underneath on a glass plate. Distilled water was used as reference liquid and was allowed to drop automatically on the electrospun nanofibers. Time to measure the water contact angle was 10s after the water droplet dropped. Measurements were recorded by CCD video camera installed inside the instrument. Five droplets for each sample were deposited and analyzed.

Preparation of PCL film for contact angle analysis

A pure PCL film was used as a reference. To prepare this film, 10wt% PCL solution was prepared by using a solvent mix of chloroform: ethanol (80:12 wt/wt) and was magnetically stirred overnight. This solution was utilized to cast a smooth film on a Teflon sheet by employing a manual bar coater of 100 μm thickness. After coating a thin film of PCL solution on Teflon sheet,

this sheet was placed in a drying oven for 3 hours at 40°C to evaporate all the solvents. After complete drying, it was used to measure the water contact angle.

3.4 Differential Scanning Calorimetry (DSC) analysis of nanofibers

Thermal properties of pure PCL, pure PEG and all samples of PCL nanofibers were determined by using Differential Scanning Calorimeter (DSC) model TA instrument Q200. Specimens of approximately 9mg in weight were sealed in non-hermetic aluminum capsules. Experiments were performed under nitrogen atmosphere with a dual cycle of heating from -80°C to 100°C at a rate of 10°C/min. The glass transition and melting temperatures of each sample were determined and the crystallinity ratios (X_c) of PCL, PCL/PEG and IBU loaded nanofibers were calculated. The crystallinity ratios of all nanofibers were calculated with reference to the content of PCL used for each sample. X_c was determined by using following Equation 2:

$$X_c (\%) = \Delta H_m / \Delta H_m \text{PCL} \times 100 \quad (2)$$

Where, ΔH_m is the melting enthalpy of PCL nanofibers and $\Delta H_m \text{PCL}$ is the melting enthalpy of 100% crystalline PCL [4]. In case of blend PCL/PEG nanofibers, the X_c of only PCL nanofibers was calculated by subtracting the content ratio of PEG.

3.5 Thermogravimetric analysis (TGA) of nanofibers

To determine the thermal stability and degradation behavior of nanofibers, thermogravimetric analysis (TGA) was performed by using TA instrument model Q500. All samples were analyzed under nitrogen with 10°C/min rate of heating ramp till 800°C.

3.6 Particle size distribution measured by light scattering

The particle size distribution of nanocapsules of chitosan in chloroform was measured by light scattering (Malvern-Mastersizer 3000). This equipment uses the laser technique of laser diffraction to measure the particle size and particle size distribution. The particle size distribution results were measured in number for their D10, D50 and D90 values. The D10 value indicates that the portion of particles with diameters smaller than this value is 10%, D50 is the portion of particles with diameters smaller and larger than this value are 50% and D90 is the portion of particles with diameters below this values are 90%.

3.7 Optical Microscopy

Optical microscopy snapshots of agglomerates of nanocapsules in PCL solution were obtained from an Olympus BX51 piloted equipment by using the software cell^A. The images were taken in reflecting mode at a 50 μ scale. Images obtained were optimized in terms of contrast in order to get well-defined photos.

3.8 Tensile strength testing of nanofibers

To study the mechanical properties of electrospun PCL nanofibers and GE films, the MTS M/20 tensile testing machine was used which used a load cell with capacity of 10N and an elongation rate of 10mm/min. To perform this test, samples were prepared by following a specific procedure reported by Hekmati *et al.* [5].

For the nanofibers, rectangular strips were cut from different areas of sample in 20mm \times 5mm dimensions using a roller cutter. Schut's digital micrometer with a precision value up to 0.001mm was used to measure the thickness of each sample at five different points to cover all the possibilities. All specimens were weighed on a micro balance before testing. The specimens were

conditioned in atmospheric conditions at 20 ± 2 °C and 65 ± 2 % relative humidity for 48h before testing according to ASTM standard. Double-edge duct tape was placed on both edges of the sample to facilitate its grip between the jaws of tensile tester. Cut samples were sandwiched between two cardboard layers which functioned as templates and made it possible to easily handle and grip the specimens in jaws for mechanical testing. The edges of the cardboard along with the specimen ends were placed between the grips of tensile testing machine so that the area of nanofibers between the two jaws remained 10mm as shown in the Figure 2.5. The cardboard templates were cut after fixing specimens between pneumatic clamps of the tensile machine and tests were performed at room temperature. Four samples for each specimen were tested to analyze the tensile strength.

For GE films, all above mentioned steps were followed. Only difference was that the rectangular strips of GE films were cut in 20mm × 5mm dimensions and no prior conditioning of samples was done. The thickness of films was measured by using Schut's digital micrometer and a mean was taken for each sample.



Figure 2.5. Specimen between the jaws of MTS M/20 Tester

4. Biological Testing

PCL, PCL/PEG and IBU loaded nanofibers were characterized for their biological aspects. These nanofibers were analyzed for their biocompatibility and safe use for biomedical applications. The IBU loaded nanofibers were studied for their drug release kinetics and drug release behavior over a defined period of time. The antibacterial efficiency of nanofibers against gram positive and gram negative bacteria was also tested. All the biological analysis and their methodologies are explained in this section.

4.1 Drug release kinetics

The in vitro drug release kinetics for IBU loaded nanofibers were studied by Pr. Leonard-Ionut Atanase and his team at the Faculty of Dental Medicine, University “Apollonia”, Iasi-Romania. The dialysis method was used to perform this analysis. Each sample was introduced into a dialysis membrane and was suspended into 10ml of phosphate buffer saline solution (PBS) with pH 7.4 at $37^{\circ}\text{C} \pm 0.5^{\circ}\text{C}$ under constant stirring. Certain volumes of solution, approximately $2\mu\text{L}$ were taken out at pre-established time intervals and the concentration was determined by UV-Vis spectroscopy according to a calibration curve shown in Figure 2.6. The release efficiency of IBU (RE%) was calculated using the following Equation 3:

$$\text{RE\%} = m_r/m_l \times 100 \quad (3)$$

Where, m_r is the amount of released IBU (mg) and m_l is the amount of loaded IBU (mg) in nanofibers.

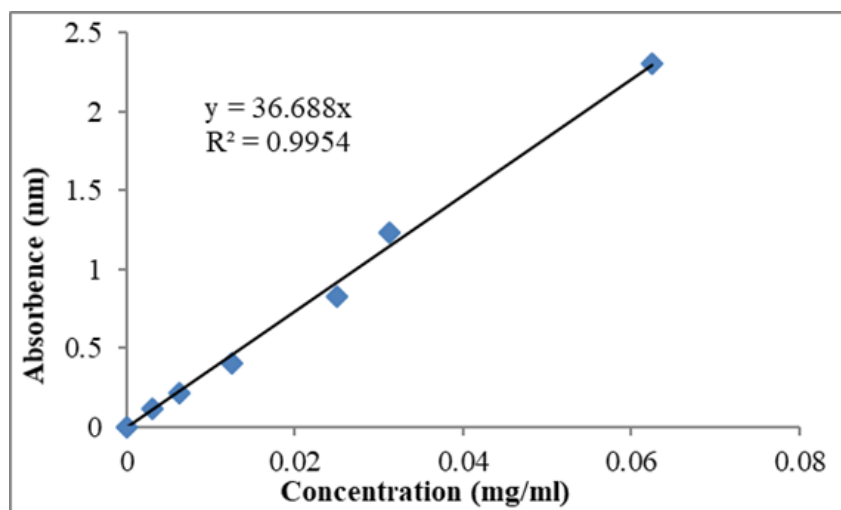


Figure 2.6. Calibration curve for IBU release

4.2 In-vitro antimicrobial assay

The IBU loaded nanofibers and the final bilayer wound dressing material were characterized for their resistance against *E. coli* (gram-negative) and *S. epidermidis* (gram-positive) bacterium. The specifications of all the materials and their suppliers are given in the Table 2.12.

Table 2.12. Specifications and Supplier Information of Materials used in Antibacterial Analysis

Materials	Specification	Supplier
<i>Escherichia coli</i>	Gram negative bacteria	Centre de Ressources Biologiques de l'Institut Pasteur (CRBIP)
<i>Staphylococcus epidermidis</i>	Gram positive bacteria	Centre de Ressources Biologiques de l'Institut Pasteur (CRBIP)
Culture media	Terrific Broth (TB)	Carl Roth-Germany
Agar media	Mueller-Hinton Agar (MHA)	Fisher Scientific-France

a) Preparation of Bacteria Culture

The lyophilized bacteria strains were rehydrated with 200 μ L of Terrific Broth (TB) medium and placed in a sterilized tube containing 2mL of TB medium. *S. epidermidis* was incubated at 37°C while *E. coli* was incubated at 30°C during 24h. Each bacterial strains were transferred in another tube containing 2mL of TB medium and incubated under agitation (120 rpm) at 37°C during 36h for *S. epidermidis* and at 30°C during 24h for *E. coli*. After the incubation, each type of bacteria was transferred with a single inoculation loop into a new tube containing 2mL of TB medium and was placed in the same conditions. After a new cycle of 36h for *S. epidermidis* and 24h for *E. coli*, these bacteria cultures were used for antibacterial analysis.

b) Antibacterial Analysis

Petri dishes, containing Mueller-Hinton Agar (MHA) medium were inoculated with bacterial cultures, thanks to an inoculation loop. Disks of nanofibers (5 mm diameter) were disposed on the surface of MHA medium as well as sterile disks impregnated with 15 μ L of chloramphenicol solution (25 mg/L in MeOH) as control. Petri dishes were then placed at 37°C during 36h for *S. epidermidis* and at 30°C during 24h for *E. coli*. The zones of inhibition were examined for each sample and all experiments were performed in triplicate.

5. Conclusion

In this chapter, all the details of materials and methodology employed for this study is narrated. The specifications of chemicals are given along with their supplier information. Procedures are described in length to carry out all the experiments and characterization. All the operating principles and conditions are mentioned with their respective procedures. Steps of sample preparations for specific characterization are also enlisted. Thus, a comprehensive outline is delineated about the two different electrospinning techniques used to produce nanofibers and then the physio-chemical and biological characterization of these nanofibers. The obtained results from all these characterizations will be discussed in the successive chapters.

References

1. Trinca, R.B., et al., *Electrospun multilayer chitosan scaffolds as potential wound dressings for skin lesions*. European Polymer Journal, 2017. 88: p. 161-170.
2. Liu H., L.K.K.a.Z.Y., *Antimicrobial Properties and Release Profile of Ampicillin from Electrospun Poly(ϵ -caprolactone) Nanofiber Yarns*. Journal of Engineered Fibers and Fabrics, 2010. 5(4): p. 1024-1031.
3. Rață D. M., P.M., Chailan J-F., Tamba B. I., Ionut Tudorancea and Peptu C. A., *Ibuprofen-loaded chitosan/ poly(maleic anhydride-alt-vinyl acetate) submicronic capsules for pain treatment*. Journal of Bioactive and Compatible Polymers, 2013. 28(4): p. 368-384.
4. Wang X., Z.H., Turng L-S. and Li Q., *Crystalline Morphology of Electrospun Poly(ϵ -caprolactone) (PCL) Nanofibers*. Industrial & Engineering Chemistry Research, 2013. 52(13): p. 4939-4949.
5. Hekmati A. H., K.N., Nazir A., Adolphe D., Schacher L. and Drean J. Y., *A Facile Approach for Sample Preparation of Electrospun Polyamide-6 Nanoweb for Mechanical Characterization*. Experimental Techniques, 2016. 40(6): p. 1549-1554.

Chapter 3: Single-Needle Electrospinning & Characterization of PCL Nanofibers

Chapitre 3: Electrofilage à une aiguille et caractérisation des nanofibres PCL et PCL/PEG

Ce chapitre présente l'ensemble des résultats des études préliminaires de l'électrofilage d'une solution à 10 wt% en PCL dans un mélange chloroforme/éthanol (88wt/12wt) en utilisant la technique d'électrofilage à une seule aiguille. Initialement, l'optimisation des paramètres d'électrofilage a été effectuée à partir d'échantillons de nanofibres obtenus en utilisant des solutions de PCL, PCL/PEG-10% et PCL/PEG-20% pures à 10% en masse de PCL dans un solvant chloroforme: éthanol (88:12 wt / wt). Les paramètres appliqués tels que la tension, la distance aiguille-collecteur et le débit d'alimentation de la solution ont été modifiés pour étudier leur impact sur la morphologie et les diamètres des nanofibres. En utilisant un outil statistique appelé «Analyse en Composantes Principales», les meilleurs paramètres d'électrofilage pour chaque échantillon ont été sélectionnés sur la base de l'homogénéité des diamètres des nanofibres. La caractérisation SEM des nanofibres PCL et PCL/PEG a révélé que leur morphologie était hétérogène avec des diamètres allant du nano au micro. Toutes les nanofibres étaient principalement de forme cylindrique et les nanofibres PCL/PEG-10% présentaient des pores à leur surface. Des nanocapsules de chitosane chargées de Na-IBU ont été incorporées à des nanofibres PCL afin de développer un système de délivrance de médicaments. Cependant, en raison de leur mauvaise dispersion et de leur agglomération dans les solutions de PCL et PCL/PEG, leur utilisation a été interrompue pour des études expérimentales supplémentaires. Pour remplacer ces nanocapsules, l'ibuprofène pur (IBU) qui est un médicament anti-inflammatoire et non stéroïdien, a été choisi comme substitut approprié. Deux concentrations différentes d'IBU, 5% en masse et 7% en masse ont été incorporées aux solutions de PCL et PCL/PEG-10%. L'étude morphologique de ces nanofibres chargées en

IBU a révélé que l'ajout d'IBU a donné des nanofibres de forme ronde avec des diamètres relativement plus grands dans la gamme du micron.

Des études DSC, il a été constaté que les taux de cristallinité des nanofibres électrofilées PCL et PCL/PEG étaient plus élevés que ceux de la PCL pure et cet effet était plus prononcé pour les nanofibres contenant du PEG-400. En revanche, les nanofibres contenant de l'IBU présente une cristallinité plus faible, malgré la présence de PEG-400 indiquant que la présence d'IBU limitait la cristallisation des chaînes PCL. Cet effet amélioré du taux de cristallinité des nanofibres PCL se reflète également dans les mesures d'angle de contact avec l'eau où un angle de contact plus élevé a été enregistré pour les nanofibres PCL par rapport à un film PCL pur vérifiant leur nature hydrophobe. En revanche, une absorption rapide des gouttelettes d'eau a été observée dans le cas des nanofibres PCL/PEG qui ont montré une mouillabilité améliorée en raison de l'ajout de PEG-400 hydrophile. Les résultats de la caractérisation thermique des nanofibres ont confirmé l'absence de solvant résiduel après électrofilage. De plus, dans les courbes de dégradation thermique des nanofibres chargés en IBU, la présence de pics intermédiaires correspondants à l'IBU a validé le chargement réussi du médicament dans la structure des nanofibres.

La détermination de la résistance à la traction uniaxiale des nanofibres PCL/PEG a montré qu'en augmentant la concentration de PEG-400 dans les nanofibres PCL, la résistance globale à la traction est diminuée car le PEG-400 agit comme un plastifiant. En outre, la courbe contrainte-déformation des nanofibres avec IBU a démontré de mauvaises propriétés mécaniques par rapport à leurs homologues PCL/PEG. Enfin, l'étude de la cinétique de libération du médicament in vitro des nanofibres chargées en IBU a été menée pour évaluer leur performance en tant que système d'administration de médicament. Une première libération rapide d'IBU a été enregistrée pendant les deux premières heures d'analyse suivie d'une libération progressive. L'efficacité du relargage de l'IBU atteint 82% en 24h d'analyse.

CHAPTER 3

SINGLE-NEEDLE ELECTROSPINNING AND CHARACTERIZATION OF PCL NANOFIBERS

1. Introduction

Electrospinning is a facile yet versatile technology that is used to create nanofibrous nonwoven structures in the nanoscale range for biomedical applications. The basic principle of this promising technique is the application of strong electrical field to eject the polymer solution from a reservoir to a collector surface to fabricate a nonwoven fiber network. Solution properties such as, concentrations of polymers, solvent nature, solution viscosity and the processing parameters like, applied voltage, electrospinning distance and solution feed rate affect the morphological, physical and mechanical properties of obtained nanofibers [1, 2]. Due to a wide variety of materials available, electrospinning has emerged as an adaptable method to develop various types of micro and nano structures for their potential use as a drug delivery system for wound dressing applications [3, 4].

Poly(ϵ -caprolactone) (PCL) is a biocompatible and biodegradable polymer which exhibits good mechanical properties. It is FDA approved polymer that has been widely used for biomedical applications over the last few decades [5]. Low cost, readily availability and slow degradation of PCL make it a good choice to be used for electrospinning [6]. However, the hydrophobic nature of PCL nanofibers is a limitation for their use as a wound dressing material [7]. In order to rectify this problem, a number of studies were dedicated to research about PCL blending with other polymers to tailor the hydrophilic properties of resulting nanofibers [8-11]. This part has already been well described in Chapter 1 where, PCL blending with several other hydrophilic polymers

like polyethylene glycol (PEG)/ polyethylene oxide (PEO), polyvinyl alcohol (PVA), polylactic acid (PLA) and polylactic co-glycolic acid (PLGA) is reported.

The novelty of this research study is the use of a low molar mass of PEG with Mn-400 for PCL blending. In literature, no study was found reporting the use of PEG-400 for PCL blend electrospinning. This is the first time when such a low molar mass of PEG is employed for the electrospinning of PCL/PEG nanofibers and their properties were investigated. The purpose of using a low molar mass PEG was to modify the physical properties of PCL nanofibers such as its hydrophobicity and rigidity. A hypothesis was drawn that addition of PEG-400 will improve the wettability of nanofibers while introducing pliability to the PCL nanofibers. A model drug, Ibuprofen (IBU) which is an anti-inflammatory, non-steroidal drug commonly known as NSAID was incorporated into the PCL nanofibers to devise a drug delivery system for the treatment of pain and inflammation in the wounds [12, 13]. Two concentrations of IBU were used and their impact on electrospinning and characteristics of PCL and PCL/PEG nanofibers was studied.

2. Viscosity of PCL in different solvents

In order to determine a suitable solvent system for electrospinning of PCL, different single and a binary solvent systems were studied. Besides chloroform, PCL is also soluble in a whole range of other solvents like tetrahydrofuran (THF), acetone, dimethylformamide (DMF), o-xylene, formic acid and acetic acid [14]. Among all these solvents, formic acid and acetic acid are the least toxic in nature but they could be responsible for the hydrolytic degradation of PCL [15]. The use of methanol and ethanol, which are non-solvents of PCL is also reported in literature in combination with chloroform to improve the electrospinnability of PCL solutions [16]. Therefore, chloroform, acetone, THF and o-xylene were used as single solvents and a binary solvent system of chloroform

and ethanol in 88:12 wt/wt ratio was employed to measure the viscosity of PCL solutions. The PCL concentration was fixed at 10wt% for all the solutions.

The viscosity (MPa.s) of all PCL solutions as a function of time (s) are presented in Figure 3.1. The viscosity values of PCL in chloroform and chloroform: ethanol (88:12 wt/wt) solvents were the highest in a range of 3200-3600 MPa.s. Whereas, the PCL solutions in THF, acetone and o-xylene exhibited an extremely different behavior with very low viscosity values of 600, 500 and 300 MPa.s respectively.

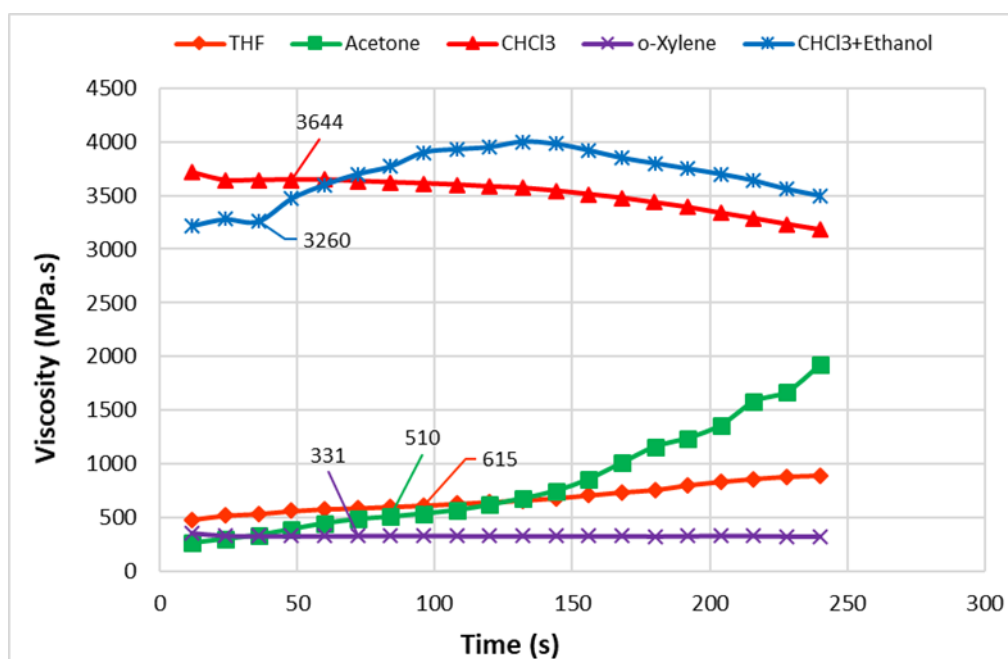


Figure 3.1. Viscosity (MPa.s) of all PCL solutions in different solvents as a function of Time (s) determined by using Anton Paar plate-plate rheometer at room temperature (25°C) under a shear rate of 100 s⁻¹

This vast difference in viscosities showed the interaction of PCL molecular chains with different solvents. Higher viscosity value indicates the better solubility of PCL in the respective solvent which translates into stronger intermolecular interactions between polymer chains and solvent molecules. For problem-free electrospinning and bead-free nanofibers, the choice of solvent and its solution viscosity plays a key role. So, a homogenous polymer solution with optimum viscosity

is needed to perform successful electrospinning process. It was found in literature that, too low or too high viscosities are not favorable for the production of continuous and bead-free nanofibers [16, 17]. Higher solution viscosity and reduced surface tension, contribute to the bead-free formation of nanofibers. Concentration of polymer controls the final solution viscosity and the coefficient of surface tension depends upon the interaction of polymer and solvent. For example, the addition of ethanol to the solvent system can reduce the surface tension coefficient that will avoid the bead formation and will ensure smooth electrospinning of nanofibers under electric field [18]. Therefore, after analyzing these viscosity values, the binary solvent system of chloroform: ethanol (88:12 wt/wt) was selected as a suitable solvent for preparing PCL solutions. All the experiments in this study were performed using this binary solvent system.

3. Morphology of nanofibers

The electrospinning of all kinds of nanofibers was carried out by following their respective DOE's (design of experiments) mentioned in Section 2.3 (a) of Chapter 2. The electrospinning parameters were varied and tested to study their impact on the morphology of resulting nanofibers and their mean diameters. Diameters were measured by ImageJ software by taking bar measurements and then the mean diameter, standard deviation and coefficient of variation were calculated for each sample.

3.1 Pure PCL nanofibers

The SEM images of 10wt% PCL nanofibers at different voltages and needle-collector distances are shown in Figure 3.2 and 3.3. All the images were taken at 50 μ m scale. Their mean diameters, standard deviation and CV% are given in Table 3.1.

F.R = 0.5 mL/h and D = 25 cm

50 μ m scale

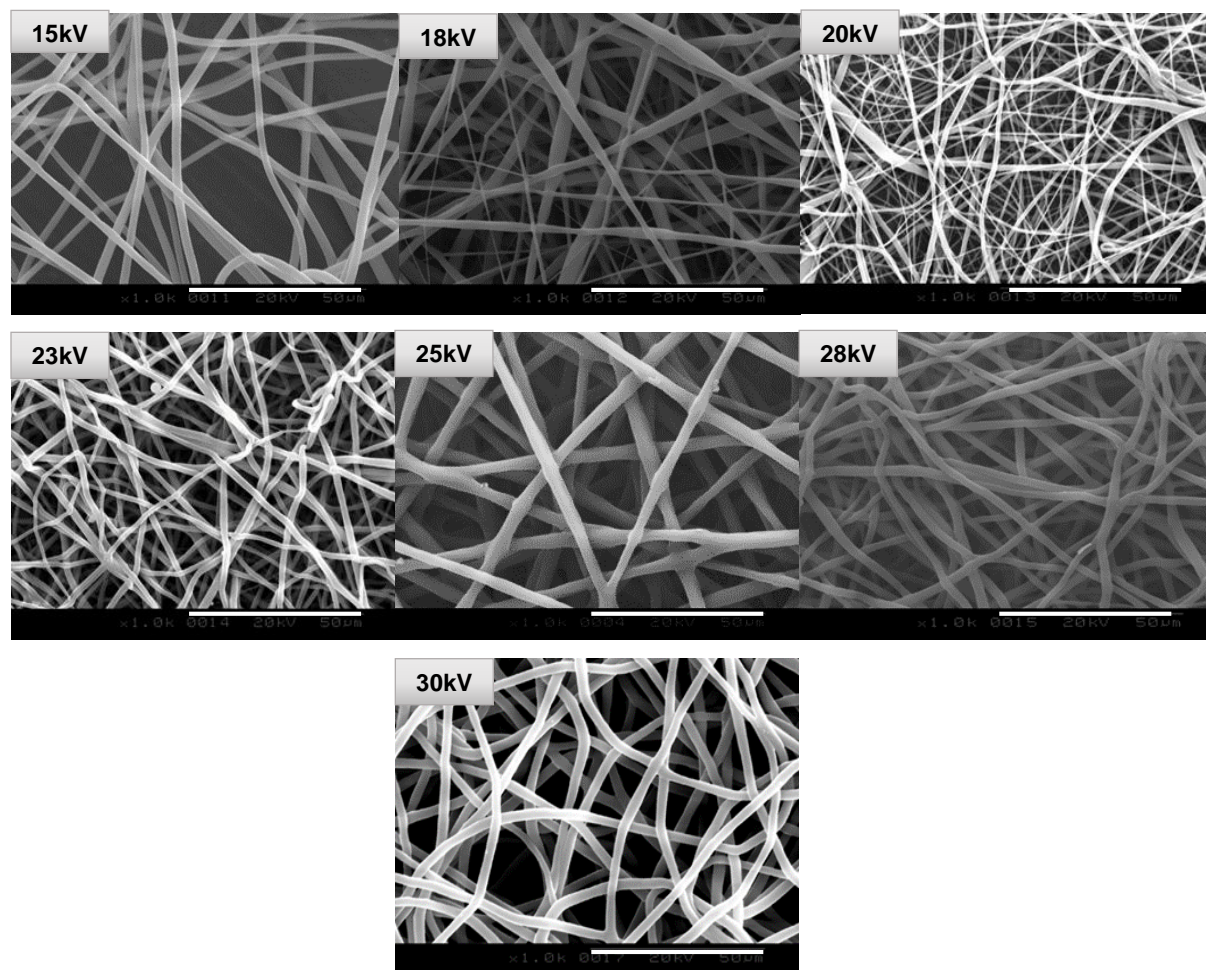


Figure 3.2. SEM images of 10wt% PCL nanofibers at different applied voltages

All the nanofibers were circular in shape with no bead formation. The overall morphology of these nanofibers was heterogeneous with a mix of micro and nano fibers. No particular alignment of nanofibers was seen. At higher voltage, larger diameters were obtained but with less variations. It is established from the literature that electrospinning of PCL in chloroform produces rather larger diameters but continuous bead-free nanofibers are obtained [19-22].

F.R = 0.5 mL/h and V = 25 kV

50 μ m scale

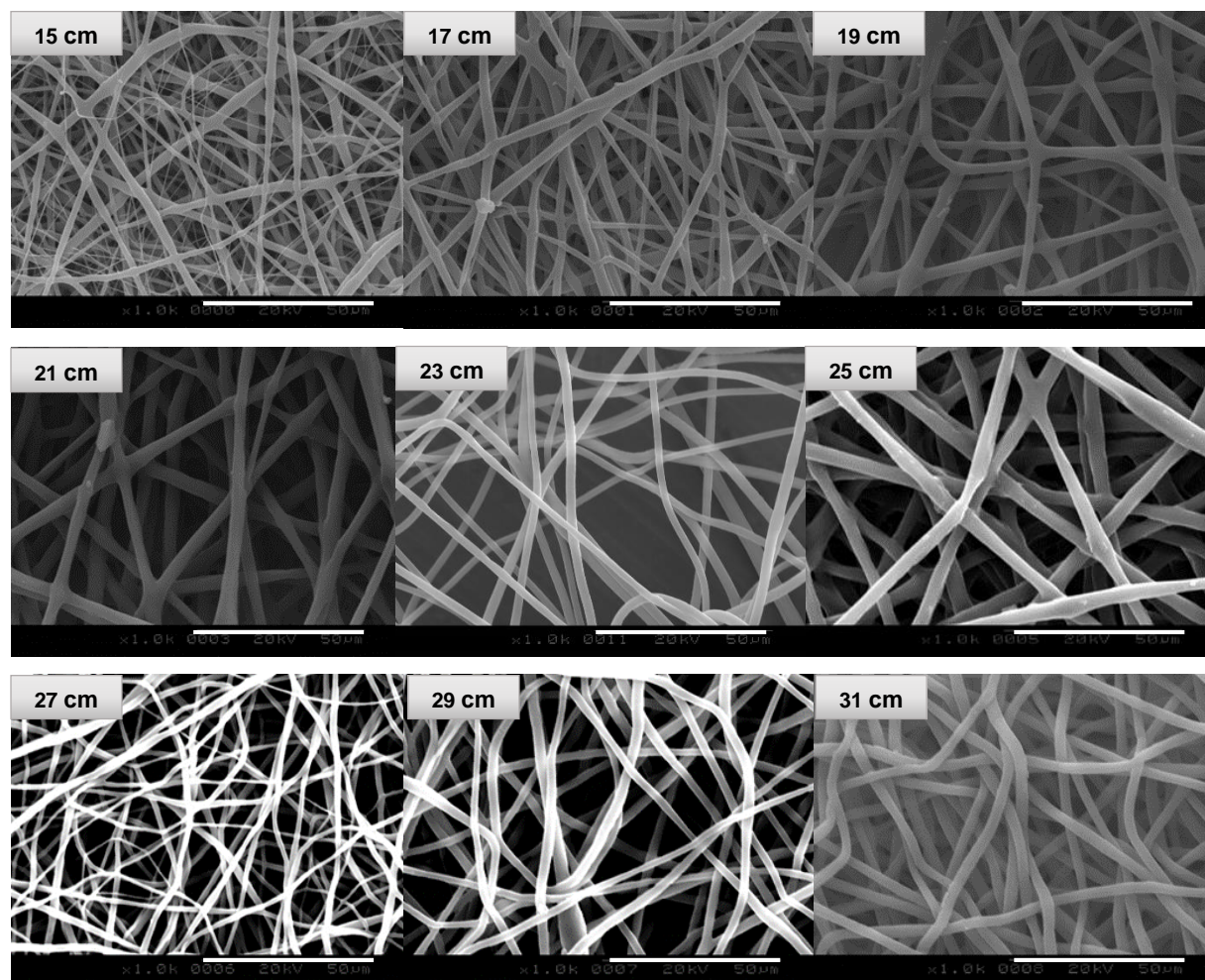


Figure 3.3. SEM images of 10wt% PCL nanofibers at different needle-collector distances

Similarly, when the needle-collector distance (D) was varied by fixing the applied voltage (V) at 25kV and feed rate (F.R) at 0.5mL/h, round-cylindrical shaped nanofibers were achieved with heterogeneous morphology. No bead formation or structural irregularity was found in nanofibers. At smaller values of D, the variation in diameters was very high as it can be seen in Figure 3.3. As the D increased, more uniform nanofibers were obtained.

Table 3.1. Mean diameters and CV% of 10wt% PCL nanofibers at different electrospinning parameters

F.R mL/h	V (kV)	D (cm)	M.D (nm)	CV%
0.5	15	25	1990 ± 340	17
	18		1125 ± 700	64
	20		520 ± 310	60
	23		1240 ± 470	37
	25		3530 ± 500	14
	28		1825 ± 435	24
	30		2340 ± 450	19
	25	15	990 ± 800	82
		17	1390 ± 570	41
		19	1680 ± 550	33
		21	2800 ± 870	31
		23	3400 ± 800	23
		25	3530 ± 500	14
		27	1220 ± 520	43
		29	2040 ± 445	21
31	2840 ± 380	13		

The bold figures in Table 3.1 are the optimum parameters selected for the electrospinning of pure PCL nanofibers. Although, the diameters of PCL nanofibers achieved at these electrospinning conditions were in micro range but they were homogenous showing less CV%.

3.2 PCL/PEG-10% nanofibers

By following the DOE described in Chapter 2, the electrospinning of PCL/PEG-10% was done. Again, the electrospinning parameters were varied to investigate their influence on the morphology of nanofibers. The SEM images of the PCL/PEG-10% nanofibers can be seen in Figure 3.4. All the images were taken at 20µm scale.

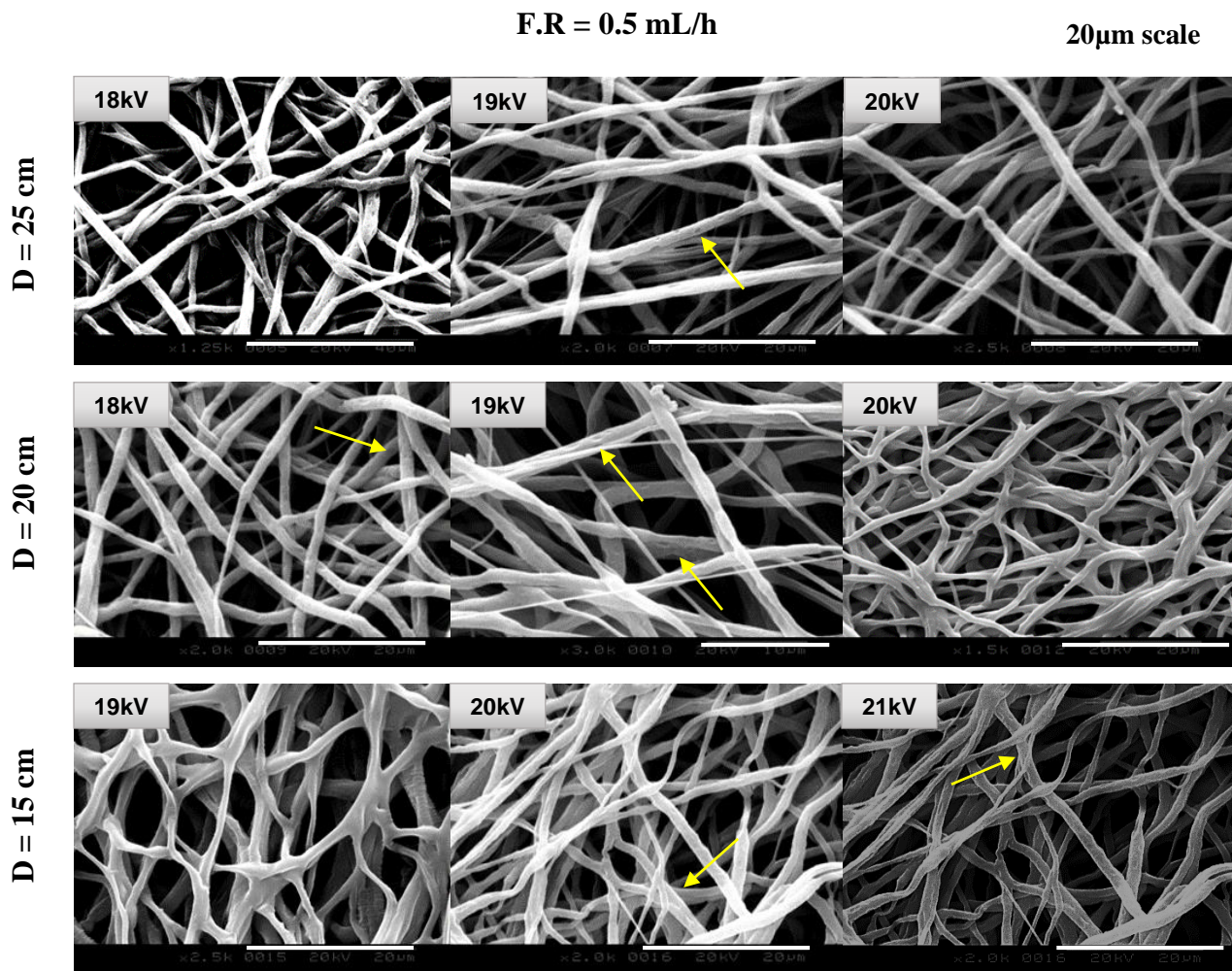


Figure 3.4. SEM images of PCL/PEG-10% nanofibers at different electrospinning parameters

***Yellow arrows indicate the presence of pores**

Impact of PEG-400 on the morphology of PCL nanofibers

The general morphology of PCL/PEG-10% nanofibers was heterogeneous with nanofibers both in nano and micro range. But, the addition of PEG-400 produced finer diameters as compared to pure PCL nanofibers. A significant drop was observed in diameters of nanofibers and dense nanofibers networks were formed. The decrease in diameters by adding PEG-400 could be due to the enhanced electrical conductivity of the polymer solution which resulted in greater bending instability in polymer jets. Consequently, further elongation of polymer jets occurred leading finer diameters of nanofibers [23]. There were pores on the surface of nanofibers that could be due to

the ejection of liquid PEG-400 during the electrospinning process. These pores can be clearly seen in Figure 3.5 marked with yellow arrows. The presence of pores on the PCL/PEG nanofibers surface was also reported in previous studies [7, 11]. The average diameters and their standard deviations along with CV% are listed in Table 3.2.

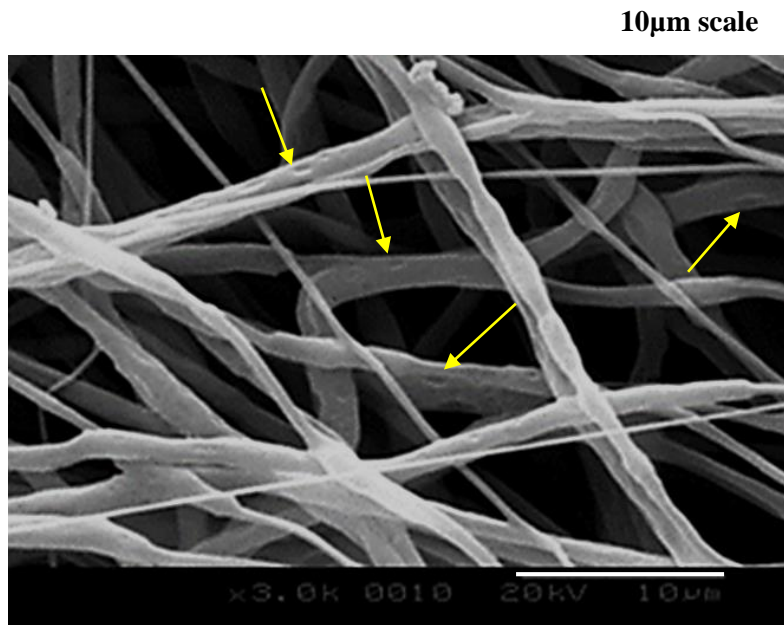


Figure 3.5. Pores on the surface of PCL/PEG-10% nanofibers

Table 3.2. Mean diameters and CV% of PCL/PEG-10% nanofibers at different electrospinning parameters

F.R mL/h	V (kV)	D (cm)	M.D (nm)	CV%
0.5	18	25	1560 ± 490	31
	19		1010 ± 495	49
	20		990 ± 365	37
	18	20	1290 ± 610	47
	19		940 ± 465	49
	20		940 ± 327	35
	19	15	970 ± 290	30
	20		920 ± 400	44
	21		450 ± 245	54

The optimum electrospinning parameters for the PCL/PEG-10% nanofibers are shown in bold figures in Table 3.2. These parameters were selected on the basis of homogeneity of nanofibers which showed less variations in their diameters. Addition of PEG-400 considerably reduced the diameters of nanofibers as compared to pure PCL nanofibers.

3.3 PCL/PEG-20% nanofibers

For PCL/PEG-20%, the DOE described in Chapter 2 was employed by varying electrospinning parameters. The SEM images of all PCL/PEG-20% nanofibers can be seen in Figure 3.6. All the images were taken at 10 μ m scale.

F.R = 0.5 mL/h

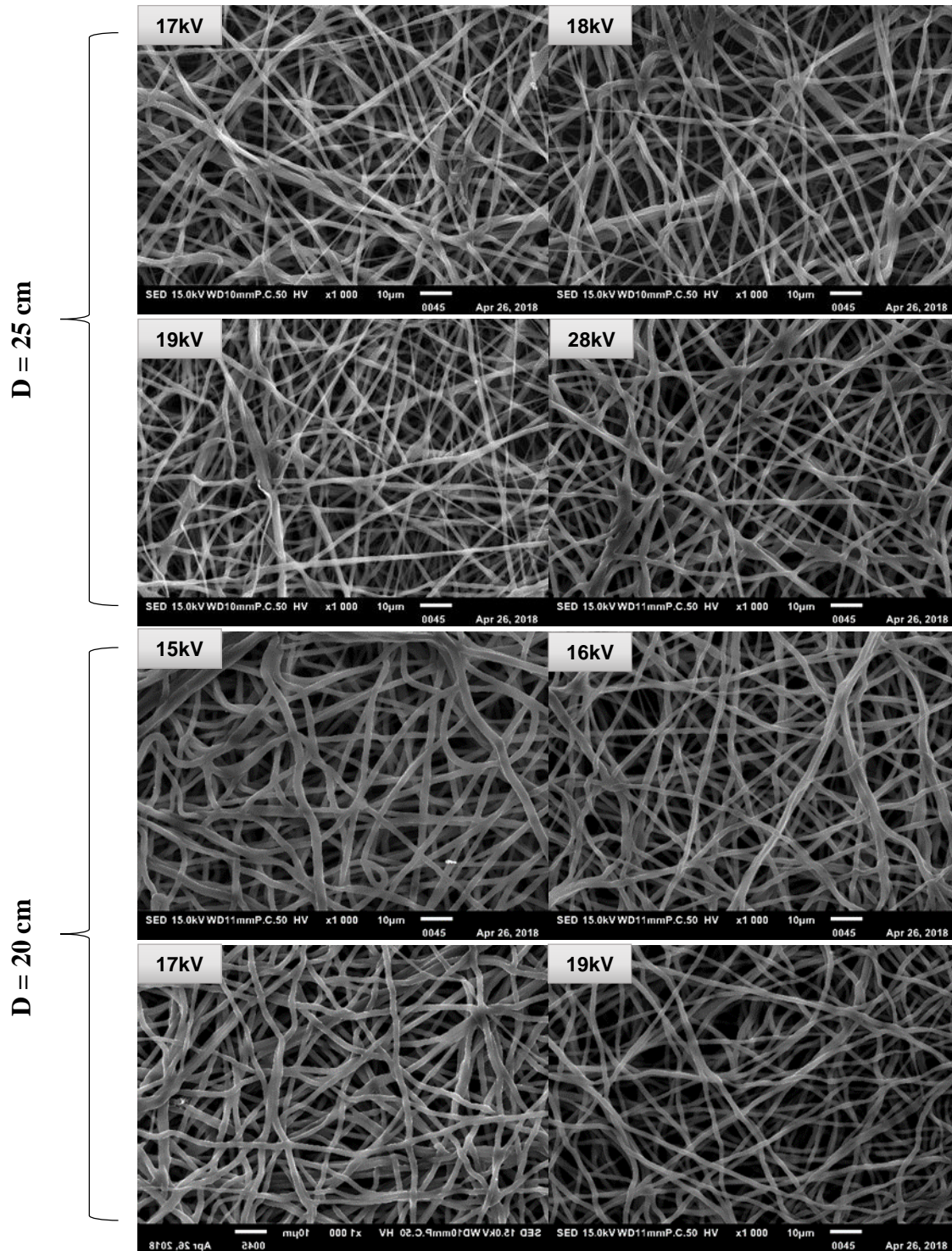


Figure 3.6. SEM images of PCL/PEG-20% nanofibers at different electrospinning parameters

No pores were observed on the surface of PCL/PEG-20% nanofibers as it was the case with PCL/PEG-10% nanofibers. A dense network of smooth cylindrical shaped nanofibers with heterogeneous morphology was created. No beads or entanglements were observed in the structure. These nanofibers lack uniformity in diameters along their length like previously described cases. Diameters were in a range of 800-1300nm scale with CV% ranging from 30-50% as shown in Table 3.3.

Table 3.3. Mean diameters and CV% of PCL/PEG-20% nanofibers at different electrospinning parameters

F.R mL/h	V (kV)	D (cm)	M.D (nm)	CV%
0.5	15	20	1370 ± 610	44
	16		830 ± 300	36
	17		1025 ± 339	33
	19		1100 ± 300	27
	17	25	840 ± 365	43
	18		910 ± 475	52
	19		675 ± 300	45
	20		862 ± 345	40

The best electrospinning conditions for PCL/PEG-20% shown in bold figures in Table 3.3 were chosen depending upon the homogeneity of nanofibers with less CV%. In this case of PCL/PEG-20% nanofibers, decrease in diameters of nanofibers was recorded. Whereas, no pores were seen on the surface of nanofibers as it was the case in PCL/PEG-10% nanofibers.

4. Statistical optimization of electrospinning parameters for PCL and PCL/PEG nanofibers

The results of preliminary experiments of single-needle electrospinning were analyzed by using a statistical tool called “Principle Component Analysis” (PCA). The working principle of this software and the details of data analysis are already described in Section 2.3 (b) of Chapter 2. This study was performed to derive a relationship between the electrospinning parameters, the mean diameters of nanofibers and their coefficient of variation. To do so, five variables were taken for the analysis which were: solution feed rate (F.R), applied voltage (V), needle to collector distance (D), mean diameters of nanofibers and their coefficient of variation (CV%). The concentration of PCL was fixed at 10wt%, so it had no impact on any parameter. PCA was done on three different DOE’s (design of experiments) such as, 10wt% PCL, PCL/PEG-10% and PCL/PEG-20%. The cumulative coefficient of variance which is also called Pearson’s coefficient (n) describes the reliability of obtained results. Normally, it is considered that if the value of Pearson’s coefficient is $n \geq 70\%$, it shows a strong relationship among the variables but values up to 50% also narrates a relationship that could be considered effective. Moreover, these values are shown in positive (+) and negative (-) figures which means a direct or inverse relationship among the variables respectively.

4.1 Observations of PCA for 10wt% PCL nanofibers

The matrix of correlation for 10wt% PCL electrospinning parameters and their Pearson’s coefficients are shown in Table 3.4 (a) and their respective circle of correlation is illustrated in Figure 3.7. For this DOE (which was explained in Section 2.3(a) of Chapter 2), the feed rate was fixed at 0.5mL/h for all the experiments and the applied voltage (V) and needle-collector distance (D) were varied to analyze their impact on the mean diameter (M.D nm) of nanofibers and their

coefficient of variation (CV%) was calculated. The homogeneity in nanofiber diameters with less CV% was the main goal of this analysis.

Table 3.4 (a). Pearson's (n) matrix of correlation between electrospinning parameters of 10wt% PCL nanofibers using chloroform: ethanol (88:12 wt/wt) solvent

Variables	V (kV)	D (cm)	M.D (nm)	CV%
V (kV)	1	-0.037	0.328	-0.0272
D (cm)	-0.037	1	0.363	-0.563
M.D (nm)	0.328	0.363	1	-0.793
CV%	-0.272	-0.563	-0.793	1

In above mentioned Table 3.4 (a), the bold figures represent the strong correlation among their respective variable.

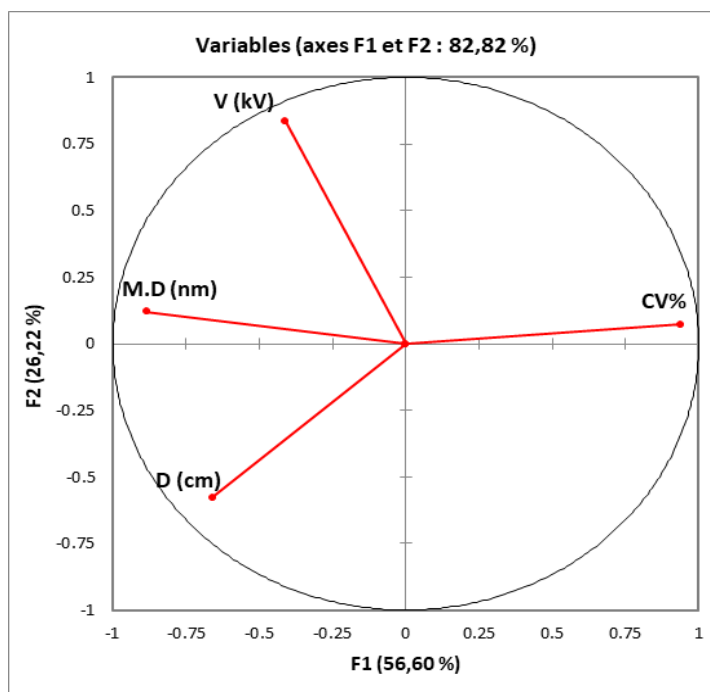


Figure 3.7. Circle of correlation between electrospinning parameters of 10wt% PCL nanofibers

From this correlation matrix, following facts were gathered:

- A strong correlation was found among the variables as total variance percentage of F1 and F2 coordinates is 82%.
- CV% has an inverse relationship with applied voltage, needle-collector distance and mean diameter of nanofibers as all the Pearson's coefficient values are negative.
- When applied voltage and needle-collector distance were increased, larger diameters of the nanofibers were achieved.
- A strong but inverse correlation of CV% was seen with needle-collector distance and mean diameters of nanofibers with Pearson's coefficient values of -0.563 and -0.793 respectively.
- As the mean diameter of nanofibers increased, their CV% decreased that means more homogenous nanofibers were achieved.

After analyzing all these factors, the selection of electrospinning parameters was done on the basis of homogeneity of nanofibers with less CV%. These optimal parameters for 10wt% PCL electrospinning are presented in Table 3.4 (b).

Table 3.4 (b). Optimized electrospinning parameters and mean diameters of 10wt% PCL nanofibers

F.R (mL/h)	V (kV)	D (cm)	M.D (nm)	CV%
0.5	25	25	3530 ± 500	14

Findings of this statistical analysis are completely aligned with the morphological study of 10wt% PCL nanofibers. The optimal electrospinning parameters were selected on the basis of less variations in nanofibers diameters.

4.2 Observations of PCA for PCL/PEG-10%

The matrix of correlation for PCL/PEG-10% electrospinning parameters and their Pearson's coefficients are shown in Table 3.5 (a) and their respective circle of correlation is illustrated in

Figure 3.8. For this DOE, two feed rates (F.R) 0.1mL/h and 0.5mL/h were employed and applied voltage (V) and needle-collector distance (D) were varied to see their impact on mean diameters (M.D nm) of nanofibers and their coefficient of variation (CV%) was calculated. The homogeneity among the nanofibers diameters was the emphasis.

Table 3.5 (a). Pearson (n) matrix of correlation between electrospinning parameters of PCL/PEG-10% nanofibers using chloroform: ethanol (88:12 wt/wt) solvent

Variables	F.R (mL/h)	V (kV)	D (cm)	M.D (nm)	CV%
F.R (mL/h)	1	0.185	-0.056	0.482	-0.147
V (kV)	0.185	1	-0.114	-0.310	0.442
D (cm)	-0.056	-0.114	1	0.198	0.241
M.D (nm)	0.482	-0.310	0.198	1	-0.367
CV%	-0.147	0.442	0.241	-0.367	1

In above mentioned Table 3.5 (a), the bold figures represent a trend among their respective variable.

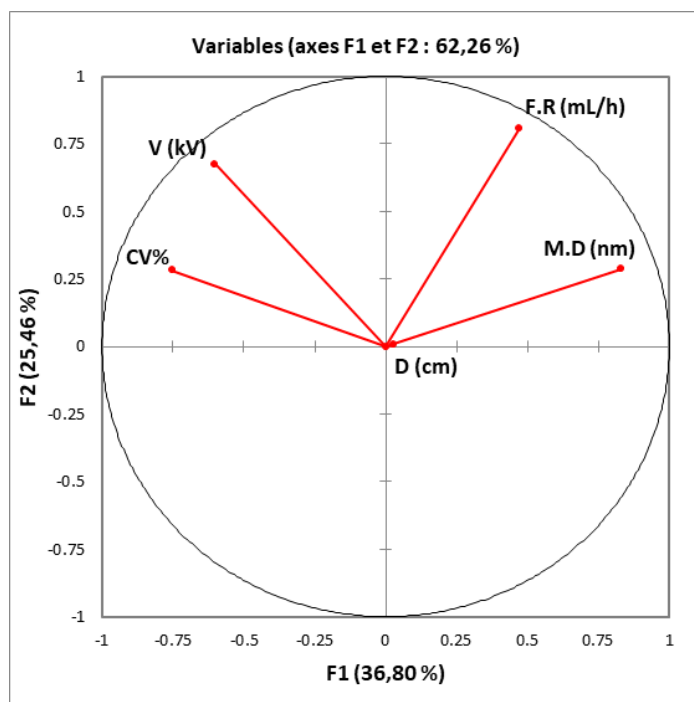


Figure 3.8. Circle of correlation between electrospinning parameters for PCL/PEG-10% nanofibers

From this correlation matrix, following facts were deduced:

- A moderate relationship was found among the variables as total variance percentage of F1 and F2 coordinates is 62%.
- D (needle-collector distance) is closer to the center which means it had no impact on the mean diameter and CV% of the nanofibers.
- CV% of the nanofibers showed a direct relationship with applied voltage with Pearson's coefficient value of 0.442.
- But both CV% and V are inversely proportional to the mean diameter of the nanofibers.
- At larger feed rate, higher applied voltages produced finer diameters of nanofibers but with less homogeneity (higher CV%).

The optimization of electrospinning parameters was done on the basis of more homogenous nanofibers that means less CV%. The optimal parameters selected for PCL/PEG-10% electrospinning are presented in Table 3.5 (b).

Table 3.5 (b). Optimized electrospinning parameters and mean diameters of PCL/PEG-10% nanofibers

F.R (mL/h)	V (kV)	D (cm)	M.D (nm)	CV%
0.5	20	20	940 ± 327	35

Results of PCA for PCL/PEG-10% electrospinning parameters are in total agreement with the morphology of these nanofibers. Optimization of electrospinning parameters was done by keeping in view the homogeneity of nanofibers diameters.

4.3 Observations of PCA for PCL/PEG-20%

The matrix of correlation for PCL/PEG-20% electrospinning parameters and their Pearson's coefficients are shown in Table 3.6 (a) and their respective circle of correlation is illustrated in Figure 3.9. In this DOE, only one feed rates (F.R) 0.5mL/h was used to prepare the samples because difficulty in electrospinning was faced by using feed rate of 0.1 mL/h. The effect of applied voltage (V) and needle-collector distance (D) on the mean diameters (M.D nm) of nanofibers and their coefficient of variation (CV%) was studied. The homogeneity of nanofibers was determined by analyzing their CV%.

Table 3.6 (a). Pearson (n) matrix of correlation between electrospinning parameters of PCL/PEG-20% nanofibers using chloroform: ethanol (88:12 wt/wt) solvent

Variables	V (kV)	D (cm)	M.D (nm)	CV%
V (kV)	1	0.488	-0.233	-0.023
D (cm)	0.488	1	-0.741	0.703
M.D (nm)	-0.233	-0.741	1	-0.541
CV%	-0.023	0.703	-0.541	1

In above mentioned Table 3.6 (a), the bold figures represent the strong correlation among their respective variable.

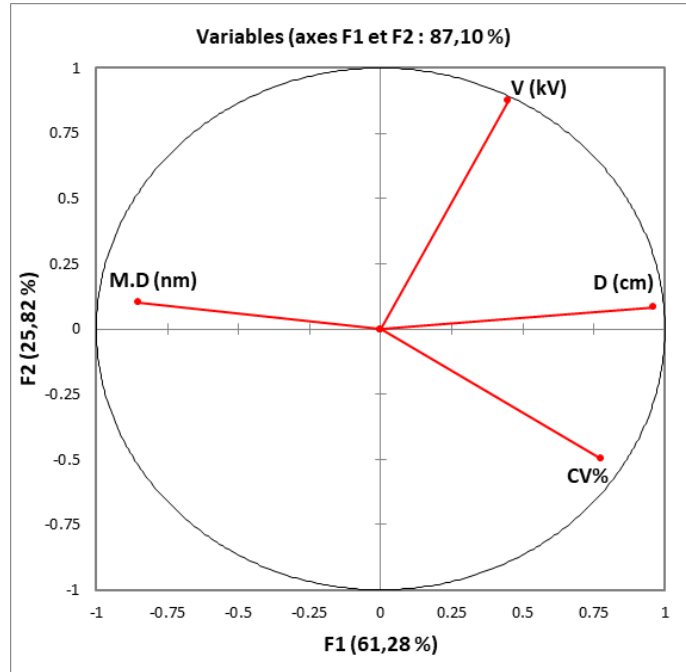


Figure 3.9. Circle of correlation between electrospinning parameters of PCL/PEG-20% nanofibers

From this matrix of correlation, following observations were made:

- A strong correlation was found among the variables as total variance percentage of F1 and F2 coordinates is 87%.
- Mean diameter of nanofibers showed strong and inverse relationship with needle-collector distance with Pearson' coefficient value of -0.741 that means if needle-collector distance will increase then, mean diameter of nanofibers will decrease.
- Applied voltage and CV% showed an inverse and strong relationship with -0.504 value of Pearson' coefficient.
- Higher voltages resulted in more homogenous nanofibers with smaller values of CV%.

All these facts were analyzed and optimal electrospinning parameters were finalized on the basis of homogenous fibers as shown in Table 3.6 (b).

Table 3.6 (b). Optimized electrospinning parameters and mean diameters of PCL/PEG-20% nanofibers

F.R (mL/h)	V (kV)	D (cm)	M.D (nm)	CV%
0.5	19	20	1100 ± 300	27

Morphological study of PCL/PEG-20% nanofibers justify these results of PCA and the selection of best electrospinning parameters according to their corresponding CV%.

4.4 Comparison between electrospinning parameters of PCL and PCL/PEG-10%, PCL/PEG-10% and PCL/PEG-20%

A comparison was drawn between PCL and PCL/PEG-10% electrospinning parameters. The purpose of this comparison was to analyze the impact of adding PEG-400 to PCL on its electrospinning process and parameters. Similarly, another comparison was made between the electrospinning parameters of PCL/PEG-10% and PCL/PEG-20% to study the impact of two concentrations of PEG-400 on PCL electrospinning. The circles of correlation for both these comparisons are shown in Figure 3.10.

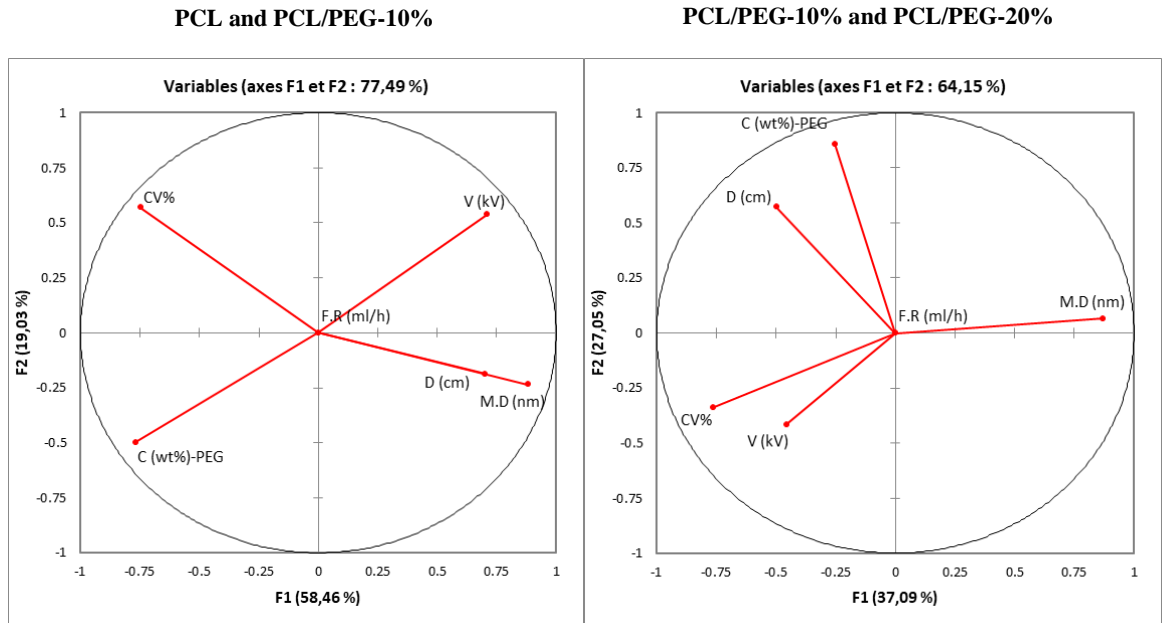


Figure 3.10. Circles of correlation for the comparison

Results of these compared correlation matrices were in agreement with their individual correlation matrices as described in above sections. PCL and PCL/PEG-10% showed a strong correlation as their percentage variance was 77%. However, PCL/PEG-10% and PCL/PEG-20%, showed a moderate correlation among their variable with their percentage variance value of 64%. The overall impact of PEG-400 addition in two different concentrations to PCL is exclusively discussed here. After analyzing their correlation matrices, following conclusions were derived:

- Feed rate has no significant impact on the electrospinning process and nanofibers diameters in both scenarios.
- With PCL/PEG-10%, finer diameters were achieved at low voltage as compared to pure PCL nanofibers.
- In PCL-PCL/PEG-10% comparison, needle-collector distance directly influenced the mean diameter of resulting nanofibers. When “D” increased, the “M.D” of nanofibers also increased.

- In both cases of PEG-10% and PEG-20%, PEG-400 concentration showed an inverse relationship with applied voltage and mean diameters of the nanofibers.
- With increase in concentration of PEG-400, lower voltages worked well in producing finer diameters of nanofibers but with larger CV%.
- Needle-collector distance showed insignificant effect on the mean diameters of nanofibers in either concentration of PEG-400.

5. Crystallinity of PCL and PCL/PEG nanofibers

The DSC analysis was performed to determine the degree of crystallinity of PCL and PCL/PEG nanofibers. All samples were sealed in non-hermetic capsules and analysis was performed under nitrogen atmosphere with a dual cycle of heating from -80°C to 100°C at a rate of $10^{\circ}\text{C}/\text{min}$. The crystallinity ratio (X_c) of all samples was calculated with reference to the used content of PCL and dividing the ΔH_m of each sample by the melting enthalpy of 100% crystalline PCL ($\Delta H_{m,\text{PCL}}$) [24]. In case of all nanofibers, only first cycle of heating was considered as true representative of their crystalline behavior. The DSC analysis of pure PCL pellets was also performed as a reference to the PCL and PCL/PEG nanofibers. DSC curves were extracted by using TA Universal Analysis software for analysis. Figure 3.11 illustrates one of those extracted thermograms of PCL nanofibers.

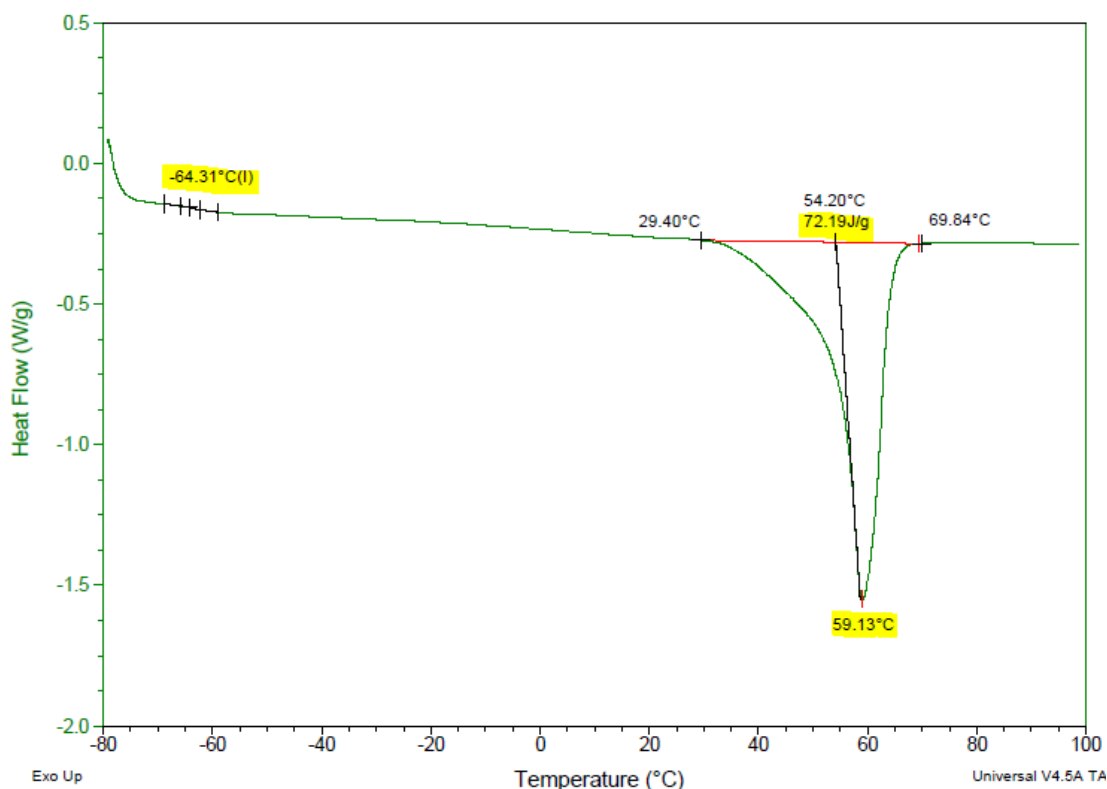


Figure 3.11. DSC curve of PCL nanofibers representing the first heating cycle from -80° to 100°C under N₂

The glass transition temperature (T_g), melting temperature (T_m) and melting enthalpy (ΔH_m) for each sample were analyzed and their values are given in Table 3.7. No substantial change in glass transition and melting temperatures of all nanofibers was observed [25]. It was found that the crystallinity ratio of PCL nanofibers was 11% higher than that of pure PCL [24, 25]. This indicates that a change occurred in alignment of PCL chains during the electrospinning process which enhanced the overall crystallinity of PCL nanofibers. It is quite understandable because the polymer solution underwent extensive stretching as it was subjected to the high voltage electric field that could have affected the crystallization phenomenon of PCL molecular chains. Another reason for this increased crystallinity ratio could be because of post-deposition crystallization of nanofibers. This effect has been reported by the scientists that when nanofibers are deposited on the collector surface, a solid layer is formed on the top of nanofibers due to quick evaporation of solvent [26]. Therefore, solvent trapped in the center of nanofibers allowed further crystallization

of molecular chains even after they were collected on the plate. Because of this phenomenon, crystallization of PCL nanofibers might have continued after their deposition on the collector plate.

Table 3.7. Glass transition temperatures (T_g), melting temperatures (T_m), melting enthalpies (ΔH_m) and crystallinity ratios ($X_c\%$) of pure PCL, PCL and PCL/PEG nanofibers determined on the first temperature ramp from -80°C to 100°C under N_2

Sample	T_g ($^\circ\text{C}$)	T_m ($^\circ\text{C}$)	ΔH_m (J/g)	$X_c\%$
Pure PCL	-64	57	63	40%
PCL nanofibers	-64	59	72	51%
PCL+PEG-10% nanofibers	-63	57	74	58%
PCL+PEG-20% nanofibers	-62	58	102	90%

Impact of PEG-400 on the crystallinity of PCL nanofibers

This effect of higher crystallinity was more pronounced in nanofibers containing PEG-400 with an upsurge up to 90% in their crystallinity ratios in case of PCL/PEG-20% nanofibers. For PCL/PEG-10% nanofibers, an increase of 18% was observed as compared to the crystallinity ratio of pure PCL pellets. Therefore, it can be stated that by increasing the PEG-400 content in PCL nanofibers, their crystallinity also increased that is a fact proved by previous research studies [7, 23]. Keeping in view the previous arguments, another reason for this augmented crystallinity could be the polarity induced by PEG-400 to the PCL solution which favored the crystalline arrangement of macro-molecular chains under the effect of electric field [10]. However, there was no significant difference in the glass transition temperatures and melting temperatures of nanofibers.

6. Tailoring the wettability of PCL nanofibers with PEG-400

PCL is a semi-crystalline hydrophobic polymer that has widely been used for its biomedical applications. Despite its good mechanical properties, slow biodegradation and biocompatibility, PCL lacks hydrophilicity which limits its applicability for wound healing. To overcome this problem, blending of PCL with other hydrophilic polymers is a tested and verified solution which is documented in literature [10]. Similarly, in this study blend electrospinning of PCL and PEG-400 was done and the obtained PCL/PEG nanofibers were analyzed for their wettability by measuring their water contact angle.

Water contact angle measurements were recorded for pristine PCL film, 10wt% PCL nanofibers, PCL/PEG-10% and PCL/PEG-20% nanofibers. The images of water droplet on the surface of pure PCL film (as control sample) and PCL nanofibers are shown in Figure 3.12.

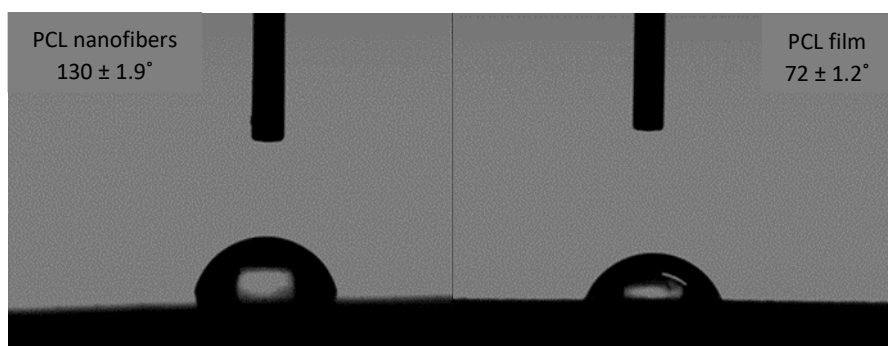


Figure 3.12. Images of water contact angle for PCL nanofibers and pure PCL film

The PCL nanofibers showed a larger water contact angle as compared to the pure PCL film. This enhanced hydrophobicity in PCL nanofibers could be due to their surface roughness as compared to smooth PCL film. Surface roughness is known to amplify hydrophobicity by mimicking the lotus effect [27]. Another reason for this phenomenon could be explained by understanding the crystallinity of nanofibers that has already been proved from their DSC analysis. It was observed

that the crystallinity ratio of PCL nanofibers was 11% higher than that of pure PCL. In fact, during the electrospinning PCL chains were stretched under the effect of high voltage and rearrangement of PCL chains took place to form nanofibers [7]. However, in case of PCL/PEG-10% and PCL/PEG-20% nanofibers it was not possible to record their contact angle as water droplet was quickly absorbed by the surface of nanofibers. This quick absorption of water droplet proved the presence of hydrophilic PEG-400 on the surface of nanofibers [28]. The observations for water contact angle for all samples are given in Table 3.8.

Table 3.8. Water contact angle measurements for pure PCL film, PCL and PCL/PEG nanofibers

Sample	Mean Contact Angle	Observations
Pure PCL film	$72 \pm 1.2^\circ$	Hydrophobic
PCL nanofibers	$130 \pm 1.9^\circ$	Hydrophobic
PCL/PEG-10% nanofibers	Rapid absorption	Hydrophilic
PCL/PEG-20% nanofibers	Rapid absorption	Hydrophilic

Therefore, it was concluded that addition of PEG-400 improved the wettability of PCL nanofibers that was in fact, the main objective of blend electrospinning. This enhanced wettability was a desired feature for these electrospun nonwoven mats for their potential application as a wound dressing material in order to absorb wound exudate [29, 30].

7. Thermal analysis of PCL and PCL/PEG nanofibers

Use of chloroform for the electrospinning of nanofibers that have a potential use for biomedical applications, is not really encouraged. Therefore, the TGA analysis of PCL and PCL/PEG nanofibers was performed to reassure that there was no solvent left in the structure of nanofibers.

All samples were analyzed under nitrogen with 10°C/min rate of heating ramp till 800°C. A degradation curve of PCL nanofibers is shown in Figure 3.13. No preliminary peaks were found until 200°C that might have corresponded to the solvent evaporation as the boiling point of chloroform is around 61°C and of ethanol round 78°C. Absence of such peaks, strongly indicates that there were no traces of any solvent left in electrospun PCL nanofibers.

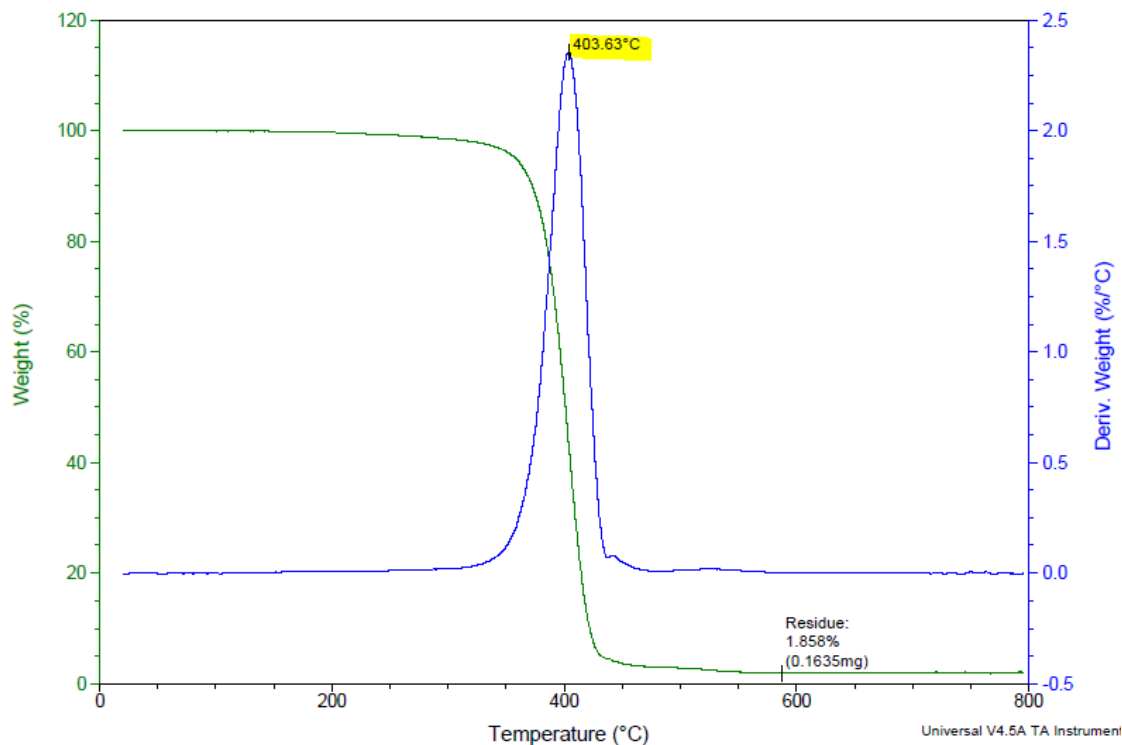


Figure 3.13. A degradation curve of electrospun PCL nanofibers showing absence of any solvent peaks

Moreover, this analysis also provided useful information about the thermal degradation behavior of PCL and PCL/PEG-10% nanofibers in comparison to their pure states. No substantial change in their 5% degradation temperatures along with their total degradation temperatures are presented in Table 3.9. No residual material was found in any sample at the end of their degradation cycles.

Table 3.9. TGA results representing 5% degradation temperatures and total degradation temperatures of pure PCL, pure PEG-400 and their nanofibers

Samples	5% Degrad. Temp. (°C)	Total Degrad. Temp. (°C)
Pure PCL	365	570
Pure PEG	245	375
PCL nanofibers	360	580
PCL/PEG-10% nanofibers	302	470

There was no significant difference between the degradation temperature of PCL nanofibers and pure PCL [31]. The degradation temperature of PCL/PEG-10% nanofibers was lower than that of PCL nanofibers which could be due to the addition of PEG-400 which has a lower degradation temperature. But this difference was not substantial proving that PEG-400 had not affected the thermal stability of PCL nanofibers to a great extent. All the samples showed good thermal stability in order to be used as wound dressing materials.

8. Incorporation of nanocapsules of chitosan

The synthesis of nanocapsules of chitosan and the drug encapsulation was done by Pr. Leonard Ionut Atanase at Faculty of Dental Medicine, University “Apollonia”, Iasi-Romania. This section has already been described in Chapter 2.

The main purpose of incorporating these chitosan nanocapsules into PCL nanofibers was to devise a targeted drug delivery system in the nanofibers network. Due to their small size and hydroxyl functional groups present around them, these nanocapsules were thought as an ideal choice for drug encapsulation and its localized delivery to the affected wound area [32]. From literature, it was proved that these biocompatible, biodegradable nanocapsules of chitosan offer prolonged

release of drug and could be loaded homogeneously into the non-woven structure of nanofibers [33-35]. The choice of drug as sodium-salt of Ibuprofen was made by considering its hydrophilic properties which would have aligned in a better manner with hydrophilic chitosan nanocapsules [36]. As the drug release analysis is performed in aqueous medium, it was supposed that use of such hydrophilic drug would result in good compatibility with nanocapsules of chitosan. However, later the agglomeration problems and their difficult electrospinning discouraged their use as a potential biomedical agent for drug delivery applications. Consequently, they were replaced by pure Ibuprofen (an anti-inflammatory and non-steroidal drug) (IBU) which was a hydrophobic drug used for inflammation and pain treatment [12].

8.1 Morphology of 1%NCs+PCL nanofibers

At first, the nanocapsules of chitosan (NCs) without drug were electrospun with PCL and PCL/PEG-10% nanofibers. The electrospinnability of the process and the obtained nanofibers morphology was studied by the preliminary experiments. 1wt% of NCs with respect to the PCL was added to the solution of PCL and PCL/PEG-10% and electrospinning was done at relative humidity of $35\pm 5\%$ and temperature was kept at $25\pm 4^\circ\text{C}$. The SEM images of 1%NCs+PCL nanofibers are presented in Figure 3.14 and all images were taken at $10\mu\text{m}$ scale.

F.R = 0.5 mL/h and D = 25cm

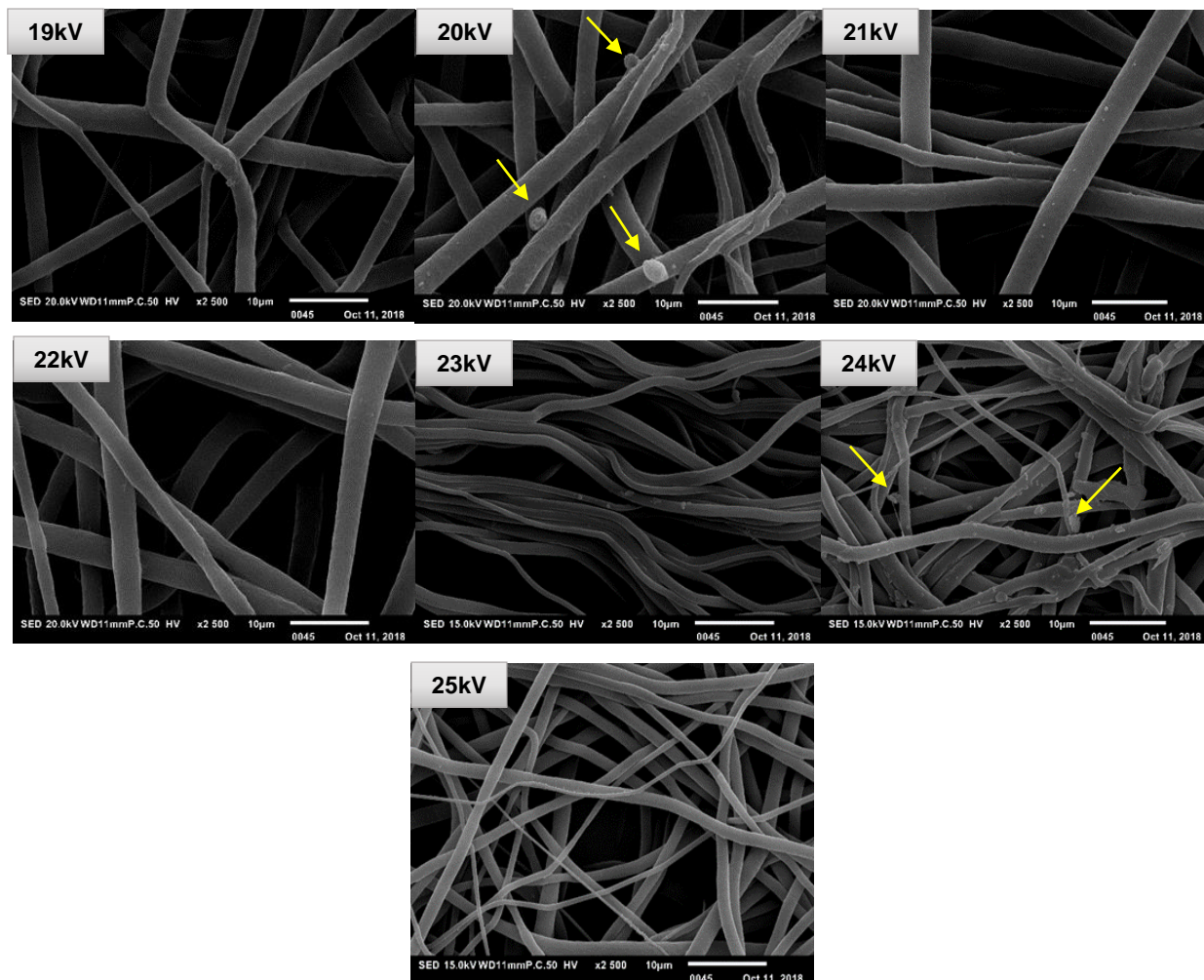


Figure 3.14. SEM images of 1%NCs+PCL nanofibers at different applied voltages

All nanofibers were cylindrical in shape and showed no beads or entanglements along the length. Like PCL nanofibers, these nanofibers too were heterogeneous in morphology with nano and micro fibers. Lower voltages produced larger diameters whereas, high voltage produced finer diameters with high CV%. Agglomerates of NCs were also observed in few samples which are indicated in Figure 3.14 with yellow arrows. The best electrospinning voltage which generated homogenous nanofibers was 19kV. The average diameters of nanofibers with their standard deviations and CV% are listed in Table 3.10.

Table 3.10. Mean diameters and CV% of 1%NCs+PCL nanofibers at different applied voltages

Sample	V (kV)	M.D (nm)	CV%
1%NCs+PCL	19	2070 ± 710	34%
	20	2195 ± 980	44%
	21	2525 ± 770	40%
	22	2670 ± 871	32%
	23	970 ± 520	53%
	24	865 ± 477	55%
	25	745 ± 430	58%

The best electrospinning conditions for 1%NCs+PCL nanofibers are shown in bold figures in Table 3.10. The selection criteria for these parameters was the homogeneity in nanofibers diameters.

8.2 Morphology of 1%NCs+PCL/PEG-10% nanofibers

Same amount of NCs was incorporated into PCL/PEG-10% solution in chloroform: ethanol (88:12 wt/wt) and electrospinning was performed. The SEM images of obtained nanofibers are shown in Figure 3.15. All images were taken at 10 μ m scale.

F.R = 0.5 mL/h and D = 25cm

10 μ m scale

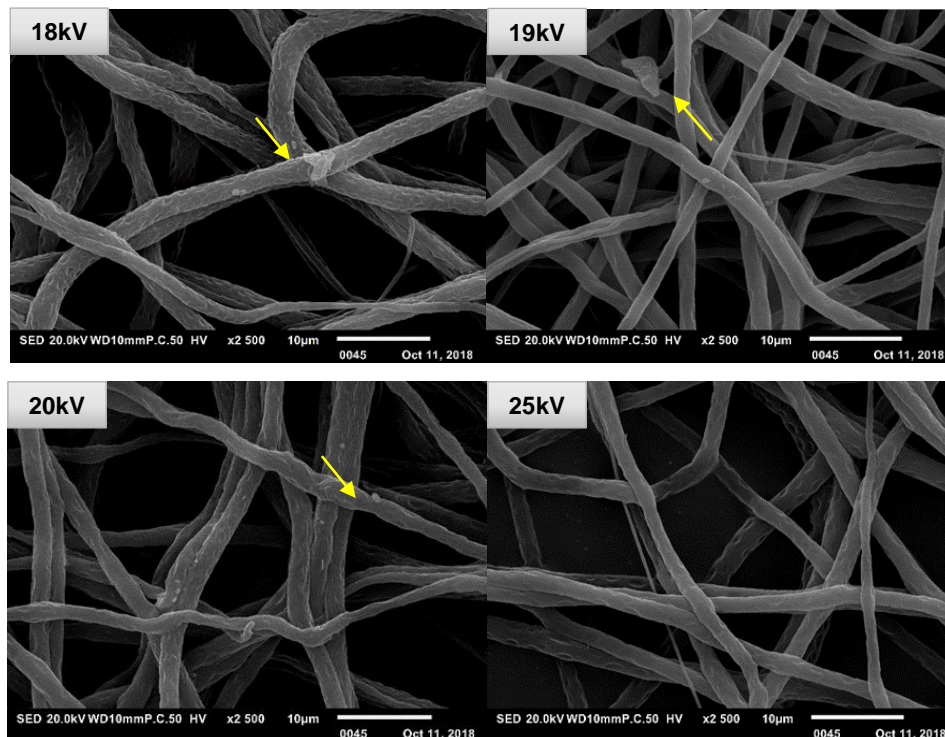


Figure 3.15. SEM images of 1%NCs+PCL/PEG-10% nanofibers at different applied voltages

The nanofibers of 1%NCs+PCL/PEG-10% showed pores along their surface which was in agreement with the previous example of PCL/PEG-10% nanofibers. Unlike previous scenario, this time no sharp decrease in the diameters of nanofibers was noticed after the addition of PEG-400. The presence of NCs may had effected the overall charge density of PCL/PEG-10% solution and hindered the polymer jets from further stretching. All diameters were above one micron in a range between 1.2 to 1.6 μ m with predominantly round shapes and irregularity in thickness along their length. As the voltage increased, nanofibers diameter decreased and showed less homogeneity. Agglomerates of NCs could be seen in the SEM images of few samples (marked with yellow arrows). The average diameters and CV% of nanofibers at given applied voltages are shown in Table 3.11.

Table 3.11. Mean diameters and CV% of 1%NCs+PCL/PEG-10% nanofibers at different applied voltages

Sample	V (kV)	M.D (nm)	CV%
1%NCs+PCL/PEG-10%	18	1610 ± 600	37%
	19	1620 ± 545	33%
	20	1255 ± 521	41%
	25	1545 ± 744	48%

The bold figures represent the best electrospinning parameters for 1%NCs+PCL/PEG-10% nanofibers. These values were chosen depending upon the less CV% of the nanofibers.

8.3 Incorporation of drug encapsulated nanocapsules of chitosan

After successful electrospinning of nanocapsules of chitosan with PCL and PCL/PEG-10%, the next step was the electrospinning of nanocapsules of chitosan (NCs) encapsulated with a drug. For this purpose, the sodium-salt of Ibuprofen (Na-IBU) was encapsulated into these nanocapsules of chitosan. The synthesis of these nanocapsules of chitosan and their drug encapsulation has already been described in length in Section 2.2 of Chapter 2.

8.4 Agglomerations of NCs.Na-IBU into PCL solution

At first, these NCs.Na-IBU were incorporated into 10wt% PCL solution with chloroform: ethanol (88:12 wt/wt) solvent to perform electrospinning. Huge agglomerations of these NCs.Na-IBU in PCL solution were observed with naked eye. Thus, the solution was stirred magnetically for 20min to disperse these NCs.Na-IBU but no improvement was seen in dispersion of NCs.Na-IBU agglomerates. These agglomerates were observed under optical microscope and are shown in Figure 3.16. When no success was realized in dispersion of NCs.Na-IBU with magnetic stirring, then solution was agitated by using ultra-turrax at a 3000 rpm speed for another 15min. Again, no improvement was seen and the solution turned greyish with some black particles settled at its base.

This change in color could be due to the degradation of nanocapsules of chitosan (as chitosan is a temperature sensitive polymer) from the heat generated by high speed mechanical agitation of solution [37]. Moreover, this technique was not suitable to disperse these drug encapsulated nanocapsules as there was high risk of drug release from them during their mechanical agitation.

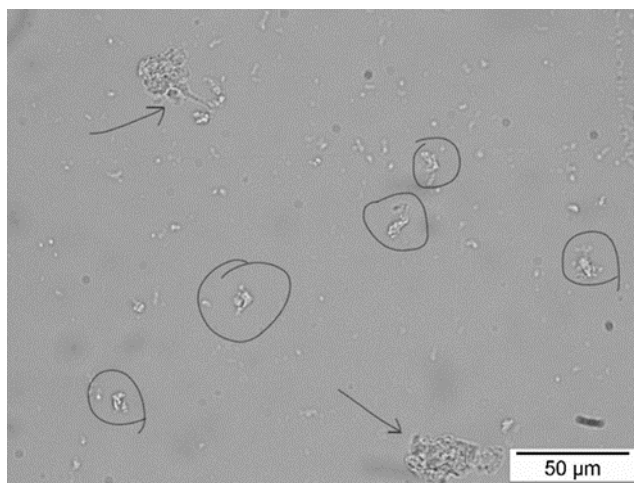


Figure 3.16. Optical microscope image of agglomerates of NCs

8.5 Size distribution analysis of NCs.Na-IBU with dispersing agents

To overcome this problem of agglomerations, another effort was made by using three different types of dispersing agents. It was assumed that these dispersing agents will solve this issue of agglomerations. Because, they were soluble in PCL/PEG solution and possessed phosphoric acid group at the end of their chains, able to interact with the hydroxyl groups present on the surface of NCs. The names of these dispersing agents are as follows:

- W996 provided by BYK
- G079 provided by Mader
- G127 provided by Mader

To analyze their impact on the dispersion of NCs.Na-IBU, these dispersing agents were first added into the binary solvent system in 2wt% amount (with respect to the PCL) and then NCs-Na-IBU were added to this mixture. This mixture was magnetically stirred for 15min and ultra-sonication for 5min was done. After that, the particle size distribution analysis of this solution was done by light scattering measurements (Mastersizer equipment). The particle size distribution of NCs.Na-IBU after adding these dispersing agents was recorded in numbers and is shown in Figure 3.17.

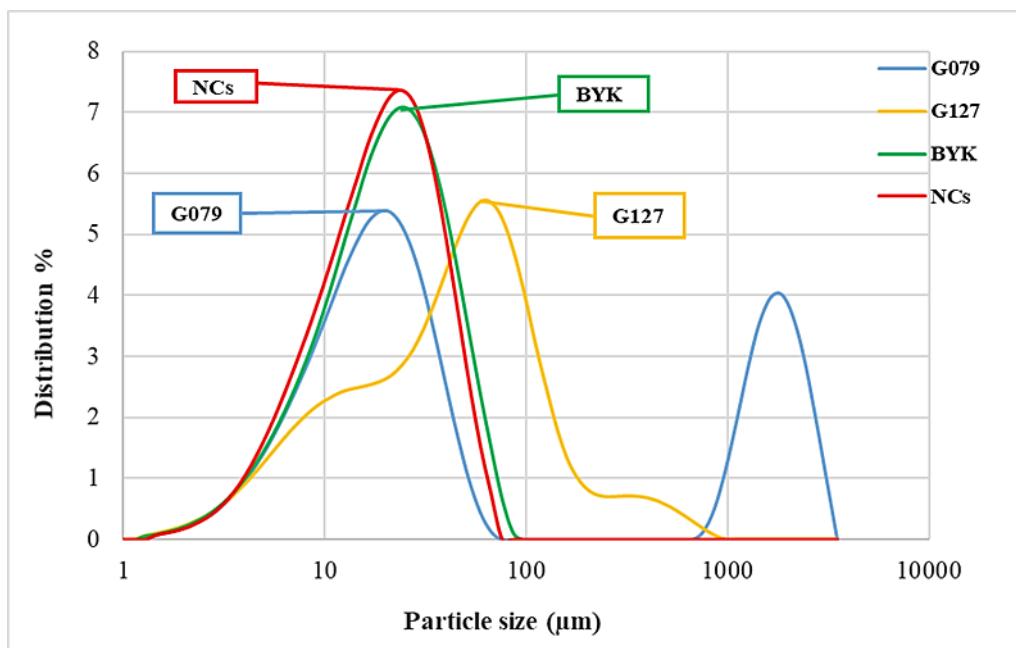


Figure 3.17. Particle size distribution of NCs.Na-IBU in number with three dispersing agents in solvent mixture of chloroform: ethanol 88:12 wt/wt ratio

From this study, our hypothesis was clearly proved wrong as there was no significant impact of any dispersing agent on the size of NCs.Na-IBU agglomerates. No reduction in size was noticed in case of BYK-W996, Mader-G079 and Mader-G127 that proved them irrelevant for this application. The agglomerates were still present and were huge in size. Thus, no progress was found in size reduction of NCs.Na-IBU agglomerates by using these dispersing agents as it was obvious from their particle size distribution elaborated in Table 3.12.

Table 3.12. Size distribution of NCs.Na-IBU with dispersing agents in solvent mixture of chloroform: ethanol 88:12 wt/wt ratio by light scattering analysis

Particle size distribution	NCs (µm)	BYK-W996 (µm)	Mader-G079 (µm)	Mader-G127 (µm)
Dx (10)	7.01	7.20	7.40	7.80
Dx (50)	20.40	21.80	24.70	47.10
Dx (90)	44.10	49.10	*2076.60	148.20

†Note: The figure with (*) mark was a disturbance that could be due to a dust particle.

The light scattering results proved that the use of these dispersing agents was not encouraging for the dispersion of NCs.Na-IBU into PCL solution. The inability of these dispersing agents to interact with the nanocapsules of chitosan and to break their clusters could be due to the presence of strong H-bonding among them which were not broken during the stirring of the PCL solution. Therefore, it was not possible to disperse these agglomerates of nanocapsules of chitosan.

8.6 Incorporation of NCs.Na-IBU into PCL/PEG-10% nanofibers

After unsuccessful dispersion of NCs.Na-IBU in PCL solution even after employing different dispersing agents, there was still a hope to try another solution for this problem. A new attempt was made by adding hydrophilic PEG-400 (10wt% with respect to PCL) into the solution for their better dispersion. A new hypothesis was made that this polar hydrophilic PEG-400 would help in homogeneous dispersion of these nanocapsules of chitosan.

To prepare this solution, 1.8wt% of NCs.Na-IBU were added to the PCL/PEG-10% solution with chloroform: ethanol (88:12 wt/wt) solvent. This solution was only magnetically stirred for 20min with a subsequent ultra-sonication for 5min to remove air bubbles. After adding PEG-400, it was seen with naked eye that agglomerations were comparatively less than they were in pure PCL

solution. Hence, this solution was subjected to the electrospinning of nanofibers. However, the electrospinning process was not problem free as several times needle was blocked by these agglomerates that disturbed the whole process of sample making. Various nanofibrous samples were made at different voltages. The SEM images of all samples of 1.8%NCs.Na-IBU+PCL/PEG-10% nanofibers are shown in Figure 3.18. All these images were taken at 10 μ m scale.

F.R = 0.5 mL/h and D = 25cm

10 μ m scale

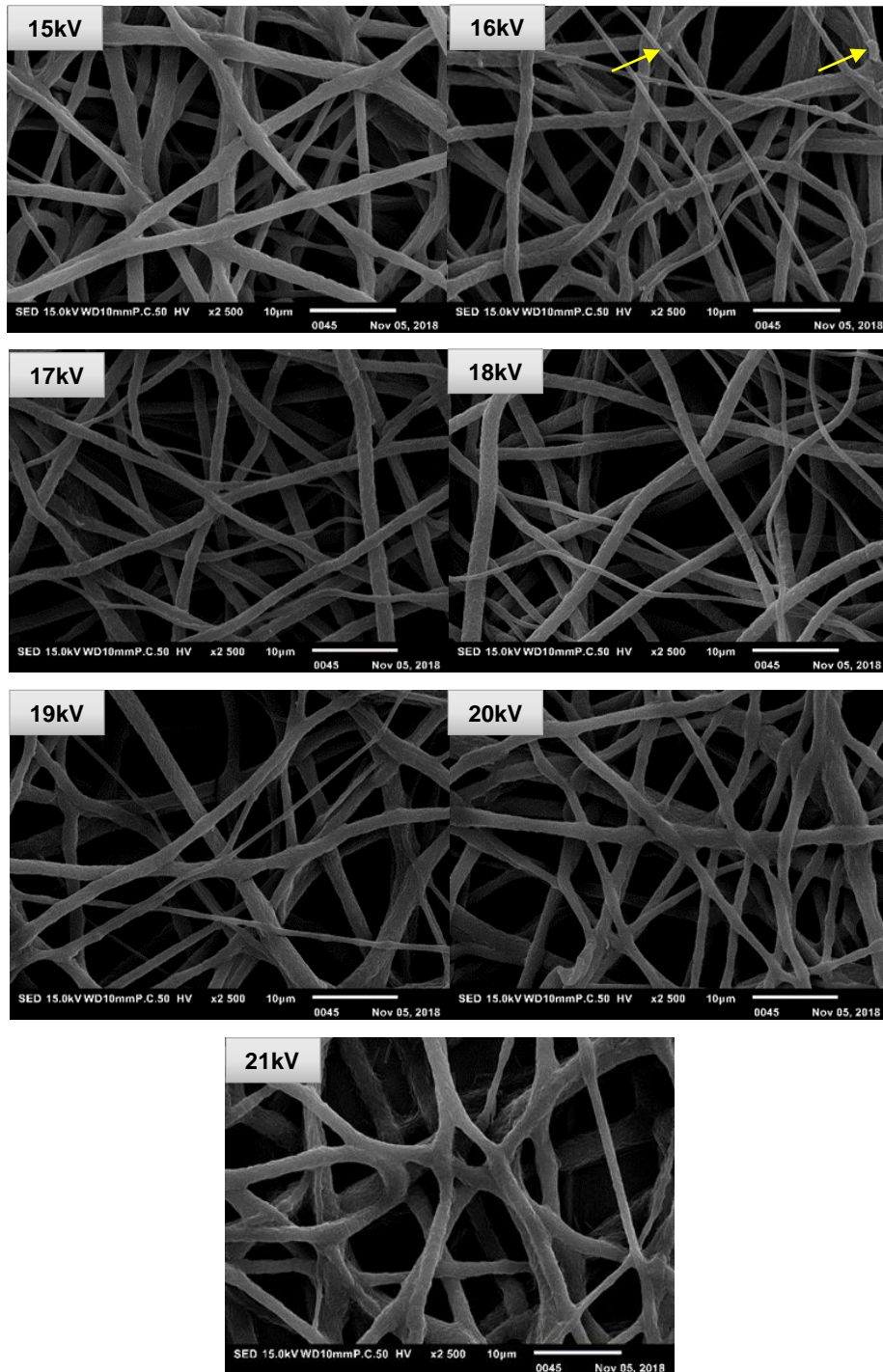


Figure 3.18. SEM images of 1.8%NCs.Na-IBU+PCL/PEG-10% nanofibers at different applied voltages

The images of electron microscopy revealed pores on the surface of these nanofibers and their non-uniform thickness. All the fibers were round in shape with rather fused boundaries at higher voltages i.e. 20kV and 21kV. This effect could be due to the rapid evaporation of solvent from the deposited nanofibers. Small agglomerates of NCs were found only in one sample electrospun at 16kV. The overall morphology of obtained nanofibers was heterogeneous in nature with diameters in a range of 900-1200nm as mentioned in Table 3.13. Initially increasing the voltage from 15kV till 19kV reduced the nanofibers diameters. After 19kV, this trend did not follow up and a rise in nanofiber diameter was observed with increased voltage. Nanofibers with lowest coefficient of variation in diameters were achieved at 20kV.

Table 3.13. Mean diameters and CV% of 1.8%NCs.Na-IBU loaded nanofibers at different applied voltages

Sample	V (kV)	M.D (nm)	CV%
1.8%NCs.Na-IBU+PCL/PEG-10%	15	1190 ± 475	40%
	16	1050 ± 545	52%
	17	1077 ± 415	43%
	18	970 ± 474	48%
	19	955 ± 437	45%
	20	1050 ± 260	25%
	21	1200 ± 480	40%

Although, the nanofibers were achieved by electrospinning of 1.8%NCs.Na-IBU+PCL/PEG-10% solution, but the dispersion of these nanocapsules of chitosan still remained a big problem. Presence of these agglomerates could be seen on the surface of many samples. Due to their poor dispersion even in PCL/PEG-10% solution, the electrospinning process was greatly affected because several times the needle was clogged due to these agglomerates. Therefore, all these facts

discouraged their use for further electrospinning experiments. Now, after the failure of nanocapsules of chitosan, an alternative product had to be selected and incorporated to devise a drug delivery system in nanofibers. For this purpose, Ibuprofen (IBU) drug in its pure form was selected as the substitute for this application.

9. Incorporation of pure IBU into PCL and PCL/PEG nanofibers

Ibuprofen is a hydrophobic drug used to cure pain and inflammation in wounds [12]. In order to develop electrospun scaffolds equipped with a drug delivery system for wound healing applications, pure IBU was incorporated into PCL and PCL/PEG-10% nanofibers. Two concentrations of IBU, 5wt% and 7wt% with respect to the PCL were added to the electrospinning solutions. Chloroform: ethanol (88:12 wt/wt) solvent was used to prepare all the solutions and electrospinning was performed at $25^{\circ}\pm 4^{\circ}\text{C}$ temperature with relative humidity of $35\pm 5\%$.

9.1 Morphology of 5%IBU+PCL nanofibers

Electrospinning of 5%IBU+PCL solution was carried out at different voltages with a constant feed rate of 0.5mL/h and a fixed needle-collector distance of 25cm. The obtained IBU loaded nanofibers of pure PCL were examined under scanning electron microscope to determine their morphology. The SEM images of all samples are shown in Figure 3.19. All images were taken at $10\mu\text{m}$ scale.

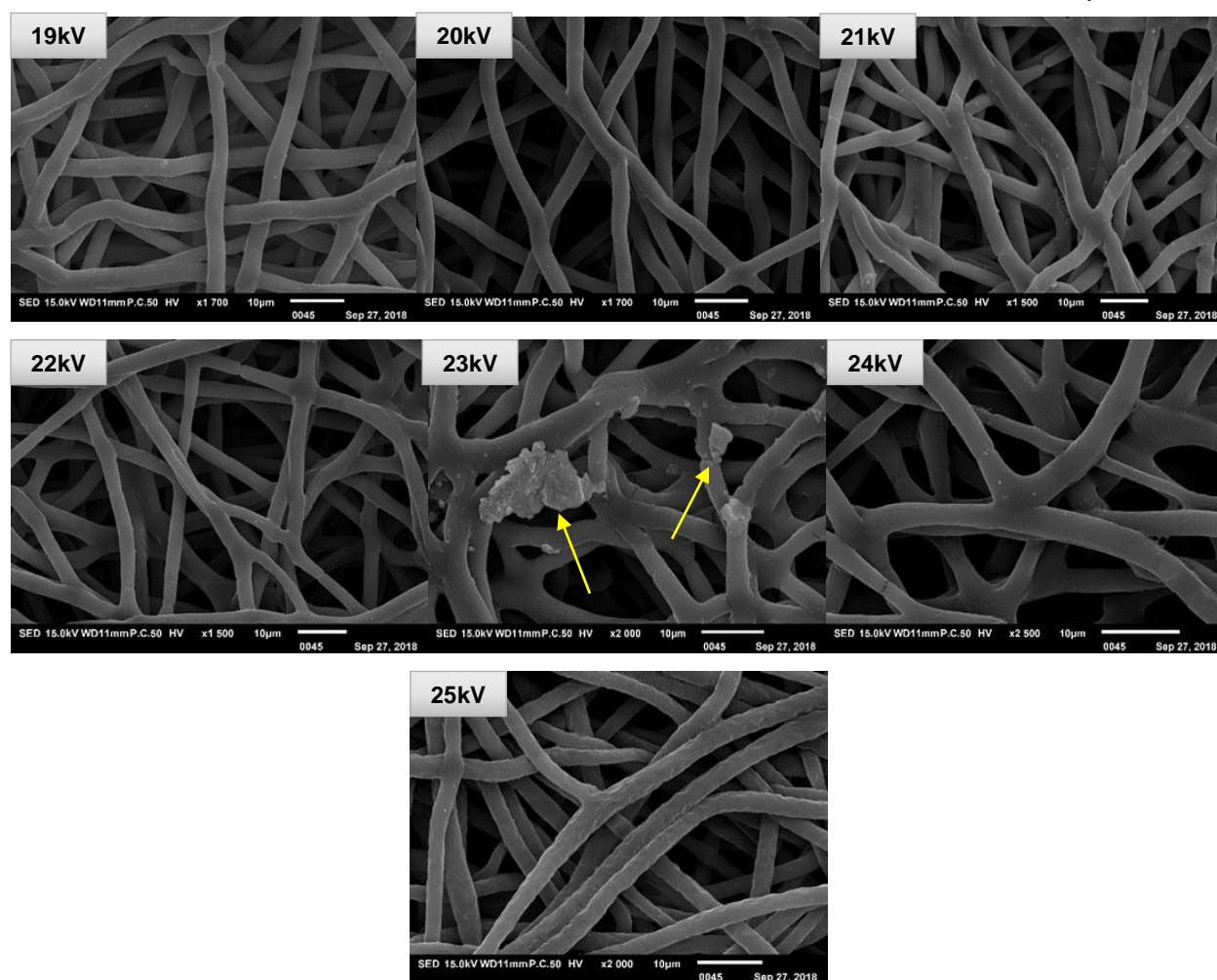


Figure 3.19. SEM images of 5%IBU+PCL nanofibers at different applied voltages

All the nanofibers were circular in shape with variable thicknesses along their length. No bead formations were observed in any sample. Agglomerates of IBU on the surface of nanofibers were found in only one sample that can be seen in Figure 3.19 marked with yellow arrows. In IBU loaded nanofibers, larger diameters were observed with more homogeneity. Instead of large variations, uniformity was seen among the diameters. All nanofibers were predominantly homogenous with diameters in micro range. This effect of increase in nanofibers diameter with drug incorporation is reported in literature by scientist [38, 39]. The mean diameters of 5%IBU+PCL nanofibers and their CV% are presented in Table 3.14.

Table 3.14. Mean diameters and CV% of 5%IBU+PCL nanofibers at different applied voltages

Sample	V (kV)	M.D (nm)	CV%
5%IBU+PCL	19	2900 ± 400	14%
	20	2840 ± 280	10%
	21	3050 ± 521	17%
	22	2890 ± 395	13%
	23	2900 ± 355	12%
	24	2222 ± 580	26%
	25	2640 ± 540	20%

The best electrospinning conditions for 5%IBU+PCL nanofibers are mentioned in bold figures in Table 3.14. It was obvious from these results that IBU loaded nanofibers were homogenous in nature with large diameters. The CV% of all samples was in a range of 10-26% with no huge differences. As the applied voltage increased, the variation in diameters also increased which concluded large CV% values.

9.2 Morphology of 7%IBU+PCL/PEG-10% nanofibers

The nanofibers of 7%IBU+PCL/PEG-10% were also electrospun at different applied voltages at a constant feed rate of 0.5mL/h and at fixed needle-collector distance of 25cm. All the acquired samples were analyzed for their morphology and their mean diameters were measured by ImageJ software by taking bar measurements. The SEM images of nanofibers at different applied voltages are shown in Figure 3.20. The analysis was done at a 10µm scale for all samples.

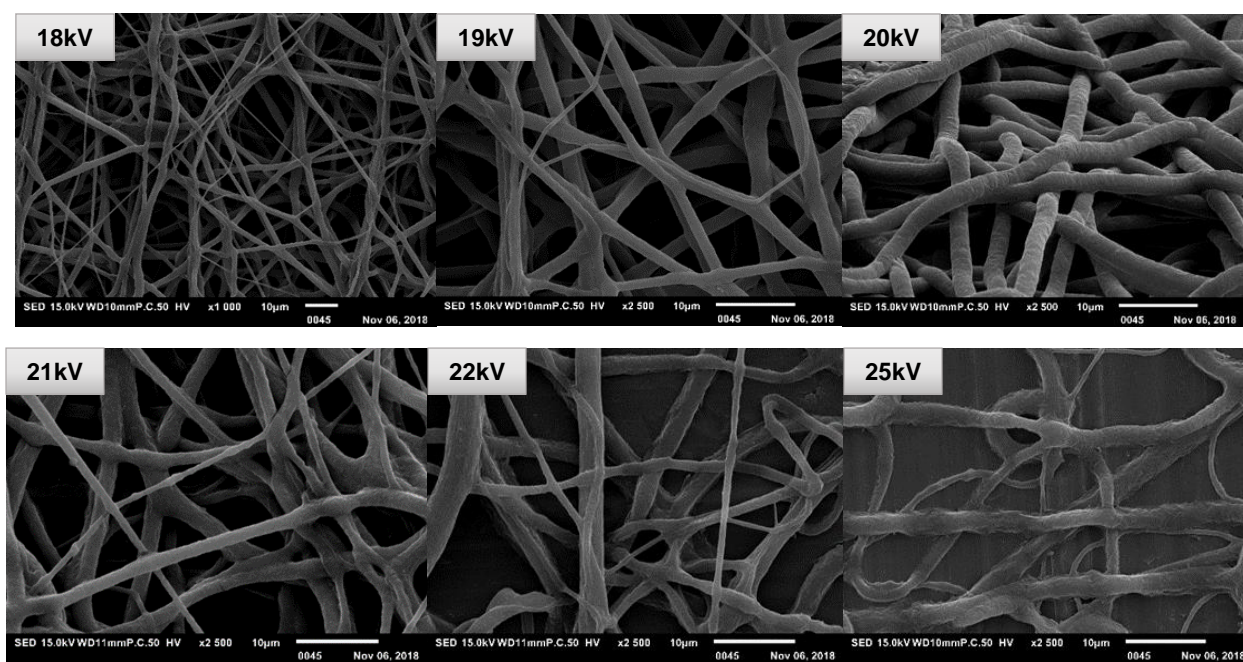


Figure 3.20. SEM images of 7%IBU+PCL/PEG-10% nanofibers at different voltages

Heterogeneous morphology of nanofibers was obvious from these SEM results. As the applied voltage was increased, the morphology of nanofibers distorted. At 25kV, nanofibers were no longer definite in shape and their boundaries looked somewhat fused. The CV% of nanofibers are higher in this case ranging from 12-80%. Neither any pores were seen on the surface of nanofibers as it was a possibility due to PEG-400 nor the agglomerates of IBU were noticed. Absence of IBU agglomerates on the surface of nanofibers endorse the possibility of IBU being embedded into the nanofibers structure [40]. Mean diameters and CV% of these nanofibers are enlisted in Table 3.15.

Table 3.15. Mean diameters and CV% of 7%IBU+PCL/PEG-10% nanofibers at different applied voltages

Sample	V (kV)	M.D (nm)	CV%
7%IBU+PCL/PEG-10%	18	1035 ± 547	53%
	19	930 ± 548	59%
	20	2155 ± 270	12%
	21	990 ± 490	50%
	22	1160 ± 929	80%
	25	1425 ± 835	58%

The bold figures represent the best selected electrospinning parameters for 7%IBU+PCL/PEG-10% nanofibers based on their less CV%.

Termination of Single-Needle Electrospinning Equipment

Due to some security reasons, the single-needle electrospinning machine was terminated for further use. Therefore, it was not possible to execute the remaining experiments of electrospinning.

Otherwise, the electrospinning of following experiments was due:

- 5%IBU+PCL/PEG-10%
- 5%IBU+PCL/PEG-20%
- 7%IBU+PCL
- 7%IBU+PCL/PEG-20%

9.3 Crystallinity of IBU loaded nanofibers

DSC analysis of IBU incorporated PCL and PCL/PEG-10% nanofibers was done to examine the impact of IBU on their crystallinity ratio, melting temperature and glass transition temperature of the nanofibers. Prior to test, all samples were sealed in non-hermetic capsules and analysis was performed under nitrogen atmosphere with a single cycle of heating from -80°C to 100°C at a rate of $10^{\circ}\text{C}/\text{min}$. The crystallinity ratio (X_c) was calculated with reference to the used content of PCL for nanofibers. Only first cycle of heating was considered to determine the crystallinity of samples. DSC curves were analyzed by using TA Universal Analysis software. Figure 3.21 demonstrates a DSC curve of 5%IBU+PCL nanofibers.

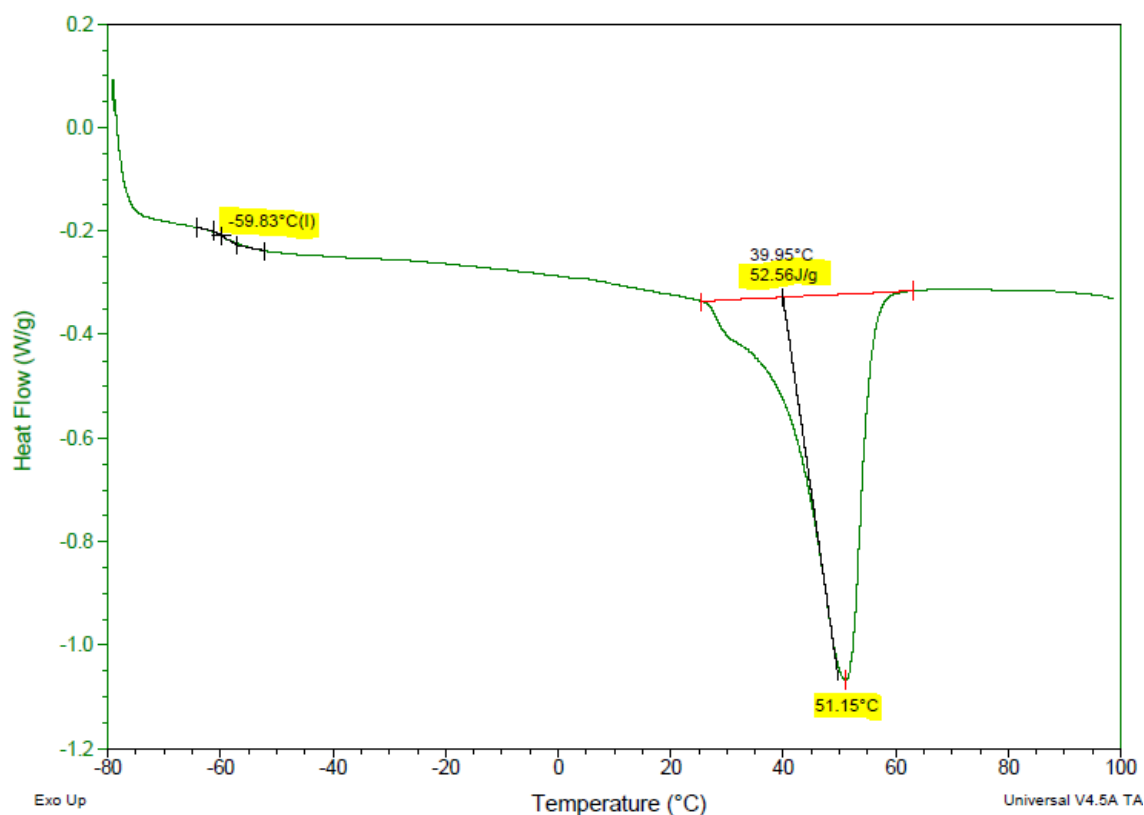


Figure 3.21. DSC curve of 5%IBU+PCL nanofibers showing first heating cycle from -80° - 100°C under N_2

It was observed that the melting temperatures of IBU loaded nanofibers were lower than that of pure PCL, PCL and PCL/PEG-10% nanofibers. The crystallinity ratios (X_c) of these 5%IBU+PCL and 7%IBU+PCL/PEG-10% nanofibers showed moderate values as shown in Table 3.16.

Table 3.16. Melting temperature (T_m), glass transition temperature (T_g) and crystallinity ratio (X_c) of 5%IBU+PCL and 7%IBU+PCL/PEG-10% nanofibers determined by their heating cycle from -80°C to 100°C under N_2

Sample	T_g ($^\circ\text{C}$)	T_m ($^\circ\text{C}$)	ΔH_m (J/g)	X_c %
Pure PCL	-64	57	63	40%
PCL nanofibers	-64	59	72	51%
5%IBU+PCL nanofibers	-60	51	53	39%
7%IBU+PCL/PEG-10% nanofibers	-61	50	59	46%

No sharp increase or decrease in crystallinity was observed due to IBU as it was the case with PCL and PCL/PEG nanofibers. Thus, it could be implied that IBU acted as a defect in nanofibers structure and hindered their crystalline arrangement. It could be possible that the PCL molecular chains had less opportunity to rearrange, nucleate and crystallize [41]. The melting temperature of pure IBU was also determined by its DSC analysis and it was at 77°C . No distinct peak of IBU melting around this temperature was seen.

9.4 Presence of IBU in nanofibers determined by thermal analysis

Thermal analysis of IBU loaded nanofibers was done in order to confirm the presence of IBU into the nanofibers. TGA analysis of pure IBU was also done to provide a reference for the nanofibers. The degradation curve of pure IBU, 5%IBU+PCL and 7%IBU+PCL-PEG-10% nanofibers are shown in Figure 3.22 (a), 3.22(b) and 3.22(c) respectively.

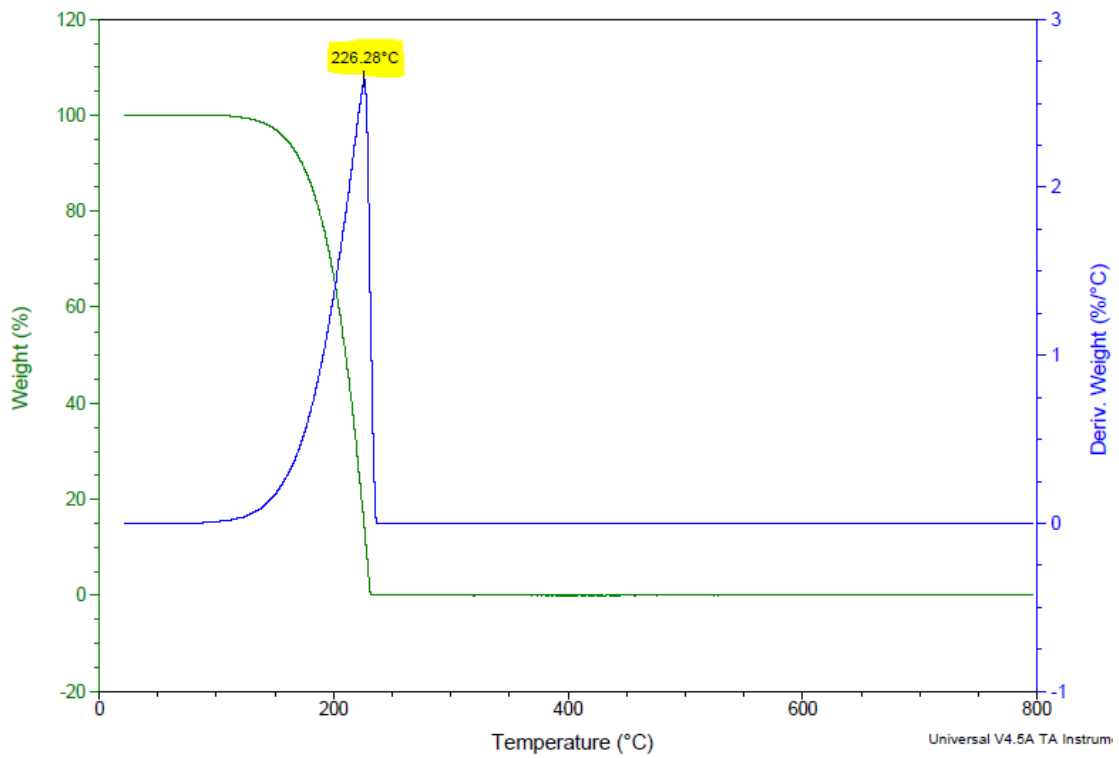


Figure 3.22 (a). Degradation curve of pure IBU at 10°C/min heating rate till 800°C under N₂

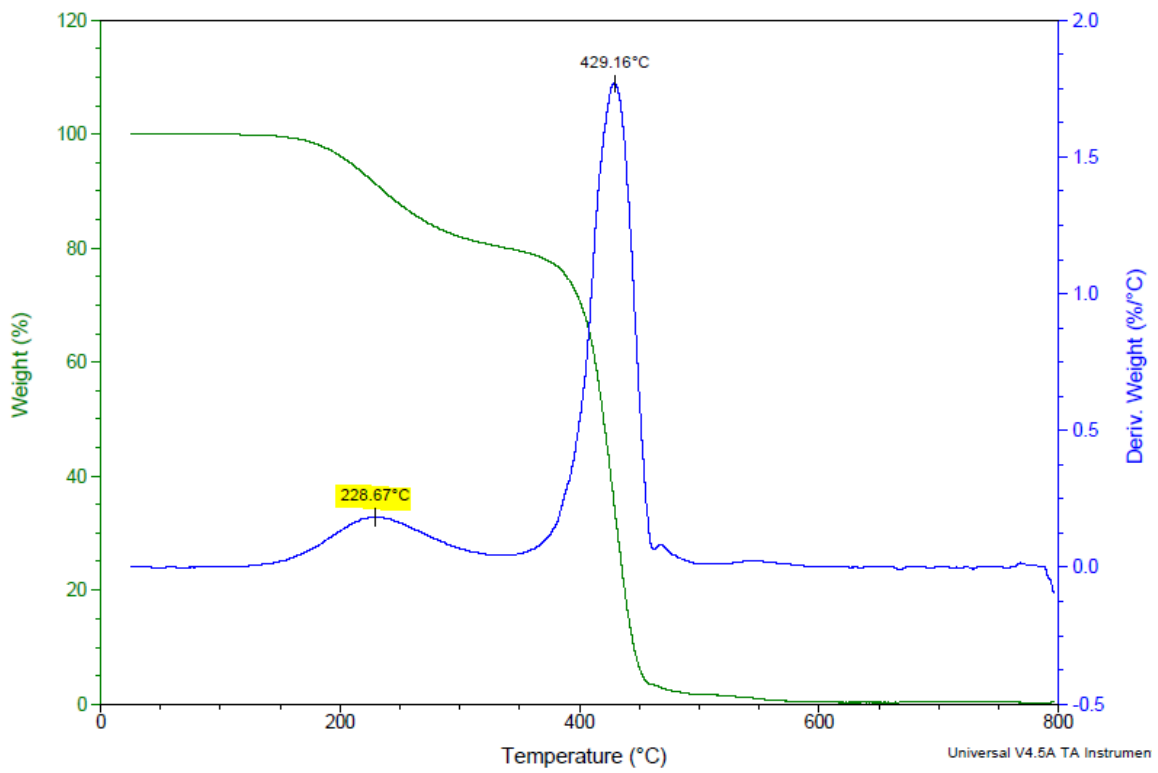


Figure 3.22 (b). Degradation curve of 5%IBU+PCL nanofibers at 10°C/min heating rate till 800°C under N₂

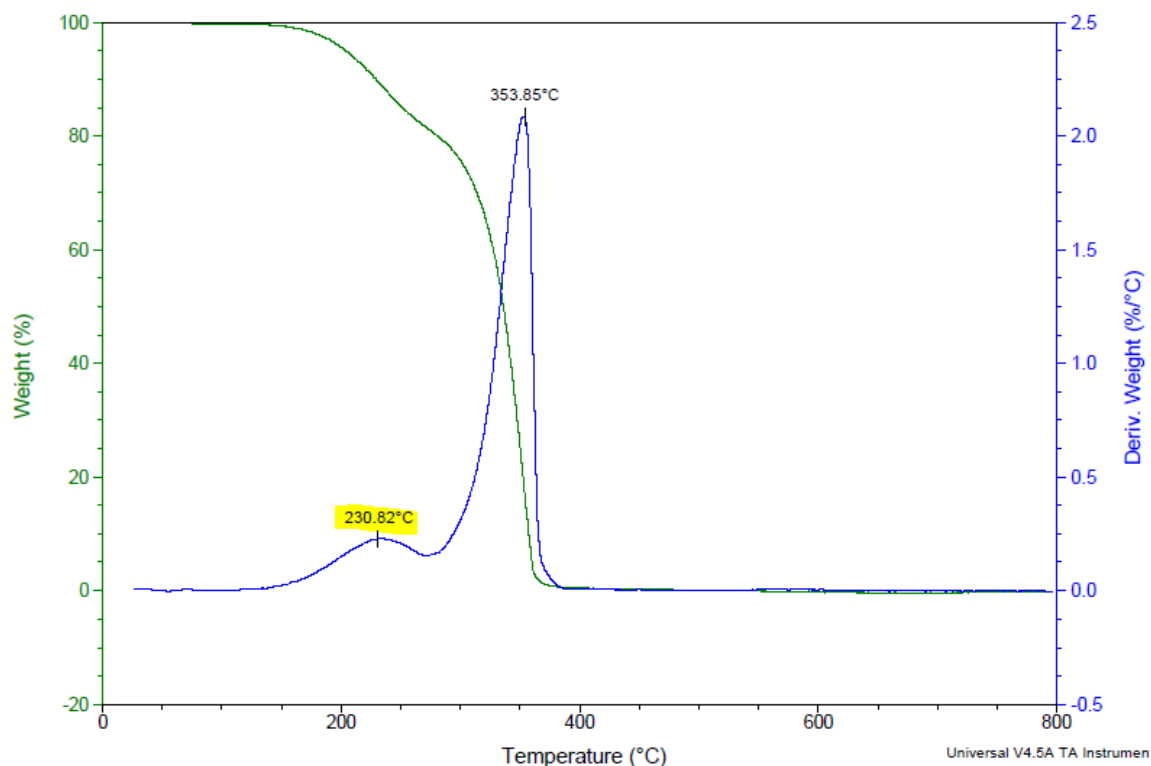


Figure 3.22 (c). Degradation curve of 7%IBU+PCL/PEG-10% nanofibers at 10°C/min heating rate till 800°C under N₂

The degradation curve of pure IBU showed that the complete degradation of drug took place at 226°C temperature that can be seen above in Figure 3.22 (a). In degradation curves of 5%IBU+PCL and 7%IBU+PCL/PEG-10% nanofibers, the presence of IBU was proved from the intermediate peaks noted at 228°C and 230°C respectively. Moreover, the quantification of IBU was done by considering the initial weight loss% of nanofibers as compared to their PCL and PCL/PEG-10% content. Theoretically, in case of 5%IBU+PCL nanofibers the amount of loaded IBU (5wt%) compared to PCL corresponds to 4.8%. So, the content of IBU calculated by its initial weight loss% was found to be 5.2% that is in agreement with the actual amount of IBU loaded into the nanofibers. Similarly, for 7%IBU+PCL/PEG-10% nanofibers added amount of IBU was 6.2% with respect to the PCL/PEG-10% content and from their degradation curve the amount of IBU was found to be 9% that is in accordance to its actual amount. These results proved that the drug was successfully incorporated into the nanofibers during their electrospinning.

10. Mechanical properties of nanofibers

Fundamental studies on mechanical properties of electrospun nanofibers typically focus on uniaxial tensile strength testing of randomly aligned nanofibers. In this study, tensile strength testing of PCL/PEG-10%, PCL/PEG-20%, and 7%IBU+PCL/PEG-10% nanofibers (electrospun with chloroform: ethanol with 88:12 wt/wt ratio as solvent) were performed. The obtained electrospun nanofibers were randomly oriented with heterogeneous morphology comprising of diameters ranging from nano to micro scale and had non-uniform thicknesses. Representative stress-strain curves of these randomly oriented PCL/PEG and IBU loaded nanofibers highlighted the intrinsic features of mechanical behavior of these nanofibers and are presented in Figures 3.23 and 3.24 respectively. Five samples of each type of nanofibers were tested. All the procedural details of this analysis have already been explained in Section 3.8 of Chapter 2.

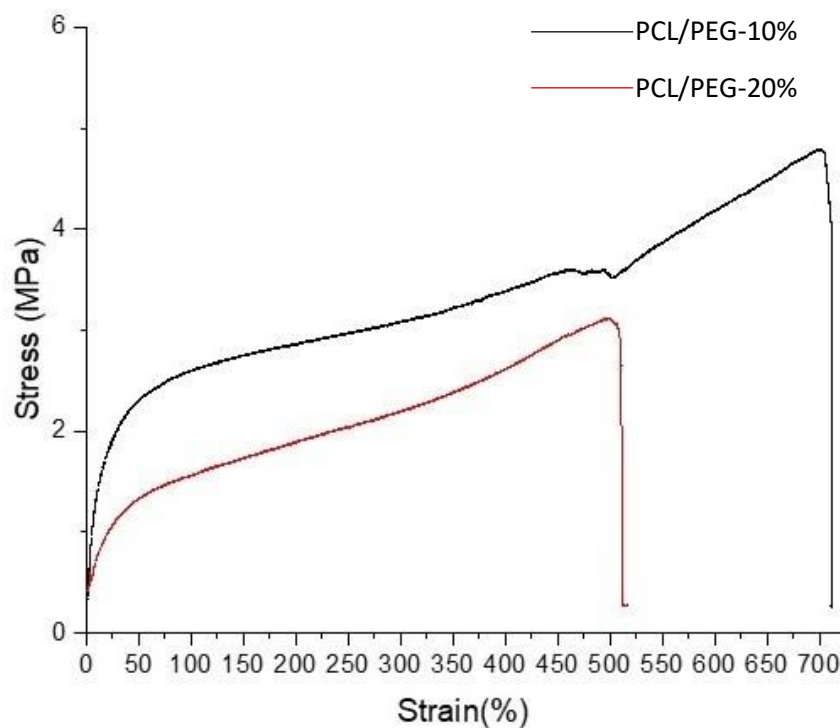


Figure 3.23. Typical stress-strain curves of PCL/PEG-10% and PCL/PEG-20% nanofibers

10.1 Influence of PEG-400 concentration

The stress-strain curves of PCL/PEG-10% and PCL/PEG-20% nanofibers can be divided into three sections: elastic, yielding and strain-hardening regions. Specifically, the initial linear elastic region occurs up to 2% strain where stretching and alignment of nanofibrous mats occurred along the direction of applied load. The values of tensile stress corresponding to the elongation at break for each sample are given in Table 3.17. It was observed that in PCL/PEG-10% nanofibers, as the applied stress increased up to 5 MPa, the percentage deformation in material was 560% with a total elongation in material up to 66mm. Whereas, in PCL/PEG-20% nanofibers, the maximum tensile stress was 3.7 MPa which produced a maximum strain of 370% with a total elongation in the material up to 47mm, as shown in Figure 3.23. Therefore, it was concluded that increasing the concentration of PEG-400 from 10wt% to 20wt%, decreased the uniaxial tensile strength of produced nanofibers [10].

Table 3.17. The maximum tensile stress corresponding to total elongation at break occurring in PCL/PEG-10%, PCL/PEG-20% and 7%IBU+PC/PEG-10% nanofibrous mats.

Sample	Nanofibers Mean Diameter (nm)	Tensile Stress (MPa)	*Strain%
PCL/PEG-10%	1200	5 ± 0.7	560%
PCL/PEG-20%	1100	3.7 ± 0.5	370%
7%IBU+PCL/PEG-10%	2100	1.8 ± 0.25	220%

*Note: The original length of the nanofibrous sample used for testing was 10mm.

10.2 Impact of IBU on mechanical properties of nanofibers

The stress-strain curve of 7%IBU+PCL/PEG-10% nanofibers is shown in Figure 3.24. It can be seen in Table 3.17 that the maximum tensile stress value reached up to 1.8 MPa and strain percentage was up to 220% with elongation at break of 32mm in the material. These stress-strain values are lower than observed in case of PCL/PEG-10% and PCL/PEG-20% nanofibers. These results depicted that PCL/PEG nanofibers were more ductile than IBU loaded nanofibers which means that incorporation of IBU reduced their tensile strength [11].

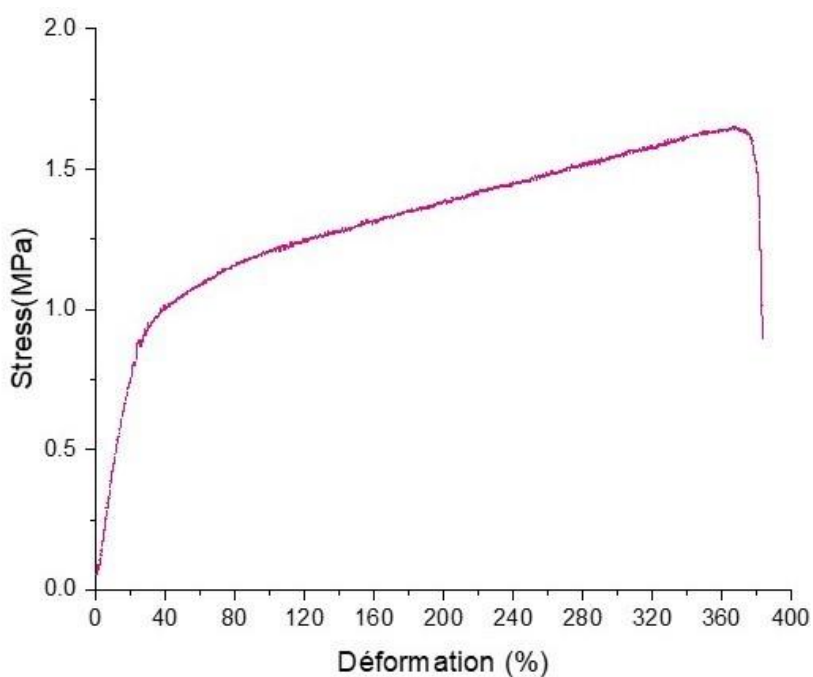


Figure 3.24. Typical stress-strain curve of 7%IBU+PCL/PEG-10% nanofibers

The relationship between these results of tensile strength and lower crystallinity values of IBU loaded nanofibers obtained from their DSC analysis, is clear and plausible. Lower crystallinity means more amorphous regions in molecular structure which eventually translates into poor tensile

strength of material. Hence, it was assumed that IBU acted as a defect in the molecular structure of nanofibers causing a decrease in their pliability and mechanical strength [9].

11. IBU release kinetics of nanofibers

The main objective of drug incorporation into PCL and PCL/PEG-10% nanofibers was to devise a drug delivery system in these non-woven electrospun mats for their wound dressing applications. The performance of these IBU loaded nanofibrous scaffolds was tested through *in vitro* drug release kinetic study. This analysis was performed by Pr. Leonard Ionut ATANASE and his team at the Faculty of Dental Medicine, University “Apollonia”, Iasi-Romania. Samples of IBU loaded nanofibers were immersed in phosphate-buffered saline (PBS) solution (pH=7) at 37°C as described in Chapter 2. The drug release efficiency of IBU was monitored for 24h duration. The percentage release efficiencies (%RE) of both samples, 5%IBU+PCL and 7wt%IBU+PCL/PEG-10% are given in Table 3.18.

Table 3.18. Initial and final release efficiency (%RE) of IBU from nanofibers

Samples	%RE (1.5h)	%RE (24h)
5%IBU+PCL	51%	85%
7%IBU+PCL/PEG-10%	39%	82%

† ES conditions: 20 kV applied voltage, 25 cm needle-collector distance and 0.5 mL/h feed rate

The graphical release profile of IBU from these samples is presented in Figure 3.25 below. Two distinct stages of IBU release were observed: a strong burst release phenomenon followed by a slower release until 24h. This initial burst release phenomenon was particularly intense during first 2h of analysis and has been described in several research studies [41]. It might be possible that a considerable amount of IBU could have migrated to the surface of ejected polymer solution during

electrospinning [42]. Additionally, IBU was incorporated into the amorphous regions of semi-crystalline PCL. In case of PCL/PEG-10% nanofibers, the dissolution of PEG-400 in aqueous medium could be responsible for a faster release of IBU from the nanofibers [43]. A phase separation phenomenon might have occurred between semi-crystalline PCL and water soluble PEG-400 that led to this abrupt drug release. There have been previous reports about the use of low molar mass PEG and leading to faster release of drug from blend nanofibers [9, 44, 45].

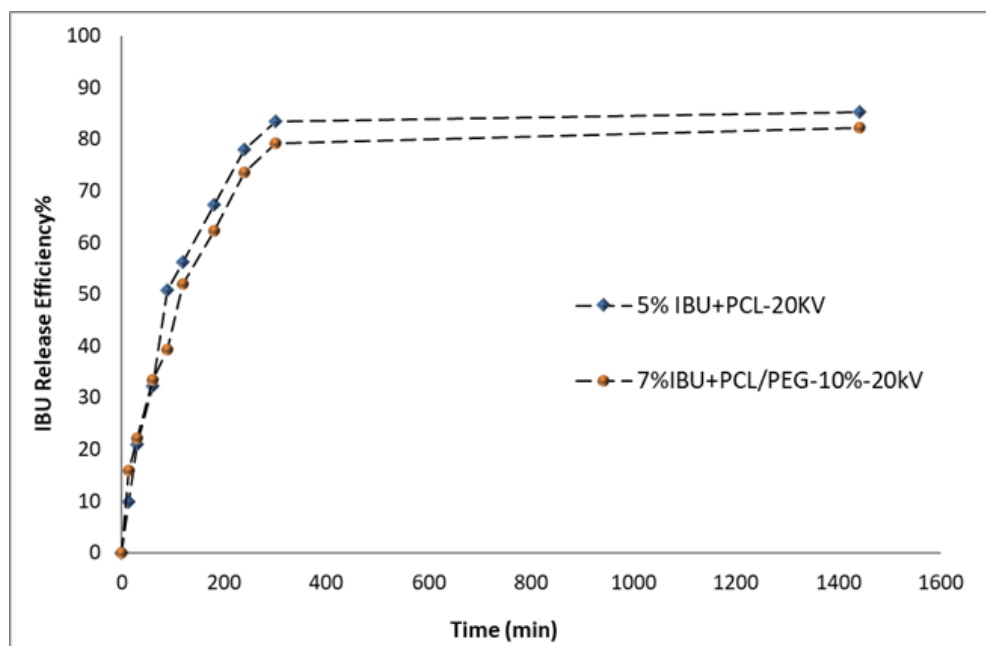


Figure 3.25. Graphical profile of IBU release kinetics from PCL and PCL/PEG-10% nanofibers during 24h.

This initial rapid release of the IBU could be attributed to the IBU agglomerates present on the surface of nanofibers. However, in case of 7wt%IBU+PCL/PEG-10% this effect of burst release of IBU was comparatively slower than for 5%IBU+PCL nanofibers [39, 46]. This steady release could be due to the reason that IBU was embedded into the nanofibers network rather than being dispersed on their surface. Moreover, the total amount of released IBU from nanofibers was not 100% which indicates that some amount of IBU was probably lost during the electrospinning process.

12. Conclusion

This chapter entailed all the results of preliminary studies of PCL electrospinning by using single-needle electrospinning technique. Initially, optimization of electrospinning parameters was done by creating samples of nanofibers using 10wt% pure PCL, PCL/PEG-10% and PCL/PEG-20% solutions in chloroform: ethanol (88:12 wt/wt) solvent. The applied parameters such as voltage, needle-collector distance and solution feed rate were varied to study their impact on the nanofibers morphology and diameters. By using a statistical tool known as “Principal Component Analysis”, the best electrospinning parameters for each sample were selected on the basis of homogeneity among nanofibers diameters. The SEM characterization of PCL and PCL/PEG nanofibers revealed their heterogeneous morphology with diameters ranging from nano to micro scale. All nanofibers were predominantly cylindrical in shape and PCL/PEG-10% nanofibers showed pores on their surface. The nanocapsules of chitosan loaded with Na-IBU were incorporated to PCL nanofibers in order to develop a drug delivery system. However, due to their poor dispersion and agglomeration problem, their use was discontinued for further experimental studies. To replace these nanocapsules, pure Ibuprofen (IBU) which is an anti-inflammatory and non-steroidal drug, was chosen as a suitable substitute. Two different concentrations of IBU, 5wt% and 7wt% were incorporated to PCL and PCL/PEG-10% nanofibers. Morphological study of these IBU loaded nanofibers revealed that the addition of IBU yielded round shaped nanofibers with relatively larger diameters in micro range.

From DSC studies, it was found that the crystallinity ratios of electrospun PCL and PCL/PEG nanofibers were higher than that of pure PCL and this effect was more pronounced in nanofibers containing PEG-400. Whereas, the nanofibers containing IBU showed decrease in crystallinity despite the presence of PEG-400 which showed that presence of IBU limited the crystallization of PCL chains. This enhanced effect of crystallinity ratio of PCL nanofibers also reflected in their

water contact angle measurements where large contact angle was recorded for PCL nanofibers in comparison to pure PCL film verifying their hydrophobic nature. However, quick absorption of water droplet was seen in case of PCL/PEG nanofibers which showed their improved wettability due to the addition of hydrophilic PEG-400. The results of thermal characterization of nanofibers confirmed the absence of any solvent left, after their electrospinning. Moreover, in thermal degradation curves of IBU loaded nanofibers, the presence of corresponding intermediate peaks of IBU validated the successful loading of drug into the nanofibers structure.

The uniaxial tensile strength of PCL/PEG nanofibers explained the fact that by increasing the concentration of PEG-400 in PCL nanofibers, the overall tensile strength will be decreased because PEG-400 acted as a plasticizer. Also, the stress-strain curve of nanofibers with IBU demonstrated poor mechanical properties as compared to their PCL/PEG counterparts. Finally, the *in vitro* drug release kinetics study of IBU loaded nanofibers was conducted to gauge their performance as a drug delivery system. An initial rapid release of IBU was recorded during first two hours of analysis followed by a gradual release. The total release efficiency of IBU up to 82% was achieved during 24h of analysis.

References

1. Bhardwaj, N. and S.C. Kundu, *Electrospinning: a fascinating fiber fabrication technique*. Biotechnol Adv, 2010. 28(3): p. 325-47.
2. Amir, D., *Effect of electrospinning process parameters of polycaprolactone and nanohydroxyapatite nanocomposite nanofibers*. Textile Research Journal, 2015. 85(14): p. 1445-1454.
3. Chou, S.-F., Carson, D., Woodrow, K. A., *Current strategies for sustaining drug release from electrospun nanofibers*. J. Control. Release., 2015. 220: p. 584-591.
4. Gizaw, M., et al., *Electrospun Fibers as a Dressing Material for Drug and Biological Agent Delivery in Wound Healing Applications*. Bioengineering (Basel), 2018. 5(1).
5. Cipitria, A., et al., *Design, fabrication and characterization of PCL electrospun scaffolds—a review*. Journal of Materials Chemistry, 2011. 21(26): p. 9419.
6. Mochane M. J., M.T.S., Sadiku E. R, Mokhena T. C. and Sefadi J. S., *Morphology and Properties of Electrospun PCL and Its Composites for Medical Applications: A Mini Review*. Applied Sciences, 2019. 9(11): p. 2205.
7. Chen, C.H., Chen, S. H., Shalumon, K. T. and Chen, J. P., *Prevention of peritendinous adhesions with electrospun polyethylene glycol/polycaprolactone nanofibrous membranes*. Colloids. Surf. B: Biointerfaces, 2015. 133: p. 221-30.
8. Bui H. T., C.O.H., Cruz J. D. and Park J. S., *Fabrication and characterization of electrospun curcumin-loaded polycaprolactone-polyethylene glycol nanofibers for enhanced wound healing*. Macromolecular Research, 2014. 22(12): p. 1288-1296.
9. Repanas A, W.W.F., Grykshov O, Müller M. and Glasmacher B., *PCL/PEG electrospun fibers as drug carriers for the controlled delivery of dipyridamole*. Journal of In Silico & In Vitro Pharmacology, 2015. 1(1:2): p. 1-10.
10. Tiwari A. P., J.M.K., Lee J., Bikendra M., Ko S. W., Park C. H. and Kim C. S., *Heterogeneous electrospun polycaprolactone/polyethylene glycol membranes with improved wettability, biocompatibility, and mineralization*. Colloids and Surfaces A: Physicochemical and Engineering Aspects., 2017. 520: p. 105-113.
11. Chou S-F. and Woodrow K.A., *Relationships between mechanical properties and drug release from electrospun fibers of PCL and PLGA blends*. J. Mech. Behav. Biomed. Mater., 2017. 65: p. 724-733.

12. Celik G. and Oksuz A. U., *Controlled Release of Ibuprofen From Electrospun Biocompatible Nanofibers With In Situ QCM Measurements*. Journal of Macromolecular Science, Part A, 2014. 52(1): p. 76-83.
13. Sigg, J., *Production of drug-delivery systems with Ibuprofen through encapsulation in nanofibers and -particles with core-shell architecture*, in *Life Science and Facility Management 2017*, ZHAW, Studieren Zürich. p. 65.
14. Qin, X. and D. Wu, *Effect of different solvents on poly(caprolactone) (PCL) electrospun nonwoven membranes*. Journal of Thermal Analysis and Calorimetry, 2011. 107(3): p. 1007-1013.
15. Gil-Castell O., B.J.D., Strömberg E., Karlsson S. and Ribes-Greus A., *Effect of the dissolution time into an acid hydrolytic solvent to tailor electrospun nanofibrous polycaprolactone scaffolds*. European Polymer Journal, 2017. 87: p. 174-187.
16. Van der Schueren L., D.S.B., Kalaoglu O. I., De Clerck K., *An alternative solvent system for the steady state electrospinning of polycaprolactone*. European Polymer Journal, 2011. 47: p. 1256-1263.
17. Ferreira J. L., G.S., Henriques C., Borges J. P. and Silva J. C., *Electrospinning Polycaprolactone Dissolved in Glacial Acetic Acid*. Journal of Applied Polymer Science, 2014. 131.
18. Angamma C. J. and Jayaram S. H., *Analysis of the Effects of Solution Conductivity on Electrospinning Process and Fiber Morphology*. IEEE Transactions on Industry Applications, 2011. 47(3): p. 1109-1117.
19. Del Gaudio C., B.A., Folin M., Baiguera S., Grigioni M., *Structural characterization and cell response evaluation of electrospun PCL membranes: micrometric versus submicrometric fibers*. J. Biomed. Mater. Res. A, 2009. 4(89A): p. 1028-1039.
20. Lowery J.L., D.N., Rutledge G.C., *Effect of fiber diameter, pore size and seeding method on growth of human dermal fibroblasts in electrospun poly(epsilon-caprolactone) fibrous mats*. Biomaterials, 2010. 31(3): p. 491-504.
21. Smith L. A., M.P.X., *Nanofibrous scaffolds for tissue engineering*. Colloid Surface B, 2004. 39(3): p. 125-131.
22. Van der Schueren, L., et al., *Polycaprolactone and polycaprolactone/chitosan nanofibres functionalised with the pH-sensitive dye Nitrazine Yellow*. Carbohydr Polym, 2013. 91(1): p. 284-93.

23. Saraf A., L.G., Haesslein A., Kasper F.K., Raphael R.M., Baggett L.S. and Mikos A.G., *Fabrication of Nonwoven Coaxial Fiber Meshes by Electrospinning*. Tissue Engineering Part C: Methods, 2009. 15(3).
24. Kolbuk D., G.-L.S., Sajkiewicz P., Maniura-Weber K. and Fortunato G., *The Effect of Selected Electrospinning Parameters on Molecular Structure of Polycaprolactone Nanofibers*. International Journal of Polymeric Materials and Polymeric Biomaterials, 2015. 64: p. 365-377.
25. Kostakova E. K., M.L., Maskova G., Blazkova L., Turcsan T. and Lukas D., *Crystallinity of Electrospun and Centrifugal Spun Polycaprolactone Fibers: A Comparative Study*. Journal of Nanomaterials, 2017. 2017: p. 1-9.
26. Wang X., Z.H., Turng L-S. and Li Q., *Crystalline Morphology of Electrospun Poly(ϵ -caprolactone) (PCL) Nanofibers*. Industrial & Engineering Chemistry Research, 2013. 52(13): p. 4939-4949.
27. Patankar N. A., *Mimicking the Lotus Effect: Influence of Double Roughness Structures and Slender Pillars*. ACS publications, 2004. 20(19): p. 8209–8213.
28. Li Y-F., R.M., Aslan H., Yu Y., Howard K. A., Dong M., Besenbachera F. and Chen M., *Ultraporous interweaving electrospun microfibers from PCL–PEO binary blends and their inflammatory responses*. Nanoscale, 2014. 6: p. 3392–3402.
29. Liu M., D.X.P., Li Y.M., Yang D.P. and Long Y.Z., *Electrospun nanofibers for wound healing*. Mater. Sci. Eng. C, 2017. 76: p. 1413-1423.
30. Wang J. and Windbergs M., *Functional electrospun fibers for the treatment of human skin wounds*. European Journal of Pharmaceutics and Biopharmaceutics, 2017. 119: p. 283–299.
31. Cipitria A., S.A., Dargaville T. R., Daltonac P. D. and Hutmacher D. W., *Design, fabrication and characterization of PCL electrospun scaffolds—a review*. Journal of Materials Chemistry, 2011. 21: p. 9419–9453.
32. Huang S. and Fu X., *Naturally derived materials-based cell and drug delivery systems in skin regeneration*. J. Control. Release, 2010. 142(2): p. 149-159.
33. Chen M., G.S., Dong M., Song J., Yang C., Howard K. A., Kjems J. and Besenbacher F., *Chitosan/siRNA Nanoparticles Encapsulated in PLGA Nanofibers for siRNA Delivery*. ACS Nano, 2012. 6(6): p. 4835–4844.

34. Wang Y., W.B., Qiao W. and Yin T., *A novel controlled release drug delivery system for multiple drugs based on electrospun nanofibers containing nanoparticles*. J Pharm Sci, 2010. 99(12): p. 4805-11.
35. Rață D. M, C.J.-F., Peptu C. A., Costuleanu M. and Popa M., *Chitosan: poly(N-vinylpyrrolidone-alt-itaconic anhydride) nanocapsules—a promising alternative for the lung cancer treatment*. Journal of Nanoparticle Research, 2015. 17(7).
36. Rață D. M., P.M., Chailan J-F., Tamba B. I., Ionut Tudorancea and Peptu C. A., *Ibuprofen-loaded chitosan/ poly(maleic anhydride-alt-vinyl acetate) submicronic capsules for pain treatment*. Journal of Bioactive and Compatible Polymers, 2013. 28(4): p. 368-384.
37. Szymańska E. and Winnicka K., *Stability of Chitosan—A Challenge for Pharmaceutical and Biomedical Applications*. Marine Drugs, 2015. 13: p. 1819-1846.
38. Gohary M. I., H.B.M., Al Saeed A. A., Tolba E., El Rashedi A. M. and Saleh S., *Electrospinning of doxorubicin loaded silica/poly(ϵ -caprolactone) hybrid fiber mats for sustained drug release*. Advances in Natural Sciences: Nanoscience and Nanotechnology, 2018. 9(2): p. 025002.
39. Tran T., H.M., Patel D., Burns E., Peterman V. and Wu J., *Controllable and switchable drug delivery of ibuprofen from temperature responsive composite nanofibers*. Nano Convergence., 2015. 2(15).
40. Potrc T., B.S., Roskar R., Planinsek O., Lavric Z., Kristl J. and Kocbek P., *Electrospun polycaprolactone nanofibers as a potential oromucosal delivery system for poorly water-soluble drugs*. Eur J Pharm Sci, 2015. 75: p. 101-13.
41. Shi Y., W.Z., Zhao H., Liu T., Dong A. and Zhang J., *Electrospinning of ibuprofen-loaded composite nanofibers for improving the performances of transdermal patches.,.* Journal of Nanoscience and Nanotechnology, 2013. 13(6): p. 3855-3863.
42. Zamani M., M.M., Varshosaz J. and Jannesari M., *Controlled release of metronidazole benzoate from poly ϵ -caprolactone electrospun nanofibers for periodontal diseases*. Eur. J. Pharm. Biopharm., 2010. 75: p. 179-185.
43. Kim T. G., L.D.S.a.P.T.G., *Controlled protein release from electrospun biodegradable fiber mesh composed of poly(ϵ caprolactone) and poly(ethylene oxide)*. Int. J. Pharm., 2007. 338: p. 276-283.

44. Saraf A., B.L.S., Raphael R. M., Kasper F. K. and Mikos A. G., *Regulated non-viral gene delivery from coaxial electrospun fiber mesh scaffolds*. J. Controlled Release, 2010. 143: p. 95-103.
45. Valarezo E., T.L., González S., Malagón O. and Vittoria V., *Fabrication and sustained release properties of poly(ϵ -caprolactone) electrospun fibers loaded with layered double hydroxide nanoparticles intercalated with amoxicillin*. Appl. Clay. Sci., 2013. 72: p. 104-109.
46. Karavasili C., B.N., Kontopoulou I., Smith A., Van der Merwe S. M., Rehman I. U. R., Ahmad Z. and Fatouros D. G., *Preparation and Characterization of Multiactive Electrospun Fibers: Poly-caprolactone Fibers Loaded with Hydroxyapatite and Selected NSAIDs*. J. Biomedical Materials Research Part A, 2014. 102(8): p. 2583-2589.

Chapter 4: Needleless Electrospinning and Characterization of PCL and PCL/PEG Nanofibers

Chapitre 4: Electrospinning sans aiguille et caractérisation des nanofibres PCL et PCL/PEG

Une technique avancée semi-industrielle sans aiguille d'électrofilage des nanofibres a été utilisée pour synthétiser des nanofibres PCL et PCL/PEG. Après optimisation des paramètres d'électrofilage, un médicament modèle, l'Ibuprofène (IBU), a été incorporé à ces nanofibres PCL et PCL/PEG en deux concentrations différentes et leur électrofilage a été réalisé. Une tentative d'électrofilage des nanofibres PCL avec du sel de sodium d'ibuprofène (Na-IBU) a également été réalisée. Cependant, en raison d'un dépôt inadéquat de nanofibres et de difficultés dans le processus d'électrofilage, l'utilisation de Na-IBU a été arrêtée. L'analyse morphologique des nanofibres obtenues a été réalisée par traitement d'image et leurs images MEB ont mis en évidence leurs formes rondes et leur nature hétérogène. Les diamètres moyens de ces nanofibres ont été mesurés par le logiciel ImageJ en prenant 50 mesures et leur CV% a été calculé. Les diamètres moyens de tous les échantillons de nanofibres chargées en PCL, PCL/PEG et IBU étaient inférieurs à un micron. L'analyse DSC de ces nanofibres a montré des taux de cristallinité plus élevés des nanofibres électrofilées par rapport au taux de cristallinité de la PCL de départ. Il a été observé qu'en augmentant la teneur en PEG-400 dans les nanofibres, leur cristallinité augmentait également. En revanche, l'incorporation d'IBU a diminué le taux de cristallinité des nanofibres car le médicament agissait comme un défaut dans leur structure. Aucun pic d'évaporation du solvant n'a été enregistré lors de l'analyse TGA des nanofibres et il a été établi que l'ajout de PEG-400 ou IBU n'avait pas d'effet substantiel sur la dégradation thermique des nanofibres. Des pics distincts de dégradation de l'IBU sont observables sur les courbes TGA des nanofibres chargées en médicament, ce qui confirme sa présence dans le réseau nanofibreux. La cinétique de libération du médicament in vitro des nanofibres chargées en IBU pendant 48h a montré une libération régulière

d'IBU suivie d'une libération complète jusqu'à 80% en 6 jours. Cette libération prolongée d'IBU à partir des nanofibres était une caractéristique souhaitée pour son application en tant que pansement. Cependant, les nanofibres contenant du PEG-400 présentaient une libération d'IBU partielle. Par conséquent, il a été décidé pour la suite de l'étude que seules les nanofibres PCL chargées d'IBU seront étudiées pour leurs profils de libération de médicaments.

CHAPTER 4

NEEDLELESS ELECTROSPINNING AND CHARACTERIZATION OF PCL AND PCL/PEG NANOFIBERS

1. Introduction

After single-needle electrospinning of PCL nanofibers, another electrospinning technique was investigated to produce nanofibers in large volumes that is called “Needleless Electrospinning”. The needleless electrospinning equipment used for this purpose was [®]Elmarco’s “NanoSpider” pilot plant (Model NS 1WS500U, Czech Republic). Instead of a needle, metallic wire electrode was used on which polymer solution was coated by a solution carriage moving across its length as shown in Figure 4.1. All the equipment details and its working principle have already been entailed in Section 2.4 of Chapter 2.



Figure 4.1. Nanofibers production from a polymer solution coated wire electrode and a solution carriage moving across its length

The main advantage of this needleless technique is the faster fabrication of nanofibers in large proportions. However, a comparison between both electrospinning techniques shows differences in their applied parameters and their impact on the properties of nanofibers. For instance, needleless electrospinning requires much higher voltages between two electrodes to create an

electric field as compared to single-needle electrospinning. Moreover, a hypothesis was made that nanofibers morphology and their yield will also differ than that of single-needle electrospinning. To testify this hypothesis, electrospinning of PCL, PCL/PEG and IBU loaded nanofibers was done followed by their characterization. Preliminary experiments were performed to optimize the electrospinning parameters. All samples were produced at $35 \pm 4\%$ relative humidity and $25 \pm 2^\circ\text{C}$ temperature. This chapter explains the fabrication of nanofibers by needleless electrospinning and their physico-chemical attributes including their morphology, nanofibers diameters, crystallinity ratios and their thermal behavior. The drug release kinetics of IBU loaded nanofibers were also studied and explained.

2. Needleless electrospinning of pure PCL, PCL/PEG and IBU loaded nanofibers

The needleless electrospinning of pure PCL, PCL/PEG-10%, PCL/PEG-20% and IBU loaded nanofibers was done by using chloroform: ethanol solvent in 88:12 wt/wt ratio. All samples were prepared by doing electrospinning for 30min. The distance between two wire electrodes was kept at 220mm and 0.5mm orifice size was used to deposit polymer solution on wire electrode. Electrospun nanofibers were deposited on aluminum foil substrate. Two voltages (-ve and +ve) were applied to create a potential difference between two electrodes and their cumulative values will be mentioned in the following sections.

Morphology of nanofibers

Morphology of all obtained nanofibers was determined by their SEM analysis. All images were taken at $10\mu\text{m}$ except on image of 7%IBU+PCL/PEG-20% that was taken at $5\mu\text{m}$ in order to show the presence of IBU agglomerates on the surface of nanofibers and are presented in Figure 4.2.

Mean diameters of nanofibers were measured by using ImageJ software by taking fifty bar measurements each specimen to ensure uniform representation of the sample. The optimum values of applied voltages were chosen after analyzing their mean diameters and CV%. Samples with less CV% values were selected as the best conditions for electrospinning.

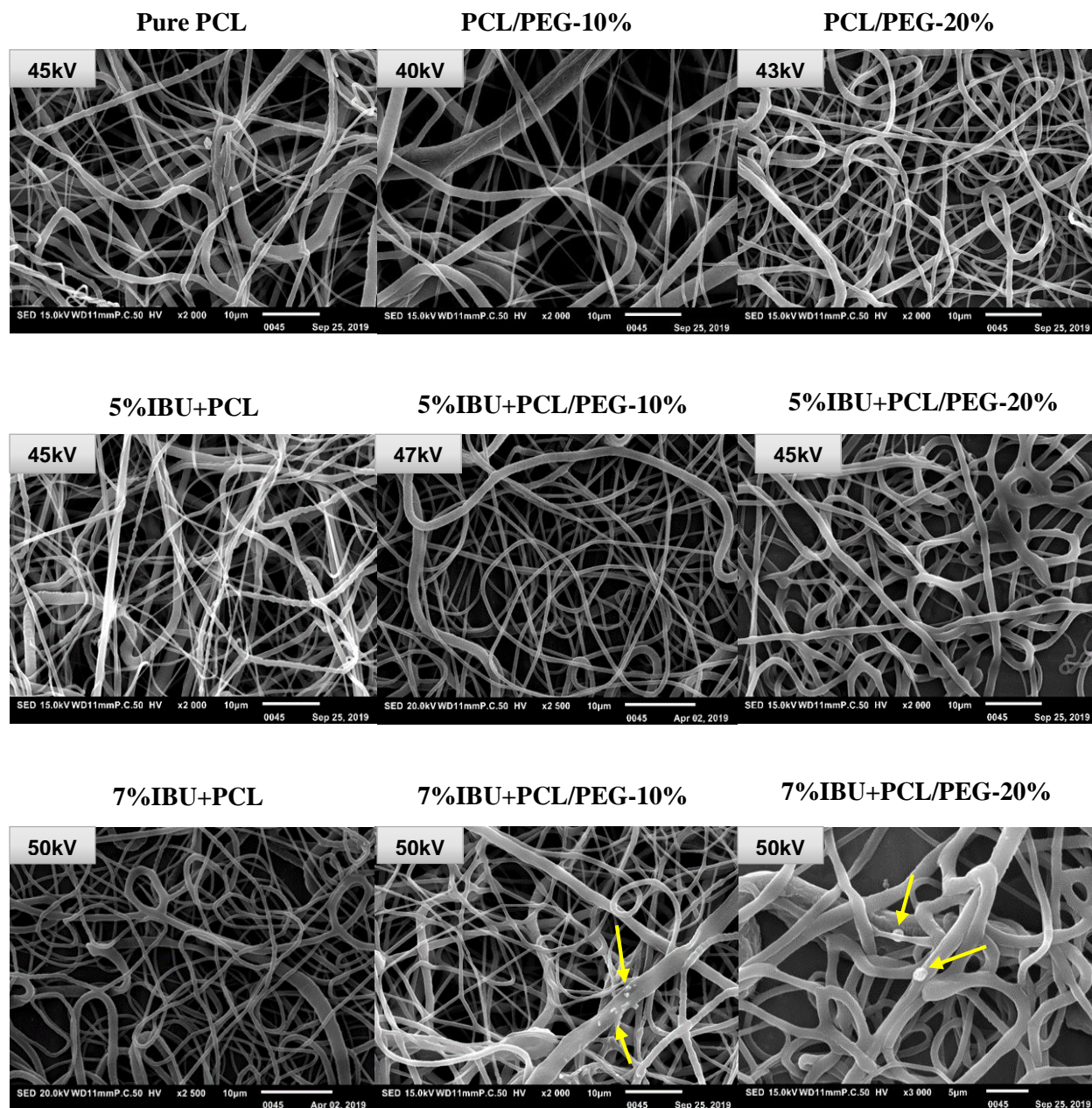


Figure 4.2. SEM images of PCL nanofibers with different concentrations of PEG and IBU electrospun by needleless electrospinning using optimized electrospinning parameters

Formation of ultrafine nanofibers network

The SEM images showed that all nanofibers were heterogeneous in nature and largely round in shape. A network of very fine nanofibers was seen among other nanofibers having relatively bigger diameters. Formation of these ultrafine nanofibers could be attributed to the additional splitting of initial jet of polymer solution under the influence of strong electric forces. At first, a single jet of polymer solution starts from the electrode surface and is stretched under electric field but due to higher charge density and Coulomb's repulsion forces, this jet further splits into multiple jets thus forming a network of ultrafine nanofibers [1-3]. Due to heterogeneous nature of nanofibers, the CV% values were higher up to 70% with mean diameters ranging from 400-800nm.

Impact of PEG-400 and IBU

In case of nanofibers with PEG-400, no sharp increase or decrease in diameters was observed as compared to pure PCL nanofibers. Contrary to the nanofibers electrospun by single-needle electrospinning, there were no pores on the surface of these PCL/PEG nanofibers obtained by needleless electrospinning. Similarly, nanofibers containing IBU did not show any significant influence of drug on the mean diameter of resulting nanofibers or their morphology. Diameters of all samples of PCL nanofibers with PEG-400 and IBU were heterogeneous with large percentage values of coefficient of variation (CV%) that are enlisted in Table 4.1. Agglomerations of IBU were observed in two samples that are illustrated with yellow colored arrows in Figure 4.2.

Table 4.1. Mean diameters and CV% of pure PCL, PCL/PEG and IBU loaded nanofibers electrospun by needleless electrospinning

Sample	Applied Voltage (kV)	Mean Diameter (nm)	CV%
Pure PCL	45	590 ± 400	68%
PCL/PEG-10%	40	740 ± 640	86%
PCL/PEG-20%	43	510 ± 300	58%
5%IBU+PCL	45	510 ± 340	66%
5%IBU+PCL/PEG-10%	47	700 ± 310	44%
5%IBU+PCL/PEG-20%	45	755 ± 345	45%
7%IBU+PCL	50	630 ± 235	37%
7%IBU+PCL/PEG-10%	50	635 ± 480	75%
7%IBU+PCL/PEG-20%	50	840 ± 320	37%

*Note: The distance between the two electrodes was 220mm and orifice size was 0.5mm.

3. Needleless electrospinning of PCL nanofibers with Na-IBU

The sodium salt of Ibuprofen (Na-IBU) was chosen to be incorporated into nanofibers due to its hydrophilic nature as compared to pure Ibuprofen (IBU) that is hydrophobic. It was supposed that the good miscibility of this drug in water will enhance its release in aqueous media from the electrospun nanofibers. Hence, the needleless electrospinning of PCL nanofibers was performed by incorporating the Na-IBU into PCL and PCL/PEG solutions by using chloroform: ethanol as solvent in 88:12 wt/wt ratio. Two different concentrations of this drug, 5wt% and 7wt% with respect to PCL were added to the PCL solution and were subjected to electrospinning process. Although, nanofibers were deposited on the substrate but their quantity was very less. Despite

increasing the sample production time from 30min to 45min, the quantity of deposited nanofibers was not appreciable. It was obvious that the addition of Na-IBU has adversely impacted the electrospinnability of PCL nanofibers thus producing very less amount of sample. Different applied voltages were tried to see their effect but no significant improvement was found.

This problem could be explained by considering the polar nature of drug and presence of Na⁺ ions in a non-polar solvent such as chloroform. Under strong electric field, the poor interaction between these Na⁺ ions and solvent could act as a disturbance in initiation of polymer jets and their stretching. The literature review offered a more logical explanation for this problem which states that the addition of salts increases the conductivity of polymer solution by increasing its overall charge density [4]. The electrostatic forces induced on the fluid surface therefore significantly increase due to the external electric field. Hypothetically, the enhanced electrostatic forces facilitate the initiation of polymer jets. On the other hand, ionic salts increase the conductivity of fluids which cause a decrease in the tangential electric field along the surface of fluid. This decrease in tangential electric field due to increased conductivity of polymer solution causes the electrostatic forces along the surface of fluid to diminish considerably. The total effect of this phenomenon thus negatively impact the formation of polymer jets that is a key factor for smooth electrospinning process [5, 6].

Morphology of Na-IBU loaded PCL nanofibers

The SEM images of PCL nanofibers incorporated with 5%Na-IBU and 7%Na-IBU are shown in Figures 4.3 and 4.4 respectively. These SEM images were taken at 10 μ m scale and the images showing size of agglomerates of Na-IBU were taken at 1 μ m. The mean diameters of nanofibers were measured by taking 50 bar measurements per sample using ImageJ software.

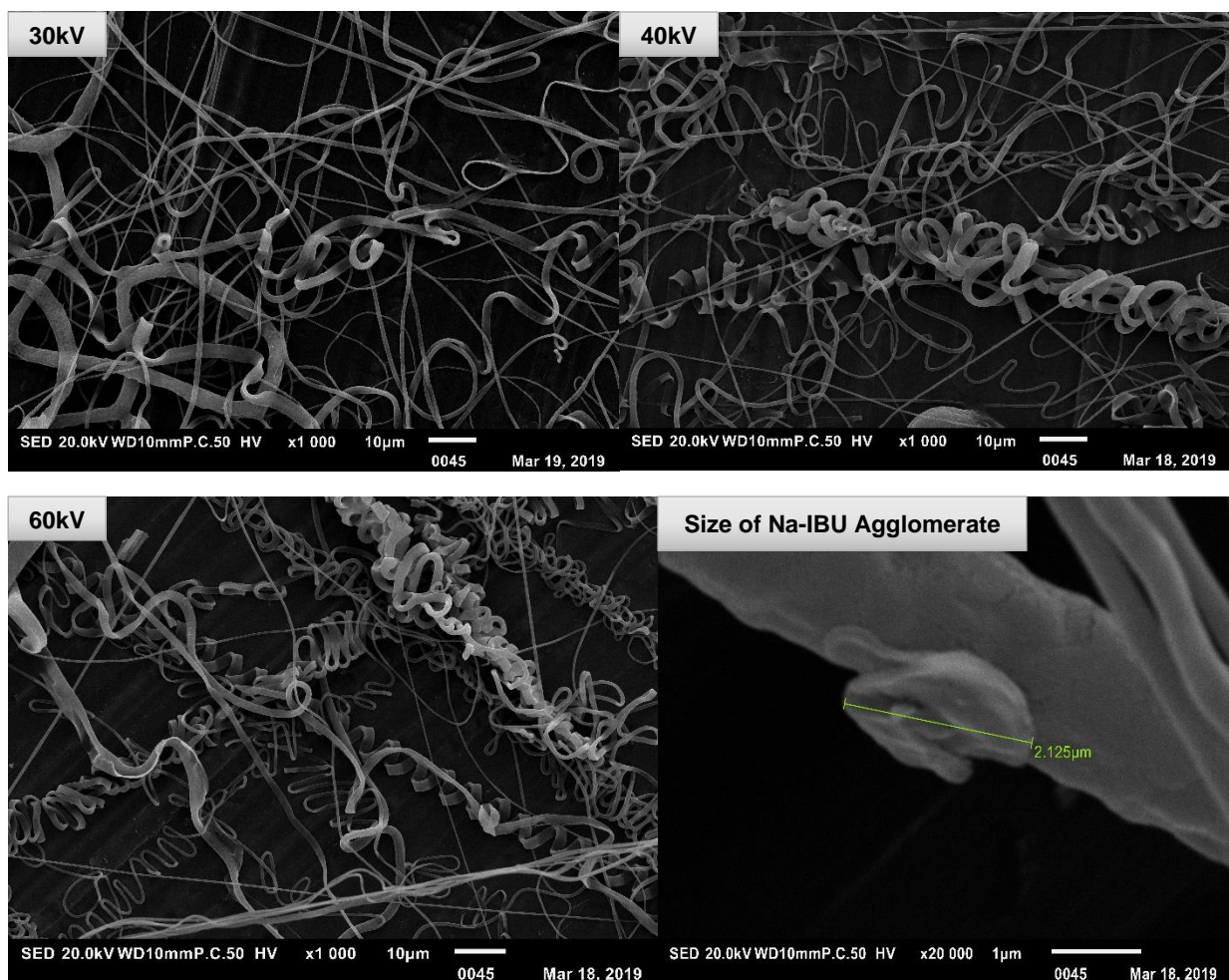


Figure 4.3. SEM images of 5%Na-IBU+PCL nanofibers at different voltages and agglomerations of Na-IBU on the surface of nanofibers

These images demonstrate a flat ribbon like shape of nanofibers instead of round/cylindrical shape with a zig-zag manner of deposition. The inadequate deposition of nanofibers can be observed visibly in these micrographs. Big agglomerates of Na-IBU (almost 2-3 µm in size) were also found on the surface of nanofibers. The diameters were heterogeneous and were in a range of 700-800nm. It can be seen in SEM images that with increasing voltage, the irregularity in nanofibers deposition also increased and was more pronounced in the form of zig-zag patterns.

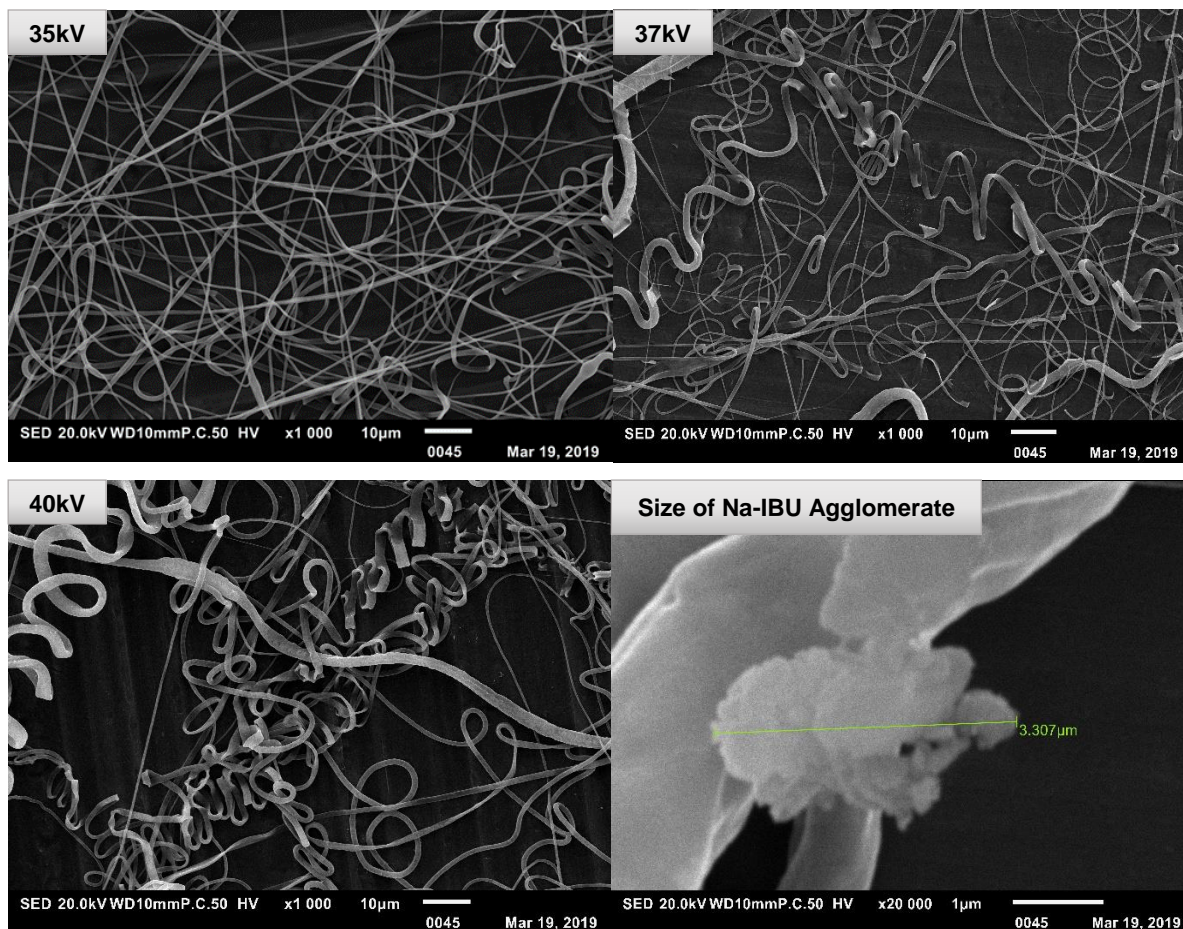


Figure 4.4. SEM images of 7%Na-IBU+PCL nanofibers at different voltages and agglomerates of Na-IBU on the surface of nanofibers

In case of 7%Na-IBU+PCL nanofibers, flat ribbon shaped nanofibers were obtained with zig-zag pattern of deposition which was more evident at higher voltages. Agglomerates of Na-IBU were also found on the surface of nanofibers of approximately $3.3\mu\text{m}$ in size as shown in Figure 4.4. Nanofibers diameters were heterogeneous ranging from 400-900nm and the amount of deposited nanofibers was insufficient. Mean diameters of all nanofibers along with their standard deviation and CV% are mentioned in Table 4.2.

Table 4.2. Mean diameters and CV% of Na-IBU loaded PCL nanofibers electrospun by needleless electrospinning

Sample	Applied Voltage (kV)	Mean Diameter (nm)	CV%
5%Na-IBU+PCL	30	715 ± 420	58%
5%Na-IBU+PCL	40	700 ± 424	60%
5%Na-IBU+PCL	60	760 ± 475	62%
7%Na-IBU+PCL	35	555 ± 185	33%
7%Na-IBU+PCL	37	435 ± 290	66%
7%Na-IBU+PCL	40	990 ± 290	29%

*Note: The distance between the two electrodes was 220mm and orifice size was 0.5mm.

Due to difficulty in electrospinning and inadequate deposition of nanofibers on the substrate, further experiments of needleless electrospinning of Na-IBU loaded nanofibers were halted.

4. Crystallinity of PCL and PCL/PEG Nanofibers Electrospun by Needleless Electrospinning

The crystallinity ratio of nanofibers electrospun by needleless technique was determined by their DSC analysis. All samples were sealed in non-hermetic capsules and analysis was performed under nitrogen atmosphere with a single cycle of heating from -80°C to 100°C at a rate of 10°C/min. The crystallinity ratio (X_c) was calculated with reference to the PCL content used and by dividing the ΔH_m of each sample by the melting enthalpy of 100% crystalline PCL ($\Delta H_{m,PCL}$) [7]. The DSC analysis of pure PCL pellets was also performed as a reference for the nanofibers. DSC curves were extracted by using TA Universal Analysis software for analysis. The DSC curves of PCL,

5% IBU+PCL/PEG-10% and 7% IBU+PCL/PEG-10% nanofibers are shown in Figures 4.5 (a), 4.5 (b) and 4.5 (c) respectively.

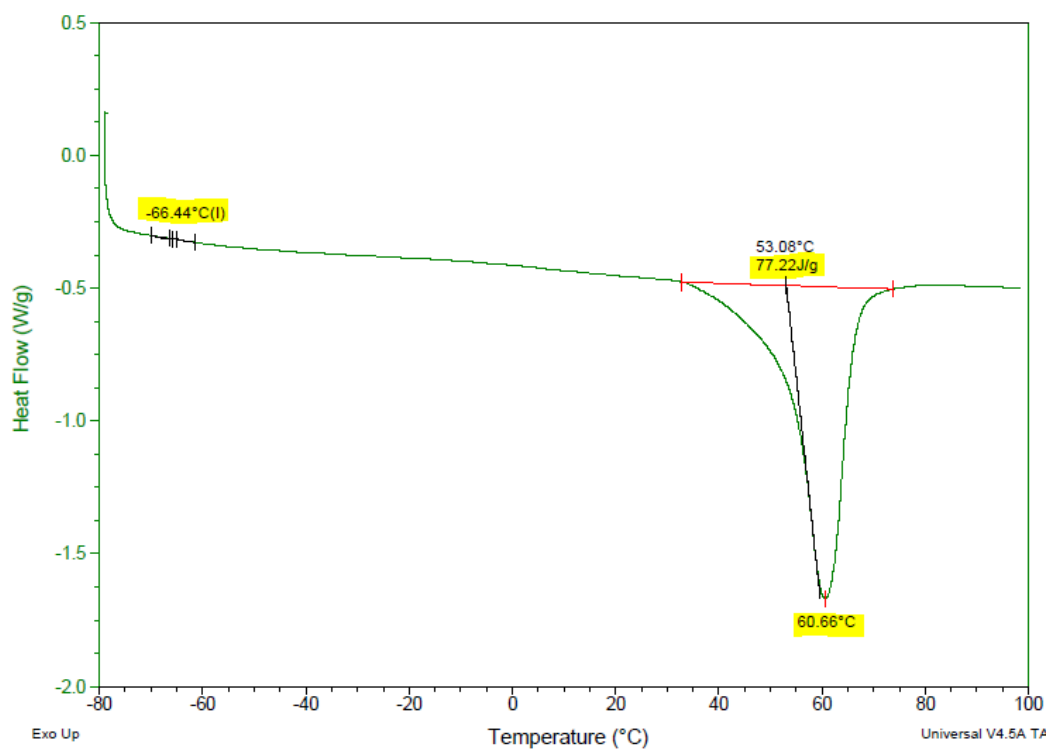


Figure 4.5 (a). DSC curve of PCL nanofibers electrospun by needleless electrospinning showing first heating cycle from -80° to 100°C under N₂

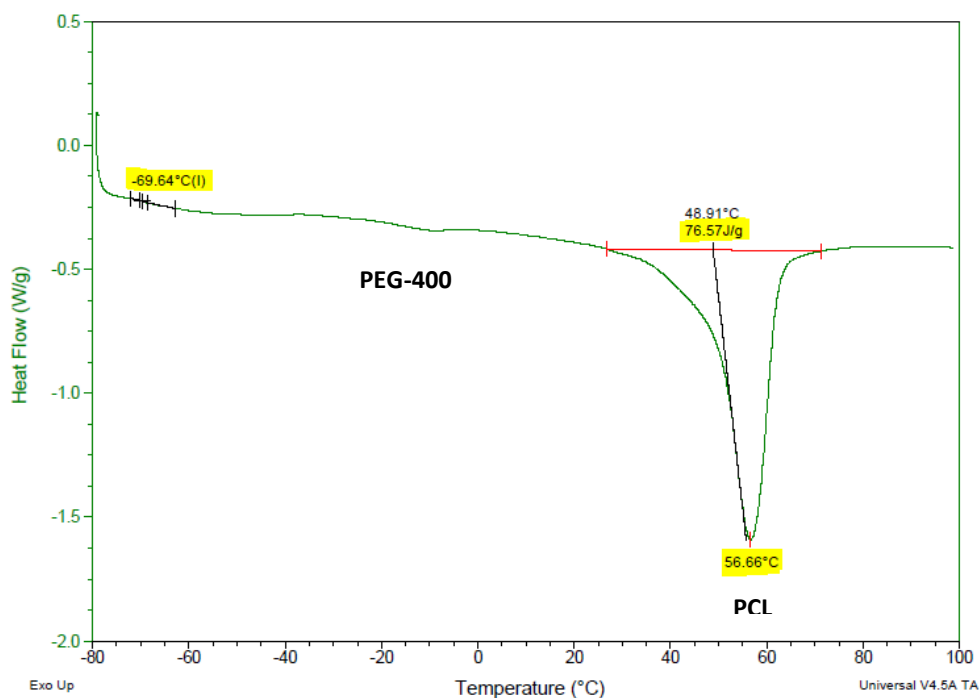


Figure 4.5 (b). DSC curve of 5%IBU+PCL/PEG-10% nanofibers electrospun by needleless electrospinning showing first heating cycle from -80° to 100°C under N₂

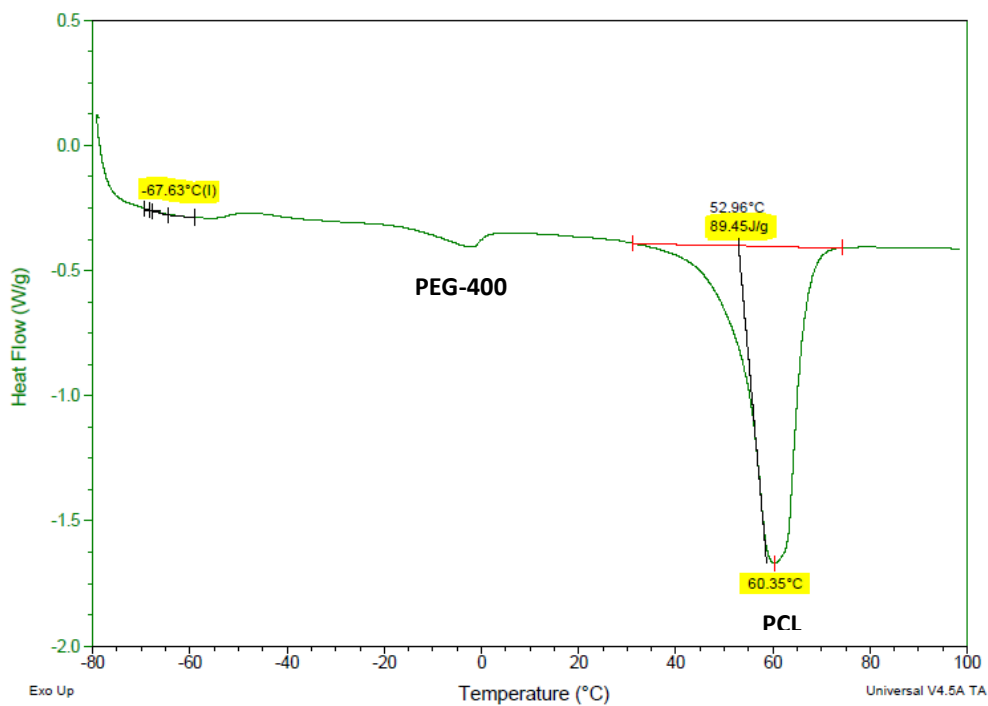


Figure 4.5 (c). DSC curve of 7%IBU+PCL/PEG-10% nanofibers electrospun by needleless electrospinning showing first heating cycle from -80° to 100°C under N₂

It was observed that the melting temperatures (T_m) of all samples of PCL, PCL/PEG and IBU incorporated nanofibers were almost same around 60°C. Small endothermic peaks of PEG-400 melting were observed in both PCL/PEG nanofibers and was more prominent in PCL/PEG-20% due to the greater content of PEG-400. There was no significant impact of PEG-400 or IBU on the glass transition temperature (T_g) of nanofibers. As far as the crystallinity ratio of nanofibers was concerned, a general upsurge in crystallinity ratios was noticed in nanofibers that were electrospun by needleless electrospinning technology as compared to the nanofibers obtained by single-needle electrospinning. All the results deducted from DSC analysis of these nanofibers are presented in Table 4.3. DSC curve of pure IBU is illustrated in Figure 4.5 (d) which shows the IBU melting at 77°C. No such peaks of IBU melting at this temperature were seen in DSC curves of IBU loaded samples that could have proved its incorporation.

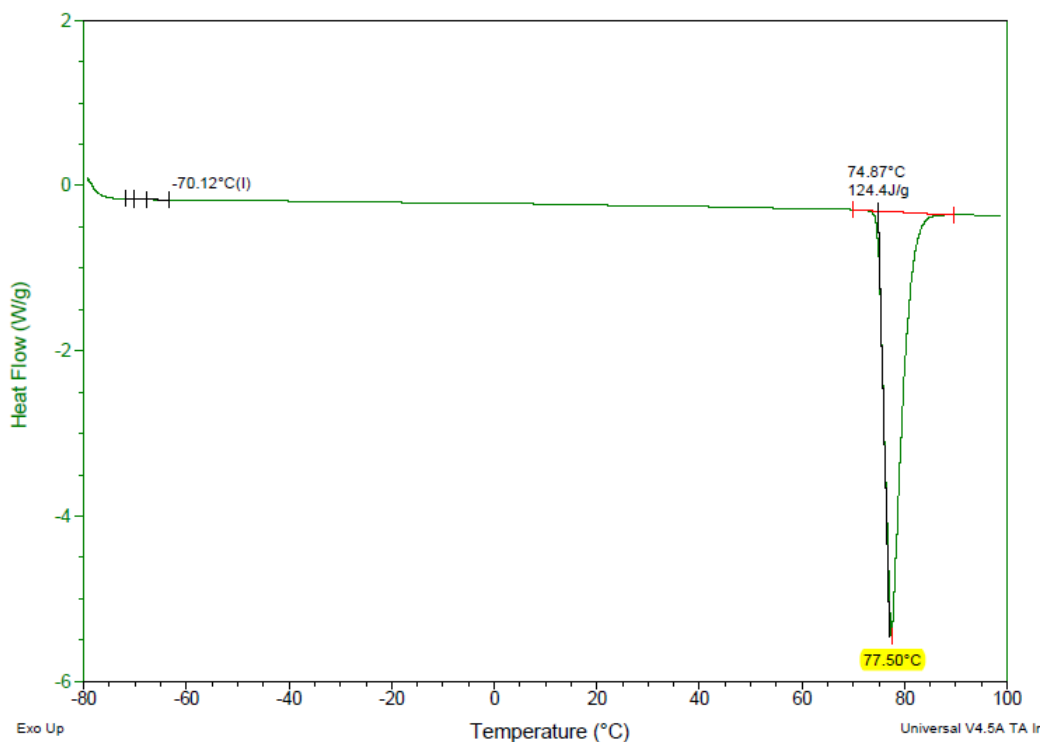


Figure 4.5 (d). DSC curve of pure IBU showing first heating cycle from -80° to 100°C under N₂

Table 4.3. Glass transition temperatures (T_g), melting temperatures (T_m), melting enthalpies (ΔH_m) and crystallinity ratios ($X_c\%$) of pure PCL, PCL, PCL/PEG and IBU loaded nanofibers electrospun by needleless electrospinning determined by their first heating cycle from -80°C to 100°C under N_2

Sample	T_g ($^\circ\text{C}$)	T_m ($^\circ\text{C}$)	ΔH_m J/g	$X_c\%$
PCL pellets	-64	57	63	40%
PCL nanofibers	-66	60	77	54%
PCL/PEG-10%	-63	58	90	70%
PCL/PEG-20%	-64	57	88	77%
5%IBU+PCL	-63	59	80	56%
5%IBU+PCL/PEG-10%	-69	56	76	59%
5%IBU+PCL/PEG-20%	-62	58	78	69%
7%IBU+PCL	-63	57	71	50%
7%IBU+PCL/PEG-10%	-67	60	89	69%
7%IBU+PCL/PEG-20%	-68	55	65	57%

Impact of PEG-400 and IBU on the crystallinity ratios of PCL nanofibers

All nanofibers electrospun by needleless electrospinning exhibited higher crystallinity ratios above 50% as compared to the crystallinity ratio of pure PCL pellets that was 40%. The highest $X_c\%$ value of 77% was recorded in PCL/PEG-20% nanofibers and 70% in PCL/PEG-10% nanofibers. It proved that by increasing the PEG-400 content in nanofibers, their crystallinity significantly increased. Whereas, in case of IBU loaded nanofibers their crystallinity was not as distinct as it

was seen in PCL/PEG nanofibers. It was noticed that the nanofibers with IBU showed less crystallinity ratio than that of PCL and PCL/PEG nanofibers. This behavior indicates that IBU acted as a defect in nanofibers structure and hindered their crystalline arrangement during the whipping phenomenon of polymer jet under electric field. This unfavorable role of IBU in nanofibers restructuring during electrospinning has already been explained with scientific references in Section 9.3 of Chapter 3. This fact is established from previously published research studies that the presence of drugs could possibly slow down the rearrangement of polymer chains hence offering them fewer opportunities to align in definite geometry and consequently lowering their crystallinity [8].

5. Thermal analysis of nanofibers electrospun by needleless electrospinning

The TGA analysis of PCL, PCL/PEG and IBU loaded nanofibers using chloroform: ethanol solvent in 88:12 wt/wt ratio and electrospun by needleless electrospinning, was performed to assert three aspects, (a) to confirm that no solvent was left in nanofibers after electrospinning, (b) to quantify the incorporated IBU in nanofibers structure and (c) to analyze thermal stability of nanofibers. As the use of chloroform for the electrospinning of nanofibers to be used for biomedical applications is not encouraged therefore, this analysis was aimed to reassure the complete evaporation of solvent from nanofibers. All samples were analyzed under nitrogen with 10°C/min rate of heating ramp till 800°C. A curve showing thermal degradation of PCL nanofibers is presented in Figure 4.6 (a).

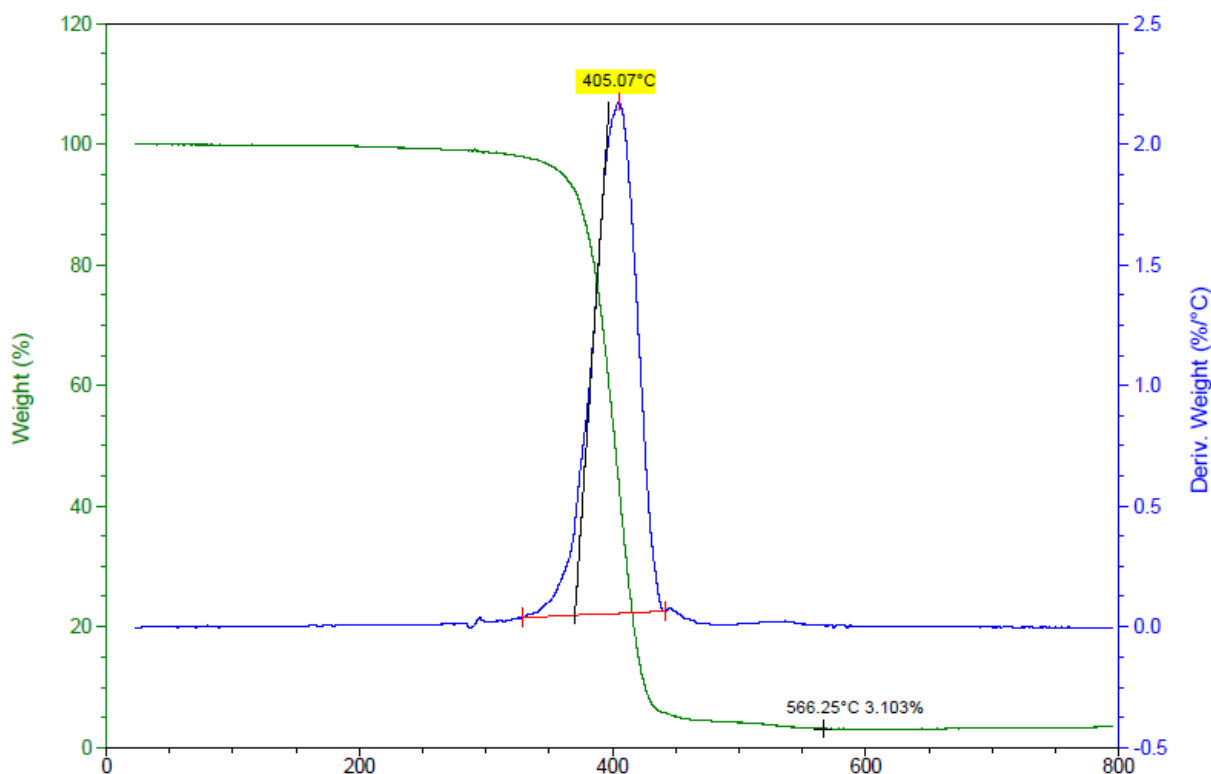


Figure 4.6 (a). A degradation curve of PCL nanofibers electrospun by needleless technique at heating rate of 10°C/min till 800°C under N₂

It can be seen that the complete degradation of PCL nanofibers took place at 405°C and it remained same for all other samples including PCL/PEG and IBU incorporated PCL nanofibers. This behavior attested that the addition of PEG-400 or IBU did not deter the thermal stability of PCL nanofibers. Also, no preliminary peaks indicating solvent evaporation were found corresponding to the boiling points of chloroform or ethanol (61°C and 78°C respectively) that could have shown their traces in nanofibers. Hence, it was verified that solvent was completely evaporated from PCL nanofibers during electrospinning and in storage under vacuum hood.

Presence of IBU in nanofibers determined by thermal analysis

In few SEM images the agglomerates of IBU were observed on the surface of nanofibers but in order to confirm its presence inside the structure of PCL nanofibers, their thermal degradation

analysis helped in a great deal. Two curves showing thermal degradation of 5%IBU+PCL/PEG-10% and 7%IBU+PCL/PEG-10% are shown in Figures 4.6 (b) and 4.6 (c) respectively. TGA analysis of pure IBU was also done as a reference to identify its corresponding peaks in drug loaded nanofibers. The results showed that the full degradation of pure IBU took place at 226°C and the degradation curve was previously presented in Section 9.4 of Chapter 3.

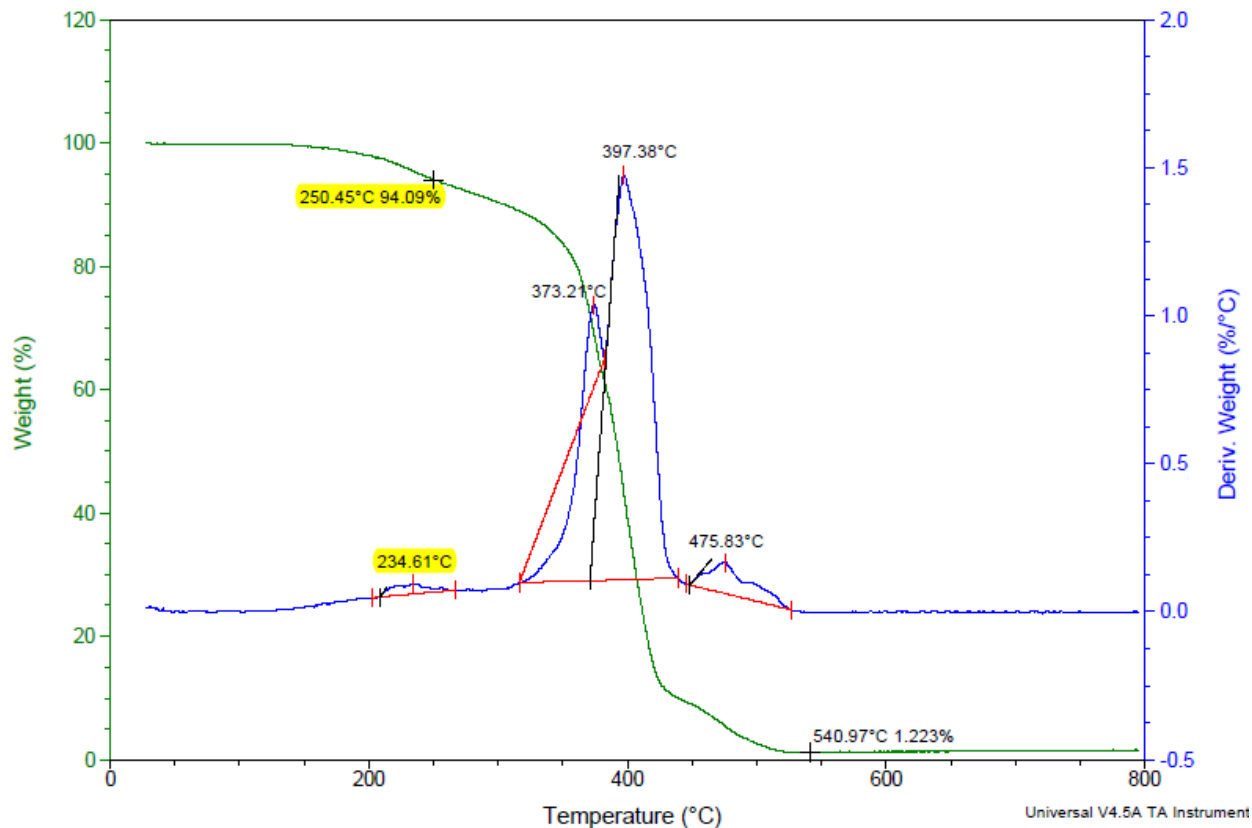


Figure 4.6 (b). Degradation curve of 5%IBU+PCL/PEG-10% nanofibers electrospun by needleless electrospinning at heating rate of 10°C/min till 800°C under N₂

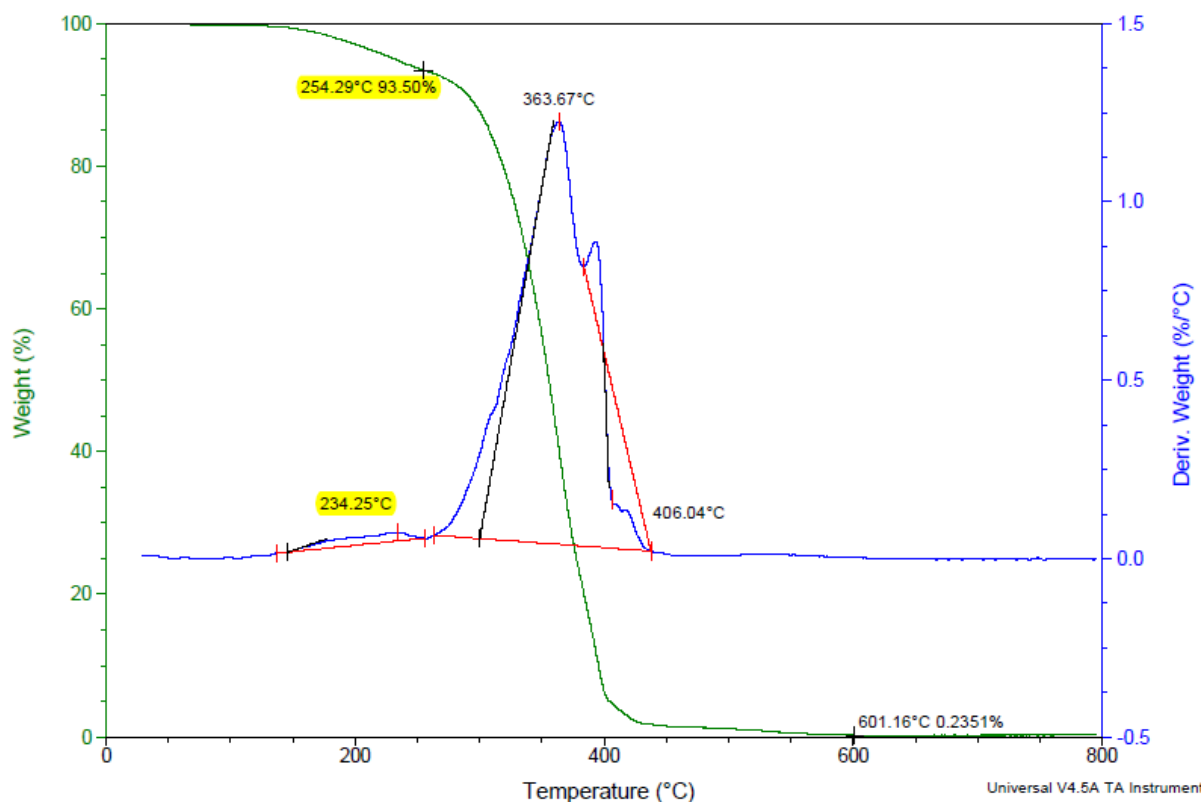


Figure 4.6 (c). Degradation curve of 7%IBU+PCL/PEG-10% nanofibers electrospun by needleless electrospinning at heating rate of 10°C/min till 800°C under N₂

At the beginning of both curves, small peaks at 234°C can be observed that corresponds to the degradation temperature of pure IBU that was 226°C. Presence of these peaks in samples of IBU loaded nanofibers provided important evidence of successful integration of IBU into their structure. Moreover, in both degradation curves their initial weight loss% at 250°C demonstrates degradation of IBU at this stage. Theoretically, in case of 7%IBU+PCL/PEG-10% sample the amount of incorporated IBU (7wt%) compared to PCL corresponds to 6.3% of IBU compared to PCL/PEG-10% and from their TGA analysis their IBU content could be calculated using the weight loss% of IBU between the T-ambient and T-250°C. By doing this calculation the amount of IBU degraded at this point was found to be 7% that is in good agreement with the actual amount of IBU initially incorporated into the nanofibers. Similarly, the quantification of IBU for

5%IBU+PCL/PEG-10% nanofibers was done from their degradation curve and their values are given in Table 4.4.

Table 4.4. Quantification of IBU by TGA analysis of drug loaded nanofibers

Sample	Theoretical amount of IBU	IBU degradation temperature	Quantified amount of IBU from TGA
5%IBU+PCL/PEG-10%	4.5%	250 °C	6%
7%IBU+PCL/PEG-10%	6.3%	254 °C	7%

In few SEM images of IBU loaded nanofibers, agglomerates of the drug were found on their surface. Despite the fact that these agglomerates were not seen in majority of samples, still their presence caused a doubt about the actual incorporation of IBU into the nanofibers structure. Even the DSC curves of IBU loaded nanofibers did not show any distinct peaks of IBU melting. Therefore, it was necessary to prove that the IBU was present into the nanofibers structure by presenting solid facts. In this regard, this quantification of IBU deducted by their TGA analysis provided a factual argument that drug was incorporated into the structure of nanofibers.

6. IBU release kinetics

The incorporation of 5wt% and 7wt% IBU into the PCL and PCL/PEG nanofibers was done using needleless electrospinning technique. *In vitro* drug release profiles of these drug loaded nanofibers was done by Pr. Leonard Ionut ATANASE and his team at the Faculty of Dental Medicine, University “Apollonia”, Iasi-Romania. The drug release efficiency was realized by UV-vis spectroscopy by immersing the nanofibrous samples in phosphate-buffered saline (PBS) solution (pH=7) at 37°C. The complete description of this analysis has already been given in Section 4.1 of

Chapter 2. The release kinetics of IBU from the nanofibers were studied over a period of 6 days at regular intervals. The percentage release efficiencies of IBU from all samples during their first 24h and 48h of analysis are given in Table 4.5.

Table 4.5. Percentage IBU release efficiencies from drug loaded nanofibers during 24h and 48h of analysis

Samples	%RE (24h)	%RE (48h)
5%IBU+PCL	36%	57%
5%IBU+PCL/PEG-10%	46%	50%
5%IBU+PCL/PEG-20%	18%	25%
7%IBU+PCL	44%	47%
7%IBU+PCL/PEG-10%	26%	30%
7%IBU+PCL/PEG-20%	25%	37%

† Samples shown in Table 4.5 were electrospun by needleless electrospinning with optimized parameters.

A graphical representation of percentage IBU release until 48h is shown in Figure 4.7. All PCL nanofibers loaded with 5wt% and 7wt% of IBU and with PEG-10% and PEG-20% are represented in this graph. This graph showed the IBU release in two stages: initial burst release during 5h and then a steady release until 48h from drug loaded nanofibers. This two-stage release phenomenon of drug release from nanofibers has previously been reported in many publications [8-11]. It was also observed that nanofibers containing PEG-400 released less amount of IBU than PCL nanofibers. This decrease in IBU release from PCL/PEG nanofibers could be due to their higher crystallinity which has already been mentioned in their DSC analysis. Higher crystallinity of these nanofibers may have delayed the release of drug particles from the nanofibers network.

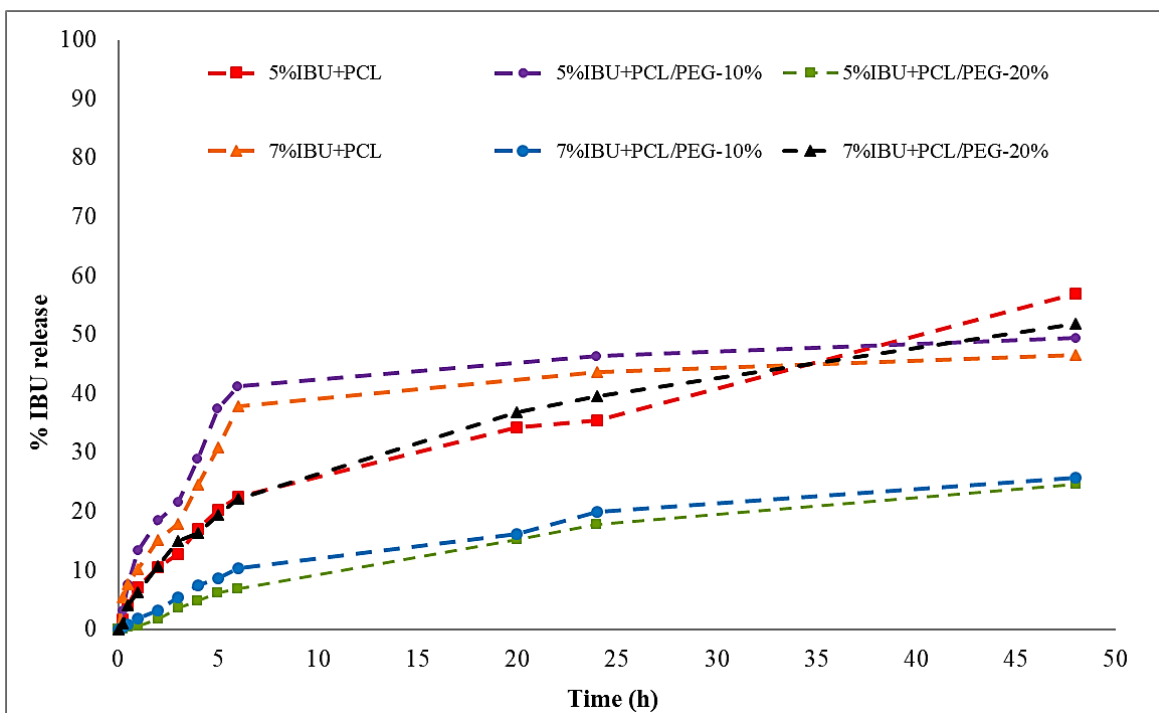


Figure 4.7. The IBU release kinetics from drug loaded PCL and PCL/PEG nanofibers during 48h

This graph only represents the release profile of IBU until 48h and it can be noticed that this release is not complete yet. This IBU release was completed until 6 days and total release efficiencies of 81% and 63% were observed in case of 5%IBU+PCL and 7%IBU+PCL/PEG-20% nanofibers respectively. Release kinetics of these drug loaded nanofibers showed a prolonged release of IBU until six days that was actually the ultimate goal of this study. In order to use these nanofibrous mats as a wound dressing, a gradual release of drug was intended to cure pain and to prevent inflammation in wound. Typical wound dressings are needed to be replaced every eight hours which itself is a time consuming and painful process. Therefore, a wound dressing equipped with a drug delivery system was required that could slowly release the medicine to relieve pain while healing the wound. These IBU loaded nanofibrous mats with steady release profiles will serve the stated purpose and will considerably reduce the fatigue and painful experience of changing the wound dressings.

7. Comparison Between Two Electrospinning Techniques

The technique of producing nanofibers with diameters in micro/nano scale by electrospinning the polymer solutions is decades old. Initially a conventional electrospinning approach was established usually known as “Single-Needle Electrospinning” that later followed by various advancements in this field thus introducing a new semi-industrial approach called “Needleless Electrospinning”. Both the techniques operate on different working principles and electrospinning parameters, the details of which have previously been explained in Section 2.3 and 2.4 of Chapter 2. These differences obviously impact the physico-chemical characteristics of resulting nanofibers such as their morphology, mean diameters, homogeneity, crystallinity ratios and thermal stability.

In this research work, the electrospinning of PCL, PCL/PEG and their IBU loaded nanofibers was carried out by using both these technologies. The characteristics of obtained nanofibers from these two different approaches are presented and discussed in Chapters 3 and 4. Several differences were noted in nanofibers fabrication and their properties and to report these differences, a tabular comparison is shown in Table 4.6.

Table 4.6. Comparison between two electrospinning techniques with respect to their operating parameters and resulting nanofibers characteristics

Single-Needle Electrospinning	Needleless Electrospinning
Applied voltage ranges from 10-30 kV	Two applied voltages (+ve and -ve) were applied ranging from 10-50 kV
Single metallic needle used to initiate polymer jet	A metallic wire electrode used to initiate thousands of polymer jets simultaneously
Polymer solution feed rate was in mL/h	Polymer solution was deposited on wire electrode selecting an orifice size in mm
Significant impact of applied voltage on nanofibers morphology	No significant impact of applied voltage on nanofibers morphology
Nanofibers were heterogeneous mix of nano and micro fibers	Nanofibers were heterogeneous and were under one micron
In every sample with nanofibers there were microfibers too Mean diameters were ranging from 400nm to 3µm	Finer nanofibers with no microfibers Mean diameters were under one micron ranging from 400-900nm
Pores were found on the surface of nanofibers with PEG-400	No pores were observed in nanofibers with PEG-400
No ultrafine (100-300 nm) nanofiber networks	Presence of ultrafine (100-300 nm) nanofiber nets
Problem of agglomerations with chitosan nanocapsules loaded with Na-IBU	Inadequate deposition of nanofibers loaded with Na-IBU
Crystallinity ratio of electrospun nanofibers was higher than pure PCL pellets	Higher crystallinity ratios of nanofibers than single-needle electrospun nanofibers
IBU release kinetics of drug loaded nanofibers showed a rapid release of IBU until 24h	IBU release kinetics of drug loaded nanofibers showed a prolonged release of IBU until 48h
Maximum percentage release efficiency of IBU was 85% in 24h	Maximum percentage release efficiency of IBU was 57% in 48h

8. Conclusion

An advance semi-industrial needleless technique of electrospinning the nanofibers was employed to synthesize PCL and PCL/PEG nanofibers. After optimization of electrospinning parameters, a model drug Ibuprofen (IBU) was incorporated to these PCL and PCL/PEG nanofibers in two different concentrations and their electrospinning was done. An attempt of electrospinning the PCL nanofibers with sodium salt of Ibuprofen (Na-IBU) was also performed. However, due to inadequate deposition of nanofibers and difficulties in electrospinning process, the use of Na-IBU for further experiments was ceased. Morphological analysis of obtained nanofibers was done by image processing and their SEM images highlighted their round shapes and heterogeneous nature. The mean diameters of these nanofibers were measured by ImageJ software taking bar measurements and their CV% was calculated. The mean diameters of all samples of PCL, PCL/PEG and IBU loaded nanofibers were under one micron. The DSC analysis of these nanofibers showed higher crystallinity ratios of electrospun nanofibers as compared to the PCL pellets. It was observed that by increasing the content of PEG-400 in nanofibers, their crystallinity also increased. While, the incorporation of IBU decreased the crystallinity ratio of nanofibers as the drug acted as defect in their structure. No peak of solvent evaporation was recorded during the TGA analysis of nanofibers. It was established that the addition of PEG-400 or IBU had no substantial effect on thermal degradation of their nanofibers. Distinct peaks of IBU degradation were found in TGA curves of drug loaded nanofibers that ascertained its presence in nanofibrous network. The *in vitro* drug release kinetics of IBU loaded nanofibers during 48h showed a steady release of IBU followed by a complete release of up to 80% until 6 days. This prolonged release of IBU from nanofibers was an anticipated feature for its application as a wound dressing material. However, nanofibers containing PEG-400 exhibited less percentage release of IBU therefore, it

was decided that in future only PCL nanofibers loaded with IBU will be studied for their drug release profiles.

References

1. Wang X., D.B., Sun G., Wang M. and Yu J., *Electro-spinning/netting: a strategy for the fabrication of three-dimensional polymer nano-fiber/nets*,. Prog. Mater. Sci., 2013. **58**(8): p. 1173-1243.
2. Li Z., X.Y., Fan L., Kang W. and Cheng B., *Fabrication of polyvinylidene fluoridetreelike nanofiber via one-step electrospinning*,. Materials & Design., 2016. **92**: p. 95-101.
3. Hu J., W.X., Ding B., Lin J., Yu J. and Sun G., *One-step electro-spinning/netting technique for controllably preparing polyurethane nano-fiber/net*,. Macromolecular Rapid Communications, 2011. **32**: p. 1729-1734.
4. Stanger J., S.M.P., Tucker N. and Kirwan K., *Effect of charge density on the Taylor cone in electrospinning*,. Solid State Phenomena, 2009. **151**(6/7): p. 54-59.
5. J. F. A. de la Mora, *The fluid dynamics of Taylor cones*,. Annual Review of Fluid Mechanics, 2007. **39**: p. 217-243.
6. Angamma C. J. and Jayaram S. H., *Analysis of the Effects of Solution Conductivity on Electrospinning Process and Fiber Morphology*. IEEE Transactions on Industry Applications, 2011. **47**(3): p. 1109-1117.
7. Kolbuk D., G.-L.S., Sajkiewicz P., Maniura-Weber K. and Fortunato G., *The Effect of Selected Electrospinning Parameters on Molecular Structure of Polycaprolactone Nanofibers*. International Journal of Polymeric Materials and Polymeric Biomaterials, 2015. **64**: p. 365-377.
8. Shi Y., W.Z., Zhao H., Liu T., Dong A. and Zhang J., *Electrospinning of ibuprofen-loaded composite nanofibers for improving the performances of transdermal patches*,. Journal of Nanoscience and Nanotechnology, 2013. **13**(6): p. 3855-3863.
9. Zamani M., M.M., Varshosaz J. and Jannesari M., *Controlled release of metronidazole benzoate from poly ϵ -caprolactone electrospun nanofibers for periodontal diseases*. Eur. J. Pharm. Biopharm., 2010. **75**: p. 179-185.

10. Tran T., H.M., Patel D., Burns E., Peterman V. and Wu J., *Controllable and switchable drug delivery of ibuprofen from temperature responsive composite nanofibers*. Nano Convergence., 2015. **2**(15).
11. Karavasili C., B.N., Kontopoulou I., Smith A., Van der Merwe S. M., Rehman I. U. R., Ahmad Z. and Fatouros D. G., *Preparation and Characterization of Multiactive Electrospun Fibers: Poly-caprolactone Fibers Loaded with Hydroxyapatite and Selected NSAIDs*. J. Biomedical Materials Research Part A, 2014. **102**(8): p. 2583-2589.

Chapter 5: Fabrication & Characterization of Bilayer Electrospun Wound Dressing

Chapitre 5: Fabrication et Caractérisation du Pansement Bicouche Électrofilé

L'objectif principal de cette étude était la fabrication et la caractérisation d'un pansement bicouche. Un pansement biomédical moderne a été développé en déposant des nanofibres PCL chargées d'IBU/HA sur un film d'hydrogel GE/HA humide via une technique d'électrofilage sans aiguille. Toutes les expériences ont été réalisées après optimisation des paramètres d'électrofilage. La caractérisation des nanofibres PCL contenant le mélange IBU/HA a été effectuée et les propriétés physiques, thermiques et mécaniques des nanofibres ont été déterminées. Les études MEB des nanofibres ont révélé leur morphologie ronde avec leurs diamètres moyens allant de 400-700nm. Il a été montré que l'HA n'avait aucun impact sur la température de fusion et la cristallinité des nanofibres PCL. La courbe de dégradation du film GE/HA indique une bonne stabilité thermique du matériau et la présence de HA et IBU dans les nanofibres PCL a été mise en évidence. La mouillabilité du film d'hydrogel GE/HA a été déterminée par mesure d'angle de contact avec l'eau montrant sa nature hydrophile, une caractéristique souhaitée pour absorber l'exsudat pour une cicatrisation rapide de la plaie. En outre, ce film d'hydrogel présente une bonne résistance à la traction avec des valeurs élevées de module de Young et assure la stabilité mécanique de ce pansement bicouche.

Les cinétiques de libération du médicament des nanofibres PCL chargées IBU/HA et de la structure bicouche ont été déterminées par spectroscopie UV-vis. Tous les échantillons présentaient un phénomène de libération de médicament en deux étapes, une libération initiale rapide suivie d'une libération prolongée et régulière d'IBU jusqu'à 48 h. Cependant, il a été observé que les profils de libération d'IBU étaient incomplets, ce qui suggère un suivi futur de la cinétique de relargage de ces échantillons pendant une période plus longue. Un test antibactérien de ces

échantillons nanofibreux chargés en IBU/HA et d'un pansement bicouche contre deux bactéries, *S. epidermidis* (gram positif) et *E. coli* (gram négatif) a été réalisé. Aucune inhibition n'a été observée contre la souche bactérienne de *S. epidermidis* dans aucun échantillon, tandis qu'une légère activité antibactérienne a été observée contre la souche bactérienne d'*E. coli*. Cela a permis de conclure que l'IBU agissait faiblement comme un agent antibactérien contre les bactéries *E. coli*.

CHAPTER 5

FABRICATION AND CHARACTERIZATION OF BILAYER ELECTROSPUN WOUND DRESSING

1. Introduction

Skin is the largest human organ, exposed to external environment and is vulnerable to various types of damages. Severe skin damages can be life threatening due to the loss of essential body fluids, electrolytes and vital nutrients from wounded area. However, day-to-day minor skin damages or surgical cuts can be treated appropriately by applying modern wound dressings [1, 2]. An ideal wound dressing should protect the wound from external contaminants and facilitate rapid recovery. Though, single layer wound dressings cannot meet all these clinical requirements due to their intrinsic features and limitations. Recently, bilayer wound dressings composed of two distinct layers with diverse properties have gained a lot of attention [1, 3]. Two different structures fabricated to offer targeted characteristics can be truly advantageous [4]. For instance, a dense top layer can protect the wound from external environment, provide mechanical support to the bilayer structure as well as absorb wound exudate [5]. The bottom layer, in contact with wounded skin should be equipped with a self-administered drug delivery system capable of releasing the drug in a controlled manner in order to cure pain and inflammation. Moreover, it should mimic the extracellular matrix (ECM) and promote cells adhesion to accelerate skin regeneration [6, 7].

An apt selection of materials to construct such a wound dressing is a key factor that predict its efficacy and performance. Hence, the choice of materials utilized for this purpose must be done objectively. Gelatin (GE) is a biocompatible biodegradable polymer that can be employed as hydrogel due to its hydrophilic properties and it offers good mechanical strength [8]. Poly(ϵ -

caprolactone) (PCL) is another biocompatible synthetic polymer which exhibit slow degradation and good thermal stability [9, 10]. However, its hydrophobicity is a limitation that could be tailored by blending it with a hydrophilic polymer such as polyethylene glycol (PEG) [11]. In previous Chapter 4, a drug delivery system was devised by incorporating Ibuprofen (IBU), a non-steroidal anti-inflammatory drug into PCL and PCL/PEG nanofibers [12]. This work was advanced by achieving the main objective of this research study by constructing a modern and versatile bilayer wound dressing by utilizing all these biopolymers and former drug delivery system. This chapter will explain the fabrication and characterization of that bilayer wound dressing. For its development, first layer was made of a hydrogel film consisting of Gelatin (GE) and Hyaluronic acid (HA) (selection and function of HA will be discussed in next section). Second layer was created by depositing PCL, PCL/PEG nanofibers containing IBU/HA on the wet GE/HA film via needleless electrospinning technology. The characterization of these nanofibers and bilayer wound dressing was done to analyze their physical, thermal, mechanical and biological aspects.

2. Preparing the first layer with GE/HA hydrogel

To fabricate a bilayer wound dressing, a two-step procedure was carried out. At first, a foundation layer of hydrogel was prepared and then immediately nanofibers were electrospun over this foundation layer to build a second layer. To construct a foundation layer, two bio-sourced polymers, Gelatin (GE) and sodium Hyaluronate (HA), were utilized. 10wt% GE solution in distilled water was prepared and another solution of 2.5wt% HA in distilled water was made separately. Later, both these solutions were mixed in definite proportions to make a hydrogel of GE/HA. The hydrogel preparation conditions and amounts of polymers used have been described earlier in Section 2.5 of Chapter 2. This solution was used to prepare a hydrogel layer of GE/HA by coating it on Teflon sheet with the help of a manual bar coater (100 μ m thickness). Instantly, this GE/HA coated Teflon sheet was installed inside the NanoSpider machine and electrospinning of nanofibers was performed on it while this GE/HA layer was still wet to promote penetration of nanofibers into the structure allowing mechanical bonding of the assembly. This hydrogel coated Teflon sheet acted as a substrate surface on which nanofibers were deposited. Use of Teflon sheet facilitated the subsequent detachment of this bilayer wound dressing, thanks to its non-adhesive properties.

3. Incorporation of sodium Hyaluronate (HA) into PCL nanofibers

Hyaluronic acid, usually called Hyaluronan, is a fascinating macromolecule that offers promising future in tissue engineering and wound healing applications. Researchers have explored the properties of this linear glycosaminoglycan (GAG) for its applications in scaffolds, surrogate tissue design [13-15] and drug delivery [16, 17]. The biological aspects of hyaluronic acid are widespread and widely appreciated specially in wound healing process [13, 18, 19]. In addition, it is well known that it associates with cells surface receptors and could help in regulating the cells mobility

and adhesion [20-22]. Its ability to interact with cells surface receptors directly affects the tissue organization thus facilitating the extracellular matrix remodeling and promoting the inflammatory responses [23, 24]. Besides, hyaluronic acid has the ability to maintain *in vitro* degradation rates and to prolong the release of anti-inflammatory drugs [25].

Hyaluronan exhibits unique biophysical characteristics and allows myriad possible functionalities. In terms of structure, hyaluronic acid is a massive unmodified GAG consisting of a linear chain of repeating disaccharides of glucuronic acid and N-acetylglucosamine as shown in Figure 5.1.

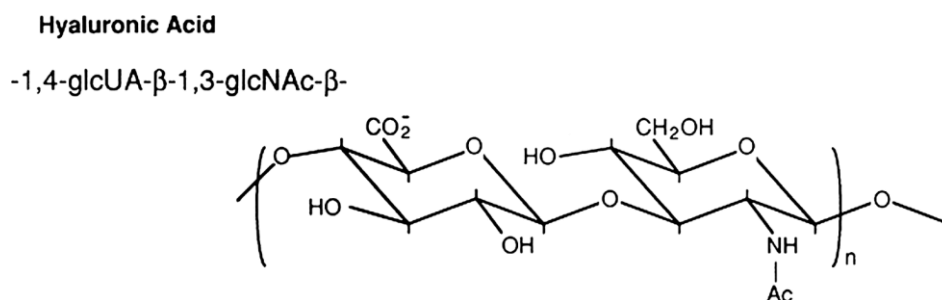


Figure 5.1. Chemical structure of Hyaluronic acid

Due to its highly negative charges, it attracts positive ions and creates an osmotic imbalance that draws water in, an intrinsic feature proven to be ideal for making hydrogels and other extracellular matrix substitutes [26]. All these wondrous attributes of Hyaluronan persuaded its incorporation into the bilayer wound dressing material. Its most common form that is widely used by cosmetic industry and for biomedical applications is the sodium salt of hyaluronic acid commonly known as sodium Hyaluronate. This sodium Hyaluronate (HA) was not only incorporated into the base layer along with GE but was also loaded into the PCL nanofibers for a two-fold benefit. In the first layer of bilayer structure, HA was added as a hydrogel to absorb wound exudate to keep wounded area dry that is needed for its speedy recovery. In second layer of nanofibers which will be in direct contact to the wound, it will assist in regeneration of extracellular matrix of damaged skin. Also,

it will improve the inflammatory responses of wound and will regulate the IBU release to the affected area.

The amount of HA incorporated in GE/HA film has already been described in above section. In nanofibers, 2wt% HA with respect to the content of PCL was added directly to PCL and PCL/PEG solutions containing IBU. For nanofibers characterization, the needleless electrospinning of HA and IBU loaded PCL and PCL/PEG nanofibers was done in two ways: (1) nanofibers were deposited on aluminum foil and (2) nanofibers were deposited on GE/HA wet film to form a bilayer structure.

4. Fabrication of bilayer wound dressing

To construct a bilayer wound dressing, the first layer was prepared by GE/HA hydrogel film and then a second layer of IBU and HA containing PCL nanofibers was fabricated by needleless electrospinning while the hydrogel film was still wet. The preparation procedure of first hydrogel layer is explained before in above section. A solvent mix of chloroform: ethanol in 88:12 wt/wt ratio was used to prepare PCL solutions. Two concentrations of IBU 5wt% and 7wt% along with 2%HA were incorporated into the PCL solution to produce a set of different samples. For these experiments only 10wt% PEG with respect to PCL content was added to the nanofibers. Optimized electrospinning parameters were applied and humidity and temperature inside the electrospinning chamber were kept at $35 \pm 4\%$ and $25 \pm 2^\circ\text{C}$ respectively. After optimization of electrospinning parameters, distance between two wire electrodes was kept at 220mm for nanofibers depositing on aluminum foil and for bilayer samples collected on Teflon sheet, this distance was reduced to 170mm. The applied voltage range was between 40-44kV and 0.5mm orifice size was used to deposit the polymer solution on wire electrode. The time of electrospinning for all samples was

30min. A schematic diagram explaining the structure and functions of this bilayer wound dressing is shown in Figure 5.2.

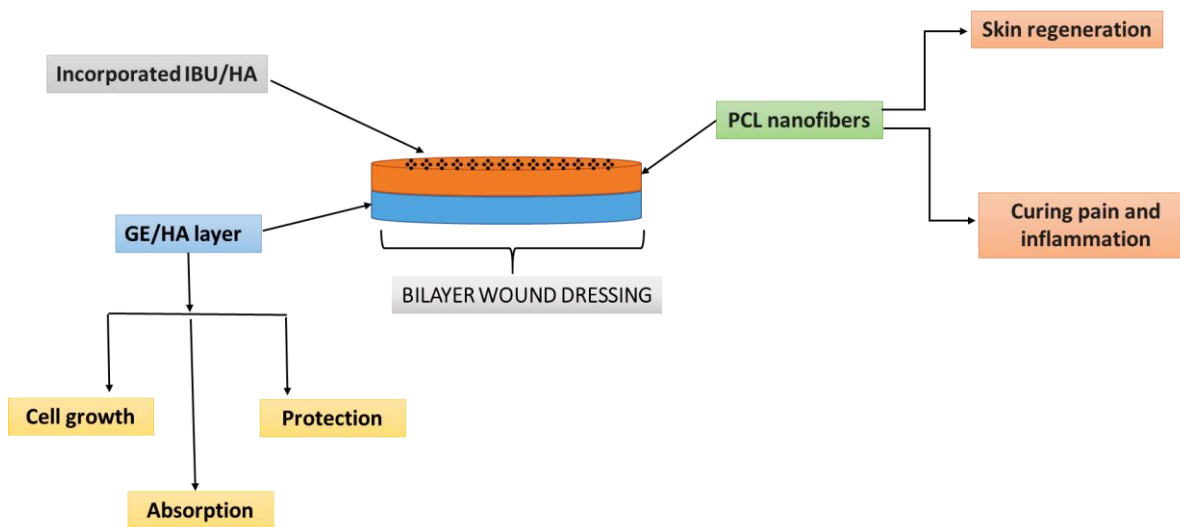


Figure 5.2. A schematic diagram explaining the structure and functioning of bilayer wound dressing

Once the nanofibers were electrospun on the GE/HA hydrogel film, these bilayer samples were placed in closed fume hoods for overnight to dry. Next day, physically dried bilayer samples were easily detached with the help of laboratory forceps and were preserved in cool-dry environment for their characterization. The physical appearance of this bilayer wound dressing is presented in Figure 5.3. It was observed that the nanofibrous layer was fused with GE/HA film and no detachment was seen between them.



Figure 5.3. Actual appearance of the bilayer wound dressing

5. Characterization of nanofibers and bilayer wound dressing

Various characterization tools were used to investigate physical properties of nanofibers such as; morphology, crystallinity, thermal stability and wettability. Characterization of bilayer wound dressing was done to analyze the morphology of electrospun nanofibers, their wettability with GE/HA film and mechanical strength of GE/HA film. All these attributes are discussed in this section in detail.

5.1 Morphology of PCL, PCL/PEG nanofibers with HA and IBU

All samples of nanofibers including the bilayer structure were studied by SEM analysis to determine their morphological properties such as shape, homogeneity and their mean diameters. SEM images were taken for each sample at 5 μ m scale. SEM images of samples are shown in Figures 5.4, 5.5 and 5.6. These images were then analyzed by ImageJ software and the average diameters of nanofibers were measured by taking 50 bar measurements per specimen. Their standard deviation and percentage of coefficient of variation (CV%) were also calculated.

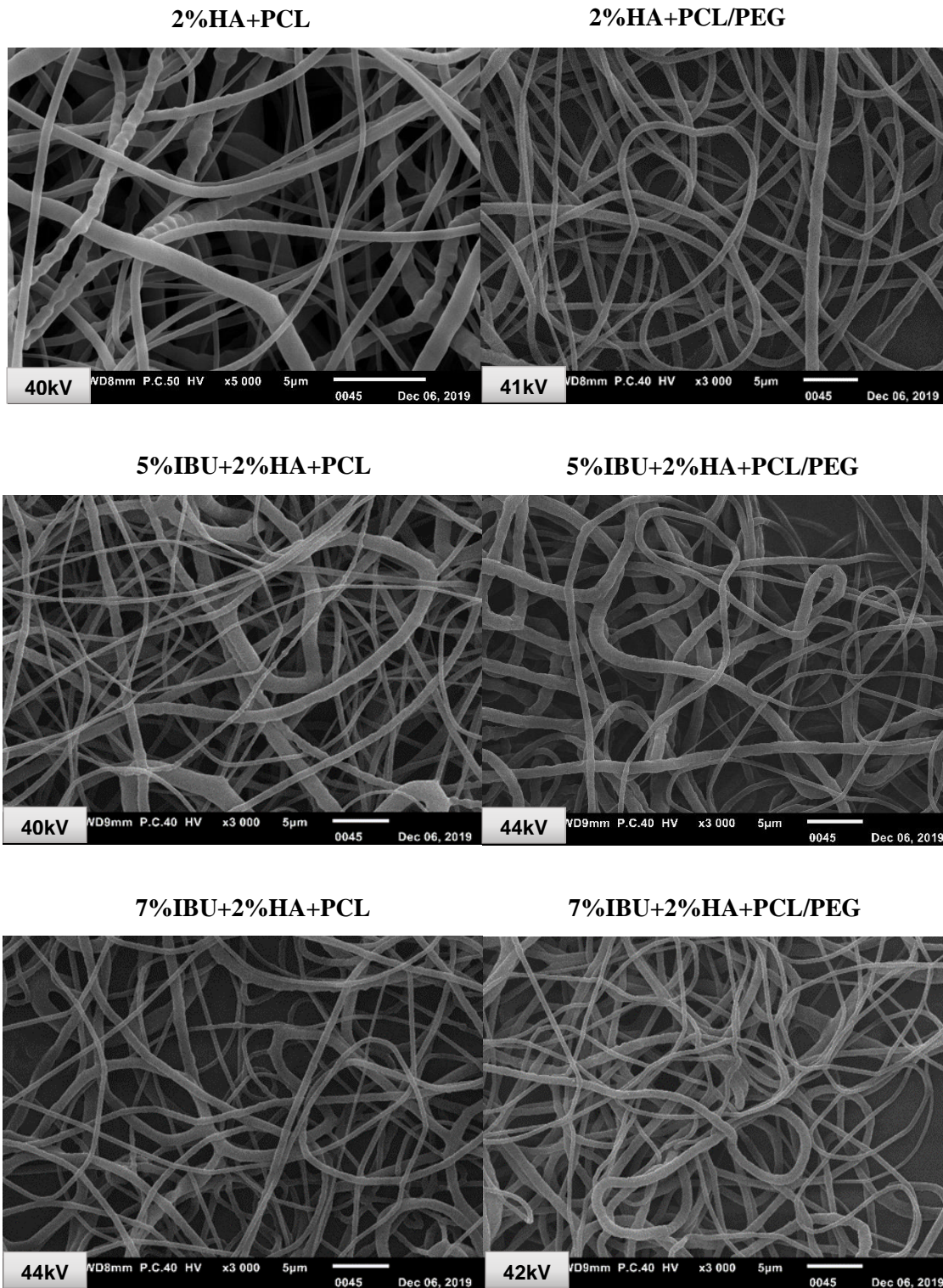


Figure 5.4. SEM images of PCL, PCL/PEG nanofibers with HA and IBU collected on aluminum foil by using optimized electrospinning parameters.

The SEM images of PCL, PCL/PEG nanofibers containing HA and IBU collected on aluminum foil revealed that all nanofibers were round in shape and their thickness varied along their length. Nanofibers were heterogeneous in nature with varying diameters. There were small voids present on the surface of 2%HA+PCL/PEG nanofibers that can be seen in Figure 5.5.

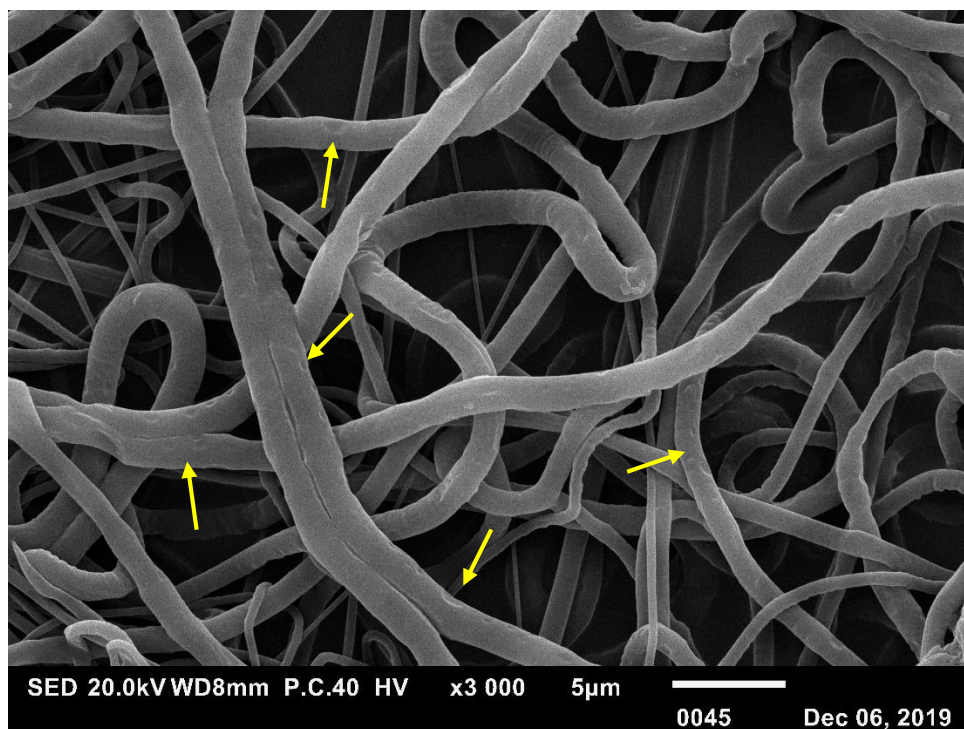
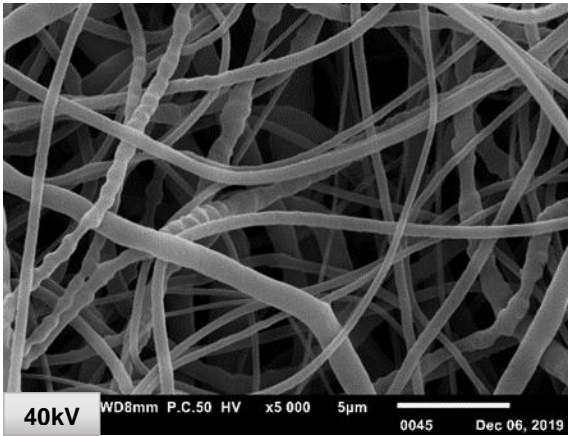


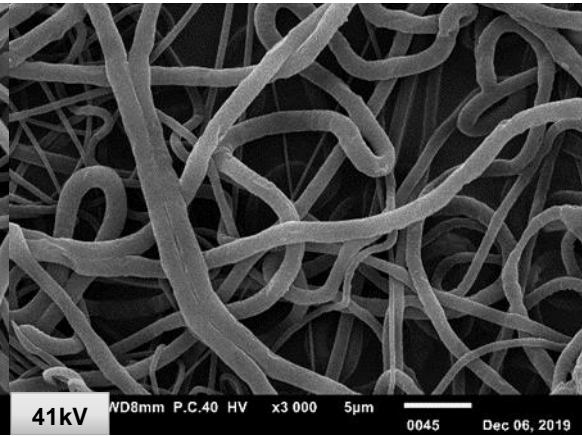
Figure 5.5. SEM image of 2%HA+PCL/PEG nanofibers with voids on their surface indicated by yellow arrows.

This effect is similar as experienced in single-needle electrospinning of PCL/PEG nanofibers. On the contrary, no pores were observed in case of PCL/PEG nanofibers electrospun by needleless electrospinning. In few samples, the appearance of nanofibers resembled to a beaded necklace that could be due to HA as it was first time that such morphology was noticed. Nanofibers mean diameters were in a range of 400-700nm with CV% as high as 78% for 5%IBU+2%HA+PCL nanofibers.

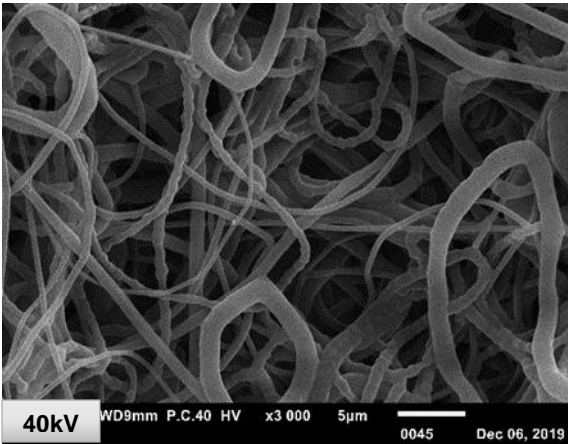
2%HA+PCL on GE/HA film



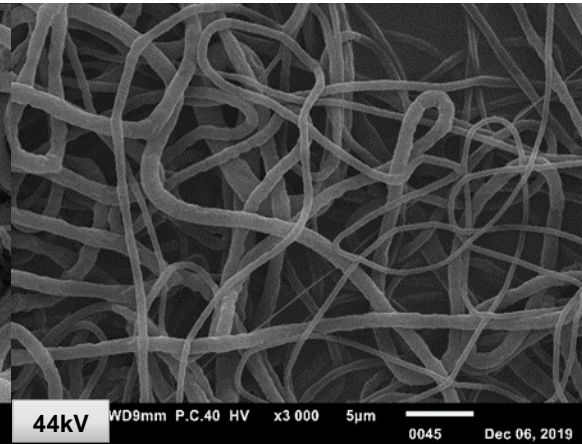
2%HA+PCL/PEG on GE/HA film



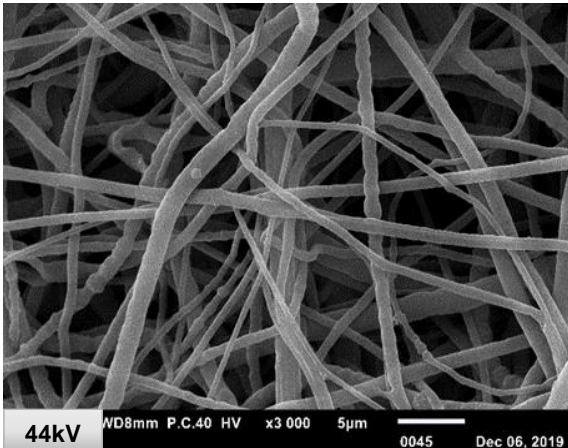
5%IBU+2%HA+PCL on GE/HA film



5%IBU+2%HA+PCL/PEG on GE/HA film



7%IBU+2%HA+PCL on GE/HA film



7%IBU+2%HA+PCL/PEG on GE/HA film

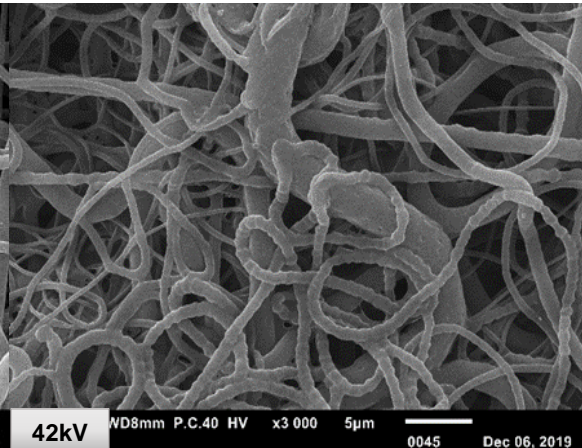


Figure 5.6. SEM images of PCL, PCL/PEG nanofibers with HA and IBU deposited on GE/HA film by using optimized electrospinning parameters.

Morphology of nanofibers being deposited on GE/HA film was a little different from the nanofibers being collected on aluminum foil. Nanofibers with beaded necklace shape were seen in most of the samples. In one of the SEM images, the fusion of nanofibers with GE/HA film was clearly observed that is shown in Figure 5.7. It demonstrated that nanofibers were glued to the wet GE/HA hydrogel layer during electrospinning.

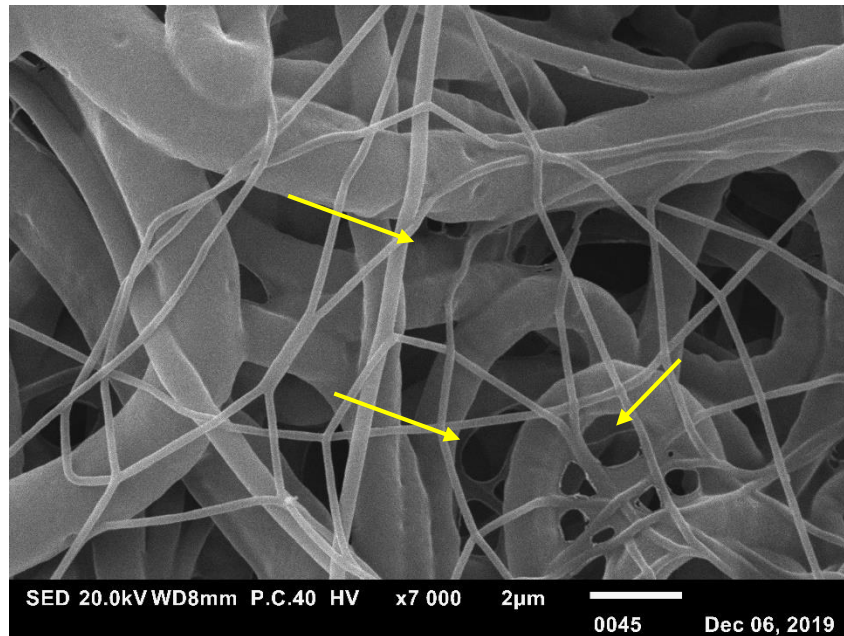


Figure 5.7. SEM image showing fused nanofibers on GE/HA film indicated by yellow arrows

Irregularities in nanofibers diameters were present and their mean diameters were ranging from 400-700nm. Nanofibers showed higher CV% in diameters that proved their heterogeneous morphology. All the findings deducted from SEM analysis are enlisted in Table 5.1.

Table 5.1. Mean diameters and CV% of PCL, PCL/PEG nanofibers with HA and IBU electrospun by needleless electrospinning by using optimized parameters.

Samples	Applied voltage (kV)	Mean diameters (nm)	CV%
Nanofibers on aluminum foil			
2%HA+PCL	40	420 ± 245	58%
2%HA+PCL/PEG	41	525 ± 159	30%
5%IBU+2%HA+PCL	40	445 ± 350	78%
5%IBU+2%HA+PCL/PEG	44	710 ± 315	44%
7%IBU+2%HA+PCL	44	445 ± 230	51%
7%IBU+2%HA+PCL/PEG	42	440 ± 222	50%
Nanofibers on GE/HA film			
2%HA+PCL	40	417 ± 235	57%
2%HA+PCL/PEG	41	685 ± 390	57%
5%IBU+2%HA+PCL	40	600 ± 300	50%
5%IBU+2%HA+PCL/PEG	44	555 ± 275	50%
7%IBU+2%HA+PCL	44	675 ± 315	46%
7%IBU+2%HA+PCL/PEG	42	460 ± 270	58%

Optimized electrospinning parameters were applied for this needleless electrospinning of nanofibers. With aluminum foil the distance between two electrodes was 220mm whereas with Teflon sheet it was kept at 170mm.

5.2 Crystallinity of PCL nanofibers with HA, PEG-400 and IBU

DSC analysis of PCL and PCL/PEG nanofibers loaded with HA and IBU was performed to study the crystallinity ratio of nanofibers. The impact of HA on the crystallinity of nanofibers was also monitored. All samples were sealed in non-hermetic capsules and analysis was performed under nitrogen atmosphere with a single cycle of heating from -80°C to 100°C at a rate of $10^{\circ}\text{C}/\text{min}$. The crystallinity ratio (X_c) was calculated with reference to the PCL content used and by dividing the ΔH_m of each sample by the melting enthalpy of 100% crystalline PCL ($\Delta H_{m,\text{PCL}}$) [7]. DSC curves were obtained and analyzed by using TA Universal Analysis software. Two DSC curves of 2%HA+PCL/PEG and 5%IBU+2%HA+PCL/PEG nanofibers are illustrated in Figures 5.8 (a) and 5.8 (b) respectively.

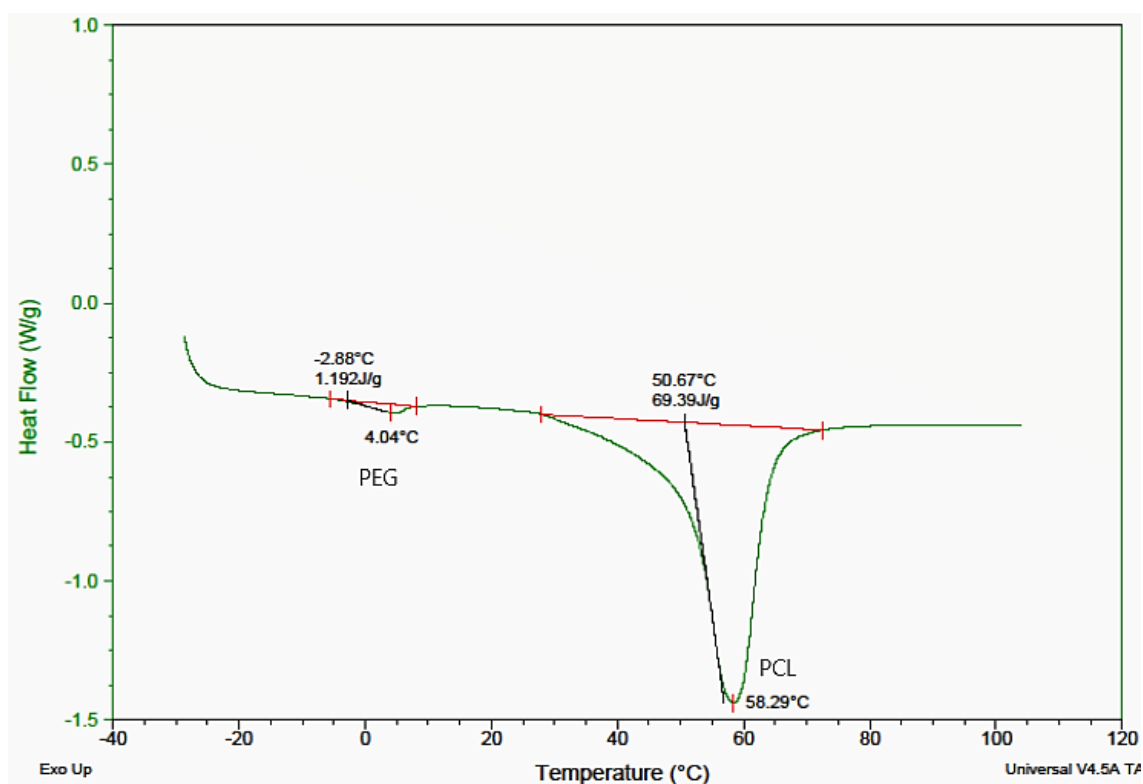


Figure 5.8 (a). A DSC curve of 2%HA+PCL/PEG nanofibers showing first heating cycle from -80° to 100°C under N_2

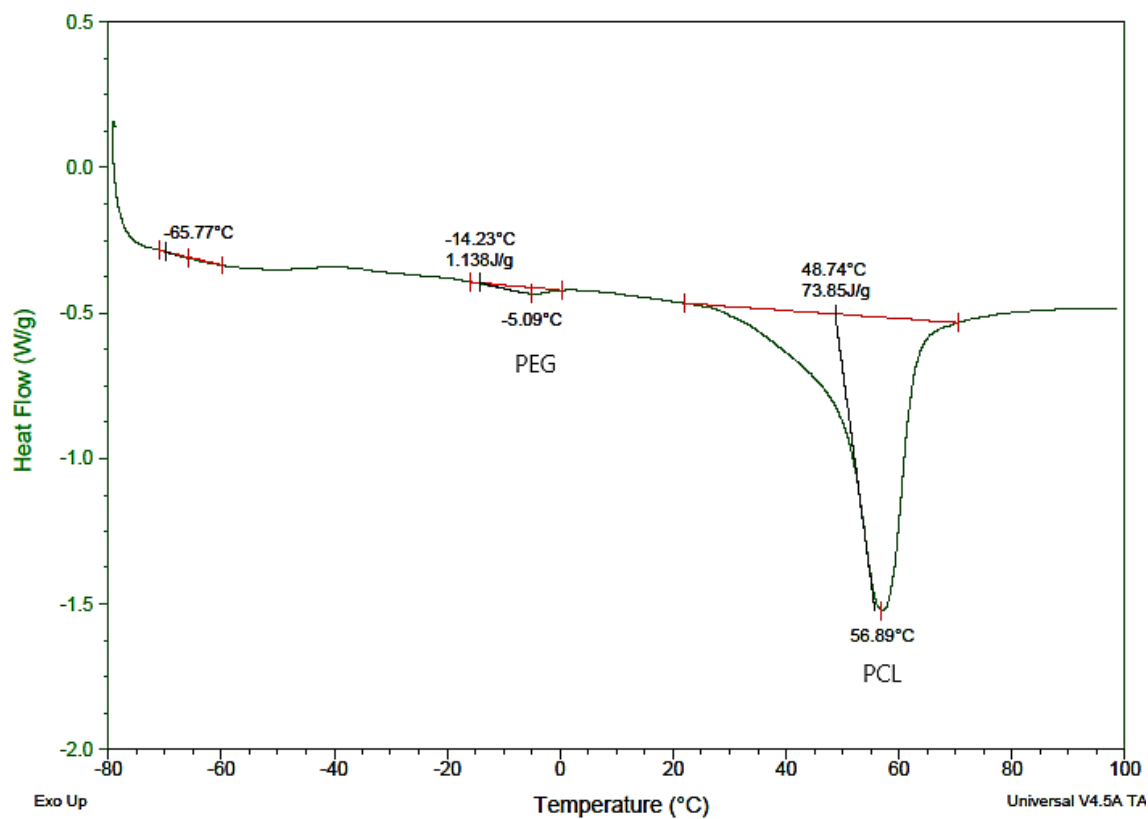


Figure 5.8 (b). DSC curve of 5%IBU+2%HA+PCL/PEG nanofibers showing first heating cycle from -80° to 100°C under N₂

The melting temperature of all PCL nanofibers was around 60°C with a slight decrease in case of IBU loaded nanofibers. Nanofibers with PEG-400 showed small melting peak of PEG before PCL melting that can be observed in above mentioned Figures 5.8 (a) and 5.8 (b). No distinct peak of IBU at 77°C was noticed in any sample. Percentage crystallinity ratio of each HA and IBU loaded sample was calculated and is given in Table 5.2 along with pure PCL crystallinity. PEG-400 was used in 10wt% concentration with respect to PCL content in order to prepare these samples.

Table 5.2. PCL Melting temperatures (T_m), melting enthalpies (ΔH_m) and crystallinity ratios ($X_c\%$) of PCL, PCL/PEG nanofibers with HA and IBU electrospun by needleless electrospinning determined by their first heating cycle from -80°C to 100°C under N_2

Samples	T_m ($^\circ\text{C}$)	ΔH_m J/g	$X_c\%$
PCL nanofibers	60	77	54%
2%HA+PCL	60	70	49%
2%HA+PCL/PEG	58	69	54%
5%IBU+2%HA+PCL	56	74	52%
5%IBU+2%HA+PCL/PEG	57	74	58%
7%IBU+2%HA+PCL	57	67	47%
7%IBU+2%HA+PCL/PEG	57	62	49%

Impact of HA and IBU on crystallinity ratio of PCL and PCL/PEG nanofibers

The crystallinity ratio of 2%HA+PCL nanofibers was turned out 49% that was less than PCL nanofibers with 54%. But, 2%HA+PCL/PEG nanofibers showed same $X_c\%$ value as of PCL nanofibers. It proved that HA had no significant impact on the crystallinity of PCL nanofibers. Incorporation of 7%IBU lowered the crystallinity of PCL nanofibers to 47% as compared to PCL nanofibers. This impact of IBU has already been described in Chapters 3 and 4 about single-needle and needleless electrospinning of IBU loaded PCL nanofibers.

5.3 Thermal stability of GE/HA film and PCL nanofibers with HA and IBU

It was necessary to understand thermal behavior of this bilayer structure to ensure its stability in order to be used as wound dressing. For this purpose, TGA analysis of GE/HA hydrogel film and PCL nanofibers with HA and IBU was performed separately for better comprehension of their features. Analysis was done under nitrogen with 10°C/min rate of heating ramp till 800°C. A degradation curve of GE/HA film showing stages of weight loss is presented in Figure 5.9.

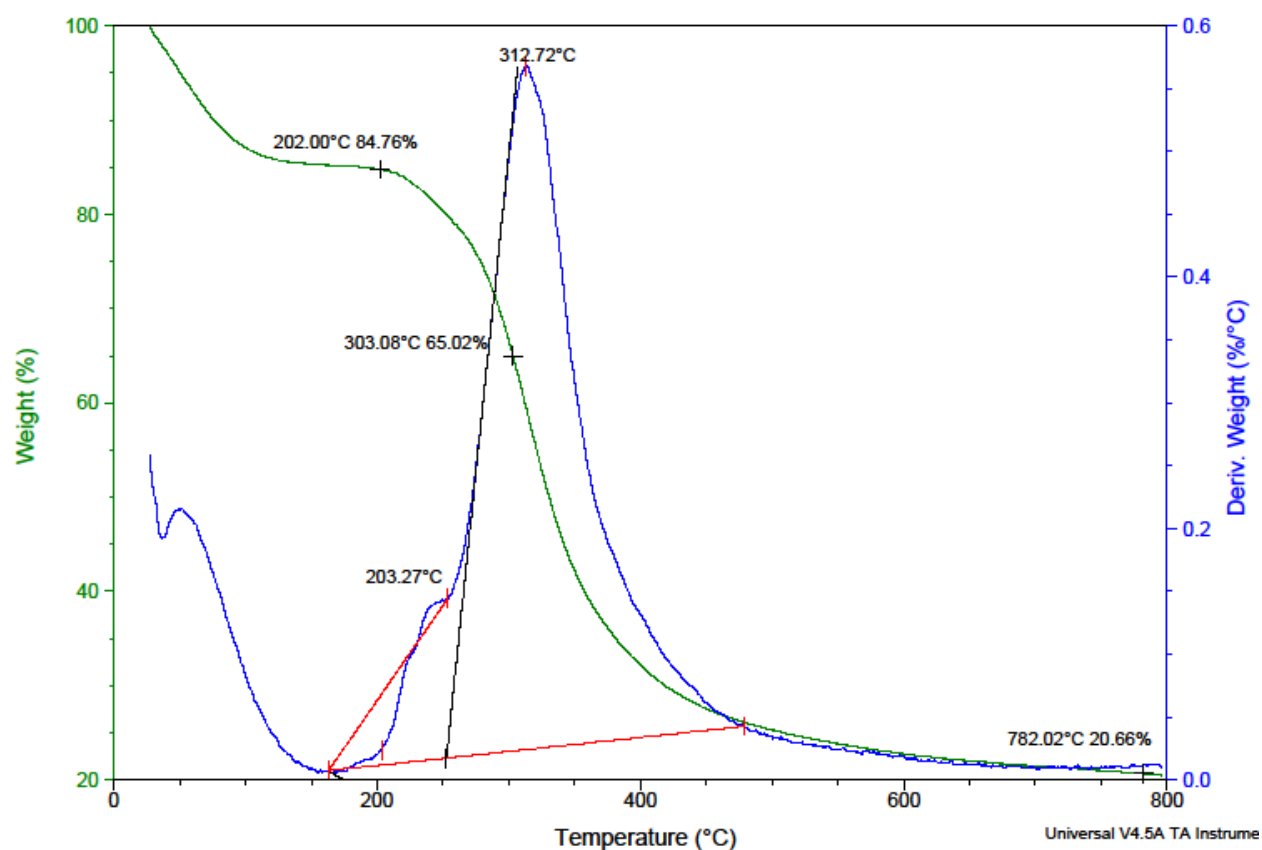


Figure 5.9. Degradation curve of GE/HA film exhibiting a two-stage weight loss

a) Degradation of GE/HA film

This GE/HA film exhibited two main stages of weight loss. The first weight loss (about 15%) occurred until 202°C that could be related to the evaporation of absorbed and bound water. This

result was in accordance with the literature [27, 28]. The second weight loss (about 65%) appeared at initial (onset) temperature of 303°C. This weight loss was associated with thermal degradation and decomposition of protein. The residual mass of gelatin film at temperature 800°C was almost 20% that is in fair agreement with previously published studies about bovine gelatin degradation [29]. This residual mass is due to the N-terminal amino acids which are the by-product of protein degradation by its hydrolysis [30]. As far as the HA degradation is concerned, it can be stated that it happened around 300°C along with gelatin degradation. According to literature, the degradation of HA is similar to gelatin because it also follows a two stage weight loss. First stage of weight loss occurs around 180°C (possibly evaporation of water) followed by a second weight loss at 280°C [31, 32]. In this degradation curve of GE/HA film, an intermediate peak at 203°C was recorded before full degradation peak of gelatin. This peak could refer to the start of second stage weight loss of HA that subsequently completed until 300°C and appeared as combined one large peak of full degradation of both GE and HA.

b) Degradation of PCL nanofibers with HA and IBU

In order to explain the thermal behavior of PCL nanofibers containing HA and IBU, their TGA analysis was done under same conditions as mentioned above. The degradation curves of 2%HA+PCL/PEG, 5%IBU+2%HA+PCL and 7%IBU+2%HA+PCL nanofibers are given in Figures 5.10 (a), 5.10 (b) and 5.10 (c) respectively.

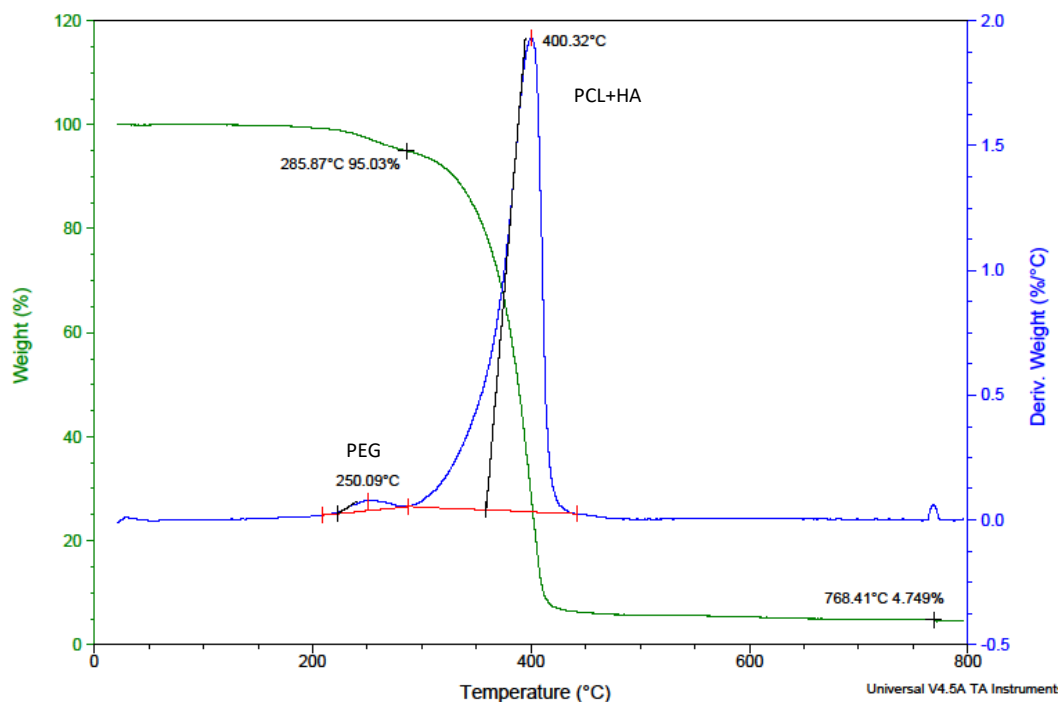


Figure 5.10 (a). Degradation curve of 2%HA+PCL/PEG nanofibers electrospun by needleless technique at heating rate of 10°C/min till 800°C under N₂

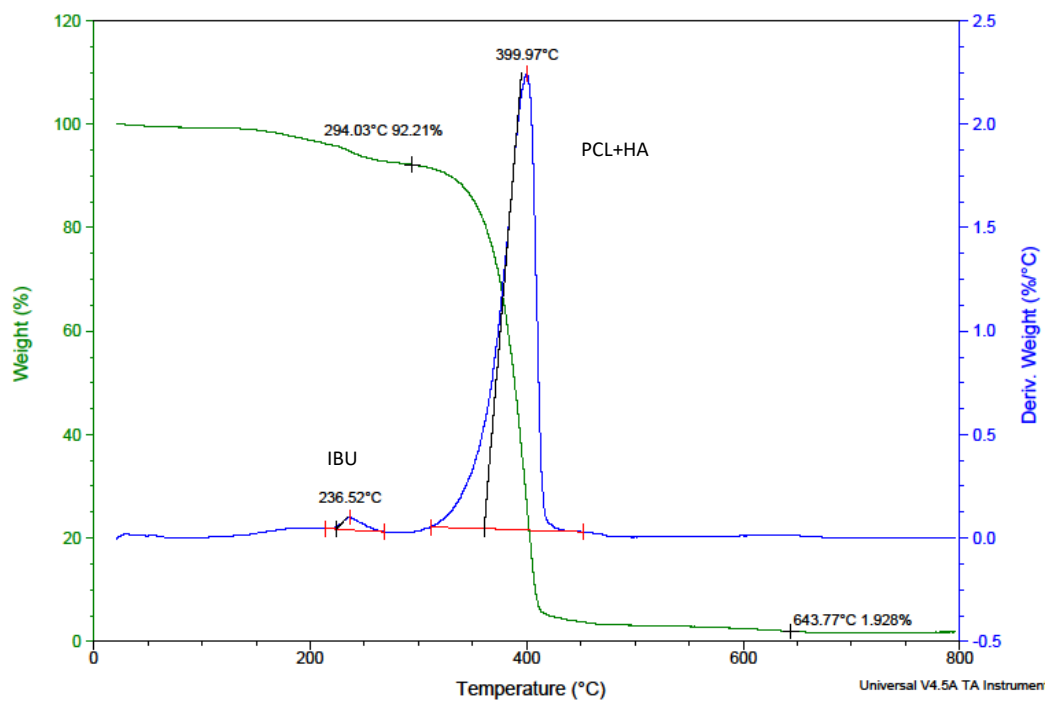


Figure 5.10 (b). Degradation curve of 5%IBU+2%HA+PCL nanofibers electrospun by needleless technique at heating rate of 10°C/min till 800°C under N₂

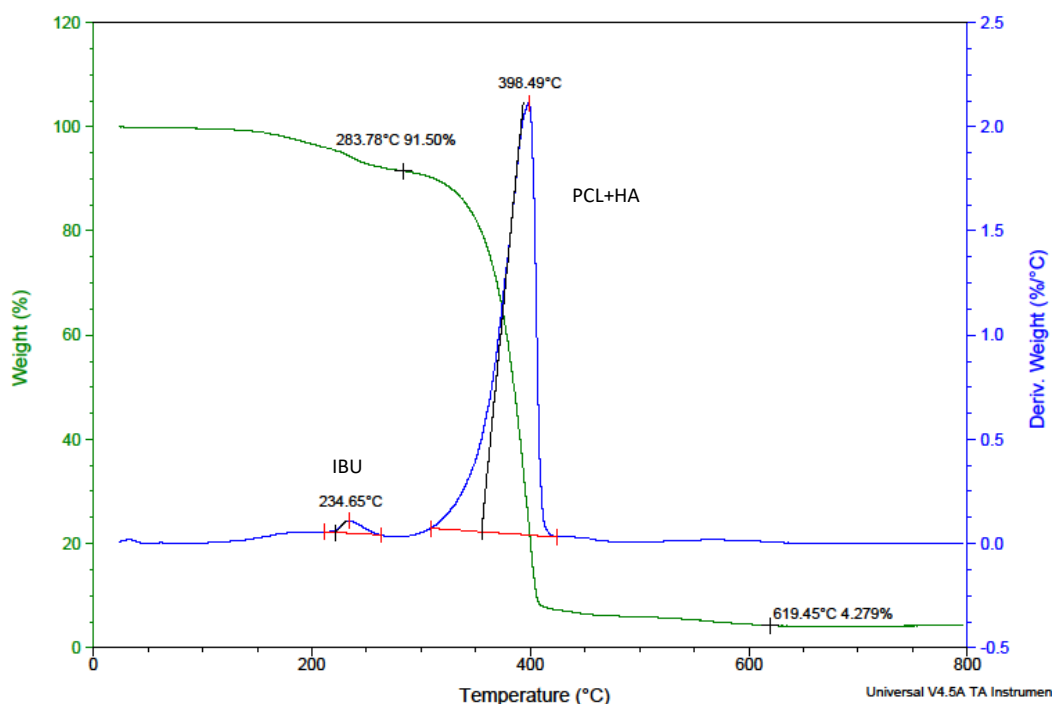


Figure 5.10 (c). Degradation curve of 7%IBU+2%HA+PCL nanofibers electrospun by needleless technique at heating rate of 10°C/min till 800°C under N₂

In all these curves, degradation of HA could be seen at around 280°C which is previously described in above section of GE/HA film degradation. PCL nanofibers displayed similar behavior as of nanofibers explained in Chapter 4 showing their full degradation at 400°C temperature. Moreover, the presence of IBU was verified from small weight loss peaks at 234°C in both samples. These results ascertained that HA and IBU had no influence on the thermal stability of PCL nanofibers. To quantify the incorporated IBU into nanofibers, the initial weight loss% of drug loaded PCL nanofibers was considered. In samples of 5%IBU+2%HA+PCL and 7%IBU+2%HA+PCL nanofibers, theoretical amount of added IBU compared to PCL was 5% and 7% respectively. The actual content of IBU was determined by using their initial weight loss% between their T-ambient and T-294°C and T-284°C and the calculated amounts of IBU were 8% and 9% respectively for both samples which were in good agreement to the theoretical incorporated percentages of IBU.

5.4 Wettability of GE/HA film and nanofibers of bilayer wound dressing

The ability to absorb water/fluids is a key feature that a material should have if it would be used as a wound dressing. Absorption of wound exudate is an essential requirement for its rapid recovery and to prevent infections. Therefore, the bilayer structure that was prepared for this specific application was tested for its wettability function. Not only the GE/HA hydrogel layer was studied for its hydrophilicity but the hydrophilic behavior of PCL nanofibers with HA alone and in its bilayer form was also analyzed. Water contact angle measurements were recorded for GE/HA film, 2%HA+PCL nanofibers on GE/HA film and 2%HA+PCL nanofibers alone. The obtained water contact angle values for these samples are mentioned in Table 5.3.

Table 5.3. Mean water contact angles of GE/HA film, 2%HA+PCL nanofibers with and without GE/HA film

Sample	Mean Contact Angle	Observations
PCL nanofibers	$130 \pm 2^\circ$	Hydrophobic
2%HA+PCL nanofibers	$123 \pm 3^\circ$	Hydrophobic
2%HA+PCL on GE/HA film	$125 \pm 2^\circ$	Hydrophobic
GE/HA film	$56 \pm 2^\circ$	Hydrophilic

This analysis disclosed that water contact angle of 2%HA+PCL nanofibers alone and on GE/HA film was almost similar to the PCL nanofibers that proved their hydrophobic nature. This indicated that HA was embedded inside the nanofibers structure and did not migrate on their surface. On the other hand, the GE/HA hydrogel film presented a smaller angle ($56 \pm 2^\circ$) which confirmed its hydrophilic nature. Thus, it was revealed that the GE/HA film of this bilayer wound dressing will act as a hydrogel and has the tendency to absorb water that was actually the desired outcome.

5.5 Mechanical strength of GE/HA film

The tensile strength testing of GE/HA film was done to anticipate the projected film integrity under conditions of stress during its handling and processing. Method of GE/HA film preparation was explained in Section 2.5 of Chapter 2. Six strips of GE/HA film were trimmed to 20mm × 10mm dimensions and their average thickness was measured by a digital micrometer with a precision of 0.001mm. All the procedural details of this analysis have already been described in Section 3.8 of Chapter 2. The mechanical strength and flexibility of GE/HA film was described by its Young's modulus (MPa) and percentage elongation at break known as strain % under maximum applied stress (MPa) and obtained results are given in Table 5.4.

Table 5.4. Results of tensile strength testing of GE/HA film samples

Samples of GE/HA film	Thickness (mm)	Stress (MPa)	Strain%	Young's Modulus (MPa)
A	0.042	32	1.6%	2280
B	0.018	23	1.2%	2330
C	0.048	38	4.7%	1900
D	0.028	44	2.2%	2360
E	0.021	47	2.4%	2190
F	0.028	30	3.4%	1890

All samples of GE/HA film displayed high values of Young's Modulus that corresponds to good mechanical strength. Lower values of maximum elongation at break (strain %) as compared to the tested length of the samples (10mm between the jaws) for all films were attained that translate

their poor flexibility. These observations are in agreement with literature where studies reported that generally, gelatin films exhibited poor elasticity and high Young's Modulus [33, 34]. A clustered column chart presenting the mechanical properties of GE/HA film samples is given in Figure 5.11.

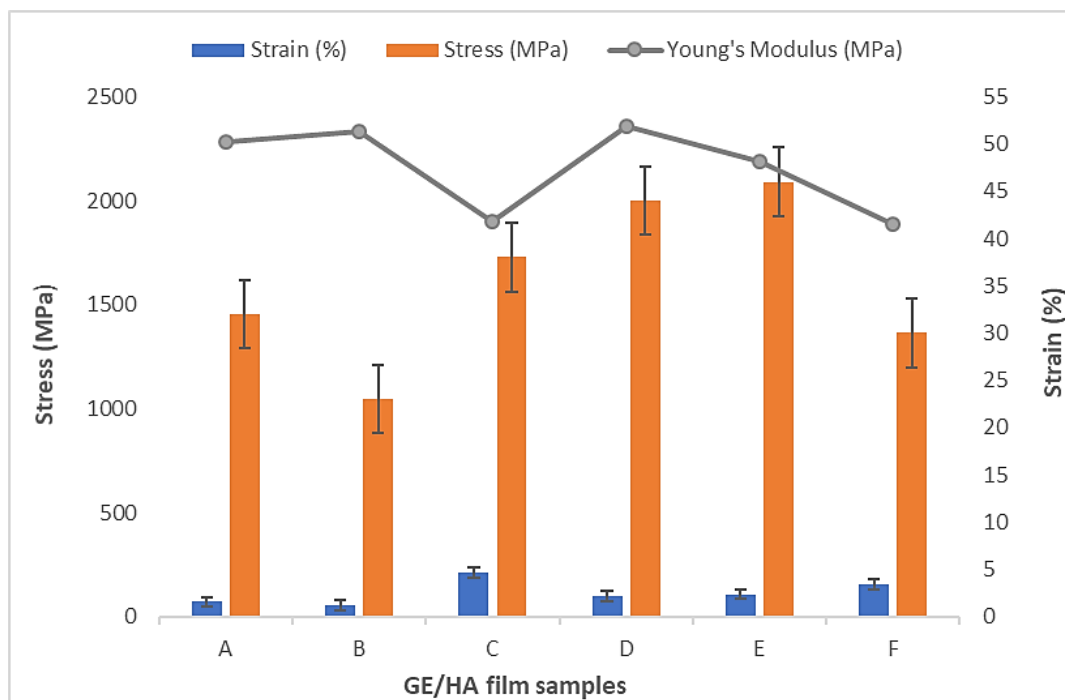


Figure 5.11. Tensile strength of GE/HA film samples in terms of their Young's Modulus and Stress-Strain%

Tensile strength analysis proved that GE/HA hydrogel film exhibited good mechanical strength that is justified by its high Young's Modulus. Hence, it is reasonable to state that this hydrogel layer of bilayer wound dressing will fairly withstand any stress during its handling and application process.

6. IBU release kinetics of HA/IBU loaded nanofibers and bilayer structure

The electrospinning of PCL nanofibers was done with 2wt% HA and two concentrations of IBU. Similar composition was followed to produce the bilayer wound dressing. The *in vitro* IBU release kinetics of these nanofibers and bilayer structure were realized by Pr. Leonard Ionut ATANASE and his research team at the Faculty of Dental Medicine, University “Apollonia”, Iasi-Romania. The details of this method have already been stated in Section 4.1 of Chapter 2. Quantification of released IBU was made by UV-vis spectroscopy and analysis was done for 48h duration. The percentage release efficiencies (%RE) of IBU for all these samples during their first 24h and then for 48h are given in Table 5.5.

Table 5.5. Percentage IBU release efficiencies (%RE) from HA/IBU loaded nanofibers and bilayer structure during their 24h and 48h of analysis

Samples	%RE (24h)	%RE (48h)
5%IBU+2%HA+PCL	37%	39%
7%IBU+2%HA+PCL	41%	43%
5%IBU+2%HA+PCL on GE/HA film	32%	34%
7%IBU+2%HA+PCL on GE/HA film	35%	37%

† Samples shown in the Table 5.5 were electrospun by needleless electrospinning with optimized parameters

A graph presenting the kinetics of IBU release from all these samples during 48h duration is displayed in Figure 5.12. This graph demonstrated the IBU release in two steps, a rapid release followed by a steady release of IBU from all these nanofibers both in case of bilayer structure and alone. At start the burst release was explained by the drug present on the surface of nanofibers

whereas, the prolonged release of IBU could be explained by the diffusion of drug through the polymer matrix [35, 36]. This behavior describes that IBU was embedded into the PCL nanofibers structure hence, it took longer time to release.

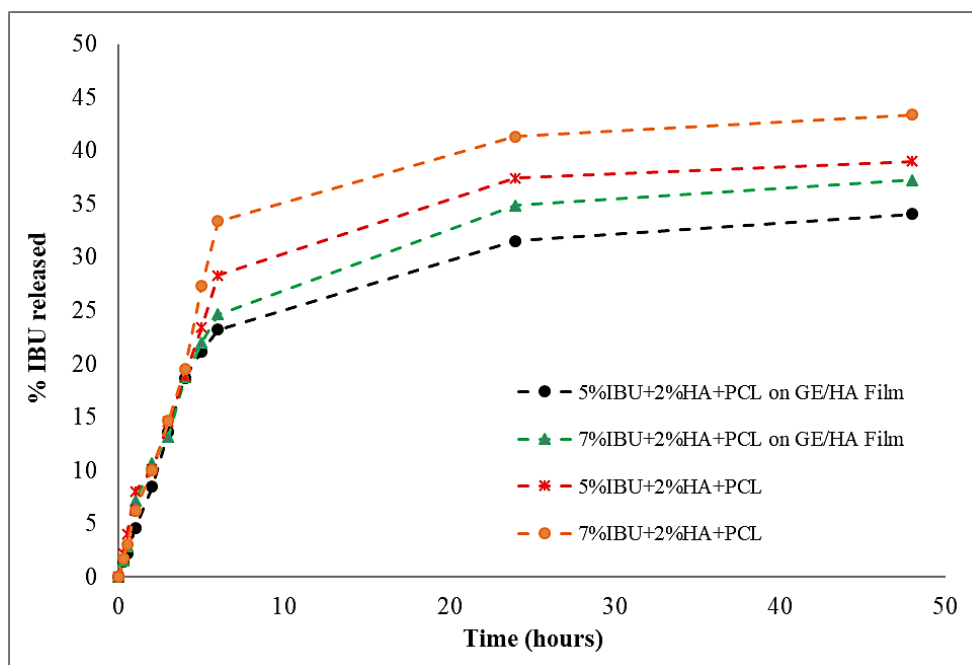


Figure 5.12. IBU release kinetics of HA/IBU loaded PCL nanofibers and bilayer wound dressing during 48h

The maximum release efficiency recorded was 43% from 7%IBU+2%HA+PCL nanofibers during 48h. It can be seen from the %RE values given in the Table 5 that there was no significant increase in IBU release rate after 24h. But, one thing was obvious from this graph that this release was not completed yet. If the analysis could have been done for a longer period of time, there was a strong possibility of further IBU release from these nanofibers. Thus, in future studies the drug release kinetics of these nanofibers will be analyzed for a longer duration such as until four days.

To construct a modern biomedical wound dressing, it was required to develop a self-sufficient drug delivery system that must be capable of controlling the drug release to the wound for days [37]. To fulfill this criteria, these results of IBU release kinetics from bilayer wound dressing are

encouraging as it offered a drug delivery system that can efficiently administer the constant release of drug ultimately, relieving pain and preventing inflammation in wound for a longer period of time. Furthermore, this bilayer wound dressing will increase patient compliance by reducing the time required to change dressing after every few hours as this bilayer wound dressing can be used unchanged for days.

7. Antibacterial analysis of bilayer wound dressing

Although, Ibuprofen (IBU) which is a non-steroidal, anti-inflammatory drug typically called NSAIDs [38], this is reported that it can inhibit few bacterial strains like, gram positive bacteria *Staphylococci aureus* and gram negative bacteria *E. coli*. available information about the relationship between bacteria and IBU is mainly focused on its anti-inflammatory response on the immune system that is stimulated by bacterial infection and not on the antibacterial activity. IBU was found to limit the effect of *E. coli* endotoxin on physiological activities of rabbits and humans [39, 40]. But, a direct action of IBU on bacterial cultures is not clearly illustrated until now. Therefore, to better understand this aspect of IBU, an *in vitro* antibacterial assay was performed on IBU loaded PCL nanofibers and their bilayer structure.

This analysis was done under the supervision of Dr. Mary-Lorène GODDARD working in the Laboratoire d'Innovation Moléculaire et Applications (LIMA-UHA, Mulhouse). The antibacterial resistance of IBU loaded nanofibrous mats was tested against two common types of bacteria, *E. coli* (gram-negative bacteria) and *S. epidermidis* (gram-positive bacteria). Five different samples of nanofibrous mats and bilayer wound dressing material were analyzed and are mentioned in Table 5.6. All samples were cut into circular disks of approximately 5mm diameters, sterile disks impregnated with chloramphenicol solution (Chl) were used as control samples. The zones of inhibition for all samples were observed and for each specimen experiments were performed in

triplicate. The description of applied method and specifications of all the materials used for this analysis were entailed in Section 4.2 of Chapter 2.

Table 5.6. Antibacterial activity of IBU/HA loaded nanofibers and bilayer wound dressing

Samples	Annotation	Inhibition for <i>E. coli</i>	Inhibition for <i>S. epidermidis</i>
5%IBU+2%HA+PCL	A	-	-
7%IBU+2%HA+PCL/PEG	B	-	-
7%IBU+2%HA+PCL	C	+	-
5%IBU+2%HA+PCL on GE/HA film	E	+	-
7%IBU+2%HA+PCL on GE/HA film	F	++	-
Chloramphenicol control disk	Chl	+++	+++

*Note: The (-) annotation depicts “no inhibition”, (+) means “Good inhibition”, (++) translates to “Fairly good inhibition” and (+++) in case of control Chl disk shows “Excellent inhibition”

After the incubation time of analysis for both bacteria, petri dishes were carefully observed for their inhibition zones. It was observed that neither IBU/HA loaded nanofibers nor bilayer wound dressing disks showed any inhibition zones against *S. epidermidis* gram positive bacteria in comparison to Chl control disk as shown in Figure 5.13 (a). These IBU loaded nanofibers revealed no inhibition to *S. epidermidis* strains. While, in case of *E. coli* bacterial strain, two bilayer samples of 5%IBU+2%HA+PCL on GE/HA film, 7%+2%HA+PCL on GE/HA film and one sample of 7%IBU+2%HA+PCL nanofibers annotated as E, F and C respectively showed inhibition zones as compared to the control sample Chl as presented in Figure 5.13 (b).



Figure 5.13. Samples showing inhibition zones for *S. epidermidis* (a) and *E. coli* (b) bacterial strains

These observations concluded that in addition to IBU anti-inflammatory and pain relieving functions, it can also act as a mild antibacterial against *E. coli* strains. However, it cannot be recommended as an efficient antibacterial agent and further research must be conducted to study IBU antibacterial resistance against other bacterial strains such as gram positive bacteria *S. aureus*. Also, advance studies are demanded to determine the correct loading concentration of IBU for effective results.

8. Conclusion

The main objective of this research study, fabrication and characterization of a bilayer wound dressing was accomplished and recounted during this final chapter. A modern biomedical wound dressing was developed by depositing PCL nanofibers loaded with IBU/HA on a wet GE/HA hydrogel film via needleless electrospinning technique. All the experiments were performed after the optimization of electrospinning parameters. Characterization of PCL nanofibers with IBU/HA was done and their physical, thermal and mechanical properties were analyzed. SEM studies of nanofibers revealed their round morphology with their mean diameters ranging from 400-700nm. It was discovered that HA had no impact on the melting temperature and crystallinity of PCL nanofibers. Degradation curve of GE/HA film indicated good thermal stability and the presence of HA and IBU in PCL nanofibers was also deliberated by their TGA curves. Wettability of GE/HA hydrogel film was determined by water contact angle measurements which showed its hydrophilic nature, a desired feature to absorb exudate for speedy recovery of wound. Furthermore, this hydrogel film exhibited good tensile strength with high values of Young's Modulus and ensured the mechanical stability of this bilayer wound dressing.

Drug release kinetics of IBU/HA loaded PCL nanofibers and bilayer structure were realized by UV-vis spectroscopy. All samples displayed a two stage drug release phenomenon, an initial burst release followed by a prolonged steady release of IBU until 48h. However, it was observed that IBU release profiles were incomplete which suggest a future study of these samples for IBU release kinetics to be analyzed for a longer period of time. Antibacterial assay of these IBU/HA equipped nanofibrous mats and bilayer wound dressing against two bacteria, *S. epidermidis* (gram positive) and *E. coli* (gram negative) was performed. No inhibition was noticed against *S. epidermidis* bacterial strain in any sample whereas, mild antibacterial activity was seen against *E. coli* bacterial strain. This concluded that IBU could act as a mild antibacterial agent against *E. coli* bacteria.

References

1. Yao C. H., L.C.Y., Huang C. H., Chen Y. S. and Chen K. Y., Novel bilayer wound dressing based on electrospun gelatin/keratin nanofibrous mats for skin wound repair. *Materials Science and Engineering: C*, 2017. 79: p. 533-540.
2. Vig K., C.A., Tripathi S., Dixit S., Sahu R., Pillai S., Dennis V. A. and Singh S. R., Advances in skin regeneration using tissue engineering. *International Journal of Molecular Sciences.*, 2017. 18(4): p. 789.
3. Xie Y., Y.Z.X., Wang J. X., Hou T. G. and Jiang Q., Carboxymethyl konjac glucomannan-crosslinked chitosan sponges for wound dressing. *International Journal of Biological Macromolecules.*, 2018. 12: p. 1225-1233.
4. Franco, R.A., et al., Fabrication and biocompatibility of novel bilayer scaffold for skin tissue engineering applications. *J Biomater Appl*, 2013. 27(5): p. 605-15.
5. Gizaw, M., et al., Electrospun Fibers as a Dressing Material for Drug and Biological Agent Delivery in Wound Healing Applications. *Bioengineering (Basel)*, 2018. 5(1).
6. Hutmacher D. W. and Cool S., Concepts of scaffold-based tissue engineering—the rationale to use solid free-form fabrication techniques. *J. Cell. Mol. Med.*, 2007. 11(4): p. 654-669.
7. Zhang L. and Webster T. J., Nanotechnology and nanomaterials: promises for improved tissue regeneration. *Nanotoday.*, 2009. 4(1): p. 66-80.
8. Mogosanu G.D and Grumezescu A.M, Natural and synthetic polymers for wounds and burns dressing. *Int. J. Pharm.*, 2014. 463: p. 127-136.
9. Khandaker, M., et al., Use of Polycaprolactone Electrospun Nanofibers as a Coating for Poly(methyl methacrylate) Bone Cement. *Nanomaterials (Basel)*, 2017. 7(7).
10. Labet M. and Thielemans W., Synthesis of polycaprolactone: a review. *Chemical Society Reviews.*, 2009. 38: p. 3484-3504.
11. Tiwari A. P., J.M.K., Lee J., Bikendra M., Ko S. W., Park C. H. and Kim C. S., Heterogeneous electrospun polycaprolactone/polyethylene glycol membranes with improved wettability, biocompatibility, and mineralization. *Colloids and Surfaces A: Physicochemical and Engineering Aspects.*, 2017. 520: p. 105-113.

12. Sigg, J., Production of drug-delivery systems with Ibuprofen through encapsulation in nanofibers and -particles with core-shell architecture, in *Life Science and Facility Management 2017*, ZHAW, Studieren Zürich. p. 65.
13. Leach J. B., B.K.A., Patrick C.W. Jr. and Schmidt C.E., Photocrosslinked hyaluronic acid hydrogels: natural, biodegradable tissue engineering scaffolds. *Biotechnol Bioeng.*, 2003. 82(5): p. 578-589.
14. Yamane S., I.N., Majima T., Funakoshi T., Masuko T., Harada K., Minami A., Monde K. and Nishimura S., Feasibility of chitosan-based hyaluronic acid hybrid biomaterial for a novel scaffold in cartilage tissue engineering. *Biomaterials*, 2005. 26(6): p. 611-619.
15. C.E., L.J.B.a.S., Characterization of protein release from photocrosslinkable hyaluronic acid-polyethylene glycol hydrogel tissue engineering scaffolds. *Biomaterials*, 2005. 26(2): p. 125-135.
16. Luo Y., K.K.R.a.P.G.D., Cross-linked hyaluronic acid hydrogel films: new biomaterials for drug delivery. . *J. Contr. Rel.*, 2000. 69(1): p. 169-184.
17. G.D., V.K.P.a.P., Hyaluronate derivatives in drug delivery. . *Crit. Rev. Ther. Drug Carrier Syst.*, 1998. 15(5): p. 513-555.
18. Pienimäki J.P., R.K., Fulop C., Sironen R.K., Karvinen S., Pasonen S., Lammi M.J., Tammi R., Hascall V.C. and Tammi M.I., Epidermal growth factor activates hyaluronan synthase 2 in epidermal keratinocytes and increases pericellular and intracellular hyaluronan. *J. Biol. Chem.*, 2001. 276(23): p. 20428-20435.
19. Foschi D., C.L., Radaelli E., Abelli P., Calderini G., Rastrelli A., Mariscotti C., Marazzi M. and Trabucchi E., Hyaluronic acid prevents oxygen free-radical damage to granulation tissue: a study in rats. *Int. J. Tissue React.*, 1990. 12(6): p. 333-339.
20. Trochon V., M.C., Bertrand P., Legrand Y., Smadja-Joffe F., Soria C., Delpech B. and Lu H., Evidence of involvement of CD44 in endothelial cell proliferation, migration and angiogenesis in vitro. *Int. J. Cancer*, 1996. 66(5): p. 664-668.
21. Ishida O., T.Y., Morimoto I., Takigawa M. and Eto S.J., Chondrocytes are regulated by cellular adhesion through CD44 and hyaluronic acid pathway. *Bone Miner. Res.*, 1997. 12(10): p. 1657-1663.
22. Lesley J., H.V.C., Tammi M. and Hyman R. J., Hyaluronan binding by cell surface CD44. *Biol. Chem.*, 2000. 275(35): p. 26967-26975.

23. McKee C.M., P.M.B., Cowman M., Burdick M.D., Strieter R.M., Bao C. and Noble P.W., Hyaluronan (HA) fragments induce chemokine gene expression in alveolar macrophages. The role of HA size and CD44. *J. Clin. Invest.*, 1996. 98(10): p. 2403-2413.
24. Evanko S.P., A.J.C.a.W.T.N., Formation of hyaluronan- and versican-rich pericellular matrix is required for proliferation and migration of vascular smooth muscle cells. . *Arterioscler. Thromb. Vasc. Biol.*, 1999. 19(4): p. 1004-1013.
25. Hahn S.K., J.S., Maier R.V., Stayton P.S. and Hoffman A.S., Anti-inflammatory drug delivery from hyaluronic acid hydrogels. . *J. Biomater. Sci. Polym. Ed.*, 2004. 15(9): p. 1111-1119.
26. Figueira D. R., M.S.P., D. de Sá K., Correia I. J. , Production and characterization of polycaprolactone- hyaluronicacid/chitosan- zein electrospun bilayer nanofibrous membrane fortissue regeneration. *International Journal of Biological Macromolecules*, 2016. 93: p. 1100-1110.
27. Barreto P. L. M., P.A.T.N.a.S.V., Thermal degradation of edible films based on milk proteins and gelatin in inert atmosphere. *Polym. Degrad. Stab.*, 2003. 79: p. 147-152.
28. Limpan N., P.T., Benjakul S. and Prasarnpran S., Properties of biodegradable blend films based on fish myofibrillar protein and polyvinyl alcohol as influenced by blend composition and pH level. *J. Food Eng.*, 2010. 100: p. 85-92.
29. Chuaynukul K. , P.T.a.B.S., Preparation, thermal properties and characteristics of gelatin molding compound resin. *Research Journal of Chemical and Environmental Sciences.*, 2014. 2(4): p. 1-9.
30. Courts A., The N-Terminal Amino Acid Residues of Gelatin. 2. THERMAL DEGRADATION. *The Biochemical Journal.*, 1954. 58(1): p. 74-79.
31. Ahire J. J., R.D., Neveling D. P, van Reenenb A. J. and Dicks L. M. T., Hyaluronic acid-coated poly(D,L-lactide) (PDLLA) nanofibers prepared by electrospinning and coating. *RSC Adv.*, 2016. 6: p. 34791–34796.
32. Jiang B. P., Z.L., Zhu Y., Shen X. C, Ji S. C., Tan X. Y., Cheng L. and Liang H., Water-Soluble Hyaluronic Acid-Hybridized Polyaniline Nanoparticles for Effectively Targeted Photothermal Therapy. *Journal of Materials Chemistry B.*, 2015. 3: p. 1-3.
33. Wang K., W.W., Ye R., Xiao J., Liu Y., Ding J., Zhanga S. and Liua A., Mechanical and barrier properties of maize starch–gelatin composite films: effects of amylose content. *J. Sci. Food Agric.*, 2017. 97(11): p. 3613-3622.

34. Cao N., F.Y.a.H.J., Mechanical properties of gelatin films cross-linked, respectively, by ferulic acid and tannin acid,. *Food Hydrocolloids*, 2007. 21(4): p. 575-584.
35. Rață D. M., P.M., Chailan J-F., Tamba B. I., Ionut Tudorancea and Peptu C. A., Ibuprofen-loaded chitosan/ poly(maleic anhydride-alt-vinyl acetate) submicronic capsules for pain treatment. *Journal of Bioactive and Compatible Polymers*, 2013. 28(4): p. 368-384.
36. Celik G. and Oksuz A. U., Controlled Release of Ibuprofen From Electrospun Biocompatible Nanofibers WithIn SituQCM Measurements. *Journal of Macromolecular Science, Part A*, 2014. 52(1): p. 76-83.
37. Kiaee, G., et al., Multilayered Controlled Released Topical Patch Containing Tetracycline for Wound Dressing. *Journal of In Silico & In Vitro Pharmacology*, 2016. 02(02).
38. Johnson J. M., Over-the-counter overdoses: A review of ibuprofen, acetaminophen, and aspirin toxicity in adults. *Advan. Emerg. Nur. J.*, 2008. 30: p. 369-378.
39. Celik I., A.A., Kilic S. S., Rahman A., Vural P., Canbaz M. and Felek S., Effects of ibuprofen on the physiology and outcome of rabbit endotoxic shock. *BMC Infect. Dis.*, 2002. 2: p. 26.
40. Bernard G. R., W.A.P., Russell J. A., Schein R., Summer W. R., Steinberg K. P., Fulkerson W. J., Wright P. E., Christman B. W., Dupont W. D., Higgins S. B. and Swindell B. B., The effects of ibuprofen on the physiology and survival of patients with sepsis. The Ibuprofen in Sepsis Study Group. *N. Engl. J. Med.* , 1997. 336(13): p. 912-918.

General Conclusion & Future Prospects

Conclusion et perspectives

Le but de cette étude était de développer un pansement bicouche polyvalent utilisant une technique d'électrofilage pour produire des nanofibres. A cet effet, la première couche d'hydrogel était constituée d'un film de gélatine (GE) et de hyaluronate de sodium (HA). La seconde couche a été fabriquée en déposant des nanofibres de PCL à 10% en masse dans un mélange chloroforme: éthanol (rapport massique 88: 12) sur le film d'hydrogel humide par électrofilage sans aiguille. La nouveauté de ce travail a été le choix d'introduire une très faible masse molaire de PEG (Mn-400 g / mol) dans la solution PCL afin d'améliorer la flexibilité et la mouillabilité de ces nanofibres. L'ibuprofène (IBU), un anti-inflammatoire non stéroïdien, a été incorporé dans les nanofibres PCL à deux concentrations, 5% en masse et 7% en masse par rapport à la teneur en PCL. L'IBU a été intégré pour concevoir un système d'administration de médicaments en nanofibres PCL afin de soulager la douleur et de prévenir l'inflammation. L'HA a été incorporé pour ses capacités de rétention d'humidité et de réparation des tissus. Les nanofibres ont été produites en utilisant deux approches d'électrofilage différentes, une technique à aiguille unique à l'échelle du laboratoire et la technologie NanoSpider sans aiguille.

Dans une étude préliminaire s'intéressant à l'électrofilage à une seule aiguille, un plan d'expérience (DOE) a été suivi en variant les paramètres d'électrofilage, la tension appliquée, la distance aiguille-collecteur et la vitesse d'alimentation. Les données obtenues à partir de ce DOE ont été analysées à l'aide d'un outil statistique d'analyse en composantes principales (ACP) qui a contribué à l'optimisation de ces paramètres d'électrofilage. Les nanofibres PCL ont été étudiées pour leur morphologie, leur cristallinité, leur stabilité thermique, leur mouillabilité et leurs propriétés mécaniques en utilisant différentes techniques de caractérisation telles que SEM, DSC, TGA, mesures d'angle de contact avec l'eau et tests de résistance à la traction. Les diamètres moyens des

nanofibres ont été mesurés en prenant 50 mesures par échantillon à l'aide du logiciel ImageJ. Les nanofibres PCL ont montré une morphologie hétérogène avec un mélange de micro et nanofibres qui étaient principalement de forme ronde tandis que les nanofibres contenant du PEG présentent des pores à leur surface. Les diamètres moyens des nanofibres PCL issues de la technique à une seule aiguille étaient dans une plage de 400nm à 3µm tandis que, dans le cas de la technique sans aiguille, les diamètres des nanofibres étaient inférieurs à un micron (400-800nm). Les taux de cristallinité des nanofibres PCL/PEG étaient plus élevés que ceux des nanofibres PCL et de la PCL pure de départ. Toutes les nanofibres PCL ont montré une bonne stabilité thermique jusqu'à 40 ° C, comparable à la température du corps humain. La présence d'IBU et HA dans les nanofibres PCL et PCL/PEG a également été confirmée à partir de leurs courbes de dégradation respectives (ATG). Les mesures d'angle de contact avec l'eau ont prouvé que l'ajout de PEG-400 améliorait la mouillabilité des nanofibres PCL. Le film GE/HA présentait également une hydrophilie appréciable qui est nécessaire pour le fonctionnement efficace de ce pansement bicouche en absorbant l'exsudat de la plaie et en maintenant un environnement humide autour de la plaie pour sa récupération rapide. Les tests de résistance à la traction du film hydrogel GE/HA ont montré une bonne résistance mécanique qui était justifiée par son module d'Young élevé. Par conséquent, on peut affirmer que cette couche d'hydrogel de pansement bicouche résistera assez bien à toute contrainte pendant son processus de manipulation et d'application.

La cinétique de libération du médicament des nanofibres PCL chargées IBU/HA et de la structure bicouche a été déterminée par spectroscopie UV-vis. Tous les échantillons présentaient un phénomène de libération de médicament en deux étapes, une libération initiale rapide suivie d'une libération prolongée et régulière d'IBU jusqu'à 48 h. Ces cinétiques de libération d'IBU sont encourageantes car le système d'administration de médicament développé permet d'administrer efficacement et de façon constant le médicament sur une période de temps longue afin de soigner

la douleur et l'inflammation. De plus, ce pansement bicouche permettra de d'augmenter le temps entre chaque remplacement du pansement car il peut être utilisé inchangé pendant des jours. Un test antibactérien a été réalisé sur des non tissés PCL nanofibreux contenant les médicaments IBU/HA et sur un pansement bicouche contre deux bactéries, *S. epidermidis* (gram positif) et *E. coli* (gram négatif). Aucune inhibition n'a été observée contre la souche bactérienne de *S. epidermidis* dans aucun échantillon. En revanche, une légère activité antibactérienne a été observée contre les bactéries *E. coli*, ce qui atteste que l'IBU peut légèrement agir comme un agent antibactérien.

L'analyse de la cytotoxicité et un test de prolifération cellulaire de ce pansement bicouche faisaient partie intégrante de cette étude mais sont restés non exécutés en raison de la fermeture des laboratoires suite à la crise sanitaire du COVID-19. Par conséquent, ces tests biologiques doivent être effectués afin d'achever cette étude. L'étude cinétique de libération du médicament a montré des profils de libération d'IBU incomplets, ce qui suggère qu'une analyse future de ces échantillons soit effectuée pendant une période plus longue pour réaliser leurs profils complets de libération d'IBU. De plus, dans une expérimentation plus poussée, un agent antibactérien biosourcé tel que la curcumine pourrait être testé afin d'améliorer les performances antibactériennes de ce pansement.

General Conclusion and Future Prospects

The aim of this study was to develop a versatile bilayer wound dressing using electrospinning technique to produce fine nanofibers. For this purpose, first hydrogel layer was comprised of gelatin (GE) and sodium hyaluronate (HA) film. Second layer was fabricated by depositing nanofibers of 10wt% PCL in a solvent mixture of chloroform: ethanol (88: 12 wt/wt ratio) on the wet hydrogel film via needleless electrospinning. The novelty of this work was the choice of a very low molar mass of PEG (Mn-400 g/mol) for PCL blending to enhance the flexibility and wettability of its nanofibers. Ibuprofen (IBU), a non-steroidal anti-inflammatory drug was incorporated into PCL nanofibers in two different concentrations 5wt% and 7wt% with respect to PCL content. IBU was integrated to devise a drug delivery system in PCL nanofibers in order to relieve pain and to prevent inflammation. HA was incorporated for its moisture retaining and tissue repairing abilities. Nanofibers were produced by employing two different electrospinning approaches, lab-scale single-needle technique and needleless NanoSpider technology.

In preliminary studies with single-needle electrospinning, a design of experiment (DOE) was followed by varying electrospinning parameters, applied voltage, needle-collector distance and feed rate. The data obtained from that DOE was analyzed using a statistical tool Principal Component Analysis (PCA) which helped in optimization of these electrospinning parameters. PCL nanofibers were studied for their morphology, crystallinity, thermal stability, wettability and mechanical properties by using different characterization techniques like SEM, DSC, TGA, water contact angle measurements and tensile strength testing. Mean diameters of nanofibers were measured by taking bar measurements using ImageJ software. PCL nanofibers showed heterogeneous morphology with a mix of micro and nanofibers which were predominantly round in shape and nanofibers with PEG showed pores on their surface. Mean diameters of PCL

nanofibers from single-needle technique were in a range of 400 nm up to 3 μm whereas, in case of needleless technique nanofibers diameters were under one micron (400-800 nm). Crystallinity ratios of PCL/PEG nanofibers were higher than that of PCL nanofibers and pure PCL pellets. All PCL nanofibers showed good thermal stability up to 40°C that is comparable to human body temperature. Presence of IBU and HA in PCL and PCL/PEG nanofibers was also confirmed from their respective degradation curves. Water contact angle measurements proved that the addition of PEG-400 enhanced the wettability of PCL nanofibers. GE/HA film also exhibited appreciable hydrophilicity that was needed for the effective functioning of this bilayer wound dressing by absorbing wound exudate and maintaining a moist environment around wound for its rapid recovery. Tensile strength testing of GE/HA hydrogel film displayed good mechanical strength that was justified by its high Young's Modulus. Hence, it can be stated that this hydrogel layer of bilayer wound dressing will fairly withstand any stress during its handling and application process.

Drug release kinetics of IBU/HA loaded PCL nanofibers and bilayer structure were realized by UV-vis spectroscopy. All samples displayed a two stage drug release phenomenon, an initial burst release followed by a prolonged steady release of IBU until 48h. These results of IBU release kinetics were encouraging because they offered a drug delivery system which can efficiently administer the constant release of drug over a longer period of time to cure pain and inflammation. Furthermore, this bilayer wound dressing will increase patient compliance by reducing the time required to change dressing after every few hours as it can be used unchanged for days.

Antibacterial assay was performed for IBU/HA equipped nanofibrous mats and bilayer wound dressing against two bacteria, *S. epidermidis* (gram positive) and *E. coli* (gram negative). No inhibition was noticed against *S. epidermidis* bacterial strain in any sample. Whereas, mild antibacterial activity was seen against *E. coli* bacteria that attested IBU could act as a mild antibacterial agent.

Cytotoxicity analysis and cells proliferation assay of this bilayer wound dressing were integral part of this study but remained unexecuted due to worldwide lab closures in the wake of COVID-19. Therefore, these biological aspects will be analyzed in future and this study will be completed. Drug release kinetic study showed incomplete IBU release profiles which suggests a future analysis of these samples to be done for a longer period of time to realize their complete IBU release profiles. Moreover, in further experimentation a bio-sourced antibacterial agent such as Curcumin could be tested to improve the antibacterial performance of this wound dressing.

